Investigating the transport mechanisms of secondary metabolites across cell membranes

Dissertation

zur

Erlangung der naturwissenschaftlichen Doktorwürde
(Dr. sc. nat.)

vorgelegt der

Mathematisch-naturwissenschaftlichen Fakultät

der

Universität Zürich

von

Krasimira MARINOVA

aus

Bulgarien

Promotionskomitee:

Dr. Markus Klein, Universität Zürich

Prof. Dr. Enrico Martinoia, Universität Zürich (Vorsitz)

Prof. Dr. Beat Keller, Universität Zürich

Dr. Isabelle Debeaujon, INRA, Frankreich

Zürich, 2006

UNIVERSITY OF ZURICH
FACULTY OF SCIENCE
BOTANICAL INSTITUTE
MOLECULAR PLANT PHYSIOLOGY

Investigating the transport mechanisms of secondary metabolites across cell membranes

Thesis presented to the Faculty of Science of the University of Zurich for the degree of Doctor of Science

by Krasimira Marinova

Members of the jury:

Dr. Markus Klein,	University of Zürich
Prof. Dr. Enrico Martinoia,	University Zürich
Prof. Dr. Beat Keller,	University Zürich
Dr. Isabelle Debeaujon,	INRA, France

Zürich, 2006

Acknowledgement

Herewith I would like to express my gratitude to my ***family*** *– they have always supported me in my life changing decisions, to my friends at home and especially to* ***Daniela Konaktchieva*** *- her mails kept me optimist that I can show the best of me during this challenge.*

I would like to address special words of admiration and respect to my supervisor ***Dr. Markus Klein*** *who believed in me and offered me the opportunity to learn and develop myself in the field of science, which was my desire after my study in the University.*

Thanks to ***Prof. Enrico Martinoia*** *for the opportunity to work within his broad and experienced team and to the* ***members of the lab*** *for their help and support during my work.*

Wish to pay respect to ***Prof. Felix Keller*** *and* ***Dr. Markus Geisler*** *for the opportunity to experience and learn about science and live some different perspectives.*

Special thanks to my best friends ***Nicola Tomasi*** *– you are with me not only when I need you and* ***Shaun Peters*** *– you showed me sites of life I wanted to see and your way of thinking enriched my personality.*

Thanks to my friends and lab mates ***Barbara Weder*** *and* ***Hanne Grob*** *for the help and the ambience they created during this time, which made the stay and work here easy and joyful. I'm glad also that I had the opportunity to meet and work with* ***Annie Frelet***, ***Tina Ballmann*** *and* ***Katharina Schmid****. I will not forget my friends* ***Vincent Vincenzetti***, ***Christine Cretton*** *and* ***Michal Jasinski*** *- they were first to listen and share my concerns.*

I also like to thanks to my teacher ***Dr. Veneta Kapchina*** *– without you I would never have had this experience.*

This work was financially supported by the Forschungskredit of the University of Zurich, (MK) and the Roche Research Foundation, Basel, CH (KM).

Summary

Despite our knowledge on flavonoid synthesis and the regulation, the mechanism(s) by which phenolic compounds are targeted and transported to the subcellular destinations (vacuolar or apoplastic) remain largely unclear. Although the vacuolar transport mechanism of differentially conjugated flavonoids has been investigated in recent years, molecular analyses are lacking. Biochemical evidence of vacuolar transport properties performed with flavonoids suggested that flavoniod transport is mediated across the tonoplast either by directly energized ABC-type transporters or H^+-antiporters driven by the proton gradients - by the two vacuolar H^+-pumps, the V-type H^+-ATPase and H^+-pyrophosphatase, respectively.

Here we demonstrate that a member of the multidrug and toxic efflux transporter (MATE) family, a novel plant membrane protein family, is involved in vacuolar accumulation of phenolic compounds. Previous phenotypic characterization of the Arabidopsis *transparent testa12* (*tt12*) mutant (carrying a mutation in a gene which encodes a membrane protein belonging to the MATE family), suggested that TT12 is involved in the vacuolar accumulation of proanthocyanidin (PA) precursors in the seed which are responsible for seed browning. Consistent with mutant analysis, it is demonstrated that the *TT12* promoter is only active in cells involved in proanthocyanidin biosynthesis. Using a GFP-TT12 fusion, we show that this transporter localizes to the tonoplast. Vesicles isolated from *Saccharomyces cerevisiae* heterologously expressing *TT12* ehibited transport activity for the anthocyanin cyanidin-3-*O*-glucoside, but not for the aglycones cyanidin and epicatechin, suggesting that sugar conjugation is an important factor in substrate recognition of TT12. Moreover, inhibitor studies demonstrated that TT12 is able to act, *in vitro,* as a cyanidin-3-*O*-glucoside/H^+-antiporter active in proanthocyanidin-accumulating cells of the seed coat.

Although the *in vivo* substrate of TT12 was not elucidated in this study, we postulate the natural substrate to be a glycosylated epicatechin derivative. We further suggest, from the available data, that homologs of TT12 are involved in the vacuolar deposition of related flavonoids such as anthocyanins into vacuoles in other cell types and/or vegetative plant parts. With the exception of *tt12*, reverse genetic analysis in various plants have not yet lead to the identification of flavonoid transporters possibly due to the redundancy of genes encoding flavonoid transporters. In order to address this possibility we propose a misexpression strategy to assign functionality of unknown genes in redundant families via complementation of a mutant phenotype, and important steps towards this goal have been performed. More specifically, the *tt12* mutant has been transformed with full-length cDNAs of related MATE transporters either under the control of (i) the constitutive CaMV 35S promoter or, (ii) a fragment of the *BANYULS* promoter driving specific expression in cells of the seed coat actively producing PAs, thereby corresponding to *TT12* expression and complementation of the transparent testa phenotype. At the same time, MATE transporters are localized as GFP fusions in transient assays. To this end, proof of concept is provided by complementing *tt12* with P_{BAN}:TT12 . Several transformations of 35S:MATE constructs into *tt12* have been performed with none found to complement the *tt12* PA-related seed phenotype. We have been able to successfully localize 13 MATE transporters. Interestingly, four highly homologous transporters differing from TT12 in only 12 amino acids, localized either to the tonoplast or the plasma membrane. This suggests that membrane

protein sorting of MATE transporters may rather require single amino acids positioned in a specific manner in the tertiary structure of the protein than 'sorting determinants' consisting of small signature sequences.

We further demonstrated that vacuolar flavonoid transport is strictly controlled by the biosynthetic pathway. Barley primary leaves naturally synthesize the flavonoid compound saponarin, and is had been previously demonstrated that saponarin is accumulated in vacuoles via a transport mechanism driven by the proton gradient. Interestingly, we showed that vacuoles isolated from the *ant310* line which carries a mutation in the chalcone isomerase (*CHI*) gene resulting in largely defective flavonoid biosynthesis exhibit a strongly reduced transport activity for saponarin and its precursor isovitexin (apigenin 6-*C*-glucoside). Naringenin treatment of *ant310* leaf segments or protoplasts resulted chemical complementation of naringenin biosyntesis and in a strong reactivation of the uptake activity of saponarin or isovitexin into isolated vacuoles. Our results demonstrate that flavonoid biosynthesis requires the presence of the vacuole and that intact flavonoid biosynthesis controls the activity of vacuolar flavonoid/H^+-antiporter in barley. Thus, the barley *ant310* mutant represents a novel model system to study posttranslational regulatory mechanisms that control the interplay of a metabolic pathway with the vacuolar storage mechanisms.

Different pieces of evidence support the hypothesis that flavonoids reach their destination in the cell via vesicle-mediated trafficking. A prominent example for this is the synthesis of 3-deoxyanthocyanidines (3-DA) in Sorghum leaves after fungal infection. Here we demonstrated that treatment of sorghum primary leaves with an non-specific elicitor led to a comparable response as that observed during fungal infection, however the metabolites synthesized were different. Xylanase-induced 3-DA biosynthesis was found to be inhibited by some but not all inhibitors known to affect vesicular sorting and time-resolved microscopy showed that a certain fraction of the characteristic red inclusions formed in response to fungal infections transited within the cell.

We propose that the identification of such transport steps in the phenylpropanoid pathway and their future genetic manipulation will lead to the development of strategies that derive transgenic crop plants synthesizing an engineered set of metabolites with beneficial properties for both livestock and humans.

Zusammenfassung

Im Gegensatz zur Biosynthese von Flavonoiden und der Regulation der Synthese, wurden Mechanismen, die an der Anreicherung phenolischer Substanzen in bestimmten Kompartimenten in der pflanzlichen Zelle - der Vakuole oder dem Apoplasten - beteiligt sind, nicht im Detail erforscht. Obwohl vakuoläre Transportmechanismen für verschieden konjugierte Flavonoide in den letzten Jahren untersucht wurden, fehlt eine molekulare Analyse. Die biochemische Analyse der vakuolären Transporteigenschaften verschiedener Flavonoide spricht für eine Beteiligung direkt energetisierter ABC-Typ Transporter oder H^+-Antiporter, die letztlich über den tonoplastidären Protonengradient, welcher von zwei Protonenpumpen, der V-Typ H^+-ATPase und H^+-Pyrophosphatase aufgebaut wird, angetrieben werden.

Hier wird gezeigt, dass ein Mitglied der Multidrug and Toxic Efflux (MATE) Transporterfamilie, eine erst kürzlich identifizierte Membranproteinfamilie, an der vakuolären Akkumulation phenolischer Substanzen beteiligt ist. Die vorhergehende phänotypische Charakterisierung der *transparent testa12* (*tt12*) Mutante in Arabidopsis als Mutante in einem Gen, das ein Mitglied der MATE-Familie kodiert, wies darauf hin, dass TT12 an der vakuolären Akkumulation von Proanthocyanidin (PA)-Vorstufen in Samen beteiligt ist. PAs sind für die braune Farbe der Samen verantwortlich. In Übereinstimmung mit dem mutanten Phänotyp, wird gezeigt, dass der *TT12*-Promoter nur in Zellen aktiv ist, die an der PA-Biosynthese beteiligt sind. Eine GFP-TT12 Fusion lokalisiert TT12 an den Tonoplasten. Vesikel, die aus Hefen gewonnen wurden, welche *TT12* heterolog exprimieren, transportieren das Anthocyan Cyanidin-3-*O*-glucosid, aber nicht die Aglykone Cyanidin und Epicatechin, was für eine Rolle der konjugierten Zucker bei der Substraterkennung spricht. Hinweise aus Inhibitorstudien weisen darauf hin, dass TT12 *in vitro* als Cyanidin-3-*O*-glucosid/H^+-antiporter agiert, der in PA-akkumulierenden Zellen der Samenschale aktiv ist.

Obwohl die *in vivo*-Substrate von TT12 nicht identifiziert sind - z.B. wäre ein glukosyliertes Epicatechin-Derivat möglich - kann in Anlehnung an unsere Daten spekuliert werden, dass Homologe von TT12 an der vakuolären Deposition strukturell verwandter Flavonoide, z.B. von Anthocyanen, in Vakuolen anderer Zelltypen oder im vegetativen Gewebe beteiligt sind. Ausser bei *tt12* führte die Analyse von Mutanten in verschiedenen Pflanzen bisher nicht zur Identifikation von Flavonoidtransportern, was in der Redundanz von Transportergenen begründet sein könnte. Um dieses Problem zu umgehen, schlagen wir eine Misexpressions-Strategie vor, welche die Zuweisung einer Funktion unbekannter Gene in redundanten Familien erlaubt, indem Komplementationsversuche in einem definierten mutanten Hintergrund durchgeführt werden. Erste Resultate werden dargestellt. Die *tt12* Mutante wird mit verwandten Voll-Länge cDNAs anderer MATE-Transporter entweder unter Kontrolle des starken, konstitutiven CMV 35S Promotor oder eines Fragmentes des *BANYULS* Promotors transformiert, der spezifische Expression in PA-produzierenden Zellen der Samenschale entspechend dem *TT12*-Expressiosmuster erlaubt, um nach Genen zu suchen, die den Samenphänotyp von *tt12* komplementieren und demnach ebenfalls Flavonoidtransporter sein könnten. Gleichzeitig wurden MATE-Transporter als GFP-Fusionen in transienten Experimenten lokalisiert. Die generelle Richtigkeit der experimentellen Strategie wird nachgewiesen. Obwohl einige Transformationen von *tt12* mit 35S:MATE-Konstrukten durchgeführt wurden, komplementiert bisher

keines dieser Gene die typische Abwesenheit von PAs in *tt12*-Samen. Stattdessen wurden 13 MATE-Transporter lokalisiert. Interessanterweise wurden vier sehr verwandte Transporter, die sich nur in 12 Aminosäuren unterscheiden, entweder auf dem Tonoplasten oder der Plasmamembran vorgefunden. Dies weist darauf hin, dass die Addressierung von MATE-Transportern an verschiedene Membranen eher von einzelnen Aminosäuren abhängt, die in einer dreidimensionalen Struktur in bestimmter Weise positioniert werden, als von kurzen ‚Verteildeterminanten', die aus kurzen Signatursequenzen bestehen.

Eine weitere Studie zeigt, dass der vakuoläre Flavonoidtransport durch den biosynthetischen Stoffwechsel strikt kontrolliert wird. Gerste-Primärblätter synthetisieren Saponarin. Es wurde bereits gezeigt, dass Saponarin protonen-getrieben in Vakuolen akkumuliert. Interessanterweise ist die Aufnahme von Saponarin und der Vorstufe Isovitexin (Apigenin-6-*C*-glucosid) in Vakuolen der *ant310* Linie, welche aufgrund einer Mutation in der Chalkon-Isomerase (*CHI*) weitgehend flavonoid-frei ist, stark reduziert. Naringenin-Behandlung von *ant310* Blattsegmenten führte zur chemischen Komplementation der Saponarinsynthese und zu einer starke Reaktivierung der vakuolären Aufnahme von Saponarin und Isovitexin. Diese Resultate zeigen, dass die Flavonoidbiosynthese die Gegenwart der Vakuole benötigt und dass die aktive Flavonoidbiosynthese die Aktivität des Flavonoid/H^+-Antiporters in der Gerste kontrolliert. Die *ant310* Mutante ist demnach ein neues Modellsystem, um posttranslationale Regulationsmechanismen, welche das Zusammenspiels zwischen metabolischen Synthesewegen und dem vakuolären Speichermechanismus kontrollieren, zu studieren.

Verschiedene Hinweise sprechen dafür, dass Flavonoide ihre Zielkompartimente in der Zelle vesikelvermittelt erreichen können. Ein bekanntes Beispiel ist die pilzinduzierte Synthese von 3-Deoxyanthocyanidinen (3-DA) in Sorghumblättern. Wir zeigen, dass auch die Behandlung der Primärblätter von Sorghum mit einem unspezifischen Elicitor zu einer vergleichbaren Antworten führt, obwohl die synthetisierten Metabolite unterschiedlich sind. Die xylanase-induzierte 3-DA-Biosynthese konnte durch einige, aber nicht alle Inhibitoren, die den Vesikelfluss in Zellen betreffen, reduziert werden. Mittels zeitauflösender Mikroskopie wurde nachgewiesen, dass sich die typischen roten Einlagerungen in der Zelle bewegen.

Die Identifizierung von Transportschritten des Phenylpropanstoffwechsels und deren Manipulation wird die Entwicklung von Pflanzen mit einem gezielt manipulierten Muster an Metaboliten mit nützlichen Eigenschaften für Tiere und Menschen in definierten Kompartimenten erlauben.

Acknowledgement

*Herewith I would like to express my gratitude to my **family** – they always support me in my life changing decisions, to my friends at home and especially to **Daniela Konaktchieva** - her mails kept me optimist that I can show the best of me during this challenge.*

*I would like to address special words of admiration and respect to my supervisor **Dr. Markus Klein** who believed in me and offer me the opportunity to learn and develop myself in the field of science, which was my desire after my study in the University.*

*Thanks to **Prof. Enrico Martinoia** for the opportunity to work within his broad and experience team and to the **members of the lab** for the help and support during my work.*

*Wish to pay respect to **Prof. Felix Keller** and **Dr. Markus Geisler** for the opportunity to experience and learn about science and live from different perspectives.*

*Special thanks to my best friends **Nicola Tomasi** – you are with me not only when I need you and **Shaun Peters** – you showed me sites of life I wanted to see and your way of thinking enriched my personality.*

*Thanks to my friends and lab mates **Barbara Weder** and **Hanne Grob** for the help and the ambience they created during this time, which made the stay and work here easy and joy. I'm glad also that I had the opportunity to meet and work with **Annie Frelet**, **Tina Ballmann** and **Katharina Schmid**. I will not forget my friends **Vincent Vincenzetti**, **Christine Cretton** and **Michal Jasinski** - they were first to listen and share my concerns.*

*I also like to thanks to my teacher **Dr. Veneta Kapchina** – without you I would never had this experience.*

This work was financially supported by the Forschungskredit of the University of Zurich, (MK) and the Roche Research Foundation, Basel, CH (KM).

Table of contents

Chapter I : Introduction **1**

1. Secondary metabolites
2. Mechanism of membrane transport for secondary metabolites
3. The function of vacuole in secondary metabolism
4. Vesicle transport
5. Aims of this study
6. Reference list

Chapter II : The Arabidopsis MATE transporter TT12 acts as a vacuolar flavonoid/H^+-antiporter active in proanthocyanidin-accumulating cells of the seed coat, **35**
Marinova et al., 2007, The Plant cell, 19(6):2023-38

Chapter III : Analysis of the subcellular localization of Arabidopsis MATE transporters and complementation of the *tt12* seed phenotype by related transporters **48**

1. Introduction
2. Materials and methods
3. Results
4. Discussion
5. Reference list

Chapter IV : Influence of the mutations in the flavonoid biosynthesis on vacuolar biogenesis (work in progress in collaboration with Christina Ballmann) **70**

Chapter V : Flavonoid biosynthesis in Barley primary leaves requires the presence of the vacuole and controls the activity of vacuolar flavonoid transport, **77**
Marinova et al.,2007, Plant Physiology, vol. 144, pp. 432-444

Chapter VI : Sorghum bicolor as a model system to study induced synthesis and compartmentation of flavonoids in inclusions **84**

1. Introduction
2. Material and methods
3. Results and discussion
4. Reference list

Chapter VII : Concluding remarks **111**

Chapter VIII : Collaborations **118**

1. **Comparative mutant analysis of Arabidopsis ABCC-type ABC transporter: AtMRP2 Contribute to Detoxification, Vacuolar Organic Anion Transport and Chlorophyll Degradation**

Chapter IX : Addendum – CD-ROM **120**

1. **Time-lapse movies for Chapter VI.**
2. **Chapter IV**

Chapter 1

1. Secondary metabolites

The plant kingdom is characterized by unique metabolic systems that convert the products of primary metabolism into numerous so-called secondary products. They are classified into three major groups - alkaloids, terpenoids, and phenylpropanoids according to their biosynthetic pathways and chemical and structural properties. Many of these products play similar roles in all plant species, for example, as plant growth substances or pigments. Others appear to have been recruited or modified during the plant evolution to serve specific functions, for example, in defense or symbiosis. To achieve their function, such as protection against UV light or pathogens, they are generally accumulated in specific tissues or cell types in which subcellular localization is highly regulated (Yazaki, 2004). Secondary metabolites are often transported from their point of synthesis to neighboring cells, or even further to other tissues or remote organs. Current progress in molecular biology has enabled us to study the transporter proteins of these secondary metabolites, in plants from the site of synthesis in the cytoplasm to final destinations in the vacuole or cell wall.

More than 8,000 different flavonoids have been identified in vascular plants (Pietta, 2000). They are grouped into major flavonoid classes which include flavonols, flavones, flavanones, catechins, anthocyanidins, isoflavones, dihydroflavonols, and chalcones, based on the modifications to the basic flavonoid scaffold (methylations, acetylations, and glycosylations). Flavonoids are involved in many aspects of plant growth and development, such as pathogen resistance, pigmentation pattern of vegetative parts and seeds, UV screens, pollen growth, and seed coat development (Harborne, 1986). They are potent antioxidants, free radical scavengers, and metal chelators and inhibit lipid peroxidation. Anthocyanin pigments and terpenoids have key roles in attraction of flower pollinators. In plants, flavonoid derivatives serve as signal molecules in plant–microbe interactions, and participate in plant defense responses (reviewed in Dixon and Paiva, 1995; Shirley, 1996). Recent studies have also stressed the involvement of flavonoids in seed coat–imposed dormancy as well as in seed storability (Shirley, 1998; Debeaujon *et al.*, 2000), as well as phytoalexins and regulators of auxin transport (for review see Harborne and Williams, 2000).

Flavonoids are receiving increasing interest as health-promoting components of animal and human diets (Lairon and Amiot, 1999). These diverse roles can be correlated with the antioxidant properties of phenylpropanoid derivatives (Rice-Evans *et al.*, 1997), and with their inhibitory effect on enzymatic activities (Castelluccio *et al.*, 1995). There is increasing evidence suggesting that flavonols (such as kaempferol and quercetin), are potentially health-protecting components in the human diet as a result of their high antioxidant capacity (Dugas *et al.*, 2000; Duthie and Crozier, 2000; Ng *et al.*, 2000). Based on these findings, it was postulated that flavonoids may offer protection against major diseases such as coronary heart diseases and

cancer (Steinmetz and Potter, 1996; Trevisanato and Kim, 2000). Phytochemicals in this class are frequently referred as 'bioflavonoids' due to their multifaceted roles in human health maintenance.

In addition, several epidemiological studies have suggested a direct relationship between cardioprotection and consumption of flavonols from dietary sources such as onion, apple, and tea (Hertog *et al.*, 1993; Keli *et al.*, 1996). Isoflavonoids have been linked to the anticancer benefits of soy-based foods, and the stilbenes in red wine are believed to contribute to reduced risk of heart disease. Based on this there is growing interest in the development of food crops enriched with health-protective flavonoids.

In recent years, much effort has been directed at elucidating the flavonoid biosynthetic pathway and investigation into the structure and regulation of the flavonoid pathway in plants may help us to better understand and monitor flavonoid metabolism with regard to properties of the end products (Weisshaar and Jenkins, 1998). In addition to biochemical approaches, classical genetics approach using loss-of-function mutations led to the elucidation of genes involved in flavonoid biosynthesis and to screen for associated phenotypes (Lepiniec *et al*., 2006).

The molecular analysis of the membrane transport of plant secondary metabolites is a fairly new field in plant biology. The dispersed localizations of both the end-products and their biosynthetic enzymes indicate that biosynthetic intermediates might move among organelles during the biosynthesis of secondary metabolites (Sanchez-Fernandez *et al.*, 2001; De Luca and St. Pierre, 2000; Zhao *et al.*, 2003). Metabolic engineering has become a popular way of increasing the production of secondary metabolites by overexpressing biosynthetic enzymes (Yazaki, 2004). The introduction of accumulation mechanisms by engineering transport systems should be an effective way to increase the production of secondary metabolites.

Since the functions in which the flavonoids are involved are mostly dose-dependent, secondary compounds have to accumulate constitutively or inducibly and often in a tissue- or cell-specific manner to minimal concentrations starting in the millimolar range. At the same time, unconjugated phenolic compounds are toxic to the cell due to their high chemical reactivity and protein denaturing properties (Matile, 1984). The major strategy of the plant to protect the cytosolic machinery against these toxic effects is the targeting of secondary metabolites to compartments with lower biosynthetic activity, notably the extracellular space (Onyilagha, 2004) and the large central vacuole (Martinoia, 2000).

1.1. Alkaloids

Alkaloids, which are nitrogen-containing substances, are a major class of plant secondary metabolites that show a wide variety of chemical structures and biological activities. Some are used in medicine as anticancer drugs and morphine is an indispensable analgesic in clinical

medicine. They also play important roles in plants as endogenous biological barriers to protect against pathogens or herbivores due to their strong antimicrobial, antifungal (Iwasa *et al.*, 1998; Mahady *et al.*, 2003), and anti-insecticidal activities (Steppuhn *et al.*, 2004). Many systems for the production of alkaloids have been established (Kutchan, 1995) and biosynthetic pathways have been actively studied (Facchini, 2001). However, the transport and accumulation mechanisms of these alkaloids in plant cells are still unknown. Interestingly, alkaloid-producing plant cells seem to have a detoxification mechanism to prevent the cytotoxicity of alkaloids. One possible explanation for such plant detoxification is the compartmentation of alkaloids into the plant vacuole. Many alkaloids are presumed to be synthesized in the cytosol and on the endoplasmic reticulum (ER) and then transported through the tonoplast to be sequestrated in the vacuolar matrix (Hashimoto and Yamada, 2003).

Plant alkaloids are often translocated from the source to a sink organ (Hartmann, 1999). Berberine in *C. japonica* is also translocated from root tissues to rhizomes, which involves transport across several membranes, i.e. at the plasma membrane in the root and rhizome and at the tonoplast in cortex cells of rhizome. It is unclear why *C. japonica* cells have two different types of transporters for berberine; i.e. an ABC transporter (CjMDR1) at the plasma membrane (Shitan *et al.*, 2003) and H^+/berberine antiporter at the tonoplast. In bacteria, several antiporters that accept berberine as their substrate have been reported (although Na^+ is the counterpart instead of H^+) and their roles as drug efflux pumps for the purpose of detoxification have been demonstrated. For example, NorM from *Vibrio parahaemolyticus* and its homolog in *Escherichia coli*, YdhE, which are both multidrug and toxic compound extrusion (MATE)-type transporters, efflux several toxic compounds, including berberine, and confer multidrug resistance to these microorganisms (Xu *et al.*, 2003). In plants, a plasma membrane-localized MATE transporter of *Arabidopsis thaliana*, AtDTX1, which also recognizes berberine as an exogenous substrate (Li *et al.*, 2002), has been reported so far as an H^+-antiporter that acts as a detoxifier.

1.2. Terpenoids

Over 25 000 terpenoids have been isolated and their structure characterized (Croteau *et al*., 2000). The terpenoids are (bio)synthesized by condensation of monomeric C5 unit, dymethylallyl diphosphate and isopentenyl diphosphate, and they are classified according to the degree of condensation as hemi-, mono-, sesqui-, di-, sester-, tri-, tetra-, and polyterpenoids. The membrane transport is still largely unknown, except for diterpene compound illustrated below. A unique plasma-membrane-localized ABC transporter (pleiotropic drug resistance (PDR) protein) for the transport of diterpenes was first identified in the leaves of *Nicotiana plumbaginifolia* (NpABC1) (Jasinski *et al.*, 2001). This study suggests that plant plasma membrane transporters might be implicated in the secretion of endogenous metabolites (sclareol) that play a role in

defense against biotic stress. PDR orthologs of NpABC1 have also been found in *Arabidopsis* (Campbell *et al.*, 2003) and *Spirodela polyrrhiza* (van der Brule *et al.*, 2002) and these proteins were strongly induced by elicitor treatment, suggesting that they are directly involved in the pathogen resistance processes by transporting diterpene metabolites.

1.3. Flavonoids

All flavonoids derive their C15 skeletons from two basic metabolites, malonyl-CoA and p-coumaroyl-CoA. The crucial biosynthetic reaction is the condensation of three molecules malonyl-CoA with one molecule p-coumaroyl-CoA to a chalcone intermediate. Based on their core structure and its modification, the flavonoids can be grouped into different classes, such as the chalcones, flavones (luteolin, apigenin), flavonols (quercetin, kaempferol), flavanones (myricetin, naringin, hesperetin, naringenin), flavan-3-ols (catechin, epicatechin, gallocatechin), anthocyanins (cyanidin, pelargonidin, petunidin), and condensed tannins (or proanthocyanidins).

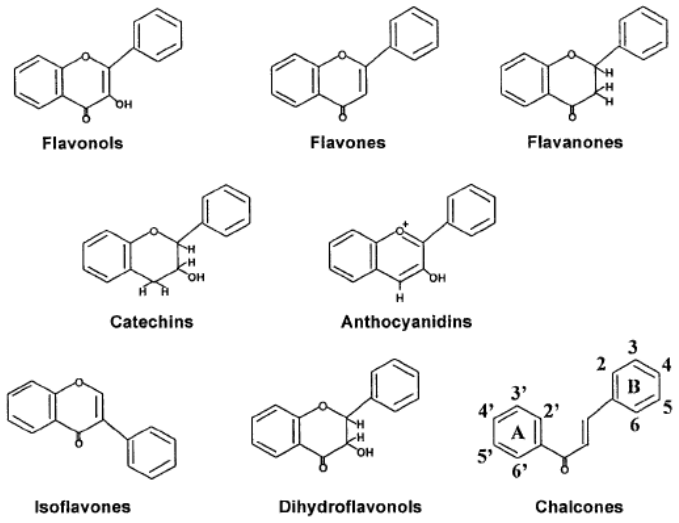

Figure 1. The chemical structures of the major classes of flavonoids (taken from Cook and Samman, 1996)

Some plant species also synthesize specialized forms of flavonoids, such as the isoflavonoids (genestein, daidzein) that are found in legumes and a small number of nonleguminous plants. Similarly, sorghum (*Sorghum bicolor*), maize (*Zea mays*), and gloxinia (*Sinningia cardinalis*) are among the few species known to synthesize 3-deoxyanthocyanins (or phlobaphenes in the polymerized form). The stilbenes, which are closely related to flavonoids, are synthesized in grape (*Vitis vinifera*), peanut (*Arachis hypogaea*), and pine (*Pinus sylvestris*).

These compounds are found in all vascular plants as well as in some mosses (Harborne and Baxter, 1999; Williams and Grayer, 2004). It is already well established that flavonoids play a significant role in various aspects of plant biology. They exhibit a wide range of functions in physiology, biochemistry, and ecology, for example in UV-protection, flower coloration, pollination, seed dispersal, allelochemical interactions, and plant defense. The flavonoid pattern is also a useful tool in chemotaxonomic studies. Other properties of certain flavonoids are their nutritional value and medicinal benefits to humans, represented by antioxidant or putative anticancer activities *inter alia*.

Arabidopsis contains three major classes of flavonoids: the anthocyanins (red to purple pigments), the flavonols (colorless to pale yellow pigments), and the proanthocyanidins (PAs, colorless pigments that turn to brown), which also are known as condensed tannins (Winkel-Shirley, 2001).

1.4. Anthocyanins and PAs

Anthocyanins are the main pigments in flowers and fruits, acting as insect and animal attractants (Bohm, 1998; Harborne and Williams, 2000). Anthocyanin biosynthesis has been extensively studied in several plant species. Two classes of genes are required for anthocyanin biosynthesis, the structural genes encoding the enzymes that directly participate in the formation of anthocyanins and other flavonoids, and the regulatory genes that control the transcription of structural genes. Transcriptional control plays an important role in regulation of the activity of flavonoid biosynthesis. The pathway is also controlled in response to different developmental and environmental signals (Mol *et al.*, 1998; Weisshaar and Jenkins, 1998; Winkel-Shirley, 2001). There is also evidence that the enzymes involved in flavonoid metabolism might be acting as membrane-associated multienzyme complexes, which are important for the efficiency, specificity, and regulation of the pathway (Stafford, 1991; Winkel-Shirley, 1999, 2001). Anthocyanin production is limited in most plants to certain tissues, and it occurs during specific stages of development.

Proanthocyanidins (PAs) are flavonoid polymers that result from the condensation of flavan-3-ol units (Xie *et al.*, 2003). In *Arabidopsis*, they are found only in the seed coat (or testa), where they confer a brown color to mature seeds after oxidation (Devic *et al.*, 1999; Debeaujon *et al.*, 2001). Tannin deposition in the testa participates in seed defense against predators and pathogens (Shirley, 1998) and in rising seed coat–imposed dormancy and longevity (Debeaujon *et al.*, 2000).

1.5. Biosynthetic pathways

Flavonoid biosynthesis has been studied extensively by several methods, from protein purification to screening libraries with heterologous probes (reviewed in Holton and Cornish, 1995). The ubiquitous nature of pigments has made it possible to identify many flavonoid mutants, which has facilitated the genetic and molecular dissection of the pathway. Mutants have been isolated in a variety of plant species based on alterations in flower and seed pigmentation. Maize, snapdragon (*Antirrhinum majus*), and petunia were established as experimental models, and work in these species led to the isolation of many flavonoid structural and regulatory genes (Holton and Cornish, 1995; Mol *et al.*, 1998; Lepiniec *et al*., 2006). More recently *Arabidopsis* has been used as a model for the analysis of the regulation and subcellular organization of the flavonoid pathway (Shirley *et al.*, 1995). Genetic loci for both structural and regulatory genes occur randomly across the *Arabidopsis* genome and have been identified on the basis of mutations that abolish or reduce pigmentation in the seed coat. Transposon and activator tagging have been used to isolate additional mutations in genes either directly or indirectly involved in flavonoid biosynthesis (Kubo *et al.*, 1999; Borevitz *et al.*, 2000).

The accumulation of flavonoids within plants or seeds is subject to fine temporal and spatial control involving several levels of regulation (e.g., transcriptional or post-translational regulation) and diverse developmental stimuli or environmental factors (Burbulis and Winkel-Shirley, 1999; Pelletier *et al.*, 1999).

The flavonoids on the plant surface form a barrier, and possibly a contact, between the cell and its environment (Zobel *et al.*, 1994a; Zobel and Brown, 1995). The defensive role of phenolic compounds relates to an increase in their concentration under stressed environmental conditions, such as air pollution (Zobel and Nighswander, 1990; Zobel *et al.*, 1990), UV radiation (Zobel and Brown, 1993; Zobel *et al*., 199b), infection (Zobel *et al.*, 1994) or mechanical damage (Hyodo and Yang, 1971).

1.5.1. *Transparent testa* mutants

Numerous flavonoid mutants have been isolated in *Arabidopsis* on the basis of altered seed color, because null mutations in *TT* genes result in reduced, abolished, or modified pigmentation of the seed coat (Shirley *et al.*, 1995; Abrahams *et al.*, 2002; Koornneef, 1990). Seed coat mutants affected in flavonoid pigmentation are represented by the *transparent testa* (*tt, tt1 to tt19*) and *transparent testa glabra* (*ttg, ttg1 and ttg2)*, *tannin deficient seeds* (*tds*) and *banyuls* (*ban*) mutants (Shikazono *et al.*, 2003; Winkel-Shirley, 2002). The seed color of *tt* and *ttg* mutants ranges from yellow (*tt1– tt5*; *tt8*; and *ttg1*) to pale brown (*tt6*, *tt7*, and *tt10*) or grayish brown (*tt9*). The *ttg1* mutant also lacks testa mucilage and trichomes and is characterized by an

aberrant root hair outgrowth due to disturbed epidermal layer structures (Koornneef, 1981, Masucci and Schiefelbein, 1996). The corresponding mutant of *banyuls* (*ban*) accumulates pink flavonoid pigments in the endothelium of immature seeds (Albert *et al.*, 1997; Devic *et al.*, 1999).

The second seed coat mutants group is represented by mutants affected in testa structure. In *aberrant testa shape* (*ats*) mutants two cell layers in the integuments are absent and as a result heart-shaped mature seeds are produced (Leon-Kloosterziel *et al.*, 1994). The *glabra2* (*gl2*) mutant has brown seeds but similar defects in mucilage production, testa surface structure, and root hair formation comparable to the *ttg1* mutant (Rerie *et al.*, 1994; Masucci and Schiefelbein, 1996). Therefore, *ttg1* combines defects of both testa mutant groups. The *tds* mutants might be defective in epimerization, transport, or condensation of PA monomers, due to a lack of enzymes that normally act to produce PA (Abrahams *et al.*, 2003).

To date, 22 *TT* loci have been identified, and several of the corresponding genes have been cloned. The mutations in *tt3*, *tt4*, *tt5*, *tt6*, *tt7*, *tt12*, *banyuls* (*ban*), and *aha10* affect the following structural genes: dihydroflavonol 4-reductase (DFR, Shirley *et al.*, 1992), chalcone synthase (CHS, Shirley *et al.*, 1995, Feinbaum and Ausubel, 1988), chalcone isomerase (CHI, Shirley *et al.*, 1992), flavanone 3-hydroxylase (F3H, Pelletier and Shirley, 1996; Wisman *et al.*, 1998), flavonoid 3'H-hydroxylase (F3'H, Koornneef *et al.*, 1982; Schoenbohm *et al.*, 2000), a multidrug secondary transporter–like protein (TT12, Debeaujon *et al.*, 2001), a putative leucoanthocyanidin reductase (LDOX, Devic *et al.*, 1999), and P-type H^+-ATPase (AHA10, Baxter *et al.*, 2005) respectively.

The effects of the *tt9*, *tt10*, *tt13*, and *tt15* mutations are restricted to seed pigmentation (Shirley *et al.*, 1995; Focks *et al.*, 1999; Debeaujon *et al.*, 2000), whereas *tt11* and *tt14* mutations also affect anthocyanin accumulation in vegetative parts (Debeaujon *et al.*, 2000). The *tt10* mutant exhibits a delay in developmentally determined browning of the seed coat (Pourcel *et al.*, 2005). TT10 is involved in the oxidative polymerization of flavonoids and functions as a laccase-type flavonoid oxidase.

It is known that pigmentation patterns are established by the cell-specific accumulation of different flavonoids. The activation of the flavonoid biosynthetic genes is regulated largely at the transcriptional level (reviewed by Weisshaar and Jenkins, 1998; Lepienec *et al.*, 2006). As a consequence, regulatory genes that activate these structural genes are major determinants of pigmentation pattern. Such regulatory genes have been identified in several plant species (Mol *et al.*, 1998; Winkel-Shirley, 2002; Weisshaar and Jenkins, 1998). A conserved model for the tissue-specific regulation of flavonoid biosynthesis in monocots and dicots involves MYB and bHLH-related proteins (Mol *et al.*, 1998). To date in *Arabidopsis*, seven proteins required for the regulation of PA biosynthesis have been described. The transcriptional regulation of the first enzyme in the flavonoid-specific part of phenylpropanoid biosynthesis, chalcone synthase, has been investigated in detail in *Arabidopsis*. MYB12 was found to be a flavonol-specific activator of

flavonoid biosynthesis in developing seedlings with the two flavonoid biosynthesis genes CHS and FLS (flavonol synthase) as its primary targets.

The regulatory genes that modulate late flavonoid biosynthetic genes *TT1*, *TT2*, *TT8*, *TT16*, *TTG1*, and *TTG2* loci have been shown to encode regulatory proteins with similarities to zinc finger motif–containing proteins (Sagasser *et al.*, 2002).

Among these genes, *TT1*, *TT2*, *TT12*, and *BAN* are expressed specifically in seeds. *TT2*, *TT8* and *TTG1* encode R2–R3 MYB, MYC/bHLH and WD40 repeat domain proteins, respectively (Nesi *et al.*, 2000, 2001, Walker *et al.*, 1999). TT2 is a master regulator as its mutation affects the expression of *DFR*, *LDOX* and *BAN* in developing siliques while its ectopic expression can induce *BAN* and *TT8* (the latter in roots only) and upregulate *DFR* and *LDOX* (Nesi *et al.*, 2000, 2001, Debeaujon *et al.*, 2003). In *Arabidopsis*, TT2 and TT8 act in concert with TTG1 to regulate *BAN* expression in the endothelium (Nesi *et al.*, 2000, 2001), and TT2 is a major determinant for *BAN* accumulation during seed development (Nesi *et al.*, 2001). TT8 also modulates the expression of other flavonoid late structural gene named *DFR* supporting a major role of the TT8 protein in the flavonoid regulatory network (Nesi *et al.*, 2000). TT1, TT16 and TTG2, regulates organ and cell development for proanthocyanidin deposition, in addition to transcription of proanthocyanidin-specific genes. TT1 and TT16 were shown to be necessary for PA biosynthesis and normal cell morphology in the seed body but not in the underlying chalaza/micropyle region. TT1 is a new zinc finger protein that defines the WIP subfamily of zinc finger transcription factors (Sagasser *et al.*, 2002). *TT16* encodes the *ARABIDOPSIS* BSISTER MADS domain (ABS) transcription factor protein (TT16/ABS) (Nesi *et al.*, 2002). TTG1, a WD domain protein, is known to interact with MYB (PAP1 and PAP2) and MYC (GL3 and EGL3) transcription factors in the yeast two-hybrid system (Payne *et al.*, 2000, Zhang *et al.*, 2003). Finally, TTG2 is zinc a finger–like transcription factor of the plant-specific WRKY gene family which modulates trichome differentiation, mucilage production and proanthocyanidin biosynthesis (Johnson *et al.*, 2002). TTG2 requires TTG1 function for regulating proanthocyanidin biosynthesis in the whole seed coat, like TT2, TT8, and TTG1. TT2, TT8, and TTG1 synergistically specify the expression of *BANYULS* and proanthocyanidin biosynthesis in *Arabidopsis thaliana* (Baudry *et al*., 2004).

This scheme closely resembles the situation in maize, in which R- and C1-like genes encode members of the bHLH and MYB transcription factor families (Cone *et al.*, 1986, Paz-Ares *et al.*, 1987, Ludwig *et al.*, 1989), and also the situation in petunia with ANTHOCYANIN2 (AN2), AN1, and AN11, which encode proteins of the MYB, bHLH, and WD repeat families, respectively (deVetten *et al.*, 1997; Quattrocchio *et al.*, 1999).

In addition, a MYB regulator of phenylpropanoid metabolism, *PAP1*, has been cloned in *Arabidopsis*, which, when overexpressed, results in intensely purple plants (Borevitz *et al.*, 2000). These observations may provide new insights into *Arabidopsis* genes that function beyond the branch to condensed tannins, a limitation of cloning genes based on the *tt* phenotype.

Genetic analysis of proanthocyanidin accumulation in the *Arabidopsis* seed coat has resulted in the identification of two genes that appear to be involved in transport processes required for PA synthesis and/or assembly. Mutations in either the *TT12* or *TT19* genes result in a transparent testa caused by reductions in the level of proanthocyanidin pigment (Debeaujon *et al.*, 2001, Kitamura *et al.*, 2004). *TT12* encodes a protein with 12 transmembrane domains exhibiting similarity to prokaryotic and eukaryotic MATE (multidrug and toxic compound extrusion) transporters, and is expressed specifically in the endothelial layer of the developing seed coat (Debeaujon *et al.*, 2001, chapter 2). *TT19* is a member of the *Arabidopsis* glutathione S-transferase (GST) multigene family (Kitamura *et al.*, 2004). TT12 and TT19 participate in the uptake of PA precursors. In contrast to the diffuse cytoplasmic distribution of PA precursors in TT12 mutants (Debeaujon *et al.* 2001), PA precursors are membrane wrapped in TT19 mutant endothelium cells (Kitamura *et al.* 2004). The functional relationship between TT12 and TT19 is unclear, and TT19 has yet to be characterized biochemically.

Analogies can be drawn between the vacuolar transport of anthocyanins in maize and the *BRONZE-2* gene, a GST homolog (Marrs *et al.*, 1995). The petunia *AN9* gene, encoding a GST involved in anthocyanin transport, can complement the *Arabidopsis tt19* mutation with respect to vacuolar accumulation of anthocyanins, but does not restore proanthocyanidin accumulation (Kitamura *et al.*, 2004).

2. Mechanism of membrane transport for secondary metabolites

The membrane transport of plant secondary metabolites is a newly developing research area. The model suggests that flavonoids are synthesized in a complex of metabolic enzymes located in the endoplasmic reticulum (Winkel-Shirley, 1999). Flavonoid-derived compounds are then transported to different locations: in many cases, flavonoids accumulate in vacuolar compartments; other flavonoids, for example polymethylated flavonoids are secreted to the appoplast or accumulate in the cell wall. Recent progress in genome and expressed sequence tag (EST) databases has revealed that many transporters and channels exist in plant genomes. Studies of the genetic sequences that encode these proteins, and of phenotypes caused by the mutation of these sequences, have been used in a few cases to characterize the membrane transport of plant secondary metabolites. They have clarified that membrane transport is fairly specific and highly regulated for each secondary metabolite. Not only are genes involved in the biosynthesis of secondary metabolites important but also those that are involved in their transport in order to successfully engineer plants for increased production of secondary metabolites.

In spite of the investigation of the flavonoid biosynthetic pathway, the mechanism(s) by which phenolic compounds reach their intracellular destinations (the vacuole or the apoplastic

space) have not been investigated in detail. The rare biochemical studies analyzing vacuolar flavonoid uptake mechanisms have led to the postulation of different transport and accumulation mechanisms. In plants, four major uptake mechanisms have been proposed for secondary metabolite transportation across the tonoplast, i.e. H^+-antiporters, ion trap (Matile, 1976), conformational trap (Rataboul *et al*., 1985), and directly energized transport by ABC transporters (Klein *et al*., 2000; Martinoia *et al*., 2000). The first three use the electrochemical gradient of H^+ across the tonoplast, whereas ABC transporters directly use the energy of Mg/ATP hydrolysis to pump their substrates into the vacuolar lumen, i.e. independent of electrochemical force.

Biochemical data presented in this work suggest that the members involved in the transport as H^+-antiporters are the multidrug secondary transporter–like proteins belonging to the MATE family. Despite their importance in compartmentation and although transport steps represent bottlenecks in flavonoid biosynthesis, proteins involved in vacuolar transport of flavonoids are largely unknown (Grotewold, 2004; Yazaki, 2005). The biochemical characterization of flavonoid transport into the vacuole argues for the existence of different transport mechanisms. Our results suggest that different transporters exist and they are divided in two major groups - H^+-antiporters vs. ABC transporters and are under investigation in the following chapters.

2.1. Vacuolar transporter of abiotic and biotic substances

In plants, secondary products such as species-specific phenolics as well as foreign compounds are often glycosylated in order to increase their water solubility. Storage of these compounds within the large central vacuole is generally assumed to protect the plant cell against potentially toxic effects of these substances, especially of their non-glucosylic form. The vacuole has the potential to detoxify and store not only endogenous but also foreign, biotic, and abiotic glucosylated substances.

Observation of directly ATP-dependent glutathione conjugate uptake into plant vacuoles (Martinoia *et al.*, 1993) triggered the identification of vacuolar ABC transporters in plants. The accumulation of secondary metabolites in vacuoles has at least two positive roles: the sequestration of biologically active endogenous metabolites inside the cells and the protection of such metabolites from catabolism (Gunawardena *et al.*, 2004).

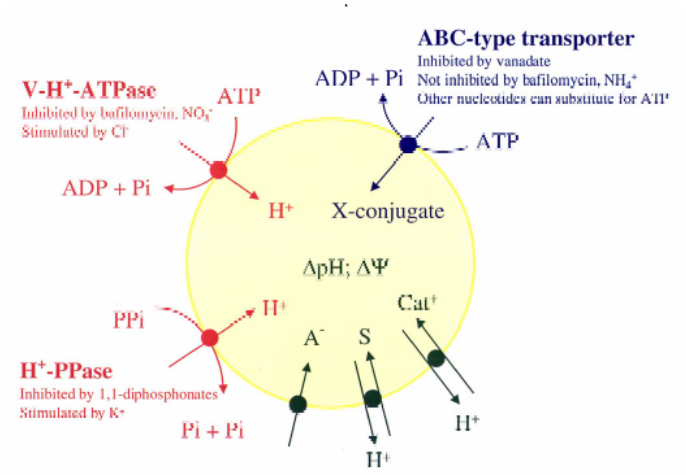

Figure 3. Vacuolar transport mechanisms of solutes: red: proton pumps, green: secondary energized uptake mechanisms, blue: directly energized ABC-type transporters. (Martinoia *et al.,* 2000).

Klein *et al.* (1996) suggested that at least two different carriers are responsible for the transport of glucosylated substances across the vacuolar membrane. In barley primary leaves different types of flavone glucosides are synthesised and finally stored in the vacuole of the mesophyll and epidermal cells. The major barley flavone, saponarin (apigenin 6-C-glucosyl-7-O-glucoside) is generated from isovitexin (apigenin 6-C-glucoside) by a terminal cytosolic glucosylation step. Uptake of isovitexin was found to be ATP-dependent and was strongly inhibited after dissipation of the ΔpH across the tonoplast. These and further results suggested that different uptake mechanisms exist in the vacuolar membrane, a ΔpH-dependent uptake mechanism for specific endogenous flavonoid-glucosides, and a directly energized, ABC-type mechanism for abiotic glucosides, which appears to be the main transport system for these substrates. In view of our recent results that MATE transporters such as TT12 are able to catalyze flavonoid/H^+-antiport it is tempting to speculate that these transporters represent the isovitexin/H^+-antiporter in barley.

Consequently, it was demonstrated that transport mechanisms for the major barley flavonoid saponarin are different in various plant species. Saponarin uptake into barley vacuoles occurred via H^+-antiport. In contrast, the transport into vacuoles from Arabidopsis, which did not synthesize flavone glucosides, displayed typical characteristics of directly energized ABC transporters. These studies concluded that different vacuolar transporters evolved for the sequestration of species-specific/endogenous and non-specific glucosylated flavonoids *in planta* (Frangne, 2002).

In contrast to glucosylated flavonoids, vacuolar uptake studies with negatively charged, glucuronidated flavonoids displayed characteristics of an ABC-type transport

mechanism. In the rye primary leaf mesophyll, two flavone glucuronides are synthesized with cell-type and developmental specificity. Both flavones were taken up into vacuoles isolated from rye via a directly energized mechanism (Klein *et al*., 2000). Apart from distinct mechanistic properties, a remarkable difference between the barley vacuolar flavone glucoside/H^+-antiporter and the MRP-type flavone glucuronide transporter was found for the species-specificity of the transport system: While the barley flavone glucoside/H^+ transport system was found to be specific for barley, the glucuronide transporter is ubiquitously present and is not species-specific (Klein *et al*., 2001; Klein *et al*., 1998).

2.1.1 MRP-type ABC transporters

Both toxins and secondary metabolites are removed from the plant cell cytoplasm and stored in the vacuole (Wink, 1997). In the case of ABC-type vacuolar sequestration, toxins or metabolites are conjugated to glutathione or other negatively charged molecules such as sulfate or glucoronide, and are then transported to the vacuole via direct energized transport (Martinoia, 1999). The MRPs (multidrug resistance-related proteins) or GS-X pumps are considered to be involved in the intracellular sequestration of toxins (reviewed by Coleman *et al.*, 1997; Rea *et al.*, 1998, 1999; Theodoulou, 2000). *Arabidopsis* AtMRPs, which are capable of vacuolar concentration of glutathione-conjugated compounds, were identified on the basis of homology with the ATPase-driven efflux pumps responsible for glutathione conjugate transport in mammalian cells (*MRP1*) and yeast (*YCF1*) (Lu *et al.*, 1997, Sanchez-Fernandez *et al.*, 1998, Tommasini *et al.*, 1998). Among several MRP genes identified in *Arabidopsis*, four have been characterized in more detail. *AtMRP1*, *AtMRP2*, and *AtMRP3* encode functional GS-X pumps and transport xenobiotics and endogenous substances, such as chlorophyll catabolites, into the vacuole (Lu *et al.*, 1997, 1998; Tommasini *et al.*, 1998).

As outlined above, genetic evidence via mutant characterization in *Arabidopsis* (Kitamura *et al., 2004*), maize, petunia and carnation (Larsen *et al.,* 2003) suggested that GSTs define late steps in anthocyanin and PA biosynthesis- In extension these studies proposed that anthocyanins are conjugated to glutathione prior to vacuolar transport. Because MRPs have a substrate preference for glutathione conjugates, anthocyanin transport by MRPs was presumed. However, maize *Bronze-2* and petunia *AN9* fail to glutathionate anthocyanins and a role of GSTs as cytosolic flavonoid-binding proteins was proposed instead (Marrs *et al*., 1995).

In spite of the unclear roles of GSTs, Goodman *et al.* (2004) reported that the maize MRP-type ABC transporter, ZmMRP3, is localized on the tonoplast and is required for anthocyanin transport. Although biochemical evidence for the transport activity of ZmMRP3 is missing, antisense *ZmMRP3*-lines produced in an anthocyanin-overproducing genetic background exhibit drastically reduced anthocyanin accumulation in leaves and tassels.

In addition to the studies mentioned above it was demonstrated that also sulphonated compounds such as the fluorescent dye Lucifer yellow CH (Klein, 1997) as well as carboxylated compounds (Fluo-3, Fura-2; Klein, unpublished) are also taken up by vacuoles via MRP-type ABC-transporters. Taken together, these studies demonstrate that plants have evolved different transport mechanisms for small molecules with various conjugation patterns. As a general rule it could be hypothesized that MRP-type ABC transporters catalyze vacuolar accumulation of negatively charged organic compounds while glycosylated flavonoids may be recognized by specific proton-dependent transport systems.

2.1.2. MATE transporters

As mentioned earlier, the *tt12* mutant displays defects in the vacuolar sequestration of PA precursors in seeds (Debeaujon *et al.*, 2001). Since TT12 was found to be a membrane protein belonging to the multidrug and toxic compound extrusion (MATE) family, it can be speculated that MATE proteins are ultimately responsible for the vacuolar deposition of flavonoids via proton-antiport. In other words, MATE transporters could be the molecular correlates of the secondary energized transport mechanisms found in vacuolar uptake studies with glucosylated flavones (Klein *et al*., 1996; Frangne *et al*., 2002). For a detailed introduction of TT12 as a PA precursor transporter see chapter 2.

The MATE family was only recently identified as a family of putative secondary transporters (Brown *et al.*, 1998). Hydropathy analysis suggests that proteins of the MATE family have a common topology consisting of 12 transmembrane (TM) domains. There are MATE family members in humans, in the yeasts *Saccharomyces cerevisiae* and *Schizosaccharomyces pombe*, in *Escherichia coli* and other bacteria, and in *Archaea*. On the basis of the analysis of two bacterial family members, NorM and YdhE (Morita *et al.*, 1998), the MATE family is thought to encode efflux pumps. In *Arabidopsis*, the MATE family consists of 56 genes (Rogers and Guerinot, 2002, Li *et al.*, 2002b) but only five have been initially characterized. Appart from TT12 mutant analysis has revealed that these genes are involved in lateral root formation (ALF5, Diener *et al.*, 2001), iron homeostasis (FRD3, Rogers and Guerinot, 2002), and salicylic acid-dependent signaling for disease resistance (EDS5, Nawrath *et al.*, 2002) (chapter 3). The complementation of the norfloxacin-hypersensitive E. coli strain KAM3, lacking AcrAB, resulted in functional cloning of AtDTX1 (Li *et al.*, 2002). AtDTX1 was shown to function in *E. coli* is as an efflux carrier of antibiotics, alkaloid berberine, and of other toxic compounds including ethidium bromide (Li *et al.*, 2002). The identification of *ALF5* as a component of the detoxification system in roots suggests the possibility of engineering plants that overexpress particular MATE proteins to achieve useful phenotypes. For example, these transgenic plants might grow in soils containing chemicals that would inhibit the growth of wild-type plants.

3. The function of vacuole in secondary metabolism

The biosynthesis of the flavonoids provides one of the best described plant metabolic pathways, with many of the structural and regulatory genes in the pathway identified and cloned (Mol *et al.*, 1998; Winkel-Shirley, 2001; Lepiniec *et al*., 2006). However information about the mechanisms by which the water-soluble anthocyanins are transported from their site of synthesis to the vacuole, where they are usually sequestered remains sparse (Grotewold, 2004). Plant vacuoles can occupy up to 90% of the cell volume, playing a key role in storage (ions, metabolites, and proteins), protein processing and degradation, Ca^{2+} signaling, digestion, pH and ion homeostasis, turgor pressure maintenance, biotic and abiotic defense responses, toxic compound sequestration, and pigmentation (De, 2000). More recently, it has been suggested that this organelle even plays important roles in tropic responses, plant development, and signal transduction (Kato *et al.*, 2002a, 2002b; Morita *et al.*, 2002; Surpin *et al.*, 2003). A large number of proteins in the tonoplast including active pumps, carriers, ion channels, receptors and structural proteins support the function of different vacuoles. Indeed there are at least two types of vacuoles found in plant cells (Paris *et al.*, 1996; De, 2000) and termed as lytic vacuoles (LV) and protein storage vacuoles (PSV). LVs are thought to be functionally analogous to the mammalian lysosome and yeast vacuole, whereas the PSV serve as a site for protein deposition within seeds and roots (Vitale and Raikhel, 1999). Both types of vacuoles may serve in both storage and degradation processes and may both be found within individual cells. In mature tissues, often the LV and PSV will fuse to form a large central vacuole that retains functional characteristics of both parent compartments. Vacuoles can therefore be distinguished by the composition of proteins localised on the tonoplast or by their soluble proteins.

Plant vacuoles are an integral part of the endomembrane system, serving as the terminal products of the secretory pathway (Marty, 1999). Several plant species store anthocyanins within vacuolar inclusions that have been loosely termed anthocyanoplasts which have been observed to start as vesicles in the cytoplasm and were defined in the past as membrane bound structures (Pecket and Small, 1980; Nozzolillo and Ishikura, 1988). More recently, the intravacuolar structures observed in the flower petals of carnation (*Dianthus caryophyllus*) and lisianthus (*Eustoma grandiflorum*), were termed anthocyanic vacuolar inclusions, or AVIs (Markham *et al.*, 2000). These inclusions were suggested to be membrane-less, proteinaceous matrixes that act as anthocyanin traps, preferentially for anthocyanidin 3,5-diglycosides (Markham *et al.*, 2000) or acylated anthocyanins (Conn *et al.*, 2003) and chapter 6.

A major function of the plant vacuole is the maintenance of turgor pressure and storage of metabolites and ions. The central vacuole is maintained at a pH of 5.5 (Sze *et al.*, 2002). This acidic environment is produced through the activity of a V-ATPase and the vacuolar pyrophosphatase (V-PPase) and is required for providing energy for the transport of ions and

organic metabolites. It has also been suggested that the proton gradient is required for protein sorting and membrane fusion events (Matsuoka *et al.*, 1997; Wickner and Haas, 2000; Peters *et al.*, 2001).

In plants, the most prominent role of the V-ATPase is to maintain ion and metabolite homeostasis by energizing secondary active transport across the tonoplast (Sze *et al.*, 1999; Kluge *et al.*, 2003). Although V-ATPases have also been found throughout the endomembrane system, including the endoplasmic reticulum, Golgi, and provacuoles (Herman *et al.*, 1994; Oberbeck *et al.*, 1994), the functions of the plant V-ATPase in secretory and endocytic trafficking are not well defined. In tobacco (*Nicotiana tabacum*) cells, inhibition of the V-ATPase interferes with secretion and leads to missorting of vacuolar proteins, suggesting that the functionality of a nonvacuolar compartment depends on V-ATPase function (Matsuoka *et al.*, 1997). Analysis of V-ATPase null mutants of *Arabidopsis thaliana* has recently shown that the V-ATPase is essential for Golgi function during the development of the male gametophyte and during embryogenesis (Dettmer *et al.*, 2005; Strompen *et al.*, 2005). Therefore, it seems possible that the growth inhibition observed in plants with reduced V-ATPase activity (Schumacher *et al.*, 1999; Padmanaban *et al.*, 2004) is caused by a defect in vesicle trafficking rather than by reduced turgor pressure attributable to a lack of osmolyte transport into the vacuole.

Another function of plant vacuoles includes stress and defense responses. Defense-related proteins previously shown to localize to the vacuole from various species include proteinase inhibitors, chitinases, peroxidases, osmotin (PR-5), glycosidases, berberine bridge enzyme, strictosidine synthase, and lectins (Neuhaus *et al.*, 1991; Bird and Facchini, 2001; Matsui *et al.*, 2003).

4. Vesicle transport

Another possibility of transport of secondary metabolites within the plant cells is presumed to be via vesicle trafficking which includes membrane bound organelles. The plant endomembrane system or secretory pathway, which is critical for biosynthetic and endocytic trafficking to the plasma membrane (PM) and vacuole, is comprised of the endoplasmic reticulum (ER), Golgi apparatus and intermediate organelles such as the prevacuolar compartment. The morphology, localization and function of these endomembrane compartments are highly dynamic throughout plant growth and development. The secretory membrane trafficking mechanisms have recently been shown to be involved in a variety of plant specific processes, including abscisic acid and auxin signaling, plant development, tropic responses, and pathogen defense.

Two hypotheses are presented for the transport of flavonoids via vesicles: (i) direct transfer of lipids from ER to the plasma membrane and (ii) Golgi-mediated exocytosis, as proposed for cuticular wax transport (Kunst and Samuels, 2003). One model of vesicle transport

has been reported in maize BMS (Black Mexican Sweet) cells transformed with P1, a regulator of 3-deoxyflavonoid synthesis, for the transport of ER-derived vesicles to the vacuole and cell wall, respectively (Grotewold, 2000). Another model is the presence of subcellular inclusions containing 3-deoxyanthocyanidins that accumulate in infected sorghum cells (Snyder and Nicholson, 1990), which first appeared to fuse before being secreted out to the apoplast (Lin *et al.*, 2003, chapter 6). This system will provide material that might be applicable for the study of vesicle-mediated transport of secondary metabolites.

The sorting of integral proteins in plants is not well understood. It has been clearly demonstrated that multiple mechanisms exist for targeting proteins to the vacuole (Vitale and Raikhel, 1999), and we are also beginning to understand the details of vacuolar membrane trafficking (reviewed in Surpin and Raikhel, 2004). It is accepted that peptidic signals exposed in the cytosol are responsible for targeting to the correct subcellular location in plant cells. Traffic of proteins within the secretory pathway of plant cells is complex because plant cells store proteins within a vacuolar compartment. These proteins must be kept separate from the active proteases that would degrade them. In contrast to yeast, plant cells may contain two functionally distinct types of vacuoles: protein storage vacuoles (PSVs) and lytic vacuoles (LVs) (Okita and Rogers, 1996). A separate vesicular pathway leads to each type of vacuole; soluble proteins are carried to the LV compartment in clathrin-coated vesicles (CCV), whereas storage proteins are carried to the PSV in smooth, dense vesicles (Hinz *et al.*, 1995; Hohl *et al.*, 1996; Okita and Rogers, 1996). In contrast to emerging knowledge about sorting of soluble proteins to plant vacuoles, relatively little is known about the biogenesis of separate vacuolar compartments, although some evidence indicates that the PSV may develop directly from the ER (Robinson *et al.*, 1995).

Plant membrane trafficking shares many features with other eukaryotic organisms, including the machinery for vesicle formation and fusion. A secretory default pathway leads from the ER via Golgi stacks to the plasma membrane. However, the plant endomembrane system lacks an ER-Golgi intermediate compartment, has numerous Golgi stacks and several types of vacuoles, and forms a transient compartment during cell division. The Golgi apparatus is a major sorting station, delivering cargo proteins to multiple destinations (Staehelin and Moore, 1995; Dupree and Sherrier, 1998). Sorting in the Golgi stacks separates bulk flow to the plasma membrane from receptor-mediated trafficking to the lytic vacuole. Cargo for the protein storage vacuole is delivered from the ER, *cis*-Golgi, and *trans*-Golgi. Trafficking to the protein storage vacuole may also involve an ER-derived route that bypasses the Golgi complex. Endocytosis includes recycling of plasma membrane proteins from early endosomes. Endosomes are still poorly defined in plants, although early studies described a partially coated reticulum as an endosomal compartment (reviewed by Battey *et al.* 1999). Recently, an endocytic multivesiculate compartment was identified as the prevacuolar compartment (PVC) known to be involved in Golgi-vacuole trafficking (Tse *et al.*, 2004). Late endosomes appear identical with the

multivesiculate prevacuolar compartment that lies on the Golgi-vacuole trafficking pathway. Thus plant cells may have at least two distinct endosomal compartments: early endosomes involved in sorting and recycling and late endosomes/PVC in route to the lytic vacuole (Paris and Neuhaus, 2002; Tse *et al.*, 2004).

Eukaryotic cells are characterized by an endomembrane system consisting of organelles with a distinct protein composition, which is partly because of the presence of specific targeting information on the resident polypeptides. This information is quite well characterized for soluble proteins but not for membrane proteins, especially polytopic proteins, such as the plasma membrane proteins of plant cells. PM integral proteins are thought to be first integrated into the ER, and then transported to the cell surface through the secretory pathway. The organization and function of the plant secretory pathway is attracting much interest (Nebenfuhr *et al.*, 2002; Ueda and Nakano, 2002), and some recent studies have identified morphological and functional aspects specific to plant cells (Brandizzi *et al.*, 2002; Saint-Jore *et al.*, 2002).

In the past, vesicle trafficking has been primarily investigated from the perspective of the transport of proteins and membranes between the different compartments of the endomembrane system. Selection of the direction of the traffic between the different compartments is dependent on the presence and identity of various coat proteins. In addition to providing target membrane specificity, coat proteins contribute to the formation of a vesicle from the donor membrane and in the selection of the cargo.

In the secretion of proteins, the process initiates in the ER, cargo passes through the Golgi, the TGN to then be directed to the cell membrane. However, recent findings using the inducible accumulation of autofluorescent compounds in maize cells suggest that there might be alternate secretory pathways that bypass the need for the Golgi apparatus and the TGN (Lin *et al.* 2003). The immuno-localization of flavonoid biosynthetic enzymes in *Arabidopsis* root cells identified intriguing cytoplasmic electron-dense structures (Saslowsky and Winkel-Shirley, 2001). Substantial evidence also supports the vesicle-mediated transport of various compounds between the vacuole and the plasma membrane (Echeverria, 2000).

5. Aims of this study

In conclusion the past few years have observed an increased understanding of the possible mechanisms by which plants deal with the transport of phytochemicals. However, presented evidence suggests that the presence of GSTs, transporters and vesicles participate together in a puzzle, waiting to be assembled. It is yet unclear how to resolve fully these divergent models involving carriers and vesicles but our major aims during this work were to elucidate and highlight their presence and biochemical characteristics within the plant cell using different species. Our study regards the mechanisms of cellular flavonoids transport on different levels and we expected to provide biochemical data supporting the theoretical data or to fill the lack of information. There is need for a better understanding of the transport mechanism of phytochemicals for the development of successful strategies for plant metabolic engineering.

Reference list

Abrahams S., Lee E., Walker A.R., Tanner G.J., Larkin P.J., Ashton A.R. 2003 The *Arabidopsis* TDS4 gene encodes leucoanthocyanidin dioxygenase (LDOX) and is essential for proanthocyanidin synthesis and vacuole development. Plant J. 35:624-636.

Abrahams S., Tanner G.J., Larkin P.J., Ashton A.R. 2002 Identification and biochemical characterization of mutants in the proanthocyanidin pathway in *Arabidopsis.* Plant Physiol. 130:561-576.

Albert S., Delseny M., Devic M. 1997 BANYULS, a novel negative regulator of flavonoid biosynthesis in the *Arabidopsis* seed coat. Plant J. 11:289-299.

Battey N.H., James N.C., Greenland A.J., Brownlee C. 1999 Exocytosis and endocytosis. Plant Cell 11:643–60.

Baudry A., Heim M.A., Dubreucq B., Caboche M., Weisshaar B., Lepiniec L. 2004 TT2, TT8, and TTG1 synergistically specify the expression of *BANYULS* and proanthocyanidin biosynthesis in *Arabidopsis thaliana*. Plant J. 39(3):366.

Baxter I.R., Young J.C., Armstrong G., Foster N., Bogenschutz N., Cordova T., Peer W.A., Hazen S.P., Murphy A.S., Harper J.F. 2005 A plasma membrane H+-ATPase is required for the formation of proanthocyanidins in the seed coat endothelium of *Arabidopsis thaliana*. PNAS 102:2649-2654.

Bird D.A., and Facchini P.J. 2001 Berberine bridge enzyme, a key branch-point enzyme in benzylisoquinoline alkaloid biosynthesis, contains a vacuolar sorting determinant. Planta 213:888–897.

Bohm B.A. 1998 Introduction to Flavonoids. Harwood, Reading.

Borevitz J.P., Xia Y., Blount J., Dixon R.A., Lamb C. 2000 Activation tagging identifies a conserved MYB regulator of phenylpropanoid biosynthesis. Plant Cell 12:2383–2393.

Brandizzi F., Snapp E.L., Roberts A.G., Lippincott-Schwartz J., Hawes C. 2002 Membrane protein transport between the endoplasmic reticulum and the Golgi in tobacco leaves is energy dependent but cytoskeleton independent:evidence from selective photobleaching. Plant Cell 14:1293–309.

Brown M.H., Paulsen I.T., Skurray R.A. 1998 The multidrug efflux protein NorM is a prototype of a new family of transporters. Mol. Microbiol. 31:393–395.

Burbulis I.E., and Winkel-Shirley B. 1999 Interactions among enzymes of the *Arabidopsis* flavonoid biosynthetic pathway. PNAS 96:12929–12934.

Campbell E.J., Schenk P.M., Kazan K., Penninckx I.A., Anderson J.P., Maclean D.J., Cammue B.P., Ebert P.R., Manners J.M. 2003 Pathogenresponsive expression of a putative ATP-binding cassette transporter gene conferring resistance to the diterpenoid sclareol is regulated by multiple defense signaling pathways in *Arabidopsis*. Plant Physiol. 133:1272-1284.

Castelluccio C., Paganga G., Melikian N., Bolwell G.P., Pridham J., Sampson J., Rice-Evans C. 1995 Antioxidant potential of intermediates in phenylpropanoid metabolism in higher plants. FEBS Lett. 368:188–192.

Chapple C.C.S., Shirley B.W., Zook M., Hammerschmidt R., Somerville S.C. 1994 Secondary metabolism in *Arabidopsis*. *In* EM Meyerowitz, CR Somerville, eds, *Arabidopsis*. Cold Spring Harbor Laboratory Press, Cold Spring Harbor, NY, pp.989–1030

Coleman J.O.D., Randall R., BlakeKalff M.M.A. 1997 Detoxification of xenobiotics in plant cells by glutathione conjugation and vacuolar compartmentalization: A fluorescent assay using monochlorobimane. Plant Cell Environ. 20:449-460.

Cook N.C., and Samman S. 1996 Flavonoids-Chemistry, metabolism, cardioprotective effects, and dietary sources. Nutritional Biochemistry 7:66-76.

Cone K.C., Burr F.A., Burr B. 1986 Molecular analysis of the maize anthocyanin regulatory locus *C1*. PNAS 83:9631–9635.

Conn S., Zhang W., Franco C. 2003 Anthocyanic vacuolar inclusions (AVIs) selectively bind acylated anthocyanins in *Vita vinifera* L. (grapevine) suspension culture. Biotech Ltrs. 25:835-839.

Croteau R., Kutchan T.M., Lewis N.G. 2000 Natural products (secondary metabolites). In: Buchanan B, Gruissem W, Jones R (eds) Biochem. Mol. Biol. Plants. American Society of Plant Physiologists, Rockville, Maryland, 1250–1318.

De D.N. 2000 Plant Cell Vacuoles. (Collingwood, Australia: CSIRO Publishing).

Debeaujon I., Leon-Kloosterziel K.M., Koornneef M. 2000 Influence of the testa on seed dormancy, germination, and longevity in *Arabidopsis*. Plant Physiol. 122:403-413.

Debeaujon I., Peeters A.J.M., Leon-Kloosterziel K.M., Koornneef M. 2001 The TRANSPARENT TESTA12 gene of *Arabidopsis* encodes a multidrug secondary transporter-like protein required for flavonoid sequestration in vacuoles of the seed coat endothelium. Plant Cell 13:853-871.

Debeaujon I., Nesi N., Perez P., Devic M., Grandjean O., Caboche M., Lepiniec L. 2003 Proanthocyanidin-accumulating cells in *Arabidopsis* testa: Regulation of differentiation and role in seed development. Plant Cell 15:2514-2531.

De Luca V., St. Pierre B. 2000 The cell and developmental biology of alkaloid biosynthesis. Trends Plant Sci 5:168-173.

Dettmer J., Schubert D., Calvo-Weimar O., Stierhof Y.D., Schmidt R., Schumacher K. 2005 Essential role of the V-ATPase in male gametophyte development. Plant J. 41:117–124.

de Vetten N., Quattrocchio F., Mol J., Koes R. 1997 The an11 locus controlling flower pigmentation in petunia encodes a novel WD-repeat protein conserved in yeast, plants, and animals. Genes & Development 11:1422-1434.

Devic M., Guilleminot J., Debeaujon I., Bechtold N., Bensaude E., Koornneef M., Pelletier G., Delseny M. 1999 The BANYULS gene encodes a DFR-like protein and is a marker of early seed coat development. Plant J. 19:387-398.

Diener A.C., Gaxiola R.A., Fink G.R. 2001 *Arabidopsis* ALF5, a multidrug efflux transporter gene family member, confers resistance to toxins. Plant Cell 13:1625-1637.

Dixon R.A., and Paiva N.L. 1995 Stress-induced phenylpropanoid metabolism. Plant Cell 7:1085–1097.

Dugas A.J., Castaneda Acosta J., Bonin G.C., Price K.L., Fischer N.H., Winston G.W. 2000 Evaluation of the total peroxyl radical-scavenging capacity of flavonoids: Structureactivity relationships. J. Nat. Prod.. 63:327–331.

Dupree P., Sherrier D.J. 1998 The plant Golgi apparatus. Biochim. Biophys. Acta 1404:259–70.

Duthie G., and Crozier A. 2000 Plant-derived phenolic antioxidants. Curr. Opin. Lipidol. 11:43–47.

Echeverria E. 2000 Vesicle-mediated solute transport between the vacuole and the plasma membrane. Plant Physiol. 123:1217–1226.

Facchini P.J. 2001 Alkaloid biosynthesis in plants: biochemistry, cell biology, molecular regulation, and metabolic engineering applications. Annu Rev. Plant Physiol. Plant Mol. Biol. 52:29-66.

Feinbaum R.L., Ausubel F.M. 1988 Transcriptional regulation of the *Arabidopsis thaliana* chalcone synthase gene. Mol Cell Biol. 8(5):1985-92.

Focks N, Sagasser M, Weisshaar B, Benning C 1999 Characterization of *tt15*, a novel transparent testa mutant of *Arabidopsis thaliana*. Planta **208:** 352–357.

Frangne N., Eggmann T., Koblischke C., Weissenboöck G., Martinoia E., Klein M. 2002 Flavone glucoside uptake into barley mesophyll and *Arabidopsis* cell culture vacuoles. Energization occurs by H^+-antiport and ATP-binding cassette-type mechanisms. Plant Physiol. 128:726-733.

Goodman C.D., Casati P., Walbot V. 2004 A multidrug resistance-associated protein involved in anthocyanin transport in *Zea mays*. Plant Cell 16:1812-1826.

Grotewold E., Sainz M.B., Tagliani L., Hernandez J.M., Bowen B., Chandler V.L. 2000 Identification of the residues in the Myb domain of maize C1 that specify the interaction with the bHLH cofactor R. PNAS 97(25):13579-84.

Grotewold E. 2004 The challenges of moving chemicals within and out of cells: insights into the transport of plant natural products. Planta 219:906-909.

Gunawardena A.H., Greenwood J.S., Dengler N.G. 2004 Programmed cell death remodels lace plant leaf shape during development. Plant Cell 16:60-73.

Harborne J.B. 1986 Nature, distribution and function of plant flavonoids. Prog. Clin. Biol. Res. 213:15-24

Harborne J.B., Baxter H. 1999 Handbook of Natural Flavonoids. 2vols., Wiley, Chichester.

Harborne J.B. and Williams C.A. 2000 Advances in flavonoid research since 1992. Phytochemistry 55:481-504.

Hartmann T., **Theuring C.**, **Schmidt J.**, **Rahier M.**, **Pasteels J.M.** 1999 Biochemical strategy of sequestration of pyrrolizidine alkaloids by adults and larvae of chrysomelid leaf beetles. J. Insect Physiol. 45(12):1085-1095.

Hashimoto T., and Yamada Y. 2003 New genes in alkaloid metabolism and transport. Curr. Opin. Biotechnol. 14(2):163-8.

Herman E.M., Li X., Su R.T., Larsen P., Hsu H., Sze H. 1994 Vacuolar-type H^+-ATPases are associated with the endoplasmic reticulum and provacuoles of root tip cells. Plant Physiol. 106:1313–1324.

Hertog M.G., Feskens E.J., Hollman P.C., Katan M.B., Kromhout D. 1993 Dietary antioxidant flavonoids and risk of coronary heart disease. The Zutphen Elderly Study. Lancet 342:1007–1011.

Hinz G., Hoh B., Hohl I., Robinson D.G. 1995 Stratification of storage proteins in the protein storage vacuole of developing cotyledons of *Pisum sativum* L. J. Plant Physiol. 145:437–442.

Hohl I., Robinson D.G., Chrispeels M.C., Hinz G. 1996 Transport of storage proteins to the vacuole is mediated by vesicles without a clathrin coat. J.Cell Sci. 109:2539–2550.

Holton T.A., Cornish E.C. 1995 Genetics and biochemistry of anthocyanin biosynthesis. Plant Cell 7:1071–1083.

Hyodo H., Yang S.F. 1971 Ethylene-enhanced synthesis of phenylalanine ammonia-lyase in pea seedling. Plant Physiol. 47:765-770.

Iwasa K., **Nanba H.**, **Lee D.U.**, **Kang S.I.** 1998 Structure-activity relationships of protoberberines having antimicrobial activity. Planta Med. 64(8):748-51.

Jasinski M., Stukkens Y., Degand H., Purnelle B., Marchand-Brynaert J., Boutry M. 2001 A plant plasma membrane ATP-binding cassette type transporter is involved in antifungal terpenoid secretion. Plant Cell 13:1095-1107.

Johnson C.S., Kolevski B., and Smyth D.R. 2002 *TRANSPARENT TESTA GLABRA2*, a trichome and seed coat development gene of *Arabidopsis*, encodes a WRKY transcription factor. Plant Cell 14:1359–1375.

Kato T., Morita M.T., Fukaki H., Yamauchi Y., Uehara M., Niihama M., Tasaka M. 2002a SGR2, a phospholipase-like protein, and ZIG/SGR4, a SNARE, are involved in the shoot gravitropism of *Arabidopsis*. Plant Cell 14, 33–46.

Kato T., Morita M.T., Tasaka M. 2002b Role of endodermal cell vacuoles in shoot gravitropism. J. Plant Growth Regul. 21:113–119.

Keli S.O., Hertog M.G., Feskens E.J., Kromhout D. 1996 Dietary flavonoids, antioxidant vitamins, and incidence of stroke. The Zutphen Study. Arch. Intern. Med. 156:637–642.

Kitamura S., Shikazono N., Tanaka A. 2004 TRANSPARENT TESTA 19 is involved in the accumulation of both anthocyanins and proanthocyanidins in *Arabidopsis*. Plant J. 37:104-114.

Klein M., Martinoia E., Hoffmann-Thoma G., Weissenböck G. 2000 A membrane-potential dependent ABC-like transporter mediates the vacuolar uptake of rye flavone glucuronides: regulation of glucuronide uptake by glutathione and its conjugates. Plant J. 21:289-304.

Klein M., Weissenböck G., Dufaud A., Gaillard C., Kreuz K., Martinoia E. 1996 Different energization mechanisms drive the vacuolar uptake of a flavonoid glucoside and a herbicide glucoside. J. Biol. Chem. 271:29666-29671.

Klein M., Martinoia E., Weissenböck G. 1997 Transport of lucifer yellow CH into plant vacuoles-evidence for direct energization of a sulphonated substance and implications for the design of new molecular probes. FEBS lett. 420(1):86-92.

Klein M., Martinoia E., Weissenböck G. 1998 Directly energized uptake of beta-estradiol 17-(beta-D-glucuronide) in plant vacuoles is strongly stimulated by glutathione conjugates. J Biol Chem. 273(1):262-70.

Klein M., Martinoia E., Hoffmann-Thoma G., Weissenböck G. 2001 The ABC-like vacuolar transporter for rye mesophyll flavone glucuronides is not species-specific. Phytochemistry 56(2):153-9.

Kluge C., Lahr J., Hanitzsch M., Bolte S., Golldack D., Dietz K.J. 2003 New insight into the structure and regulation of the plant vacuolar H^+-ATPase. J. Bioenerg. Biomembr. 35:377–388.

Koornneef M. 1981 The complex syndrome of *ttg* mutants. *Arabidopsis* Inf. Serv. 18: 45–51.

Koornneef M., Luiten W., de Vlaming P., Schram A.W. 1982 A gene controlling flavonoid-3'-hydroxylation in *Arabidopsis*. Arabid Inf Serv **19:**113–115

Koornneef M. 1990 Mutations affecting the testa colour in *Arabidopsis*. *Arabidopsis* Inf. Serv. 27:1–4.

Kubo H., Peeters A.J.M., Aarts M.G.M., Pereira A., Koornneef M. 1999 *ANTHOCYANINLESS2*, a homeobox gene affecting anthocyanin distribution and root development in *Arabidopsis*. Plant Cell 11:1217–1226.

Kunst L., Samuels A.L. 2003 Biosynthesis and secretion of plant cuticular wax. Prog Lipid Res 42:51-80.

Kutchan T.M. and Dittrich H. 1995 Characterization and mechanism of the berberine bridge enzyme, a covalently flavinylated oxidase of benzophenanthridine alkaloid biosynthesis in plants. J. Biol. Chem. 270(41):24475–24481.

Lairon D., and Amiot M.J. 1999 Flavonoids in food and natural antioxidants in wine. Curr Opin Lipidol. 10(1):23-8.

Larsen E.S., Alfenito M.R., Briggs W.R., Walbot V. 2003 A carnation anthocyanin mutant is complemented by the glutathione S-transferases encoded by maize *Bz2* and petunia *An9*. Plant Cell Rep. 21:900-904.

Lepiniec L., Debeaujon I., Routaboul J.M., Baudry A., Pourcel L., Nesi N., Caboche M. 2006 Genetics and biochemistry of seed flavonoids. Annu Rev Plant Biol. 57:405-30.

Leon-Kloosterziel K.M., Keijzer C.J., Koornneef M. 1994 A seed shape mutant of *Arabidopsis* that is affected in integument development. Plant Cell 6:385–392

Li L., He Z., Pandey G.K., Tsuchiya T., Luan S. 2002 Functional cloning and characterization of a plant efflux carrier for multidrug and heavy metal detoxification. J.Biol.Chem. 277:5360-5368.

Lin Y., Irani N.G., Grotewold E. 2003 Sub-cellular traficking of phytochemicals using autofluorescent compounds in maize cells. BMC Plant Biol 3:10.

Lu Y.P., Li Z.S., Rea P.A. 1997 AtMRP1 gene of *Arabidopsis* encodes a glutathione S-conjugate pump: Isolation and functional definition of a plant ATP-binding cassette transporter gene. PNAS 94:8243–8248.

Lu Y-P., Li Z-S., Drozdowicz Y.M., Hortensteiner S., Martinola E., Rea P.A. 1998 AtMPR2, an *Arabidopsis* ATP binding cassette transporter able to transport glutathione S-conjugates and chlorophyll catabolites: functional comparisons with AtMRP1. Plant Cell 10:267.

Ludwig S.R., Habera L.F., Dellaporta S.L., Wessler S.R. 1989 *Lc*, a member of the maize *R* gene family responsible for tissue-specific anthocyanin production, encodes a protein similar to transcriptional activators and contains the *myc*-homology region. PNAS 86:7092–7096.

Mahady G.B., **Pendland S.L.**, **Stoia A.**, **Chadwick L.R.** 2003 *In vitro* susceptibility of *Helicobacter pylori* to isoquinoline alkaloids from *Sanguinaria canadensis* and *Hydrastis canadensis.* Phytother Res. 17(3):217-21.

Matile P. 1976 Localization of alkaloids and mechanism of their accumulation in vacuoles of Chelidonium majus laticifers. Nova Acta Leopold Suppl 7:139–156.

Matile P. 1984 The toxic compartment of plant cells. Naturwissenschaften 71:18-24.

Markham K.R., Gould K.S., Winefeld C.S., Kevin A. Mitchell K.A., Bloor S.J., Boase M.R. 2000 Anthocyanic vacuolar inclusiona and their nature and significance in flower colouration. Phytochemistry 55:327-336.

Marrs K.A., Alfenito M.R., Lloyd A.M., Walbot V. 1995 A glutathione S-transferase involved in vacuolar transfer encoded by the maize gene *Bronze-2*. Nature 375:397–400.

Marty F. 1999 Plant vacuoles. Plant Cell 11:587-599.

Martinoia E., Grill E., Tommasini R., Kreuz K., Amrhein N. 1993 ATP dependent glutathione *S*-conjugate export pump in the vacuolar membrane of plants. Nature 364: 247–249.

Martinoia E., Massonneau A., Frangne N. 2000 Transport processes of solutes across the vacuolar membrane of higher plants. Plant and Cell Physiology 41:1175-1186.

Martinoia E., Klein M., Geisler M., Bovet L., Forestier C., Kolukisaoglu U., Muller-Rober B., Schulz B. 2002 Multifunctionality of plant ABC transporters — more than just detoxifiers. Planta 214:345-355.

Masucci J.D., Schiefelbein J.W. 1996 Hormones act downstream of *TTG* and *GL2* to promote root hair outgrowth during epidermis development in the *Arabidopsis* root. Plant Cell 8:1505–1517.

Matsui T., Nakayama H., Yoshida K., Shinmyo A. 2003 Vesicular transport route of horseradish C1a peroxidase is regulated by N- and C-terminal propeptides in tobacco cells. Appl. Microbiol. Biotechnol. 262:517–522.

Matsuoka K., Higuchi T., Maeshima M., Nakamura K. 1997 A vacuolar-type H^+-ATPase in a nonvacuolar organelle is required for sorting of soluble vacuolar protein precursors in tobacco cells. Plant Cell 9:533–546.

Mol J., Grotewold E., Koes R. 1998 How genes paint flowers and seeds. Trends Plant Sci. 3:212–217.

Morita Y., Kodama K., Shiota S., Mine T., Kataoka A., Mizushima T., Tsuchiya T. 1998 NorM, a putative multidrug efflux protein, of *Vibrio parahaemolyticus* and its homolog in *Escherichia coli*. Antimicrob.Agents Chemother. 42:1778-1782.

Morita M.T., Kato T., Nagafusa K., Saito C., Ueda T., Nakano A., Tasaka M. 2002 Involvement of the vacuoles of the endodermis in the early process of shoot gravitropism in *Arabidopsis*. Plant Cell 14:47–56.

Nawrath C., Heck S., Parinthawong N., Metraux J.P. 2002 EDS5, an essential component of salicylic acid-dependent signaling for disease resistance in *Arabidopsis*, is a member of the MATE transporter family. Plant Cell 14:275-286.

Nebenfuhr A., Ritzenthaler C., Robinson D.G. 2002 Brefeldin A: Deciphering an enigmatic inhibitor of secretion. Plant Physiol. 130:1102-1108.

Nesi N., Jond C., Debeaujon I., Caboche M., Lepiniec L. 2001 The *Arabidopsis* TT2 gene encodes an R2R3 MYB domain protein that acts as a key determinant for proanthocyanidin accumulation in developing seed. Plant Cell 13:2099-2114.

Nesi N., Debeaujon I., Jond C., Pelletier G., Caboche M., Lepiniec L. 2000 The TT8 Gene encodes a basic helix-loop-helix domain protein required for expression of DFR and BAN genes in *Arabidopsis* siliques. Plant Cell 12:1863-1878.

Nesi N., Debeaujon I., Jond C., Stewart A.J., Jenkins G.I., Caboche M., Lepiniec, L. 2002 The *TRANSPARENT TESTA16* locus encodes the *ARABIDOPSIS* BSISTER MADS domain protein and is required for proper development and pigmentation of the seed coat. Plant Cell 14:2463–2479.

Neuhaus J.M., Sticher L., Meins F. Jr., Boller T. 1991 A short C-terminal sequence is necessary and sufficient for the targeting of chitinases to the plant vacuole. PNAS 88:10362–10366.

Ng T.B., Liu F., Wang Z.T. 2000 Antioxidative activity of natural products from plants. Life Sci. 66:709–723.

Nozzolillo C., Ishikura N. 1988 An investigation of the intracellular site of anthocyanoplasts using isolated protoplasts and vacuoles. Plant Cell Rep 7:389-392.

Oberbeck K., Drucker M., Robinson D. 1994 V-type ATPase and pyrophosphatase in endomembranes of maize roots. J. Exp. Bot. 45:235–244.

Okita T.W., and Rogers J.C. 1996 Compartmentation of proteins in the endomembrane system of plant cells. Annu. Rev. Plant Physiol. Plant Mol. *Biol.* 47:327–350.

Onyilagha J.C., Lazorko J., Gruber M.Y., Soroka J.J., Erlandson M.A. 2004 Effect of flavonoids on feeding preference and development of the crucifer pest *Mamestra configurata Walker.* J Chem Ecol. 30(1):109-24.

Padmanaban S., Lin X., Perera I., Kawamura Y., Sze H. 2004 Differential expression of vacuolar H^+-ATPase subunit c genes in tissues active in membrane trafficking and their roles in plant growth as revealed by RNAi. Plant Physiol. 134:1514–1526.

Paris N., Stanley C.M., Jones R.L., Rogers J.C. 1996 Plant cells contain two functionally distinct vacuolar compartments. Cell 85(4):563-72.

Paris N., and Neuhaus J.M. 2002 BP-80 as a vacuolar sorting receptor. Plant Mol. Biol. 50:903–914.

Payne C.T., Zhang F., Lloyd A.M. 2000 GL3 encodes a bHLH protein that regulates trichome development in *Arabidopsis* through interaction with GL1 and TTG1. Genetics 156:1349-1362.

Paz-Ares J., Ghosal D., Wienand U., Peterson P.A., Saedler H. 1987 The regulatory *c1* locus of *Zea mays* encodes a protein with homology to *myb* proto-oncogene products and with structural similarities to transcriptional activators. EMBO J. 6:3553–3558.

Pecket C.R., Small C.J. 1980 Occurrence, location and development of anthocyanoplasts. Phytochemistry 19:2571-2576.

Pelletier M.K., and Shirley B.W. 1996 Analysis of flavanone 3-hydroxylase in *Arabidopsis* seedlings: Coordinate regulation with chalcone synthase and chalcone isomerase. Plant Physiol. 111:339–345.

Pelletier M.K., Burbulis I.E., Winkel-Shirley B. 1999 Disruption of specific flavonoid genes enhances the accumulation of flavonoid enzymes and end-products in *Arabidopsis* seedlings. Plant Mol. Biol. 40:45–54.

Peters C., Bayer M.J., Buhler S., Andersen J.S., Mann M., Mayer A. 2001 Trans-complex formation by proteolipid channels in the terminal phase of membrane fusion. Nature 409:581–588.

Pietta P.G. 2000 Flavonoids as antioxidants. J Nat Prod. 63:1035-1042.

Pourcel L., Routaboul J.M., Kerhoas L., Caboche M., Lepiniec L., Debeaujon I. 2005 TRANSPARENT TESTA10 encodes a laccase-like enzyme involved in oxidative polymerization of flavonoids in *Arabidopsis* seed coat. Plant Cell 17:2966-2980.

Quattrocchio F., Wing J., van der Woude K., Souer E., de Vetten N., Mol J., Koes R. 1999 Molecular analysis of the anthocyanin2 gene of petunia and its role in the evolution of flower color. Plant Cell 11:1433-1444.

Rataboul P., Alibert G., Boller T., Boudet A.M. 1985 Intracellular transport and vacuolar accumulation of o-coumaric acid glucoside in *Melitolus alba* mesophyll cell protoplasts. Biochim Biophys Acta 816:25–36.

Rea P.A. 1999 MRP subfamily ABC transporters from plants and yeast. J. Exp. Bot. 50:895-913.

Rerie W.G., Feldmann K.A., Marks M.D. 1994 The *GLABRA2* gene encodes a homeodomain protein required for normal trichome development in *Arabidopsis*. Genes Dev 8:1388–1399.

Rice-Evans C.A., Miller N.J., Paganga G. 1997 Antioxidant properties of phenolic compounds. Trends Plant Sci. 2:152–159.

Robinson D.G., Hoh B., Hinz G., Jeong B.-K. 1995 One vacuole or two vacuoles: do protein storage vacuoles arise *de novo* during pea cotyledon development? J. Plant Physiol. 145:654–664.

Rogers E.E. and Guerinot M.L. 2002 FRD3, a member of the multidrug and toxin efflux family, controls iron deficiency responses in *Arabidopsis*. Plant Cell 14:1787-1799.

Sagasser M., Lu G.H., Hahlbrock K., Weisshaar B. 2002 *Arabidopsis thaliana* TRANSPARENT TESTA 1 is involved in seed coat development and defines the WIP subfamily of plant zinc finger proteins. Genes & Development 16:138-149.

Saint-Jore C.M., Evins J., Batoko H., Brandizzi F., Moore I., Hawes C. 2002 Redistribution of membrane proteins between the Golgi apparatus and endoplasmic reticulum in plants is reversible and not dependent on cytoskeletal networks. Plant J. 29:661–78.

Sanchez-Fernandez R., **Ardiles-Diaz W.**, **Van Montagu M.**, **Inze D.**, **May M.J.** 1998 Cloning and expression analyses of AtMRP4, a novel MRP-like gene from *Arabidopsis thaliana*. Mol Gen Genet. 258(6):655-62.

Sanchez-Fernandez R., Davies T.G.E., Coleman J.O.D., Rea P.A. 2001 The *Arabidopsis thaliana* ABC protein superfamily,a complete inventory. J. Biol. Chem. 276:30231-30244.

Saslowsky D. and Winkel-Shirley B. 2001 Localization of flavonoid enzymes in *Arabidopsis* roots. Plant J. 27:37-48.

Schoenbohm C., Martens S., Eder C., Forkmann G., Weisshaar B. 2000 Identification of the *Arabidopsis thaliana* flavonoid 3'-hydroxylase gene and functional expression of the encoded P_{450} enzyme. Biological Chemistry 381:749–753.

Schumacher K., Vafeados D., McCarthy M., Sze H., Wilkins T., Chory J. 1999 The *Arabidopsis det3* mutant reveals a central role for the vacuolar H^+-ATPase in plant growth and development. Genes Dev. 13:3259–3270.

Shikazono N., Yokota Y., Kitamura S., Suzuki C., Watanabe H., Tano S., Tanaka A. 2003 Mutation rate and novel *tt* mutants of *Arabidopsis thaliana* induced by carbon. Genetics 163:1449-1455.

Shitan N., Bazin I., Dan K., Obata K., Kigawa K., Ueda K., Sato F., Forestier C., Yazaki K. 2003 Involvement of CjMDR1, a plant MDRtype ABC protein, in alkaloid transport in *Coptis japonica*. PNAS 100:751-756.

Shirley B.W., Hanley S., Goodman H.M. 1992 Effects of ionizing-radiation on a plant genome - analysis of 2 *Arabidopsis* transparent-testa mutations. Plant Cell 4:333-347.

Shirley B.W., Kubasek W.L., Storz G., Bruggemann E., Koornneef M., Ausubel F.M., Goodman H.M. 1995a Analysis of *Arabidopsis* mutants deficient in flavonoid biosynthesis. Plant J. 8:659-671.

Shirley B.W. 1996 Flavonoid biosynthesis: 'New' functions for an 'old' pathway. Trends Plant Sci. 1:377-382.

Snyder B.A., and Nicholson R.L. 1990 Synthesis of phytoalexins in sorghum as a site specific response to fungal ingress. Science 248:1637-1639.

Staehelin L.A., Moore I. 1995 The plant Golgi apparatus: structure, functional organization and trafficking mechanisms. Annu. Rev. Plant Physiol. Plant Mol. Biol. 46:261–88.

Staford H.A. 1991 Flavonoid evolution: an enzymatic approach. Plant Physiology 96: 680–685.

Steinmetz K.A., and Potter J.D. 1996 Vegetables, fruit, and cancer prevention: A review. J. Am. Diet. Assoc. 96:1027–1039.

Steppuhn A., Gase K., Krock B., Halitschke R., Baldwin I.T. 2004 Nicotine's defensive function in nature. PLoS Biol 2(8):e217.

Surpin M., Zheng H., Morita M.T., Saito C., Avila E., Blakeslee J.J., Bandyopadhyay A., Kovaleva V., Carter D., Murphy A.,Tasaka M., Raikhel N. 2003 The VTI family of SNARE proteins is necessary for plant viability and mediates different protein transport pathways. Plant Cell 15:2885–2899.

Surpin M., and Raikhel N. 2004 Traffic jams affect plant development and signal transduction. Nat. Rev. Mol. Cell Biol. 5:100–109.

Sze H., Li X., Palmgren M.G. 1999 Energization of plant cell membranes by Hþ-pumping ATPases. Regulation and biosynthesis. Plant Cell 11:677–690.

Sze H., Schumacher K., Muller M.L., Padmanaban S., Taiz L. 2002 A simple nomenclature for a complex proton pump VHA genes encode the vacuolar H^+-ATPase. Trends Plant Sci. 7:157–161.

Theodoulou F.L. 2000 Plant ABC transporters. Biochim Biophys Acta 1465:79–103

Tommasini R., Vogt E., Fromenteau M., Hortensteiner S., Matile P., Amrhein N., Martinoia E. 1998 An ABC-transporter of *Arabidopsis thaliana* has both glutathione-conjugate and chlorophyll catabolite transport activity. Plant J. 13:773–780.

Trevisanato S.I., and Kim Y.I. 2000 Tea and health. Nutr. Rev. 58:1–10.

Tse Y.C., Mo B., Hillmer S., Zhao M., Lo S.W., Robinson D.G., Jiang L. 2004 Identification of multivesicular bodies as prevacuolar compartments in *Nicotiana tabacum* BY-2 Cells. Plant Cell 16:672-693.

Ueda T., Yamaguchi M., Uchimiya H., Nakano A. 2001 Ara6, a plant-unique novel type Rab GTPase, functions in the endocytic pathway of *Arabidopsis thaliana*. EMBO J. 20:4730–41

van den Brule S., Muller A., Fleming A.J., Smart C.C. 2002 The ABC transporter SpTUR2 confers resistance to the antifungal diterpene sclareol. Plant J. 30:649-662.

Vitale A., and Raikhel N.V. 1999 What do proteins need to reach different vacuoles? Trends Plant Sci. 4:149–155.

Walczak H.A., Dean J.V. 2000 Vacuolar transport of the glutathione conjugate of trans-cinnamic acid. Phytochemistry 53:441-446.

Walker A.R., Davison P.A., Bolognesi-Winfield A.C., James C.M., Srinivasan N., Blundell T.L., Esch J.J., Marks M.D., Gray J.C. 1999 The *TRANSPARENT TESTA GLABRA1* locus, which regulates trichome differentiation and anthocyanin biosynthesis in *Arabidopsis*, encodes a WD40 repeat protein. Plant Cell 11:1337–1349.

Weisshaar B., and Jenkins G.I. 1998 Phenylpropanoid biosynthesis and its regulation. Curr. Opin. Plant Biol. 1:251–257.

Wickner W., and Haas A. 2000 Yeast homotypic vacuole fusion: A window on organelle trafficking mechanisms. Annu. Rev. Biochem. 69, 247–275.

Williams C.A., Grayer R.J. 2004 Anthocyanins and other flavonoids. Natural Products Repopts 21:539–573.

Wink M. 1997 Compartmentation of secondary metabolites and xenobiotics in plant vacuoles. Advances in Botanical Research Incorporating Advances in Plant Pathology **25**:141-169.

Winkel-Shirley B. 1998 Flavonoids in seeds and grains: Physiological function, agronomic importance and the genetics of biosynthesis. Seed Sci. Res. 8:415–422.

Winkel-Shirley B. 1999 Evidence for enzyme complexes in the phenylpropanoid and flavonoid pathways. Physiologia Plantarum 107:142–149.

Winkel-Shirley B. 2001 Flavonoid biosynthesis. A colorful model for genetics, biochemistry, cell biology, and biotechnology. Plant Physiol. 126:485–493.

Winkel-Shirley B. 2002 A mutational approach to dissection of flavonoid biosynthesis in *Arabidopsis*. In Recent Advances in Phytochemistry:Proceedings of the Annual Meeting of the Phytochemical Society of North America, Vol. 36, J.T. Romeo, ed (New York:Elsevier), pp. 95–110.

Wisman E., Hartmann U., Sagasser M., Baumann E., Palme K., Hahlbrock K., Saedler H., Weisshaar B. 1998 Knock-out mutants from an En-1 mutagenized *Arabidopsis thaliana* population generate phenylpropanoid biosynthesis phenotypes. PNAS 95:12432–12437.

Xie D.Y., Sharma S.B., Paiva N.L., Ferreira D., Dixon R.A. 2003 Role of anthocyanidin reductase, encoded by BANYULS in plant flavonoid biosynthesis. Science 299:396-399.

Xu X.J., Su X.Z., Morita Y., Kuroda T., Mizushima T., Tsuchiya T. 2003 Molecular cloning and characterization of the HmrM multidrug efflux pump from *Haemophilus influenzae* Rd. Microbiol Immunol. 47(12):937-43

Yazaki K. 2004 Natural products and metabolites. In Handbook of Plant Biotechnology, vol 2. Edited by Klee H, Christou P. John Wiley & Sons Ltd; pp 811-857.

Zhao P., Inoue K., Kouno I., Yamamoto H. 2003 Characterization of leachianone G 2”-dimethylallyltransferase, a novel prenyl side-chain elongation enzyme for the formation of the lavandulyl group of sophoraflavanone G in *Sophora flavescens* Ait. cell suspension cultures. Plant Physiol. 133:1306-1313.

Zhang F., Gonzalez A., Zhao M., Payne C.T., Lloyd A. 2003 A network of redundant bHLH proteins functions in all TTG1-dependent pathways of *Arabidopsis*. Development. 130(20):4859-69.

Zobel A.M., Maxwell C., Kuras M., Tykarska T. 1990 Phenolic compounds as a defence system in covering tissue of plant shoot. Joint Meeting of Canadian Botanical Association and American Botanical Society, Windsor, Canada.

Zobel A.M., Nighswander J.E. 1990 Accumulation of phenolic compounds in the necrotic areas of austrian and red pine needles due to salt spray. Annals of Botany 66: 629-640.

Zobel A.M., Chen Y., Brown S.A. 1994a Influence of UV on furanocoumarins in *Ruta graäeolens* leaves. Acta Hortica 381:355-360.

Zobel A.M., Crelin J., Brown S.A., Glowniak K. 1994b Concentration of furanocoumarins under stress conditions and their histological localization. Acta Hortica 381:510-516.

Zobel A.M., Brown S.A. 1995 Coumarins in the interactions between the plant and its environment. Allelopathy Journal 2:9-20.

Chapter 2

This article is published in *The Plant Cell* Online, *The Plant Cell* Preview Section, which publishes manuscripts accepted for publication after they have been edited and the authors have corrected proofs, but before the final, complete issue is published online. Early posting of articles reduces normal time to publication by several weeks.

The *Arabidopsis* MATE Transporter TT12 Acts as a Vacuolar Flavonoid/H^+-Antiporter Active in Proanthocyanidin-Accumulating Cells of the Seed Coat [W]

Krasimira Marinova,[a,1] Lucille Pourcel,[b] Barbara Weder,[a] Michael Schwarz,[c] Denis Barron,[d] Jean-Marc Routaboul,[b] Isabelle Debeaujon,[b] and Markus Klein[a,2]

[a] Zurich Basel Plant Science Center, University of Zurich, CH 8008 Zurich, Switzerland
[b] Seed Biology Laboratory, Jean-Pierre Bourgin Institute, Unité Mixte de Recherche 204 Institut National de la Recherche Agronomique/AgroParisTech, Center of Versailles-Grignon, F 78026 Versailles Cedex, France
[c] Technical University of Braunschweig, Institute of Food Chemistry, D 38106 Braunschweig, Germany
[d] Nestlé Research Center, CH 1000 Lausanne 26, Switzerland.

Phenotypic characterization of the *Arabidopsis thaliana transparent testa12* (*tt12*) mutant encoding a membrane protein of the multidrug and toxic efflux transporter family, suggested that TT12 is involved in the vacuolar accumulation of proanthocyanidin precursors in the seed. Metabolite analysis in *tt12* seeds reveals an absence of flavan-3-ols and proanthocyanidins together with a reduction of the major flavonol quercetin-3-*O*-rhamnoside. The *TT12* promoter is active in cells synthesizing proanthocyanidins. Using translational fusions between TT12 and green fluorescent protein, it is demonstrated that this transporter localizes to the tonoplast. Yeast vesicles expressing *TT12* can transport the anthocyanin cyanidin-3-*O*-glucoside in the presence of MgATP but not the aglycones cyanidin and epicatechin. Inhibitor studies demonstrate that *TT12* acts in vitro as a cyanidin-3-*O*-glucoside/H^+-antiporter. TT12 does not transport glycosylated flavonols and procyanidin dimers, and a direct transport activity for catechin-3-*O*-glucoside, a glucosylated flavan-3-ol, was not detectable. However, catechin-3-*O*-glucoside inhibited TT12-mediated transport of cyanidin-3-*O*-glucoside in a dose-dependent manner, while flavan-3-ol aglycones and glycosylated flavonols had no effect on anthocyanin transport. It is proposed that TT12 transports glycosylated flavan-3-ols in vivo. Mutant *banyuls* (*ban*) seeds accumulate anthocyanins instead of proanthocyanidins, yet the *ban tt12* double mutant exhibits reduced anthocyanin accumulation, which supports the transport data suggesting that TT12 mediates anthocyanin transport in vitro.

INTRODUCTION

Plants synthesize secondary metabolites for a multitude of biological functions, including UV protection or insect attraction via flower coloration. Since these functions are mostly dose dependent, secondary compounds accumulate constitutively or inducibly and often in a tissue- or cell-specific manner to concentrations starting in the millimolar range. At the same time, phenolic compounds are toxic to the cell due to their high chemical reactivity and protein denaturing properties (Matile, 1984). The major strategy of the plant to protect the cytosolic machinery against these toxic effects is the targeting of secondary metabolites in compartments with lower biosynthetic activity, notably the extracellular space and the large central vacuole. For many phenolic compounds, vacuolar accumulation is usually preceded by oxidation reactions mediated by cytochrome P450-dependent monoxygenases or dioxygenases and followed by conjugation to small hydrophilic (e.g., glycosyl) groups resulting in more water-soluble compounds (Coleman et al., 1997).

Flavonoids representing one class of phenolic compounds possess diverse chemical structures but share a common C6-C3-C6 body. Major classes are the monomeric red to purple anthocyanins in flowers and fruits that often form color-shifted copigments with UV-absorbing colorless to pale yellow flavonols or flavones (Harborne and Williams, 2000) and condensed tannins (proanthocyanidins [PAs]), which are colorless polymers of flavan-3-ols (e.g., epicatechin) that become brown after oxidation. Flavonoids appeared in the first land plants during evolution. In angiosperms, flavonoids are associated with sexual reproduction via pollination, seed dispersal, germination, and longevity (Debeaujon et al., 2000). In *Arabidopsis thaliana*, anthocyanins are found in sporophytic tissues but not in seeds, while the accumulation of PAs is restricted to PA-producing cells of the seed coat, and flavonols can be found in all plant parts (Shirley et al., 1995; Devic et al., 1999; Debeaujon et al., 2003; Routaboul et al., 2006). A histochemical analysis of developing *Arabidopsis*

[1] Current address: Clinical Pharmacology and Toxicology, Division of Internal Medicine, University Hospital Zurich, Ramistrasse 100, CH 8091 Zurich, Switzerland.
[2] To whom correspondence should be addressed. E-mail mklein@botinst.uzh.ch; fax 41-44-634-82-04.
The author responsible for distribution of materials integral to the findings presented in this article in accordance with the policy described in the Instructions for Authors (www.plantcell.org) is: Markus Klein (mklein@botinst.uzh.ch).
[W] Online version contains Web-only data.
www.plantcell.org/cgi/doi/10.1105/tpc.106.046029

seeds suggested that PA accumulation is found in three different cell types: (1) in the innermost layer of the inner integument (ii1 layer or endothelium), (2) in a few cells of the ii2 layer at the micropyle, and (3) in cells forming the pigment strand at the chalaza (Debeaujon et al., 2003). Mutants deviating from the normal brown seed color arising from the oxidation of the colorless PAs at maturity have been termed *transparent testa* (*tt*), *transparent testa glabra* (*ttg*), *tannin deficient seeds* (*tds*), *banyuls* (*ban*), and *aha10* (Lepiniec et al., 2006). Figure 1 displays a partial model of the flavonoid biosynthetic pathway in *Arabidopsis*. The *BAN* gene has recently been described to encode anthocyanidin reductase separating the anthocyanin and flavan-3-ol-derived (PA) side branches of the flavonoid pathway (Xie et al., 2003). It is essentially active in PA-producing cells of the seed coat (Debeaujon et al., 2003). Another gene, *TT10*, which encodes a laccase involved in oxidative flavonoid polymerization in late stages of seed development, is expressed mainly in PA-producing cells and the outer integument (Pourcel et al., 2005). By contrast, several mutants, such as *tt4*, *tt5*, *tt7*, and *tt18*/*tds4*, exhibit changes in overall flavonoid composition in vegetative tissues apart from affecting PA biosynthesis in the seed coat (Lepiniec et al., 2006).

With regard to secondary metabolites, biochemical analysis of vacuolar uptake mechanisms has led to the proposition of different transport and accumulation systems (Grotewold, 2004; Yazaki, 2005). Available data suggest that (1) vacuolar accumulation can involve trapping mechanisms, such as trapping of conformational isomers; (2) the conjugated moieties, such as sugar or acyl residues, are important determinants of transport specificity; and (3) plants possess specific transporters for their endogenously synthesized compounds as opposed to xenobiotic compounds possessing comparable conjugation patterns. Different transport mechanisms exist depending on the plant species chosen: while barley (*Hordeum vulgare*) uses a H^+-antiport mechanism for the vacuolar uptake of endogenous glucosylated flavones, *Arabidopsis*, which does not synthesize flavones, uses an ATP binding cassette (ABC)–type directly energized vacuolar transport when supplied with barley flavones (Klein et al., 1996). In accordance with this latter observation, *Zea mays* plants with a reduced amount of transcript of the vacuolar ABC transporter Zm *MRP3* exhibit reduced levels of anthocyanin accumulation in different plant parts (Goodman et al., 2004).

Vacuolar compartmentation and associated transport steps are important for proper flavonoid accumulation. Furthermore, in *H. vulgare* mesophyll cells, vacuolar flavonoid transport is directly controlled by the presence of the intact flavonoid biosynthetic pathway, suggesting that a biosynthetic intermediate posttranslationally activates the flavonoid transporter (Marinova et al., 2007). However, the molecular identity of the membrane proteins involved in flavonoid transport is just starting to be uncovered. A T-DNA insertion in the *TT12* gene (At3G59030 or At *DTX41*) identified the first transporter-like membrane protein involved in PA biosynthesis as *tt12* seeds lack accumulation of the flavan-3-ol epicatechin and PAs in vacuoles of the seed coat endothelium (Debeaujon et al., 2001). *TT12* encodes a membrane protein with 12 predicted transmembrane helices and belongs to the multidrug and toxic compound extrusion (MATE) family (Brown et al., 1999). MATE proteins in prokaryotes, as exemplified by the NorM multidrug resistance protein from *Vibrio parahaemolyticus* and its homolog in *Escherichia. coli*, YdhE, mediate resistance against diverse drugs, including fluoroquinolone antibiotics (Morita et al., 1998). Functionally, NorM has been described as a Na^+-driven multidrug efflux pump (Morita et al., 2000). *MATE1*, one of two orthologous genes in humans, encodes a transporter-mediating H^+-coupled cellular efflux of toxic organic cations, such as tetraethylammonium, and thus represents the polyspecific organic cation exporter that transports toxic organic cations into urine and bile (Otsuka et al., 2005). In *Arabidopsis*, the MATE family consists of 56 genes (Li et al., 2002; Rogers and Guerinot, 2002). Apart from *TT12*, four *MATE* genes have been initially characterized by mutant analysis. They are involved in lateral root formation (*ALF5*/At *DTX19*; Diener et al., 2001), iron homeostasis (*FRD3*/At *DTX43*; Rogers and Guerinot, 2002), or disease resistance (*EDS5*/At *DTX47*; Nawrath et al., 2002). Complementation of the norfloxacin-hypersensitive *E. coli* strain KAM3, lacking the multidrug efflux pump AcrAB, resulted in functional cloning of At *DTX1* (Li et al., 2002). Notably, recent evidence suggests that FRD3 is responsible for citrate secretion into the xylem and the rhizosphere, which extends the spectrum of potential substrates of MATE transporters from toxic substances or secondary compounds also to primary metabolites (Durrett et al., 2007).

Here, we identify the TT12 MATE transporter as a tonoplastic membrane protein with a clear biochemical function in the vacuolar deposition of flavonoids in the PA-synthesizing cells of the *Arabidopsis* seed coat. The substrate specificity of TT12 suggests that it mediates the transport of monomeric glycosylated flavan-3-ols as PA precursors in vivo, while it is able to transport anthocyanins in vitro as long as they are glycosylated. Mechanistically, TT12 acts as a proton antiporter.

RESULTS

Seeds of *tt12* Have an Altered Flavonoid Metabolite Composition

It was previously demonstrated that *tt12* seeds exhibit a defect in the vacuolar accumulation of PAs in immature seeds (Debeaujon et al., 2001). Apart from PAs, other flavonoid compounds, including flavonols, are synthesized during seed development in a cell type–specific manner (Pourcel et al., 2005; Kerhoas et al., 2006; Routaboul et al., 2006). To investigate the changes in the flavonoid composition in seeds caused by the absence of the TT12 MATE transporter, we performed a targeted metabolite analysis of mature wild-type and *tt12* seeds by liquid chromatography–mass spectrometry (LC-MS).

In contrast with the wild type, neither the PA precursor epicatechin nor PA polymers (dimers to heptamers) were detected in *tt12* seeds (Figure 2B). Acid-catalyzed hydrolysis of flavonoid extract and pellet remaining after extraction demonstrated that *tt12* mutant seeds contained a small amount of PAs in the insoluble fraction (~15% of the wild-type PAs) but no PAs in the soluble fraction (Figure 2C). Thus, absence of the transport activity mediated by TT12 ultimately leads to absence of epicatechin and its polymers in *tt12* seeds.

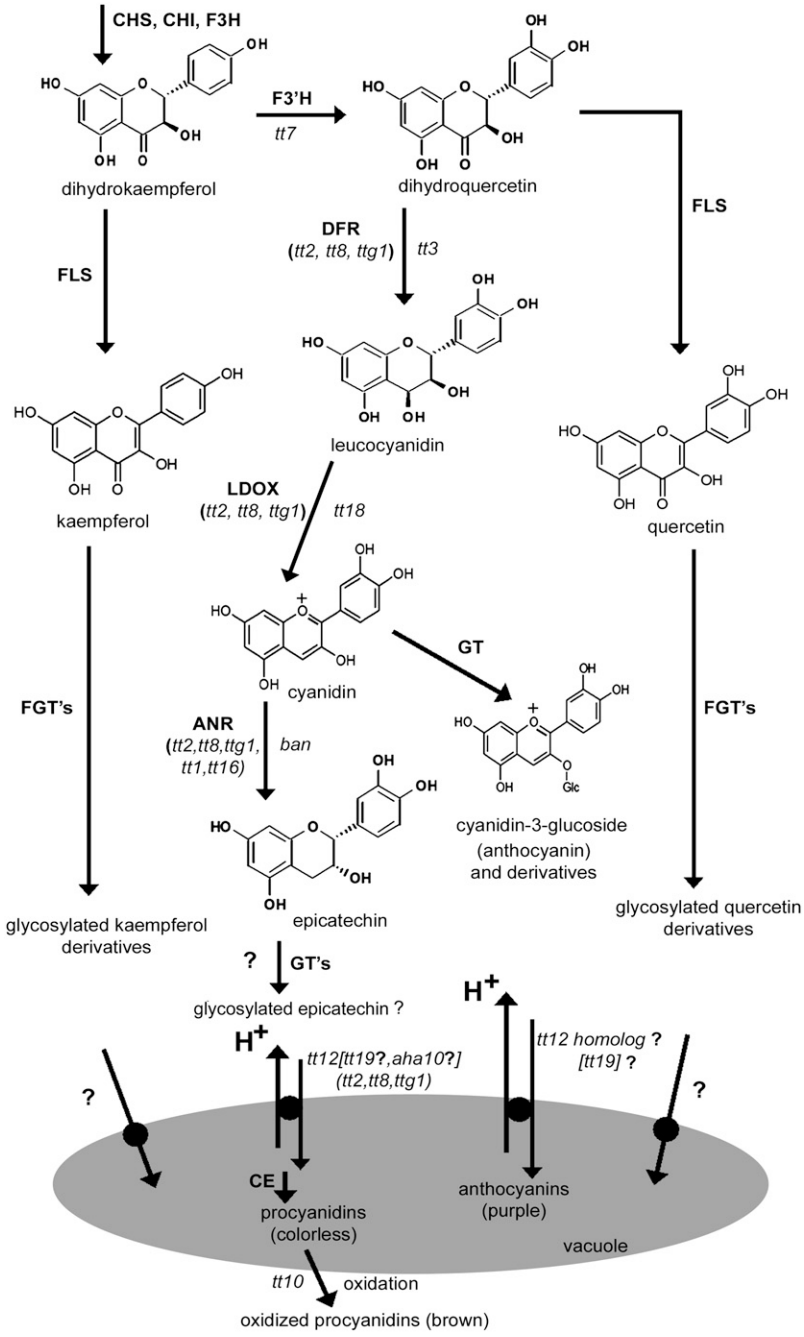

Figure 1. Simplified Scheme of the Biosynthetic Pathway in *Arabidopsis* Leading to PAs, Flavonols, and Anthocyanins, Including Proposed Vacuolar Transport Steps.

Dihydrokaempferol is synthesized from 4-coumaroyl CoA and three molecules of malonyl CoA by the sequential action of chalcone synthase (CHS), chalcone isomerase (CHI), and flavanone 3-hydroxylase (F3H). Enzymes are represented in uppercase bold letters. Corresponding genetic mutations are in lowercase italic letters. Regulatory mutants are indicated by parentheses. AHA10, P-type H^+-ATPase; ANR, anthocyanidin reductase; CE, condensing enzyme; DFR, dihydroflavonol reductase; F3′H, flavonol 3′-hydroxylase; FLS, flavonol synthase; (F)GT, (flavonol) glycosyltransferase; LDOX, leucoanthocyanidin dioxygenase.

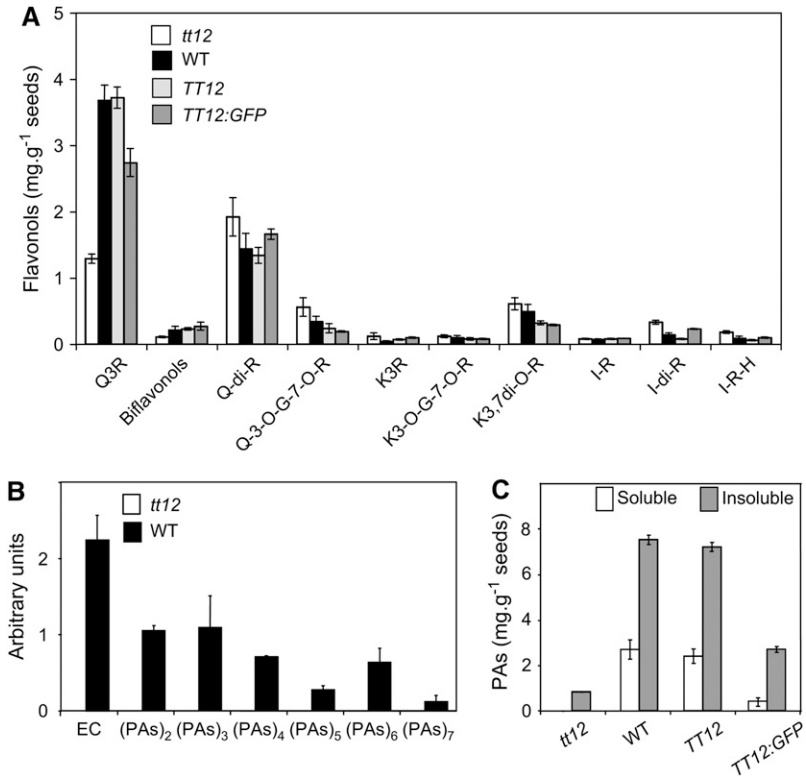

Figure 2. Flavonoid Composition of Mature Seeds.

(A) Flavonol composition of seeds from the *tt12* mutant, the wild type, *TT12* overexpressor (*TT12*), and *GFP5:TT12* overexpressor. Values represent the average and SE of six independent measurements. Q-di-R, quercetin-3,7-di-*O*-rhamnoside; G, glucoside; H, hexoside; I, isorhamnetin; K, kaempferol; Q, quercetin; R, rhamnoside.

(B) Detection of epicatechin and soluble PAs (dimers to heptamers) by LC-MS. EC, epicatechin.

(C) Analysis of soluble and insoluble PAs measured after acid-catalyzed hydrolysis.

For **(B)** and **(C)**, values represent the average and SE of three independent measurements.

Wild-type seeds contained glycosylated quercetin and kaempferol derivatives, with quercetin-3-*O*-rhamnoside (Q3R) being quantitatively the most prominent compound, followed by quercetin-3,7-di-*O*-rhamnoside and kaempferol-3,7-di-*O*-rhamnoside (Figure 2A). In *tt12*, the amount of Q3R and biflavonols (dimers of Q3R) was reduced to ~30 and 50% of wild-type levels, respectively, while the quantities of all other flavonols were not significantly affected by the *tt12* mutation.

The *TT12* Promoter Is Active Only in PA-Accumulating Cells

Previous in situ hybridization studies detected *TT12* mRNA in the endothelium at ~3 to 4 d after flowering (DAF) (Debeaujon et al., 2001). To specify the spatio-temporal expression pattern of *TT12* during seed development, we analyzed the *TT12* promoter activity using a 1.8-kb genomic fragment corresponding to the putative *TT12* promoter region (*ProTT12*) together with the 5′ untranslated region fused to the *uidA* reporter gene. β-Glucuronidase (GUS) activity was analyzed in seeds at different stages of development. Faint GUS activity was restricted to the inner integument close to the micropyle on the day of flowering (Figure 3A). *ProTT12:uidA* expression progressed from the micropyle within the ii1 layer (2 DAF; Figure 3B) until GUS activity was observed in all cells of the ii1 layer and in cells of the chalaza from 3 DAF on (Figures 3C to 3E and 3G). Sectioning of immature transgenic *ProTT12:uidA* seeds 3 DAF confirmed *TT12* expression in the ii1 layer of the seed coat, in chalazal cells, and in ii2 cells at the micropylar end (Figure 3G). At 6 DAF, GUS activity decreased in all cell types (Figure 3F). Taken together, *TT12* is expressed specifically in cells actively synthesizing PAs in developing seeds, and *TT12* expression correlates with the expression of *BAN* (Debeaujon et al., 2003).

TT12 Is Localized to the Tonoplast

To examine the subcellular localization of TT12, the full-length *TT12* cDNA was fused to the coding sequence of *GFP5*, resulting in N- and a C-terminal fusion of green fluorescent protein (GFP) to TT12. Expression of both fusions was driven by the dual cauliflower mosaic virus 35S RNA promoter (*Pro35Sdual:GFP5:TT12:t35S* and *Pro35Sdual:TT12:GFP5:t35S* simplified as *GFP-cTT12* and *cTT12-GFP* in Figure 4, respectively) and analyzed after both stable and transient expression in plants. While expression of the unmodified *TT12* cDNA fully complemented the

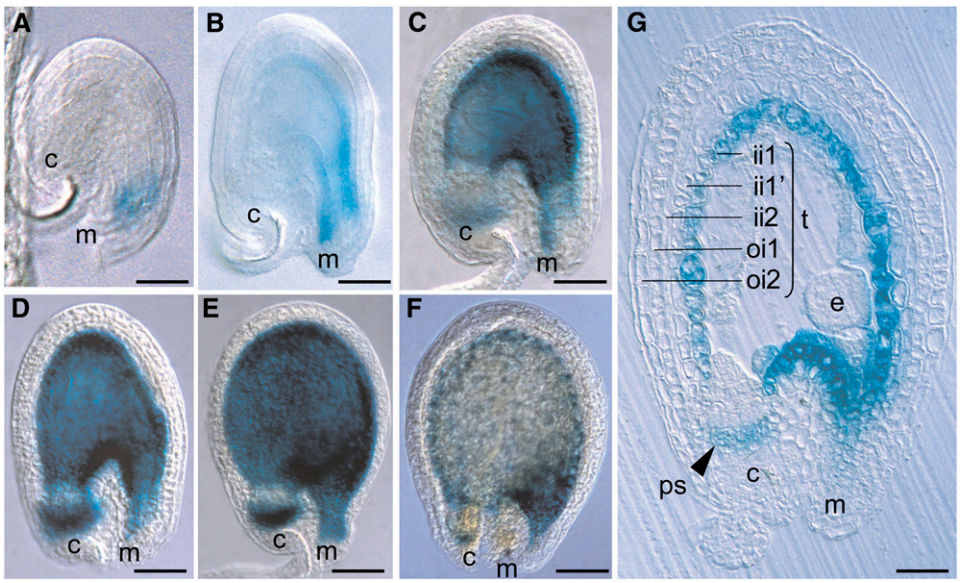

Figure 3. Activity of the TT12 Promoter in Wild-Type Developing Seeds of *Arabidopsis*.

The expression of the *ProTT12:uidA* cassette was exclusively observed in developing seeds at 0 DAF **(A)**, 2 DAF **(B)**, 3 DAF (**[C]** and **[G]**), 4 DAF **(D)**, 5 DAF **(E)**, and 6 DAF **(F)**. GUS activity was observed with Nomarski optics on whole mounts for **(A)** to **(F)** and on section for **(G)**. The ii1 layer is also called endothelium. c, chalaza; e, embryo; ii, inner integument; m, micropyle; oi, outer integument; ps, pigment strand (chalazal tissue); t, testa. Bar = 25 μm in **(A)**, 40 μm in **(B)**, 65 μm in **(C)**, 70 μm in **(D)**, 80 μm in **(E)** and **(F)**, and 33 μm in **(G)**.

tt12 mutant phenotype (including returning Q3R and insoluble and soluble PAs to wild-type levels; Figure 2), the *Pro35S-dual:GFP5:TT12:t35S* construct restored flavonoid levels at ~75, 37, and 20% of the wild-type amount of Q3R and insoluble and soluble PAs, respectively (Figure 2), suggesting that a significant portion of GFP-cTT12 protein reached its proper destination within the cell and was functional.

Transient expression by biolistic particle delivery of *GFP-cTT12* together with the established tonoplast marker *TPK1* (Czempinski et al., 2002) fused to *DsRed2* in onion bulb epidermis cells demonstrated that both proteins coreside on membranes (see Supplemental Figure 1A online). Importantly, fluorescence of both fusion proteins is visible on strands traversing the vacuole. Transient expression of a translational GFP fusion of the *Arabidopsis* P31 protein (At3G01290), a protein containing prohibitin motives that was recently localized to the plasmalemma based on a plasma membrane–proteomic approach and verified by microscopy analysis of the corresponding GFP fusion (Marmagne et al., 2004), exhibited GFP fluorescence restricted to the cell periphery (see Supplemental Figure 1B online). In contrast with *GFP-cTT12* and *DsRed2-TPK1*, *P31-GFP*-fluorescence was not detectable on transvacuolar strands, suggesting that TT12, in contrast with P31, does not reside on the plasmalemma.

The localization of TT12 was further investigated by transient expression of both *TT12-GFP* fusions in *Nicothiana benthamiana* leaves by infiltration of agrobacteria followed by isolation of mesophyll protoplasts (Figures 4A and 4B). The GFP signal obtained after expression of *cTT12-GFP* is restricted to a membrane that intracellularly surrounds the chloroplasts exhibiting red autofluorescence (Figure 4A). Gentle lysis of these mesophyll protoplasts demonstrates clearly that the GFP fluorescence surrounds the vacuole and thus localizes to the tonoplast (Figure 4B). This localization was identical when the N-terminal GFP fusion *GFP-cTT12* was expressed, suggesting that the position of the GFP did not affect the targeting of the fusion protein (data not shown). As a control, *TPK1* was separately expressed as a translational fusion with GFP fusion (Figure 4C). *cTPK1-GFP* fluorescence in *N. benthamiana* mesophyll protoplasts was restricted to the vacuolar membrane surrounding plastids and the nucleus, and its localization was therefore similar to TT12.

Confocal microscopy analysis of *tt12* mutants ectopically expressing the *GFP-cTT12* transgene exhibited membrane-bound GFP fluorescence in different tissues, such as roots or epidermis cells. Figure 4D illustrates GFP fluorescence of *GFP-cTT12* on internal membranes of a root tip. Detailed inspection of single root cells in the apex of the primary root verified the presence of *GFP-cTT12* on the tonoplast: GFP-fluorescence surrounded the vacuoles as seen after counterstaining of the cell walls with propidium iodide (red) (Figure 4E). When mesophyll protoplasts were isolated from these transgenic plants, GFP fluorescence of *GFP-cTT12* was again visible on the intracellular membrane delimiting the vacuole and excluding the red autofluorescent chloroplasts (Figure 4F and Supplementary Figure 1C). Finally, tonoplast localization of GFP-cTT12 was confirmed by isolation of vacuoles starting from mesophyll protoplasts of transgenic *Pro35Sdual:GFP5:TT12:t35S/tt12* plants. GFP fluorescence was detected on the membrane surrounding the vacuole (Figure 4G). Taken together, TT12 localizes to the tonoplast in plant cells.

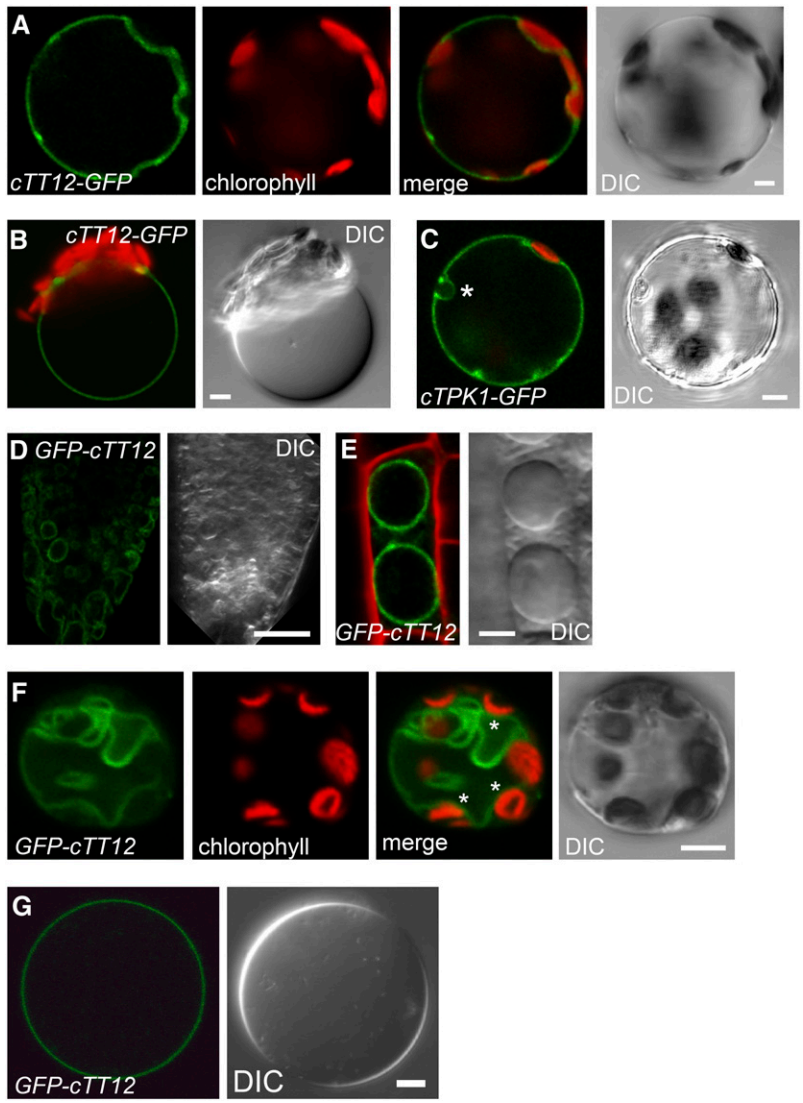

Figure 4. Subcellular Localization of the TT12 Protein after Transient and Stable Expression.

(A) to **(C)** Mesophyll protoplasts isolated after transient expression of *cTT12-GFP* (**[A]** and **[B]**) or the tonoplast control *cTPK1-GFP* **(C)** by infiltration of *N. benthamiana* leaves with agrobacteria carrying the corresponding constructs. DIC, differential interference contrast. Bars = 5 μm.
(A) GFP and chlorophyll autofluorescence were false-colored in green and red, respectively. GFP fluorescence surrounds the plastids (see merged image).
(B) A vacuole released by gentle lysis exhibits GFP fluorescence on the tonoplast.
(C) Transient *cTPK1-GFP* expression is similar to *cTT12-GFP*, resulting in GFP fluorescence surrounding plastids and the nucleus (asterisk).
In **(B)** and **(C)**, the green GFP and the red chlorophyll autofluorescence channels are merged.
(D) to **(G)** Confocal microscopy of *Arabidopsis* roots (**[D]** and **[E]**), mesophyll protoplasts **(F)**, and isolated vacuoles **(G)** after stable transformation of *GFP-cTT12* in the *tt12* background.
(D) GFP fluorescence (green) of a root tip of a 7-d-old seedling. Bar = 20 μm.
(E) Merged image of *GFP-cTT12* fluorescence (green) after propidium iodide counterstaining of cell walls (red). A single root cell possessing two large vacuoles exhibiting *GFP-cTT12* fluorescence exclusively on the tonoplast membranes is shown. Bar = 5 μm.
(F) *GFP-cTT12* fluorescence (green) is visible on an intracellular membrane surrounding the plastids exhibiting red chlorophyll autofluorescence (asterisks in the merged image) that delimits the vacuole(s) (DIC). Bar = 5 μm.
(G) Isolated leaf mesophyll vacuole prepared from stably transformed *GFP-cTT12*/*tt12* plants exhibits GFP fluorescence on the tonoplast. Bar = 5 μm.

TT12 Mediates Cyanidin-3-*O*-Glucoside Transport in Yeast Vesicles

To investigate the transport activity of TT12 biochemically, the full-length *TT12* cDNA was expressed in *Saccharomyces cerevisiae* under the control of the strong constitutive *PMA1* promoter. The presence of the TT12 protein and its subcellular localization was investigated in yeasts transformed with modified versions of *TT12*. As can be seen from the Supplemental Methods and Supplemental Figure 2 online, GFP fluorescence in yeasts cells transformed with *GFP5-cTT12* was not restricted to the vacuolar membrane but was also present on other endomembranes and the plasma membrane. Based on this result, we decided to isolate total microsomal membrane vesicles rather than vacuolar membrane vesicles for transport experiments. Using N- and C-terminally His_6-tagged versions of *TT12*, the presence of the TT12 proteins was verified in all independent yeast transformants tested (see Supplemental Figure 2B online). Finally, physiological intactness of the vesicle fractions isolated from yeasts that were either transformed with *TT12* or with the empty vector control (NEV) was confirmed by the ability of the vesicle fractions to accumulate the weak base [^{14}C]-methylamine in the presence of MgATP due to acidification of the vesicle lumen (see Supplemental Figure 2C and Supplemental Methods online). Since the uncharged methylamine base is membrane permeable but trapped inside the vesicles after protonation, this latter experiment also verifies the activity of the MgATP-dependent proton pumps regardless of the presence or absence of TT12.

Transport experiments with various structurally different flavonoids were performed with a standard substrate concentration of 1 mM using the rapid filtration technique (Tommasini et al., 1996). Since epicatechin represents the suggested immediate monomeric precursor of the PA polymers and since epicatechin is absent in *tt12* seeds (Figure 2), we first tested the flavan-3-ols epicatechin and catechin. In the presence of MgATP, no time-dependent increase in the amounts of vesicle-associated flavan-3-ols was detectable either after photometric detection (see Supplemental Figure 3 online) or HPLC analysis (data not shown). These results suggested that under our experimental conditions, these substances are not transported by TT12.

Due to the absence of a leucoanthocyanidin reductase in *Arabidopsis* seeds, only epicatechin (*cis*-flavan-3-ol) and its derivatives are synthesized in this species (Abrahams et al., 2003; Routaboul et al., 2006). In our experiments, the PA precursor epicatechin was not modified by glycosylation. It has been shown in various experimental systems that sugar residues attached to the aglycone flavonoid core are important determinants of substrate recognition and transport activity. To test the influence of a sugar moiety, a related glucosylated flavonoid, the anthocyanin cyanidin-3-*O*-glucoside (C3G), was tested as a substrate for TT12-dependent transport and compared with its aglycone cyanidin.

In the presence of MgATP and C3G, TT12-containing vesicles exhibited a time-dependent increase in the absorption spectrum maximum at 535 nm (corresponding to C3G) within 1 min of incubation, suggesting that uptake had occurred (Figure 5A). By contrast, absorption at 535 nm remained unchanged over time when vesicles isolated from empty vector–transformed yeasts were incubated with C3G and MgATP. In the absence of MgATP, no increase in absorption occurred when C3G was incubated with TT12-expressing vesicles (Figure 5B). The absorption spectra recorded after the vesicle transport experiment and filter elution were identical to authentic C3G standard (Figure 5B), which demonstrated that C3G was not subject to structural modification during TT12-mediated uptake. HPLC diode array analysis with detection at 520 nm of samples eluted from filters after transport confirmed the results of simple absorption measurements: single peaks, corresponding to C3G in retention time (Figure 5C) and absorption spectra (data not shown), increased over time only in the presence of both MgATP and TT12-containing vesicles (Figure 5D). We next investigated whether C3G transport by TT12 was time dependent. In the presence of MgATP, TT12-containing vesicles took up C3G linear with time for ~90 s, while no further increase in vesicle-associated C3G was detectable between 2 and 5 min of transport (Figure 5E). By contrast, empty vector control vesicles exhibited only a marginal increase in the amount of vesicle-associated C3G. Taken together, C3G was transported into vesicles in a TT12-dependent manner and when energization by MgATP occurred (Figure 5F).

By contrast, when cyanidin was added as substrate, no time- and TT12-dependent changes in absorption or HPLC peak sizes were observed (see Supplemental Figure 3 online). Therefore, transport via TT12 is either specific for glucosylated flavonoids or low TT12-dependent transport rates of cyanidin and the flavan-3-ols are not detected because of the background caused by unspecific flavonoid binding to the membranes.

To confirm that the absorption differences observed for C3G were related to transport as well as to elucidate the type of energization mechanism, inhibitor experiments were performed (Table 1). None of the inhibitors tested altered the baseline level of C3G transport into vesicles isolated from empty vector–transformed yeasts. C3G uptake into TT12-containing vesicles, however, was almost completely inhibited by the sulfhydryl group blocker *p*-chloromercuribenzenesulfonic acid (PCMBS) (Bush, 1993). In the presence of NH_4Cl-disrupting pH gradients or bafilomycin A1, a specific inhibitor of the vacuolar H^+-ATPase (Dröse and Altendorf, 1997), C3G uptake was strongly reduced to ~15% of the control or completely abolished, respectively. Therefore, TT12-mediated C3G uptake depends on a proton gradient established by the vacuolar proton pump and acts in vitro as a C3G/H^+-antiporter.

To further investigate the substrate specificity of TT12-mediated transport, we next tested the glycosylated flavonols Q3R, quercetin-3-*O*-glucoside (Q3G), and the procyanidin dimers B1 and B2. In our vesicle uptake assay, all of these flavonoids were not transported (Table 2; see Supplemental Figure 3 online).

Due to the specific expression of *TT12* in the seed coat (Figure 3), a direct comparison of vacuolar transport activities using wild-type and mutant vacuoles is technically impossible. In an attempt to avoid heterologous expression, we isolated mesophyll vacuoles from the wild type and plants ectopically expressing *ProCaMV35S:TT12* in the *tt12* background to directly demonstrate the transport activity of TT12 in planta. However, anthocyanins and flavan-3-ols almost quantitatively formed precipitates in the presence of Percoll or Ficoll, which are osmotically inactive

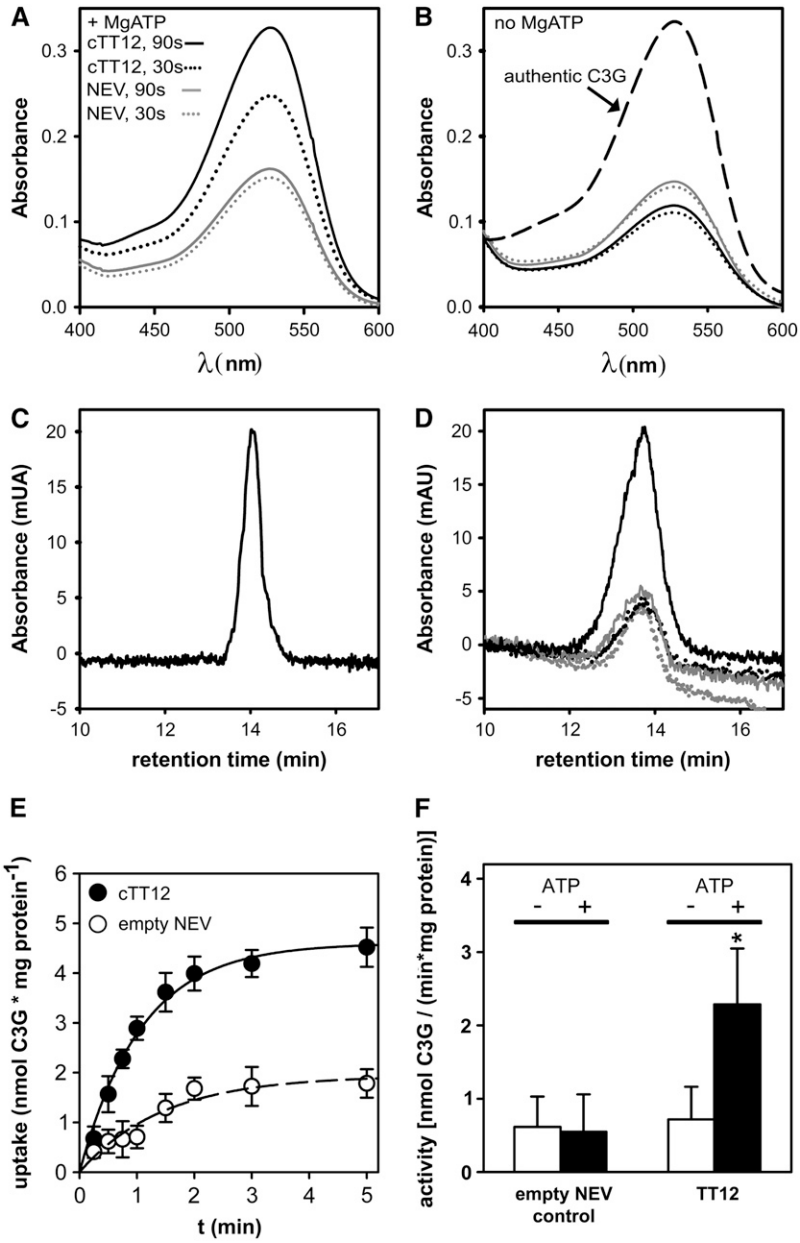

Figure 5. TT12-Mediated Transport of C3G in Yeast Microsomal Vesicles.

(A) and **(B)** Absorption scans of C3G washed off from filters after the transport experiment representing the vesicle-associated amount of C3G.
(A) Result of a transport experiment in the presence of MgATP.
(B) Corresponding control in the absence of ATP. Transport was stopped by filtration after 30 (dotted lines) or 90 s of vesicular uptake (solid lines). Black and gray lines represent uptake experiments performed with vesicles isolated from *cTT12*- or empty vector control (NEV)–transformed yeasts, respectively. Dashed line in corresponds to authentic C3G standard.
(C) HPLC profile of authentic C3G standard.
(D) HPLC analysis of the uptake of C3G into microsomal vesicles prepared from yeasts transformed with *TT12*. Vesicles isolated from *TT12*-transformed yeasts have taken up C3G after 90 s (black solid line) compared with 30 s (black dotted line) of incubation. Corresponding control vesicles (empty vector; gray lines) do not display any time-dependent increase in C3G.
(E) Time-dependent uptake of C3G into vesicles isolated from yeasts transformed either with *TT12* (closed symbols) or the empty vector (open symbols) in the presence of MgATP.
(F) Quantification of uptake activity. Averages ± SE of 20 transport experiments performed with independent vesicle preparations are presented. Black and white bars stand for yeasts transformed with TT12 (pNEV-TT12) and empty vector (pNEV), respectively.

Table 1. Effect of Different Inhibitors on Vesicle Uptake of C3G Performed in the Presence of MgATP

	C3G Uptake (% of the Control)	
Condition	Empty Vector (pNEV)	TT12
None	24 ± 31 ($n = 20$)	100 ($n = 20$)
1 mM PCMBS	32 ± 27 ($n = 4$)	2 ± 4 ($n = 4$)
5 mM NH_4Cl	17 ± 13 ($n = 4$)	13 ± 19 ($n = 4$)
0.1μM bafilomycin A1	20 ± 20 ($n = 4$)	0 ± 0 ($n = 4$)

The uptake activity measured in TT12 vesicles in the absence of inhibitors was set to 100% (control). *n* corresponds to the number of independent experiments.

substances that are necessary to adjust the density of the vacuoles in the transport medium prior to silicone oil layer centrifugation.

A Glucosylated Flavan-3-ol Specifically Inhibits TT12-Mediated Cyanidin-3-*O*-Glucoside Transport

If TT12 mediates transport of C3G but not the aglycone cyanidin in vitro, it can be speculated that monomeric flavan-3-ols need to be glycosylated in order to be accepted by TT12 as a substrate. In support of this hypothesis, an epicatechin hexoside has been detected by LC-MS in mature seeds of Landsberg *erecta* and Cvi (J.-M. Routaboul, unpublished results). As a substantial step toward the identification of the in vivo substrate of TT12, we therefore wanted to investigate whether a glycosylated flavan-3-ol is transported by TT12. Unfortunately, glycosylated epicatechin was not available to us in preparative amounts. However, we were able to obtain chemically synthesized catechin-3-*O*-glucoside (cat3G).

As for epicatechin and catechin, direct TT12-mediated transport of cat3G in yeast vesicles could not be detected (data not shown). However, cat3G inhibited C3G transport in a dose-dependent manner (Figure 6). With both C3G and cat3G at a concentration of 1 mM, MgATP-dependent C3G transport into TT12-containing yeast vesicles was reduced to ~60% of the control activity in the absence of cat3G. Addition of 2 mM cat3G completely abolished C3G transport. To confirm that cat3G inhibition of TT12-mediated C3G transport is specific for the glucosylated flavan-3-ol, the unconjugated flavan-3ols epicatechin and catechin were added at 2 mM as competitors of C3G transport. In contrast with cat3G, neither catechin nor epicatechin inhibited C3G transport. Furthermore, the flavonols Q3R and Q3G had no effect on C3G transport (Figure 6). Based on these competition experiments, we suggest that a glucosylated flavan-3-ol is the in vivo TT12 substrate, while glycosylated flavonols are not transported by TT12.

TT12 Contributes to Vacuolar Anthocyanin Deposition in *ban* Seeds

Our transport experiments suggest that TT12 mediates transport of glucosylated anthocyanidins and flavan-3-ol monomers. However, anthocyanins are not in vivo substrates in PA-accumulating cells of the *Arabidopsis* seed coat. To investigate whether anthocyanin accumulation is affected by *TT12* in support of our in vitro data, we analyzed the seed phenotype of a *ban tt12* double mutant (Figure 7). Immature seeds of the *ban* mutant contain anthocyanins of unknown conjugation pattern instead of PAs in PA-producing testa cells since they lack the anthocyanidin reductase activity (Albert et al., 1997; Devic et al., 1999; Xie et al., 2003), while wild-type and *tt12* immature seeds do not exhibit any red coloration (data not shown). In contrast with *ban*, red coloration in immature *ban tt12* seeds was strongly reduced. Furthermore, the amount of anthocyanins measured in extracts prepared in acidic methanol as absorption at 525 nm of either complete siliques or immature seeds was reduced to ~50% in the *ban tt12* double mutant compared with *ban* (Figure 7C).

DISCUSSION

Although flavonoid biosynthesis is one of the most thoroughly studied enzymatic pathways in plants, the mechanism(s) by which phenolic compounds reach their cellular destination, the vacuole or the apoplastic space, has not been investigated in detail (Grotewold, 2004). Biochemical investigation of vacuolar transport properties performed with flavonoids or simple phenolics, such as salicylic acid glucoside, as substrates indicated the presence of either directly energized ABC-type transporters or secondarily energized antiporters (for review, see Yazaki, 2005). The latter are usually driven by the H^+ gradient across the tonoplast, which is ultimately established by the two vacuolar H^+-pumps, the V-type H^+-ATPase and H^+-pyrophosphatase (Gaxiola et al., 2002). With regard to ABC transporters, the recent characterization of the maize multidrug resistance–associated protein (MRP) gene Zm *MRP3* via an antisense approach suggests that MRP-type transporters are involved in vacuolar anthocyanin accumulation in this species since antisense plants lack accumulation of anthocyanins in leaves and tassels of

Table 2. Synopsis of Transport Activities of TT12 Tested with Different Flavonoids as Substrates and Inhibition of TT12-Mediated C3G Transport by These Compounds

Flavonoid Class	Compound	Transport by TT12	Inhibition of C3G Transport by TT12
Flavan-3-ol monomers	Epicatechin	−	−
	Catechin	−	−
	Cat3G	−	+
Flavan-3-ol dimers	Procyanidin B1	−	ND
	Procyanidin B2	−	ND
Anthocyani(di)ns	C3G	+	NA
	Cyanidin	−	ND
Flavonols	Q3R	−	−
	Q3G	−	−

Presence and absence of a transport activity with the corresponding substrate and of an inhibitory effect on C3G transport is indicated by + and −, respectively. ND, not determined; NA, not applicable.

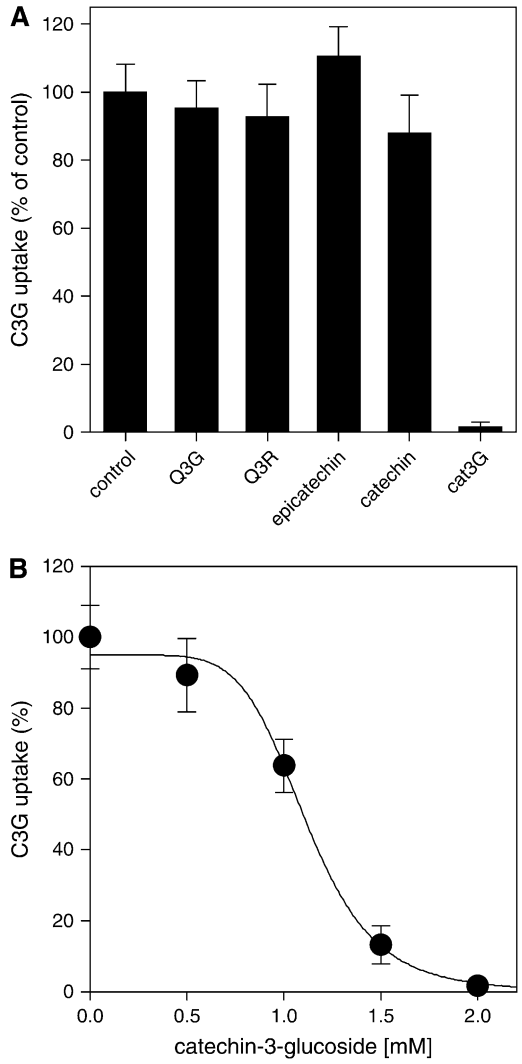

Figure 6. C3G Specifically Inhibits TT12-Mediated C3G Transport.

(A) Inhibition of the uptake of 1 mM C3G by the flavonols Q3G, Q3R, the nonglucosylated flavan-3-ols epicatechin and catechin, and by cat3G. All competitors were added at a final concentration of 2 mM. Experiments were performed in the presence of MgATP. The C3G transport activity with vesicles isolated from *TT12*-transformed yeasts in the absence of competitors was set to 100%. Transport rates were calculated after subtraction of unspecific binding.

(B) Dose-dependent inhibition of C3G uptake by cat3G. All experiments were performed in triplicate with two independent vesicle preparations.

pigmented maize plants (Goodman et al., 2004). However, the biochemical transport activity of tonoplast-localized Zm MRP3 has not been established.

Here, we demonstrate that the MATE transporter TT12 localizes to the tonoplast and mediates flavonoid transport by an H^+-antiport mechanism. Therefore, and in accordance with genetic evidence, MATE transporters define a novel plant membrane protein family involved in vacuolar accumulation of phenolic compounds.

TT12 Is a H^+-Driven Vacuolar Transporter for Flavonoids

The MATE superfamily has been identified recently as a membrane protein family (Brown et al., 1999) with 9 to 12 membrane-spanning domains (Schwacke et al., 2003). Biochemical data on transport properties and functional aspects of family members are scarce, as is the identification of functional conserved signatures or domains. MATE proteins in prokaryotes function as drug/Na^+- or drug/H^+-transporters (Morita et al., 2000; Chen et al., 2002; He et al., 2004), while extrusion of norfloxacin, the plant alkaloid berberine, and ethidium bromide mediated by the *Arabidopsis* MATE At DTX1 expressed in *E. coli* occurred in a H^+-dependent fashion (Li et al., 2002). By contrast, the substrates transported by the MATE proteins encoded by *ALF5* or *EDS5* discovered via genetic mutant screens are unknown (Diener et al., 2001; Nawrath et al., 2002). Notably, FRD3 acts as a proton-coupled citrate exporter on the plasma membrane, extruding citrate into the xylem or the rhizosphere (Durrett et al., 2007).

Vesicle uptake experiments performed with transformed yeasts expressing TT12 demonstrated that TT12 exhibits time- and ATP-dependent transport of C3G. The strong inhibitory action of bafilomycin A1 and NH_4Cl suggests that TT12-catalyzed C3G transport is H^+ dependent. Thus, TT12 acts mechanistically like At DTX1 (Li et al., 2002), FRD3 (Durrett et al., 2007), and the human MATE1, which mediates H^+-coupled extrusion of toxic organic cations (Otsuka et al., 2005). Moreover, GFP-tagged TT12 resides on the tonoplast. These data demonstrate that TT12 acts as a vacuolar anthocyanin/H^+-antiporter under our heterologous expression conditions. In extension to these results, we hypothesize that plant MATE transporters represent the H^+-dependent flavonoid transporters previously characterized in vacuolar uptake studies (Klein et al., 1996; Frangne et al., 2002; Marinova et al., 2007). Interestingly, a recent study provides circumstantial evidence for this hypothesis. The *ant1* tomato (*Solanum lycopersicum*) mutant overexpressing a MYB transcription factor by activation tagging overproduces anthocyanins. Upregulated genes in the *ant1* background include a MATE transporter gene exhibiting 36% amino acid sequence identity to TT12 and 61% to At4G25640 (Mathews et al., 2003). Therefore, it is tempting to speculate that *TT12* homologs are ultimately responsible for vacuolar anthocyanin transport in vegetative plant parts.

What Are the in Vivo Substrates of TT12?

Three findings presented here extend the view on potential functions of TT12 in seeds. First, it was proposed that TT12 acted as a transporter for the PA precursors epicatechin and catechin. However, no detectable transport of nonglycosylated flavan-3-ol monomers and dimers was observed in TT12-expressing yeast vesicles (Table 2). Since TT12 mediated transport of C3G but not the aglycone cyanidin, we speculated that PA precursors need to be glycosylated to be transported by TT12. However, the activity of a glycosyltransferase providing the glycosylated PA precursor remains to be established. While modifications of flavan-3-ols by conjugation reactions have been reported for catechin (Porter, 1993), glucosylated epicatechin is presently not available in

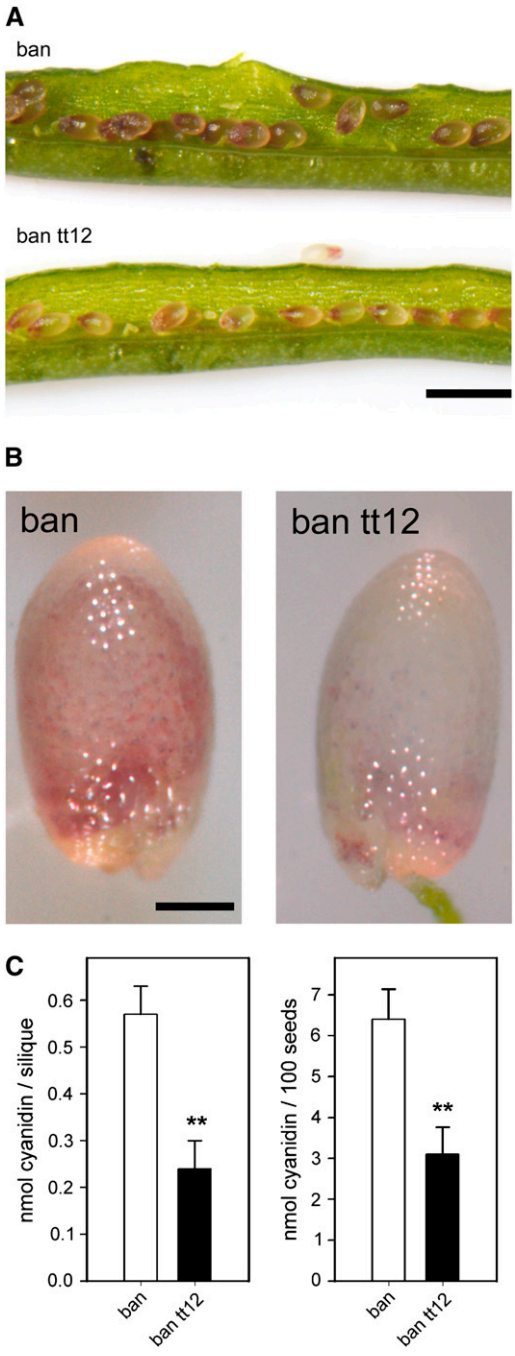

Figure 7. Anthocyanin Deposition in Immature Seeds of *ban* and the Double Mutant *ban tt12*.

(A) and **(B)** The characteristic red color observed in the endothelial layer of *ban* seed caused by anthocyanins is reduced and more diffuse in immature *ban tt12* seeds as seen in whole siliques (**[A]**; bar = 1 mm) or individual immature seeds (**[B]**; bar = 250 μm).

(C) Entire siliques (left panel) or immature seeds (right panel) of identical developmental stages were extracted in acidic methanol, and the anthocyanin content was determined photometrically at 525 nm. *ban tt12* siliques or seeds contain significantly less anthocyanins compared with *ban* (Student's *t* test, two-tailed distribution, $P < 0.01$).

sufficient amounts for transport experiments with TT12. Although direct transport of chemically synthesized cat3G was undetectable, cat3G, but not the flavan-3-ol aglycones, was an efficient inhibitor of TT12-mediated C3G transport. Furthermore, cat3G inhibition was dose dependent (Figure 6, Table 2). Based on these findings, we suggest that TT12 is a transporter for glycosylated flavan-3-ol monomers in vivo, while TT12 exhibits an extended substrate specificity in vitro, accepting glycosylated anthocyanidins. Reduction of anthocyanins in *ban tt12* double mutant seeds (Figure 7) suggests that absence of *TT12* produced a novel phenotype in the *ban* background, which may be interpreted as a partial defect in vacuolar deposition of anthocyanins. However, since anthocyanins were not completely absent in the double mutant seeds, additional transporters that are able to transport the anthocyanins present in *ban* seeds have to be suggested.

Second, LC-MS analysis of *tt12* seeds established that no soluble flavan-3-ols, PAs, and only low levels of insoluble PAs are present in the absence of the transporter. Furthermore, *TT12* promoter activity (this work) and the *TT12* mRNA (Debeaujon et al., 2001) were shown to colocalize with cells involved in PA biosynthesis. This situation is identical to the one encountered with the *BAN* gene and is relevant with the fact that the spatiotemporal patterns of expression for both genes are regulated by the same MYB, bHLH, and WD40 factors, respectively: TT2, TT8, and TTG1 (Nesi et al., 2002; Debeaujon et al., 2003). In view of the fact that *TT12* is a member of a large gene family, it can be speculated that due to this specific pattern of expression and the strong *tt12* mutant phenotype, TT12 is functionally unique in *Arabidopsis* in spite of potential redundancy.

Third, LC-MS analysis of *tt12* seeds demonstrated a specific reduction in Q3R (the major flavonol component in dry seeds; Routaboul et al., 2006), while all other flavonol derivatives remained unchanged (Figure 2). Pourcel et al. (2005) showed with histochemical staining on immature seed sections that flavonols are essentially present in the oi1 layer of the outer integument in the *Arabidopsis* wild-type seed coat. *TT12* is not expressed in this cell layer, according to the pattern of TT12 promoter activity during seed development (Figure 3). Moreover, neither Q3R nor the corresponding glucoside Q3G was a substrate for TT12-mediated transport into yeast vesicles (Table 2), and these flavonol glycosides were also unable to inhibit C3G transport (Figure 6). Thus, in extension to our results demonstrating that cat3G acts as an efficient competitor of C3G transport, it has to be suggested that flavonol glycosides are unlikely to be substrates of TT12. With regard to our expression and transport results, the finding that levels of Q3R accumulating in the outer integument are reduced in *tt12* seeds is puzzling, as is the recent finding that in *tt12* mutants, cytosolic flavonoids (presumably mainly flavonols) are not loaded from the cytosol into the tapetosomes of tapetum cells during pollen formation in anthers (Hsieh and Huang, 2007). Additional experiments will be necessary to understand the relationship between TT12 function and flavonol composition. It is possible that histochemical detection of Q3R is masked by tannins in endothelial cells, which may be investigated by looking for flavonol presence in *Arabidopsis* mutants deprived of tannins but having flavonols (e.g., *tt3*). It will be particularly important to know whether the flavonol

phenotype results from a direct effect of TT12 absence or is an indirect consequence of PA metabolism modification.

If TT12 acts as a flavan-3-ol glycoside/H^+-antiporter, the vacuolar lumen must be acidic to support epicatechin accumulation. Seeds of a knockout mutation in the *Arabidopsis* plasma membrane H^+-pump gene *AHA10* display features of a transparent testa phenotype, suggesting that AHA10 (though not predicted to localize to the tonoplast) could be involved in establishing a transmembrane H^+-gradient driving TT12-mediated vacuolar flavonoid accumulation in PA-accumulating cells (Baxter et al., 2005). In *tt18*/*tds4*, *aha10*, and *tt12* mutants, a fluorescent dye, which is targeted to the vacuole in wild-type endothelial cells, accumulates in multiple vesicular structures, suggesting that PA biosynthesis involves vesicle fusion to form the large vacuole (Abrahams et al., 2003; Baxter et al., 2005). Although it remains to be shown how PA biosynthesis affects vacuolar biogenesis in endothelial cells, a prospective model to flavonoid transport proposes vesicle-mediated trafficking of these compounds after their synthesis at large multienzyme complexes located at the cytoplasmic face of the endoplasmic reticulum, involved in channeled production of end products (Winkel, 2004). Vesicles implicated in the transport of flavonoid-derived compounds have been previously described (Grotewold, 2004). Following the model of Baxter et al. (2005) and including our results on the transport function of TT12, the rather static biosynthetic scheme presented in Figure 1 will have to be revised: PAs and other flavonoids are either directly loaded into vesicles or are guided through the cytosol by binding to glutathione *S*-transferases, such as TT19, toward vesicles destined to form the central vacuole. However, our localization of TT12 to the vacuolar membrane suggests that the transport step itself takes place on the level of the vacuole and not at the endoplasmic reticulum where the precursors are synthesized. TT12-mediated proton-dependent transport of PA precursors into vacuoles could be energized by the proton gradient established by AHA10. The subcellular localization of AHA10, predicted to be the plasma membrane, has not been determined experimentally. In extension of our results, we speculate that AHA10 also localizes to the tonoplast and is therefore a P-type H^+-ATPase with an unusual localization. However, due to the effects of *AHA10* absence on the vacuolar ultrastructure in the endothelium, it is also possible that AHA10 travels on vesicles (e.g., from the endoplasmic reticulum toward the vacuole or between the plasma membrane and prevacuolar compartments, as proposed by Baxter et al. [2005]). In the latter case, it remains to be determined whether the formation of the pH gradient takes place on the level of the vacuole or in vesicles destined to fuse with the vacuole.

The transport specificities of TT12 suggest a second extension of the late steps of PA biosynthesis in *Arabidopsis* seeds. According to our transport results, it has to be hypothesized that flavan-3-ols need to be glycosylated prior to vacuolar transport by TT12. However, a glycosylation step acting on the level of epicatechin is biochemically and molecularly unknown. Furthermore, since epicatechin and the derived PA polymers are not glycosylated according to the metabolite analysis of *Arabidopsis* seeds (Figure 2; Routaboul et al., 2006), an efficient glycosidase must be active in the vacuoles. Both steps have not yet been described on the level of mutants exhibiting a deviation in the seed color, which may reflect gene redundancy. Using the Botany Array Resource Expression Angler tool (Toufighi et al., 2005) with the AtGenExpress Plus and the Botany Array Resource data sets, we searched in silico for genes that are coexpressed with *TT12*. Three glycosylhydrolases (At2G39640, At4G13600, and At4G33850) and one glucosyltransferase (At3G01620) were found to be coexpressed with *TT12* with r-values higher than 0.77. Hierarchical clustering analysis of these four genes together with *TT12*, *BAN*, and *AHA10*, all of which are closely related to PA metabolism in the seed coat, using the clustering tool integrated into Genevestigator V3 (Zimmermann et al., 2004) and the anatomy profile, reveals that the transferase and one of the hydrolases (At4G33850) that cluster together are highly expressed in pollen and stamen (see Supplemental Figure 4 online for details). Thus, it is rather unlikely that these genes are involved in glycosylation of flavan-3-ols and the subsequent hydrolysis of the vacuolar glycoside. By contrast, the hydrolase-encoding gene At2G39640, like *AHA10*, *TT12*, and *BAN*, is preferentially expressed in siliques, and its expression profile clusters closely with *TT12* and *AHA10*. As a consequence, this glycosylhydrolase could be a putative candidate that processes glycosylated flavan-3-ol monomers once these enter the vacuole via TT12-mediated transport.

Our results support the hypothesis that different transporters are responsible for the vacuolar transfer of flavonoids, depending on their modification pattern. In *Arabidopsis* and tomato, glycosylated flavonoids are handled by MATE transporters, such as TT12 (Debeaujon et al., 2001; Mathews et al., 2003). On the other hand, the major maize anthocyanins, which are malonylated derivatives of C3G and therefore negatively charged at cytosolic pH, have been implicated to be substrates of typical MRP-type ABC transporters, such as Zm MRP3 (Goodman et al., 2004). Therefore, the molecular identification of MATE and ABC transporters as important but independent elements of vacuolar flavonoid accumulation confirms biochemical data suggesting the presence of secondary versus directly energized vacuolar uptake systems when glucosylated versus glucuronidated flavones were compared in rye (*Secale cereale*) and barley (Klein et al., 1996, 2000; Frangne et al., 2002).

In conclusion, we demonstrate that the *Arabidopsis* MATE transporter TT12 acts as a flavonoid/H^+-antiporter on the vacuolar membrane of PA-synthesizing cells of the seed coat. Its substrate specificity, the ability of cat3G to reduce the transport of C3G, and the phenotype of the *ban tt12* double mutant seeds suggests that TT12 can mediate the transport of anthocyanins and flavan-3-ols as long as they are glycosylated, while aglycones, flavan-3-ol dimers, and flavonol glycosides are not TT12 substrates. It therefore has to be postulated that PA precursors undergo a glycosylation step prior to TT12-mediated transfer into the seed coat vacuoles.

METHODS

Chemicals, Strains, Plant Material, and Cloning Procedures

C3G was isolated from blackberries by countercurrent chromatography, and its identity was confirmed by HPLC diode array detection, HPLC coupled to electron spray ionization–mass spectrometry, and nuclear magnetic resonance spectroscopy as described previously (Schwarz

et al., 2003). cat3G was from the Nestlé Research Center collection of standard compounds. All other flavonoid compounds were from Extrasynthèse. For uptake experiments, C3G and cyanidin were dissolved as a 0.1 M stock in 50% methanol/0.1% HCl. Stocks of catechin, epicatechin (0.5 M), cat3G (0.2 M), PA dimers (0.1 M), and quercetin glycosides (0.1 M) were prepared in DMSO. Bafilomycin A1 was a kind gift of K. Altendorf (University Osnabrück, Germany). Cellulase YC and pectolyase Y23 were from Kyowa Chemical. PCMBS (Toronto Research Chemicals) was directly dissolved in transport buffer. All other chemicals were from Sigma-Aldrich.

The yeast strain YPH 499 (MATa ura3-52 lys2-801 ade2-101 trp1-Δ63 his3-Δ200 leu2-1) was used for heterologous expression of the *TT12* cDNA and its derivatives and for the isolation of microsomal membrane vesicles. The *Arabidopsis thaliana tt12* mutant isolated from a collection of T-DNA transformants in the Ws-1 background (Errampalli et al., 1991) and the *ban tt12* double mutant have been described elsewhere (Debeaujon et al., 2000, 2001). For our analysis, *ban tt12* F2 plants were grown and the F3 seeds were analyzed.

Plasmid Constructions and Transformation Procedures

Construction of a 2μ yeast expression vector pNEV-Ura (Sauer and Stolz, 1994) containing the *TT12* cDNA (*cTT12*) or *GFP5:TT12* was performed by amplification of *cTT12* and *GFP5:TT12* from *Pro35Sdual:cTT12/pBIB-HYG* and *Pro35Sdual:GFP5:TT12:t35S/pAVA393* with the primers TT12-up (5′-ATAAGAATGCGGCCGCATGAGCTCCACAGAGAC-3′) or GFP-TT12-up (5′-ATAAGAATGCGGCCGCATGAGTAAAGGAGAA-3′), respectively, and TT12-low (5′-ATAAGAATGCGGCCGCTTAAACACC-TGCGTTAG-3′), where *Not*I restriction sites are underlined. PCR products were cloned into the *Not*I site of pNEV-Ura, resulting in pN-TT12 and pN-GFPTT12, respectively. Likewise, N- and C-terminally $RGSH_6$-tagged versions of TT12 cDNA in pNEV-Ura were obtained using the following primers: H_6N-TT12up (5′-ATAAGAATGCGGCCGCATG*AGAGGATCGCAT-CACCATCACCATCAC*TCCTCGATGAGCTCCACAGAGACATACG-3′) and TT12-low for pN-H_6NTT12 (N-terminal $RGSH_6$ tag) and TT12-up in combination with H_6C-TT12low (5′-ATAAGAATGCGGCCGCTTA*GTGATGGT-GATGGTGATGCGATCCTCT*CGAGGAAACACCTGCGTTAGCCATC-3′) for pN-TT12H_6C (C-terminal $RGSH_6$ tag) (*Not*I sites underlined; $RGSH_6$ motif in italics). Yeast transformation followed standard procedures (Gietz and Woods, 2002), and transformants were selected on minimal synthetic dropout medium lacking uracil (SD-Ura).

To construct the *ProTT12:uidA:t35S* cassette, a 1.8-kb *TT12* promoter was amplified by PCR from the pEB-junction plasmid (Debeaujon et al., 2001) using primers pTT12-5′SalI (5′-GTAGTCGACGAATTCACAATCG-GAAAGTCAC-3′) and pTT12-3′NcoI (5′-TCTGTGGAGCCCATGGTC-CGTTTATTAGTTC-3′; *Sal*I and *Nco*I sites underlined, respectively). The *Sal*I-*Nco*I–digested fragment was cloned into the *Xho*I and *Nco*I sites of the pBS-GUS vector described previously (Debeaujon et al., 2003). The *ProTT12:uidA:t35S* cassette was cloned as a *Sma*I-*Kpn*I fragment into the *pBIB-HYG* binary vector (Becker, 1990). The *Pro35Sdual:GFP5:TT12:t35S* construct was generated as follows. Using primers TT12-ATG-BclI (5′-GG-AACTAATAAATGATCAATGAGCTCCACAGAG-3′) and TT12-STOP-BclI (5′-GTATGATCATGCTGTTATCTTAAACACCTGC-3′; *Bcl*I sites underlined), the TT12 coding sequence was amplified and cloned at the *Bgl*II site of the pAVA393 plasmid. The resulting construct was *Kpn*I-*Sma*I digested and transferred into *pBIB-HYG* at the *Kpn*I-*Sma*I sites to give the *Pro35S-dual:GFP5:TT12/pBIB-HYG* plasmid. The *Pro35Sdual:TT12:GFP/pMDC83* plasmid was obtained by Gateway cloning (Invitrogen). The *TT12* cDNA was amplified omitting the stop codon by PCR using the primers 5′-GGGGACAAGTTTGTACAAAAAAGCAGGCTCCATGAGCTCCACAGA-GACATACG-3′ and 5′-GGGGACCACTTTGTACAAGAAAGCTGGGTCAA-CACCTGCGTTAGCCATC-3′, where attB1 and attB2 sites are underlined, respectively. The resulting PCR product was transferred into pDONR Zeo (Invitrogen) and subsequently into pMDC83 (Curtis and Grossniklaus, 2003) by BP and LR clonase reactions according to the manufacturer's instructions.

Plasmids carrying the *Pro35S:TPK1:GFP* (Czempinski et al., 2002) or the *Pro35S:P31:GFP* cassette (Marmagne et al., 2004) were kindly obtained from K. Czempinski (University of Potsdam, Germany) and G. Ephritikhine (Centre National de la Recherche Scientifique, Gif-sur-Yvette Cedex, France). The *DsRed2:TPK1* marker was constructed by replacing the GFP5 cDNA from pAVA393 by the *DsRed2* cDNA (Clontech) to build the *DsRed2/pAVA393* vector. Afterwards, the *TPK1* cDNA (Czempinski et al., 2002) was amplified with primers cKCO1-5BamHI (5′-GTAGGATC-CATGTCGAGTGATGCAGCTCGTAC-3′) and cKCO1-3BamHI (5′-GTAG-GATCCTTACCTTTGAATCTGAGACGTG-3′), *Bam*HI-digested, and cloned into the *Bgl*II site of *DsRed2/pAVA393*.

Complementation of the *tt12* mutant was performed with *cTT12*, placed under the control of the dual 35S promoter. The cDNA was amplified from the λ clone isolated by Debeaujon et al. (2001) using the primers TT12-ATG-BspMI (5′-GTAACCTGCGGACCATGGGCTCCACA-GAGAC-3′) and TT12-Stop-BclI(-) (5′-GTATGATCATGCTGTTATCTTA-AACGCCTGC-3′; *Bsp*MI and *Bcl*I sites underlined). Finally, the cDNA was cloned at the *Sma*I site of the pMagic plasmid (Nesi et al., 2002) to generate the *Pro35Sdual:cTT12/pBIB-HYG* construction.

For all constructs, PCR amplifications were performed using the proofreading Pfu Ultra DNA Polymerase (Stratagene) or the Expand High Fidelity PCR system (Roche). Correct integration and absence of errors was ultimately verified by sequencing. Stable transformation of *Arabidopsis* plants was realized as performed previously (Nesi et al., 2000).

Analysis of Seeds

GUS staining, sample mounting in a chloral hydrate solution, and inclusion in resin for the realization of sections and observations were performed according to Debeaujon et al. (2003). Seed flavonoids were extracted and analyzed as described previously (Routaboul et al., 2006).

Preparation of Yeast Membrane Vesicles and in Vitro Transport Studies

Yeast membrane vesicles for in vitro transport studies were isolated essentially as described by Tommasini et al. (1996) with the modifications reported by Klein et al. (2002). Uptake experiments to study transport of flavonoid substrates into membrane vesicles were performed using the rapid filtration technique with nitrocellulose filters (0.45-μm pore size; Millipore). One part of thawed vesicles was mixed with three parts of transport buffer (0.4 M glycerol, 0.1 M KCl, 20 mM Tris-MES, pH 7.4, and 1 mM DTT) in the presence of 1 mM flavonoids and in the absence or presence of 5 mM MgATP in a total reaction volume of 0.8 mL. At time points indicated, 0.35 mL were removed and added to 3 mL of ice-cold transport buffer, and the mixture was loaded on a prewet filter that was rapidly washed with 3× 2 mL of ice-cold transport buffer. Immediately after the experiment, filter-bound flavonoids were dissolved by adding 50% methanol/0.1% HCl. Flavonoid content eluted from the filters was analyzed in two ways: (1) absorption spectra scans between 220 and 600 nm with a Beckman Coulter DU 800 spectrophotometer, and (2) HPLC separation was performed on a CC 250/4 Nucleosil 100-5 C18HD column (Macherey-Nagel) with water/0.6% perchloric acid (A) and methanol (B) at a total flow rate of 1 mL/min and the following gradient: 0 to 20 min from 5 to 60% B over A. Parameters were controlled by a Gynkotek liquid chromatograph (Dionex) equipped with a UVD340S diode array detector set at 520, 330, and 280 nm for identification of anthocyanins, flavonols, and flavan-3-ols, respectively.

Subcellular Localization and Confocal Laser Scanning Microscopy Analysis

Subcellular localization of TT12-GFP fusions was investigated in transient assays and after stable transformation of *Arabidopsis* plants. Transient

expression in onion blub epidermal cells was performed by biolistic particle delivery of *Pro35Sdual:GFP5:TT12:t35S/pAVA393* alone or in the presence of equimolar amounts of *Pro35Sdual:DsRed2:TPK1* using DNA-coated 0.6 μm gold particles as microcarriers and the BioRad He Biolistic PDS-1000/He system following the manufacturer's instructions. Transient expression in *Nicotiana benthamiana* leaves using infiltration of *Agrobacterium tumefaciens* GV31 01 transformed with the corresponding plasmids by electroporation was performed according to published procedures (Voinnet et al., 2003; Walter et al., 2004). Microscopic observations were made after 48 h at 25°C. Mesophyll protoplasts from infiltrated *N. benthamiana* leaves or stably transformed *Pro35S-dual:GFP5:TT12/tt12 Arabidopsis* plants were prepared as described (Frangne et al., 2002), and vacuoles were released during confocal analysis by gentle addition of water. Roots of sterile-grown transgenic *tt12* plants ectopically expressing *GFP5-cTT12* were analyzed after 7 d and were counterstained with 1 mM propidium iodide (Molecular Probes). Single optical sections were captured by confocal laser scanning microscopy using a TCS SP2-x1 full-spectrum confocal microsope attached to a Leica DM IRE2 inverted fluorescence microscope. GFP and DsRed or GFP and propidium iodide were simultaneously excited with a 488-nm Ar and a 543-nm HeNe laser, and fluorescence emission images averaged over eight frames were captured in independent channels (GFP, 500 to 520 nm; DsRed, 580 to 615 nm; propidium iodide and chlorophyll autofluorescence, 620 to 700nm; DD488/543 beam splitter). Images were false-colored in green (GFP) or red (DsRed, propidium iodide, and chlorophyll autofluorescence) using Adobe Photoshop 7.0.

Accession Numbers

The Arabidopsis Genome Initiative identifiers for the genes/proteins described in this article are as follows: *TT12*/At *DTX41* (At3G59030), *BAN/ANR* (At1G61720), *TT10* (At5G48100), *ALF5*/At *DTX19* (At3G23560), *FRD3*/At *DTX43* (At3G08040), *EDS5*/At *DTX47* (At4g39030), At *DTX1* (At2G04070), *Arabidopsis* P31 protein (At3G01290), *AHA10* (At1G17260), *TT19* (At5G17220), *chalcone synthase* (At5G13930), *chalcone isomerase* (At3G55120), *flavanone 3-hydroxylase* (At3G51240), *flavonol 3′-hydroxylase* (At5G07790), *flavonol synthase* (At5G08640), and *leucoanthocyanidin dioxygenase* (At4G22880).

Supplemental Data

The following materials are available in the online version of this article.

Supplemental Figure 1. Localization of *GFP-cTT12* after Transient and Stable Expression in Plant Cells.

Supplemental Figure 2. Expression and Localization of TT12 in *Saccharomyces cerevisiae* and ATP-Dependent Formation of a pH Gradient.

Supplemental Figure 3. TT12 Transport Activity toward Various Flavonoid Substrates.

Supplemental Figure 4. Hierarchical Clustering Analysis of the Expression of *TT12*, *BANYULS*, *AHA10*, and Putative Coexpressed Glycosyltransferases or Glycosylhydrolases.

Supplemental Methods. Heterologous Expression of *cTT12* in *Saccharomyces cerevisiae* and MgATP-Dependent pH Gradient Formation in Yeast Membrane Vesicles.

ACKNOWLEDGMENTS

We thank E. Martinoia, S.E. Schauer (both of the University of Zurich), and L. Lepiniec (Institut National de la Recherche Agronomique Versailles) for comments on the manuscript, K. Czempinski (University of Potsdam) for the *TPK1* clone, G. Ephritikhine (Centre National de la Recherche Scientifique, Gif-sur-Yvette Cedex, France) for *P31-GFP*, A. von Arnim (University of Tennessee, Knoxville) for pAVA393, and J.-D. Faure and C. Smyczynski (both of the Institut National de la Recherche Agronomique Versailles) for the *DsRed2* cDNA. We also thank the reviewers for constructive and interesting suggestions. This work was supported by the Forschungskredit of the University of Zurich (M.K.), by the Swiss National Foundation (3100A0-116051; M.K.), by the Roche Research Foundation (Basel) (K.M. and M.K.), and by the Integrated Action Program ''Germaine de Staël'' (I.D. and M.K.).

Received July 20, 2006; revised May 31, 2007; accepted June 6, 2007; published June 29, 2007.

REFERENCES

Abrahams, S., Lee, E., Walker, A.R., Tanner, G.J., Larkin, P.J., and Ashton, A.R. (2003). The *Arabidopsis TDS4* gene encodes leucoanthocyanidin dioxygenase (LDOX) and is essential for proanthocyanidin synthesis and vacuole development. Plant J. **35:** 624–636.

Albert, S., Delseny, M., and Devic, M. (1997). *BANYULS*, a novel negative regulator of flavonoid biosynthesis in the *Arabidopsis* seed coat. Plant J. **11:** 289–299.

Baxter, I.R., Young, J.C., Armstrong, G., Foster, N., Bogenschutz, N., Cordova, T., Peer, W.A., Hazen, S.P., Murphy, A.S., and Harper, J.F. (2005). A plasma membrane H^+-ATPase is required for the formation of proanthocyanidins in the seed coat endothelium of *Arabidopsis thaliana*. Proc. Natl. Acad. Sci. USA **102:** 2649–2654.

Becker, D. (1990). Binary vectors which allow the exchange of plant selectable markers and reporter genes. Nucleic Acids Res. **18:** 203.

Brown, M.H., Paulsen, I.T., and Skurray, R.A. (1999). The multidrug efflux protein NorM is a prototype of a new family of transporters. Mol. Microbiol. **31:** 394–395.

Bush, D.R. (1993). Inhibitors of the proton-sucrose symport. Arch. Biochem. Biophys. **307:** 355–360.

Chen, J., Morita, Y., Huda, M.N., Kuroda, T., Mizushima, T., and Tsuchiya, T. (2002). VmrA, a member of a novel class of Na^+-coupled multidrug efflux pumps from *Vibrio parahaemolyticus*. J. Bacteriol. **184:** 572–576.

Coleman, J.O.D., Randall, R., and Blake-Kalff, M.M.A. (1997). Detoxification of xenobiotics in plant cells by glutathione conjugation and vacuolar compartmentalization: A fluorescent assay using monochlorobimane. Plant Cell Environ. **20:** 449–460.

Curtis, M.D., and Grossniklaus, U. (2003). A gateway cloning vector set for high-throughput functional analysis of genes *in planta*. Plant Physiol. **133:** 462–469.

Czempinski, K., Frachisse, J.M., Maurel, C., Barbier-Brygoo, H., and Mueller-Roeber, B. (2002). Vacuolar membrane localization of the *Arabidopsis* 'two-pore' K^+ channel KCO1. Plant J. **29:** 809–820.

Debeaujon, I., Leon-Kloosterziel, K.M., and Koornneef, M. (2000). Influence of the testa on seed dormancy, germination, and longevity in Arabidopsis. Plant Physiol. **122:** 403–413.

Debeaujon, I., Nesi, N., Perez, P., Devic, M., Grandjean, O., Caboche, M., and Lepiniec, L. (2003). Proanthocyanidin-accumulating cells in Arabidopsis testa: Regulation of differentiation and role in seed development. Plant Cell **15:** 2514–2531.

Debeaujon, I., Peeters, A.J.M., Leon-Kloosterziel, K.M., and Koornneef, M. (2001). The *TRANSPARENT TESTA12* gene of Arabidopsis encodes a multidrug secondary transporter-like protein required for flavonoid sequestration in vacuoles of the seed coat endothelium. Plant Cell **13:** 853–871.

Devic, M., Guilleminot, J., Debeaujon, I., Bechtold, N., Bensaude, E., Koornneef, M., Pelletier, G., and Delseny, M. (1999). The *BANYULS*

gene encodes a DFR-like protein and is a marker of early seed coat development. Plant J. **19:** 387–398.

Diener, A.C., Gaxiola, R.A., and Fink, G.R. (2001). Arabidopsis *ALF5*, a multidrug efflux transporter gene family member, confers resistance to toxins. Plant Cell **13:** 1625–1637.

Dröse, S., and Altendorf, K. (1997). Bafilomycins and concanamycins as inhibitors of V-ATPases and P-ATPases. J. Exp. Biol. **200:** 1–8.

Durrett, T.P., Gassmann, W., and Rogers, E.E. (2007). The FRD3-mediated efflux of citrate into the root vasculature is necessary for efficient iron translocation. Plant Physiol. **144:** 197–205.

Errampalli, D., Patton, D., Castle, L., Mickelson, L., Hansen, K., Schnall, J., Feldmann, K., and Meinke, D. (1991). Embryonic lethals and T-DNA insertional mutagenesis in *Arabidopsis*. Plant Cell **3:** 149–157.

Frangne, N., Eggmann, T., Koblischke, C., Weissenböck, G., Martinoia, E., and Klein, M. (2002). Flavone glucoside uptake into barley mesophyll and *Arabidopsis* cell culture vacuoles. Energization occurs by H^+-antiport and ATP-binding cassette-type mechanisms. Plant Physiol. **128:** 726–733.

Gaxiola, R.A., Fink, G.R., and Hirschi, K.D. (2002). Genetic manipulation of vacuolar proton pumps and transporters. Plant Physiol. **129:** 967–973.

Gietz, R.D., and Woods, R.A. (2002). Transformation of yeast by lithium acetate/single-stranded carrier DNA/polyethylene glycol method. Methods Enzymol. **350:** 87–96.

Goodman, C.D., Casati, P., and Walbot, V. (2004). A multidrug resistance-associated protein involved in anthocyanin transport in *Zea mays*. Plant Cell **16:** 1812–1826.

Grotewold, E. (2004). The challenges of moving chemicals within and out of cells: Insights into the transport of plant natural products. Planta **219:** 906–909.

Harborne, J.B., and Williams, C.A. (2000). Advances in flavonoid research since 1992. Phytochemistry **55:** 481–504.

He, G.X., Kuroda, T., Mima, T., Morita, Y., Mizushima, T., and Tsuchiya, T. (2004). An H^+-coupled multidrug efflux pump, PmpM, a member of the MATE family of transporters, from *Pseudomonas aeruginosa*. J. Bacteriol. **186:** 262–265.

Hsieh, K., and Huang, A.H.C. (2007). Tapetosomes in *Brassica* tapetum accumulate endoplasmic reticulum-derived flavonoids and alkanes for delivery to the pollen surface. Plant Cell **19:** 582–596.

Kerhoas, L., Aouak, D., Cingoz, A., Routaboul, J.M., Lepiniec, L., Einhorn, J., and Birlirakis, N. (2006). Structural characterization of the major flavonoid glycosides from *Arabidopsis thaliana* seeds. J. Agric. Food Chem. **54:** 6603–6612.

Klein, M., Mamnun, Y.M., Eggmann, T., Schuller, C., Wolfger, H., Martinoia, E., and Kuchler, K. (2002). The ATP-binding cassette (ABC) transporter Bpt1p mediates vacuolar sequestration of glutathione conjugates in yeast. FEBS Lett. **520:** 63–67.

Klein, M., Martinoia, E., Hoffmann-Thoma, G., and Weissenböck, G. (2000). A membrane-potential dependent ABC-like transporter mediates the vacuolar uptake of rye flavone glucuronides: Regulation of glucuronide uptake by glutathione and its conjugates. Plant J. **21:** 289–304.

Klein, M., Weissenböck, G., Dufaud, A., Gaillard, C., Kreuz, K., and Martinoia, E. (1996). Different energization mechanisms drive the vacuolar uptake of a flavonoid glucoside and a herbicide glucoside. J. Biol. Chem. **271:** 29666–29671.

Lepiniec, L., Debeaujon, I., Routaboul, J.M., Baudry, A., Pourcel, L., Nesi, N., and Caboche, M. (2006). Genetics and biochemistry of seed flavonoids. Annu. Rev. Plant Biol. **57:** 405–430.

Li, L., He, Z., Pandey, G.K., Tsuchiya, T., and Luan, S. (2002). Functional cloning and characterization of a plant efflux carrier for multidrug and heavy metal detoxification. J. Biol. Chem. **277:** 5360–5368.

Marinova, K., Kleinschmidt, K., Weissenböck, G., and Klein, M. (2007). Flavonoid biosynthesis in barley (*Hordeum vulgare* L.) primary leaves requires the presence of the vacuole and controls the activity of vacuolar flavonoid transport. Plant Physiol. **144:** 432–444.

Marmagne, A., Rouet, M.-A., Ferro, M., Rolland, N., Alcon, C., Joyard, J., Garin, J., Barbier-Brygoo, H., and Ephritikhine, G. (2004). Identification of new intrinsic proteins in *Arabidopsis* plasma membrane proteome. Mol. Cell. Proteomics **3:** 675–691.

Mathews, H., Clendennen, S.K., Caldwell, C.G., Liu, X.L., Connors, K., Matheis, N., Schuster, D.K., Menasco, D.J., Wagoner, W., Lightner, J., and Wagner, D.R. (2003). Activation tagging in tomato identifies a transcriptional regulator of anthocyanin biosynthesis, modification, and transport. Plant Cell **15:** 1689–1703.

Matile, P. (1984). The toxic compartment of plant cells. Naturwissenschaften **71:** 18–24.

Morita, Y., Kataoka, A., Shiota, S., Mizushima, T., and Tsuchiya, T. (2000). NorM of *Vibrio parahaemolyticus* is an Na^+-driven multidrug efflux pump. J. Bacteriol. **182:** 6694–6697.

Morita, Y., Kodama, K., Shiota, S., Mine, T., Kataoka, A., Mizushima, T., and Tsuchiya, T. (1998). NorM, a putative multidrug efflux protein, of *Vibrio parahaemolyticus* and its homolog in *Escherichia coli*. Antimicrob. Agents Chemother. **42:** 1778–1782.

Nawrath, C., Heck, S., Parinthawong, N., and Metraux, J.P. (2002). EDS5, an essential component of salicylic acid-dependent signaling for disease resistance in Arabidopsis, is a member of the MATE transporter family. Plant Cell **14:** 275–286.

Nesi, N., Debeaujon, I., Jond, C., Pelletier, G., Caboche, M., and Lepiniec, L. (2000). The *TT8* gene encodes a basic helix-loop-helix domain protein required for expression of *DFR* and *BAN* genes in Arabidopsis siliques. Plant Cell **12:** 1863–1878.

Nesi, N., Debeaujon, I., Jond, C., Stewart, A.J., Jenkins, G.I., Caboche, M., and Lepiniec, L. (2002). The *TRANSPARENT TESTA16* locus encodes the Arabidopsis BSISTER MADS domain protein and is required for proper development and pigmentation of the seed coat. Plant Cell **14:** 2463–2479.

Otsuka, M., Matsumoto, T., Morimoto, R., Arioka, S., Omote, H., and Moriyama, Y. (2005). A human transporter protein that mediates the final excretion step for toxic organic cations. Proc. Natl. Acad. Sci. USA **102:** 17923–17928.

Porter, L.J. (1993). Flavans and proanthocyanidins. In The Flavonoids: Advances in Research Since 1986, J.B. Harborne, ed (London: Chapman and Hall), pp. 23–55.

Pourcel, L., Routaboul, J.M., Kerhoas, L., Caboche, M., Lepiniec, L., and Debeaujon, I. (2005). *TRANSPARENT TESTA10* encodes a laccase-like enzyme involved in oxidative polymerization of flavonoids in Arabidopsis seed coat. Plant Cell **17:** 2966–2980.

Rogers, E.E., and Guerinot, M.L. (2002). FRD3, a member of the multidrug and toxin efflux family, controls iron deficiency responses in Arabidopsis. Plant Cell **14:** 1787–1799.

Routaboul, J.M., Kerhoas, L., Debeaujon, I., Pourcel, L., Caboche, M., Einhorn, J., and Lepiniec, L. (2006). Flavonoid diversity and biosynthesis in seed of *Arabidopsis thaliana*. Planta **224:** 96–107.

Sauer, N., and Stolz, J. (1994). SUC1 and SUC2: Two sucrose transporters from *Arabidopsis thaliana*; expression and characterization in baker's yeast and identification of the histidine-tagged protein. Plant J. **6:** 67–77.

Schwacke, R., Schneider, A., van der Graaff, E., Fischer, K., Catoni, E., Desimone, M., Frommer, W.B., Flügge, U.I., and Kunze, R. (2003). ARAMEMNON, a novel database for Arabidopsis integral membrane proteins. Plant Physiol. **131:** 16–26.

Schwarz, M., Hillebrand, S., Habben, S., Degenhardt, A., and Winterhalter, P. (2003). Application of high-speed countercurrent chromatography to the large-scale isolation of anthocyanins. Biochem. Eng. J. **14:** 179–189.

Shirley, B.W., Kubasek, W.L., Storz, G., Bruggemann, E., Koornneef, M., Ausubel, F.M., and Goodman, H.M. (1995). Analysis of Arabidopsis mutants deficient in flavonoid biosynthesis. Plant J. **8:** 659–671.

Tommasini, R., Evers, R., Vogt, E., Mornet, C., Zaman, G.J.R., Schinkel, A.H., Borst, P., and Martinoia, E. (1996). The human multidrug resistance-associated protein functionally complements the yeast cadmium resistance factor 1. Proc. Natl. Acad. Sci. USA **93:** 6743–6748.

Toufighi, K., Brady, S.M., Austin, R., Ly, E., and Provart, N.J. (2005). The botany array resource: e-Northerns, expression angling, and promoter analyses. Plant J. **43:** 153–163.

Voinnet, O., Rivas, S., Mestre, P., and Baulcombe, D. (2003). An enhanced transient expression system in plants based on suppression of gene silencing by the p19 protein of tomato bushy stunt virus. Plant J. **33:** 949–956.

Walter, M., Chaban, C., Schutze, K., Batistic, O., Weckermann, K., Nake, C., Blazevic, D., Grefen, C., Schumacher, K., Oecking, C., Harter, K., and Kudla, J. (2004). Visualization of protein interactions in living plant cells using bimolecular fluorescence complementation. Plant J. **40:** 428–438.

Winkel, B.S.J. (2004). Metabolic channeling in plants. Annu. Rev. Plant Biol. **55:** 85–107.

Xie, D.Y., Sharma, S.B., Paiva, N.L., Ferreira, D., and Dixon, R.A. (2003). Role of anthocyanidin reductase, encoded by *BANYULS* in plant flavonoid biosynthesis. Science **299:** 396–399.

Yazaki, K. (2005). Transporters of secondary metabolites. Curr. Opin. Plant Biol. **8:** 301–307.

Zimmermann, P., Hirsch-Hoffmann, M., Hennig, L., and Gruissem, W. (2004). GENEVESTIGATOR. Arabidopsis microarray database and analysis toolbox. Plant Physiol. **136:** 2621–2632.

Supplemental Figure 4, Marinova et al.

Hierarchical clustering analysis of the expression of *TT12*, *BANYULS, AHA10* and putative coexpressed glycosyltransferases or glycosylhydrolases .

By *in silico*-analysis, three glycosylhydrolases (GH; At2g39640; At4g33850; At4g13600) and one glycosyltransferase (GT; At3g01620) were identified to be co-expressed with *TT12* with r-values higher than 0.77 using the expression angler function of the Botany Array Resource (http://bbc.botany.utoronto.ca/) (Chip datasets: AtGenExpress Plus, Botany Array Resource). All these genes were not co-expressed with the related MATE transporter gene *ALF5*. Illustrated is the hierarchical clustering analysis of these genes together with the seed-coat specific genes *TT12* (At3g59030), *BANYULS* (At1g61720) and *AHA10* (At1g17260) which are all involved in PA biosynthesis. Hierarchical clustering was performed using the clustering tool integrated into Genevestigator V3 (www.genevestigator.ethz.ch) after selection of the ATH1 22k chiptype and the anatomy profile (Distance measure: Pearson correlation). Increasing intensity of the blue coloration relates to an increase in expression signal strength.

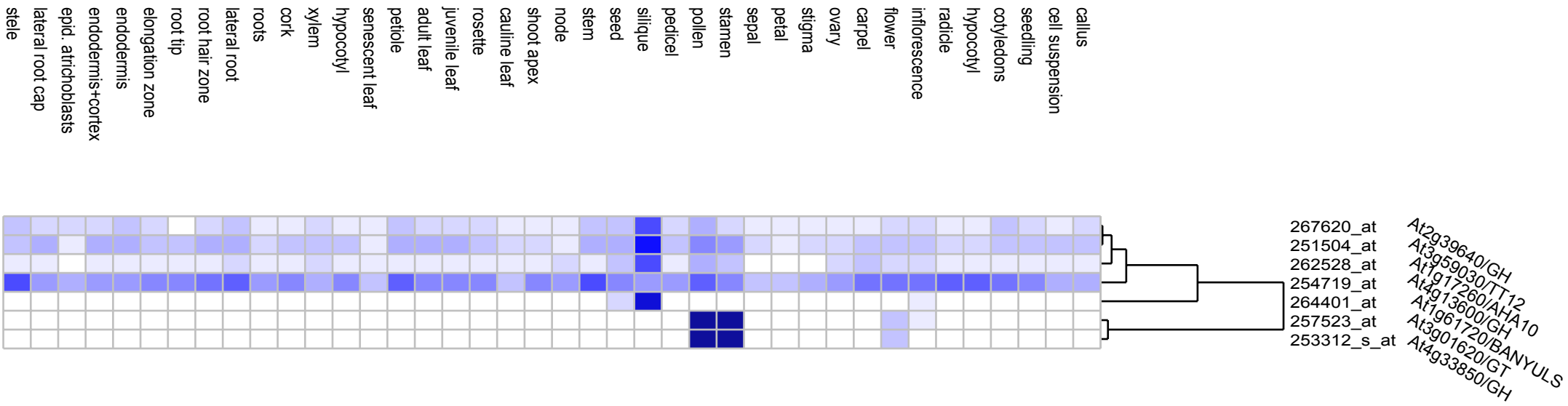

Supplemental Figure 1, Marinova et al.

Localization of *GFP-cTT12* after transient (A, B) and stable expression in plant cells (C).

(A, B) Transient expression of different fusion protein constructs in onion bulb epidermal cells. Bars = 20μm. (A) Expression of *GFP5:TT12* (*GFP-cTT12*) and the tonoplast marker *DsRed2:TPK1*, false-colored in green and red, respectively, in shows colocalization of TT12 with TPK1 on the vacuolar membrane (merged green and red channels). (B) Transient expression of *P31* (At3g01290) fused to GFP (*P31-GFP*) in onion cells exhibiting plasma membrane localization. The arrows in the differential interference contrast (DIC) images highlight transvacuolar strands suggesting that TT12 and TPK1 localize to the tonoplast while P31 fluorescence is absent from intracellular membranes. (C) A small mesophyll protoplasts isolated from a stably transformed *Pro$_{35Sdual}$:GFP5:TT12/tt12* plant. GFP fluorescence (*GFP-cTT12*) and chlorophyll autofluorescence (chlorophyll) are false-colored in green and red, respectively. The green fluorescence of GFP-cTT12 surrounds the plastid (arrow) and the nucleus (asterisk) as can be seen in the merged image. Bar = 5μm.

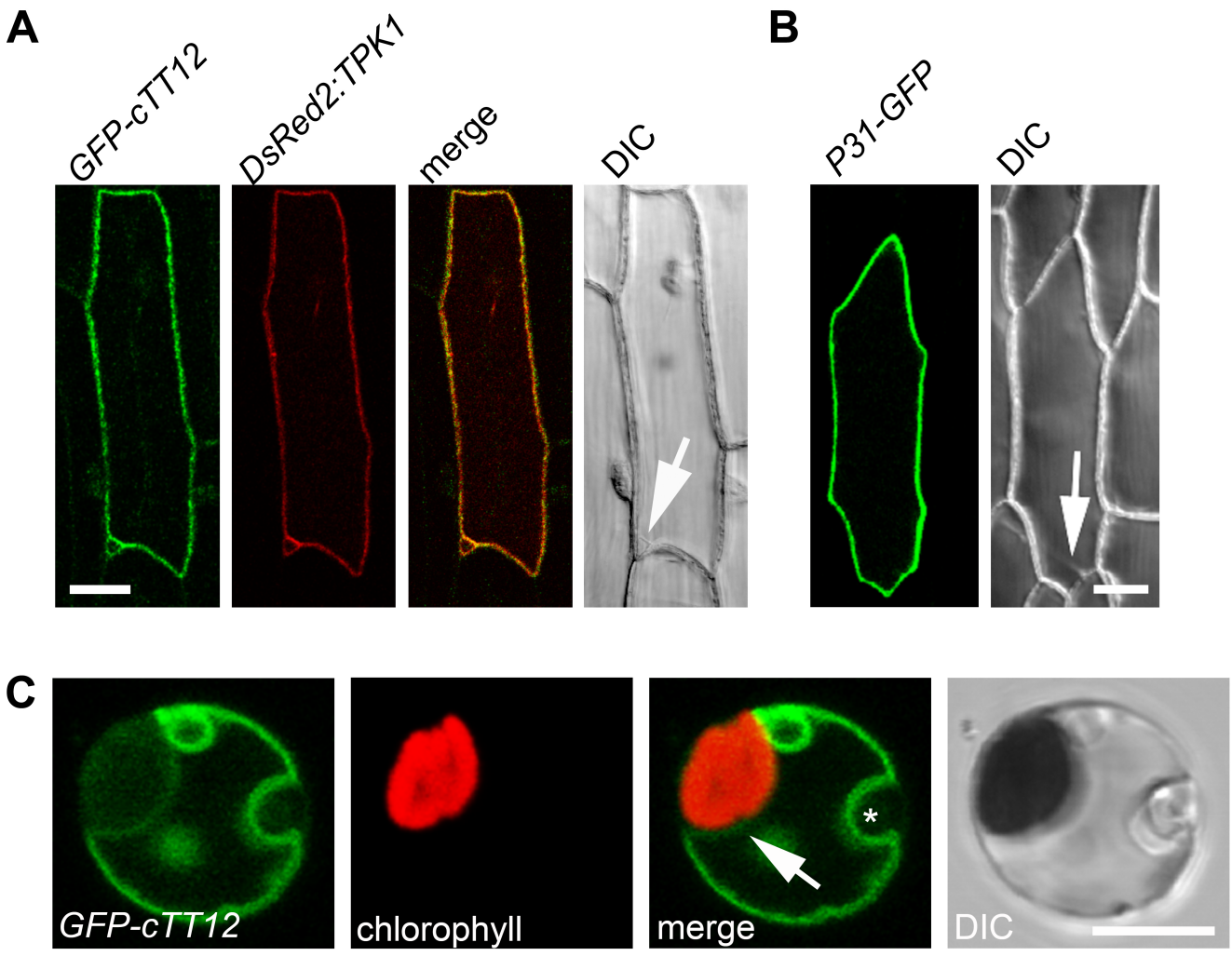

Supplemental Figure 2, Marinova et al.

Expression and Localization of TT12 in *Saccharomyces cerevisiae* and ATP-Dependent Formation of a pH-Gradient.

(A) Yeast strain YPH 499 transformed with *GFP5:TT12* was cultivated in selective medium to the exponential growth phase and subjected to confocal microscopy. GFP fluorescence of GFP5:TT12 (upper left panel). Vacuolar membranes were stained *in vivo* by adding the styryl dye FM4-64 to the growth medium for 15 min (upper right panel, red). Merging of pseudo-colored GFP and FM4-64 images confirms strong labelling of vacuolar membranes (lower left panel). In addition, weaker GFP5:TT12 fluorescence is also detected on the plasma membrane and intracellular structures. DIC, differential interference contrast image of the depicted yeast cell, Bar = 4 μm. (B) Western blot analysis of whole-cell protein extracts (1μg per lane) prepared from yeasts transformed either with the empty vector (control) or from five randomly picked colonies transformed with epitope-tagged TT12 variants either carrying an $RGSH_6$-motif at the N-terminal (upper panel; N-$RGSH_6$-TT12-C) or added to the C-terminal end (lower panel; N-TT12-$RGSH_6$-C) of TT12 (indicated by numbers below the blots). (C) [^{14}C]-methylamine accumulates in yeast vesicles transformed with either *cTT12* (filled symbols) or the empty vector (open symbols) in the presence of MgATP (circles) in a time-dependent manner. In contrast, no methylamine trapping occurs in the absence of MgATP (squares). This indicates formation of a transmembrane pH-gradient as a result of the activity of MgATP-dependent proton pumps.

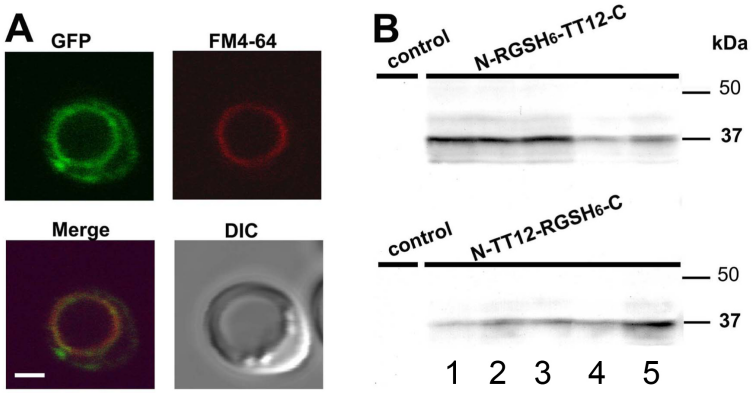

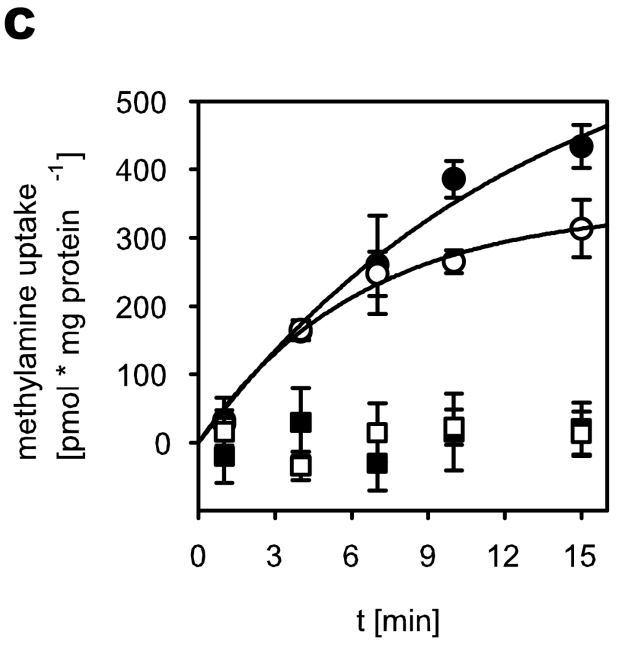

Supplemental Figure 3, Marinova et al.

TT12 transport activity towards various flavonoid substrates

The flavan-3-ol epicatechin (A), the rhamnosylated flavonol Q3R (B) and the nonglucosylated anthocyanidin cyanidin (C) do not exhibit TT12-dependent transport in the presence of MgATP. Absorbance scans of filter-associated substrates after transport assays performed with vesicles isolated from *TT12*- (black lines) or empty vector-transformed yeasts (grey lines) following 30 and 90s of transport (dotted and solid lines, respectively) are shown.

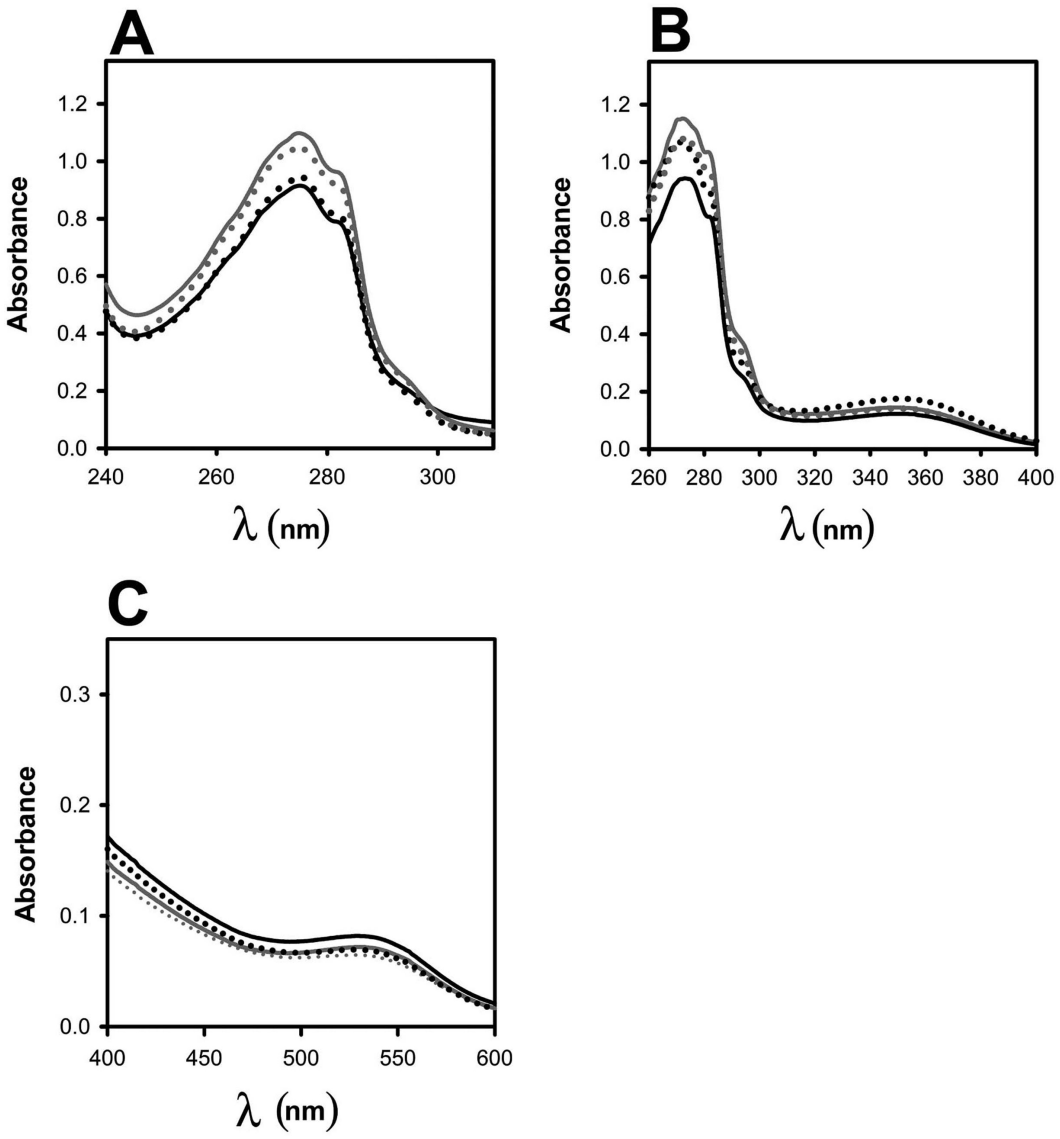

Supplemental Materials and Methods

Heterologous expression of *cTT12* in *Saccharomyces cerevisiae*

For the analysis of TT12 membrane localization in yeast, the *TT12* cDNA, *GFP5:TT12* and *TT12* variants with a $RGSH_6$-epitope fused to either the N- or the C-terminus were expressed in the YPH499 wild-type yeast strain from a *2μ* plasmid under the control of the strong and constitutive *pma1* promoter. Yeast cells expressing pN–TT12GFP and controls were cultured to the exponential growth phase in SD-Ura. Vacuolar membranes were stained by incubating cells with the styryl dye FM4-64 (10 µM; Invitrogen) (Humair et al., 2001). For CLSM analysis, GFP and FM4-64 were simultaneously excited with a 488 nm Ar and a 543 HeNe laser and fluorescence emission images averaged over eight frames were captured in independent channels (500 - 520 nm and 620 - 750 nm for GFP and FM4-64, respectively; DD488/543 beam splitter). CLSM analysis of yeasts transformed with *GFP5:TT12* revealed strong GFP fluorescence on the vacuolar membrane as verified by co-labeling with the styryl dye FM4-64 which, after endocytosis, reached the membrane surrounding the yeast vacuole (Supplementary Figure 2A). However, GFP fluorescence was also present to a lower degree on the plasma membrane and in intracellular membranes. Therefore, transport experiments were performed with microsomal membrane vesicles without any further membrane subfractionation.

For immunodetection by Western blotting, 5 ml of yeast cells grown in SD-Ura to an OD_{600} of 1 were washed twice with water followed by lysis in 150 µl of 1.85 M NaOH / 7.5% β-mercaptoethanol for 10 min on ice. After addition of 150 µ1 50% trichloroacetic acid, samples were incubated another 10 min on ice and centrifuged at 13’000x g for 10 min. The precipitate was dissolved in 10 mM Tris-HCl (pH 7.5). The equivalent of 1 µg protein was subjected to standard denaturing polyacrylamide gel electrophoresis (Laemmli, 1970) using a 10% polyacrylamide gel. Proteins were transferred onto nitrocellulose membrane by semi-dry transfer. Epitope-tagged TT12 protein was detected using anti-RGSHis (Qiagen, Germany) and alkaline phosphatase-conjugated anti-mouse IgG.

Western blot analysis performed with only 1µg of crude yeast protein extracts isolated from randomly chosen colonies transformed with TT12 carrying an $RGSH_6$ tag either fused to the N- or C-terminus (N-$RGSH_6$-TT12-C or N-TT12-$RGSH_6$-C, respectively) exhibited intense labelling of a single band comigrating with the 37-kDa molecular weight marker after detection with anti-RGSHis antibody (Supplementary Figure 2B). The TT12 protein has a

predicted molecular weight of 55 kDa. Since the molecular weight detected was lower than predicted irrespective of the tag position, it was improbable that the deviating migration was a result of protein degradation. Western blots repeated with microsomal vesicles isolated in the presence of an excess of a protease inhibitor cocktail resulted again in labelling of a band migrating at 37 kDa (data not shown). TT12 is a highly hydrophobic protein with 12 putative transmembrane segments and 48% of amino acids predicted to be within membrane-spanning helices. Therefore, it was assumed that the unusual migration of TT12 in denaturing polyacrylamide gels was due to its strongly hydrophobic nature. We concluded that *TT12* overexpressed in yeasts resulted in effective production of TT12 protein travelling to different membranes.

Independent yeast transformants transformed either with *cTT12*, *GFP5:TT12* or the empty vector were subjected to growth tests in the presence of different flavonoids including the flavan-3-ols catechin or epicatechin up to concentrations of 20 mM added to the medium. None of the flavonoids tested clearly inhibited yeast growth irrespective of the presence or absence of TT12 suggesting that the YPH499 yeast strain is not a good experimental system to study resistance towards phenolic compounds at least in a WT genetic background (data not shown).

MgATP-dependent pH-gradient formation in yeast membrane vesicles.

In order to evaluate the physiological intactness (absence of leaks) of the isolated membrane vesicles and to verify the presence and activity of MgATP-dependent proton pumps acidifying the vesicular lumen and thereby providing the proton gradient necessary for the flavonoid/H^+-antiport activity mediated by TT12, MgATP-dependent trapping of the weak base [^{14}C]-methylamine (45 mCi/mmol, Moravek Biochemicals, Brea, U.S.A.) was assayed in vesicles prepared from *cTT12*- and empty vector-transformed yeasts. In a final volume of 3.6 ml, one part of vesicles was mixed with five parts of medium (0.4 M glycerol, 0.1M KCl, 20 mM Tris-Mes pH 7.4, 1 mM dithiothreitol) containing either 1 mM $MgSO_4$ (no ATP condition) or 6 mM $MgSO_4$ and 5 mM ATP (+ ATP condition) and 1.5 µCi [^{14}C]-methylamine (given are final concentrations). At different time-points three times 0.1 ml were rapidly filtered on nitrocellulose filters and washed with ice-cold transport medium as stated in Methods. In the presence of MgATP, methylamine accumulates in the vesicles in a time-dependent manner (Supplemental Figure 2C). Methylamine trapping in vesicles is independent of the presence of TT12 and does not occur in the absence of MgATP. This result

demonstrates that the membrane-bound MgATP-dependent proton pumps on yeast vesicles are present forming a pH gradient in the presence of ATP which can be used by TT12 to transport flavonoids. Furthermore, absence of flavonoid transport into empty vector control vesicles is due to absence of a flavonoid transporter and not caused by absence of acidification.

References to Supplemental Material and Methods:

Humair, D., Felipe, D.H., Neuhaus, J.M., and Paris, N. (2001) Demonstration in yeast of the function of BP-80, a putative plant vacuolar sorting receptor. Plant Cell **13**, 781-792.

Laemmli, U.K. (1970) Cleavage of Structural Proteins during the Assembly of the Head of Bacteriophage T4. Nature **227**, 680-685.

Chapter 3

Analysis of the subcellular localization of Arabidopsis MATE transporters and complementation of the *tt12* seed phenotype by related MATE transporters

Introduction

The MATE (multidrug and toxic compound extrusion family of putative secondary transporters) (Brown *et al.*, 1999) is an extensive group of membrane proteins with largely unknown function. MATE family members have been reported in humans, in yeasts *Saccharomyces cerevisiae* and *Schizosaccharomyces pombe*, *Escherichia coli*, and many other bacteria, and in *Archaea*. Arabidopsis has 56 MATE family members, 10 times more than any other sequenced organism (Arabidopsis Genome Initiative, 2000). Hydropathy analysis suggested that proteins of the MATE family have a common topology consisting of 10-12 transmembrane (TM) domains. Biochemical data on transport properties and functional aspects of family members is scarce as is the identification of characteristic conserved signatures or domains.

In Chapter 2, a functional analysis of the *Arabidopsis* MATE transporter TT12/DTX41 was undertaken. It was shown that the *tt12* mutant largely lacks epicatechin, proanthocyanidins (PA) and the major seed flavonol quercetin 3-*O*-rhamnoside (Q3R). The *TT12* gene is expressed in cells of the seed coat that are actively involved in biosynthesis of PAs. A GFP-TT12 fusion localized TT12 to the tonoplast. Furthermore, TT12 expressed in yeast was demonstrated to function as a proton-antiporter for cyanidin 3-*O*-glucoside but not for cyanidin, epicatechin and Q3R. Although in this study the *in vivo* substrate of TT12, which could be a glycosylated epicatechin derivative, was not elucidated it might be hypothesized based on the available data that homologs of TT12 are involved in the vacuolar deposition of related flavonoids into vacuoles in other cell types and tissues. Thus, it might be hypothesized that homologs of TT12 expressed in vegetative plant parts could be ultimately responsible for the vacuolar accumulation of flavonols and anthocyanins. It is interesting to note that the TT12 homolog from tomato is presumably involved in anthocyanin deposition has been reported although a functional description of this gene is still missing. The *ant1* tomato mutant overexpressing a MYB transcription factor by activation tagging overproduces anthocyanins in fruits. Upregulated genes in the *ant1* background include a MATE transporter gene exhibiting 36% amino acid sequence identity to TT12 and 61% to DTX 35/At4g25640 (Mathews *et al.*, 2003). The fact that TT12 catalyzes transport of a glucosylated anthocyanin although this substance is not known to appear in the seed coat suggests that the substrate specificity of a given MATE transporter is not absolute.

Thus, one can speculated that functional homologs of TT12 – e.g. a vacuolar anthocyanin transporter – are also able to transport PA precursors when expressed in the *TT12* context.

Due to the large number of MATE genes one can expect that there is functional redundancy between closely related members. Due to redundancy the analysis of single knock-out mutants complicated since close homologs could overtake the function encoded by the mutated protein.

Here, we proposed a novel misexpression strategy to assign function of unknown genes in redundant families via complementation of a mutant (*tt12*) phenotype by using the promoter of the BAN gene, which encodes anthocyanidin reductase and is specifically active in PA accumulating cells of the seed coat (Xie *et al*., 2003, Debeaujon *et al*., 2003). The strategy to assign function of unknown genes in redundant families via complementation of a mutant phenotype has been termed ME MC (misexpression and mutant complementation) strategy by us. Available full length MATE cDNAs were fused to the ban or CaMV promoter in order to be expressed in the *tt12* mutant background. Subsequently, T1 plants of $Pro_{CaMV35S}$:$MATE_{XY}$GFP/*tt12* (figure 4) and Pro_{ban}:$MATE_{XY}$GFP/*tt12* (in progress, figure 3) are used in screening for the reversion of the phenotype to wild-type using vanillin staining of immature seeds demonstrating presence of PAs as a red coloration of the seed coat. The $Pro_{CaMV35S}$:$MATE_{XY}$GFP constructs were used also for the localization study (figure 2). *tt12*-reverting MATE transporters which are expressed in aerial plant parts will therefore define novel flavonoid transporters whose overexpression may ultimately allow the overproduction of health-promoting flavonoids or the realization of novel flower colors. An intriguing but unresolved problem in plant cell research regards how integral membrane proteins reach their proper destination within the cell. It is widely accepted that peptide signals exposed in the cytosol are responsible for targeting to the correct subcellular location in plant cells. Specific sorting signals are supposed to act dominant over a default pathway which targets membrane proteins to an unspecified membrane in the absence of signals (Törmäkangas *et al*., 2001, Brandizzi *et al*., 2002). Conflicting results have been reported for the tonoplast intrinsic protein α-TIP. On the one hand, the last 48 amino acids of α-TIP including the sixth transmembrane domain were sufficient to target a reporter protein to the tonoplast (Höfte and Chrispeels, 1992). On the other hand, Jiang and Rogers (1998) reported that the isolated sixth transmembrane domain of α-TIP used in a chimeric reporter construct was unable to send the reporter protein to the lytic compartment and to the Golgi. A recent study aimed at the analysis of the contribution of the absolute length of a transmembrane domain to sorting of fusion proteins with the green fluorescent protein GFP followed by the transmembrane domain of the human lysosomal protein LAMP1 (Brandizzi *et al.*, 2002). Interestingly, transient expression assays in tobacco leaves demonstrated that a transmembrane domain consisting of 17 hydrophobic amino acids was retained in the

endoplasmic reticulum while a length of 20 and 23 amino acids led to an accumulation of the GFP reporter in membranes of the Golgi apparatus and plasma membrane, respectively.

The ongoing characterization of gene families encoding membrane proteins elucidates differences in the subcellular localization of related integral proteins. In spite of a high degree of overall similarity in the prediction of numbers and positions of transmembrane α-helices in proteins belonging to the multidrug-related associated protein (MRP) subfamily of ATP-binding cassette transporters in Arabidopsis have been proposed to localize to the tonoplast or the plasma membrane (Klein *et al.*, 2006). Thus, it is obvious that yet undefined cellular machinery must be able to detect specific but unknown structural signals in plant membrane proteins defining the sorting to the destination membrane.

In chapter 2 we showed that GFP-TT12 fusion localized on the vacuolar membrane. Li *et al.* (2002) reported plasma membrane localization of a DTX1-GFP fusion. One approach to define signals involved in membrane protein sorting processes is to raise chimeras between closely related membrane proteins which reside on different membranes when expressed as fusion proteins. As shown in the phylogenetic tree presented in Figure 1, DTX1 (At2g04070) is only distantly related to TT12 (At3g59030) suggesting that the sequence variation between these two members of the MATE family is too large to clearly define signals in chimeras. Therefore, our approach was to localize several of the MATE proteins in a transient assay with the hope to either identify close TT12-homologs localized on the plasma membrane or DTX1-homologs with tonoplast localization. Proposed subcellular localizations of the Arabidopsis MATE transporters used in this study as defined by the Aramemnon plant membrane protein database are depicted in Table 1.

In order to achieve both goals we used the available full-length cDNAs of MATE transporter-coding genes from *Arabidopsis thaliana* kindly provided by the RIKEN Bioresource Center (Ibaraki, Japan, http://www.brc.riken.jp) and transferred these genes into entry vectors using Gateway™ technology. Afterwards, they were transferred by recombination-mediated cloning either into binary destination vectors suitable for *Agrobacterium*-mediated plant transformation or used for localization studies. In these destination vectors, the MATE gene cDNA was either under the control of the strong constitutive Cauliflower Mosaic Virus 35S promoter and at the C-terminus of the MATE protein a translational fusion with the gene coding for the GFP protein was obtained (Curtis and Grossniklaus, 2003; localization) or the gene was placed under control of the *BAN5* promoter defining specific expression in PA-producing seeds of the testa (Debeaujon *et al.*, 2003; ME MC approach).

Table 1. Members of MATE family used in this study

DTX* code	MIPS code	NCBI acc.No	Aramemnon predictions	
			No. TMD	predicted place
2	At2g04080	AK118147	12	none
6	At2g04100	AY093126	12	ch
9	At1g66760	AY052222	11	none
10	At1g15150	AY070445	12	none
12	At1g15170	AY139985	12	none
13	At1g15180	NP563964.1	12	none
16	At5g52450	AY046054	12	none
18	At3g23550	AY062511,AY070032	12	none
19/ALF5	At3g23560	AF370531	11	none
21	At1g33110	NP174587.1	12	none
23	At1g33080	AY080844	11	mx
25	At5g17700	AY099666	12	none
27	At5g65380	NP201341.1	13	none
29	At3g26590	AY057664	11	none
30	At5g38030	AF372972,AY054277	12	none
31	At1g12950	NP172755.1	12	none
33	At1g47530	AY058871	12	none
34	At4g00350	NP567173.3	10	secretory pathways
36	At1g11670	AY140018	12	none
37	At1g61890	AY048279,AY057622	12	none
39	At4g21910	AY054235	12	none
40	At3g21690	AY099744	12	ch
41/TT12	At3g59030	NP191462.1	12	mx
42/FDRL	At1g51340	NP974000.1	12	secretory pathways
43/FRD3	At3g08040	AY056439,AY057517	12	none
44	At2g38330	NP181367.2	12	ch
46	At2g21340	NP181367.2	12	ch
47/EDS5	At4g39030	NP195614.2	9	mx
48	At1g58340	NP564731.1	12	none
50	At5g52050	NP200018.1	10	mx
56	At4g22790	NP194010.1	12	none

*DTX (detoxification) nomenclature for the Arabidopsis MATE family, the DTX nomenclature proposed by Li *et al*., (2002)

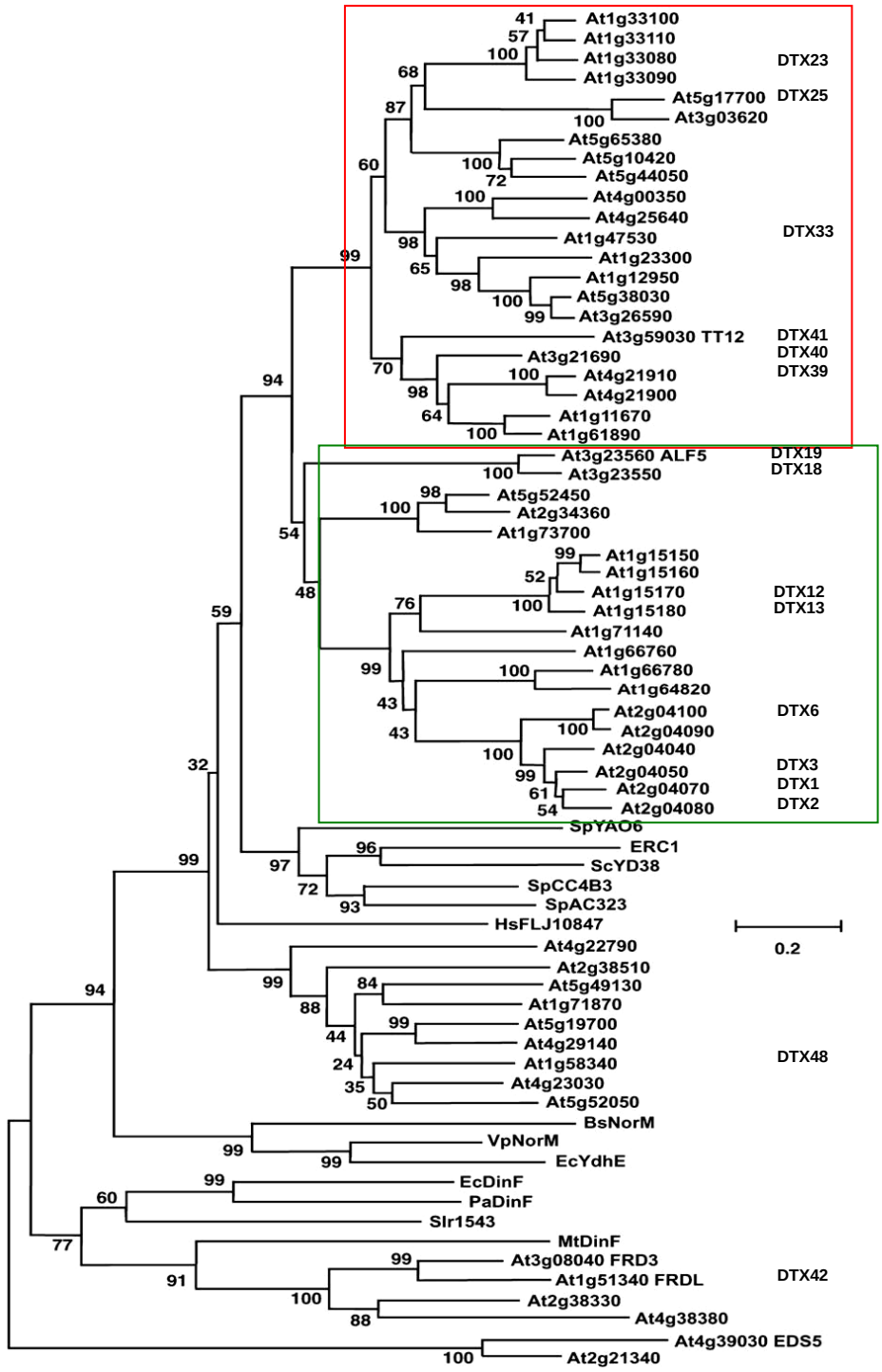

Figure 1. Dendrogram showing the amino acid sequence similarity among multidrug and toxic extrusion (MATE) family members (from Rogers and Guerinot, 2002). 56 Arabidopsis MATE proteins, 1 human protein, 5 proteins from yeast, and selected bacterial members were included in the dendogram. Clades including genes exhibiting high homology to TT12 or ALF5 and DTX1 were boxed in red and green, respectively, and the DTX nomenclature was added.

Material and methods

1. Cloning procedures

1.1 Entry clones

Table. 1 Primers, upper (B1) and lower (B2) used for the amplification of full length cDNA clones obtained from RIKEN Bioresource Center. The original pda identifier of Riken is given. cDNAs marked with asterisks were amplified with two step adapter PCR approach as described in the text. Primers were designed to allow a translational fusion of the genes if the Gateway cassette A is used in the destination vector.

*At2g04080, pda11176	DTX2-B1	AAAAAGCAGGCTCC ATGGAAGAGCCATTTCTTC
	DTX2-B2	AGAAAGCTGGGT TAACCAATCCATTTTCAGT
*At2g04100, pda08161	DTX6-B1	AAAAAGCAGGCTCC ATGCAAGATCCACTTTTATTG
	DTX6-B2	AGAAAGCTGGGT TAGCAAGTCCATTGCCAAA
At1g15180, pda01371	DTX13-B1	GGGGACAAGTTTGTACAAAAAAGCAGGCTCCATGGGAGACGCAGAGAGC
	DTX13-B2	GGGGACCACTTTGTACAAGAAAGCTGGGTTTGTTCCATAGGCCAAAGC
*At3g23550, pda05792	DTX18-B1	AAA AAG CAG GCT CCA TGG CTG ATC CCA CGT CCA
	DTX18-B2	AGA AAG CTG GGT TGA CAG TGG CAG CAG TCA
*At3g23560, pda01251	DTX19-B1	A GAA AGC TGG GTT TAC CGT AGC AAC ATT CA
	DTX19-B2	AA AAA GCA GGC TCC ATG GCT GAT CCG GCA
*At1g33080, pda07809	DTX23-B1	AAAAAGCAGGCTCCATGGCGAGAAGAGAA
	DTX23-B2	AGAAAGCTGGGTTTTCGTTTTGTAAAGT
*At5g17700, pda08645	DTX25-B1	AAAAAGCAGGCTCCATGAGTGGAGGTGGTGGA
	DTX25-B2	AGAAAGCTGGGTTCTTTCTCTCTTCATCTCT
At1g12950, pdx38008	DTX31-B1	GGGGACAAGTTTGTACAAAAAAGCAGGCTCCATGGAGAAAGATAATGAC
	DTX31-B2	GGGGACCACTTTGTACAAGAAAGCTGGGTTGTTCAAAAGAGTCTCTTT
*At1g47530, pda05274	DTX33-B1	AAA AAG CAG GCT CCA TGG GAA AGG ATA AGA C
	DTX33-B2	AGA AAG CTG GGT TCT CCT GCG CCG TTC C
At4g00350, pda13032	DTX34-B1	GGGGACAAGTTTGTACAAAAAAGCAGGCTCCATGGAGATCCCGGTTCGA
	DTX34-B2	GGGGACCACTTTGTACAAGAAAGCTGGGTTAGTTGCTATTTTTTCTAA
*At4g21910, pda05543	DTX39-B1	AAAAAGCAGGCTCC ATGGATGTGTCAAATGAGA
	DTX39-B2	AGAAAGCTGGGTTGTTT TGGAGAGGCTCC
*At3g21690, pda08799	DTX40-B1	AAAAAGCAGGCTCC ATGGACTCGTCTCCAAACGA
	DTX40-B2	AGAAAGCTGGGTTT TCAGGAACAACTTCTTGT
At1g51340, pda04738	DTX42-B1	GGGGACAAGTTTGTACAAAAAAGCAGGCTCCATGATGTCTGAAGATGGC
	DTX42-B2	GGGGACCACTTTGTACAAGAAAGCTGGGTTGCTCCTAAGAAAAGACCA
*At3g08040, pda05967	DTX43-B1	AAAAAGCAGGCTCCATGACGGAAACTGGTGAT
	DTX43-B2	AGAAAGCTGGGTTGGAAGATGAAGAGGATGA
At2g21340, pda05075	DTX46-B1	GGGGACAAGTTTGTACAAAAAAGCAGGCTTATGCAAAACCCTAACTTT
	DTX46-B2	GGGGACCACTTTGTACAAGAAAGCTGGGTCCGCAGCTTTCACTTTCTC
At1g58340, pda14579	DTX48-B1	GGGGACAAGTTTGTACAAAAAAGCAGGCTTATGTGTAATTCAAAACCA
	DTX48-B2	GGGGACCACTTTGTACAAGAAAGCTGGGTCAACCAACATGGTTCTCAT
At5g52050, pda11014	DTX50-B1	GGGGACAAGTTTGTACAAAAAAGCAGGCTTATGAGTCAATCAAATCGT
	DTX50-B2	GGGGACCACTTTGTACAAGAAAGCTGGGTCCTTATCAACCATCCCAGC

At4g22790, pda12556	DTX56-B1	GGGGACAAGTTTGTACAAAAAAGCAGGCTTATGTCAGAAACATCAAAG
	DTX56-B2	GGGGACCACTTTGTACAAGAAAGCTGGGTCTGAGTGGCTATCTTGTCC

The MATE-transporter cDNAs obtained from RIKEN were sequenced first using the oligos M13fw - TGTAAAACGACGGCCAGT and M13rev - CAGGAAACAGCTATGACC to confirm identity with the predicted sequences of *Arabidopsis thaliana* proteins TIGR v.5. Subequently, for Gateway-mediated cloning into the vectors pDONR207 or pDONR Zeo (Invitrogen), the MATE transporter coding sequences were amplified with the polymerase chain reaction (PCR) using the upper and lower primers listed in Table 1 and the Expand High Fidelity System® (Roche) according to the manufacturer's instructions in 50 µl rections. The lower primers omitted the stop codon in all cases in order to ensure a functional C-terminal fusion to GFP for localization purposes. In the destination vectors lacking a C-terminal fusion before the terminator, multiple stop codons in all three reading frames were present in the vector sequence downstream of the *att*R2 site.

Two PCR approaches were used to obtain the full length cDNAs possessing the *att*B1 and *att*B2 sites necessary for the recombination cloning into pDONR207 or pDONR Zeo vectors by the BP reaction. In the first approach primers which contained the full *att*B1 and *att*B2 sequences were used and the PCR reaction was performed as follows:

1 cycle	denaturation	5 min	95°C
30 cycles	denaturation	45 sec	95°C
	primer annealing	45 sec	50-60°C
	hybridization	1 min per 1kb	72°C
1 cycle	elongation	5 min	72°C

The second approach consisted of two step adaptor PCR were used when the specific for the DTX genes primers contained only the terminal 12 bases of the *att*B1 and *att*B2 sequences (marked with asterisks in table 1). In the first step 10 cycles PCR reaction was performed with the template-specific primers. 10µl of this PCR product served as template for a second PCR reaction containing universal *att*B primers (*att*B1 – GGG GAC AAG TTT GTA CAA AAA AGC AGG CT and *att*B2 – GGG GAC CAC TTT GTA CAA GAA AGC TGG GT, Invitrogen) and resulted in amplification of the full-*att*B PCR products.

The cycling program for the two steps PCR was as follows:

First step:

1 cycle	denaturation	2 min	95°C
9 cycles	denaturation	45 sec	95°C
	primer annealing	45 sec	60°C
	hybridization	1 min per 1kb	72°C
1 cycle	elongation	5 min	72°C

Second step:

1 cycle	denaturation	5 min	95°C
24 cycles	denaturation	45 sec	95°C
	primer annealing	45 sec	50-60°C
	hybridization	1 min per 1kb	72°C
1 cycle	elongation	5 min	72°C

2 µl of the PCR product were separated on a 1% (w/v) Agarose/1xTAE (40 mM Tris-acetate and 1 mM EDTA, pH 8.0) gel and visualized by ethidium-bromide staining under an UV-transilluminator.

The remaining PCR product was cleaned with the GFX^{TM} PCR DNA and Gel Band Purification Kit (Amersham) and subjected for the BP reaction. The BP recombination reaction (Invitrogen) was performed according to the manufacturer's instructions using ½ of the recommended reaction volumes. The product was later used to transform XL1blue by electroporation (Biorad) competent *E. coli* strain (XL1blue) and selection was performed on LB plates containing 10µm/ml of gentamycin for resistant clones. All constructs were subsequently sequenced as described in point 1.4.

1.2 Construction of the binary, gateway-compatible *Pro$_{BAN5}$* expression vectors pBAN5pr32 and pBAN5pr83.

We have used the Pro$_{ban5}$ promoter described by Debeaujon *et al.* (2003). This fragment was used to replace the constitutive CaMV 35S promoter in two binary Gateway-compatible vectors pMDC32 and pMDC83, respectively which are suitable for stable plant transformation, in order to give pBAN5pr32 or pBAN5pr83. The primers used to amplify the fragment are listed in the following table:

Ban5pr-low-AscI	AGA AAG CTG GGT TGG CGC GCC CAT GAT TGT ACT TTT GAA ATT AC
Ban5pr-low-PacI	AGA AAG CTG GGT TTT AAT TAA CAT GAT TGT ACT TTT GAA ATT AC
Ban5pr-up	AAA AAG CAG GCT CCA AGC TTT GAC TCG TGT AAT TCG

The cycling program for the PCR was as follows:

1 cycle	denaturation	5 min	95°C
29 cycles	denaturation	45 sec	95°C
	primer annealing	45 sec	58°C
	hybridization	30 sec	72°C
1 cycle	elongation	5 min	72°C

The fragment was cleaned with the GFX^{TM} PCR DNA and Gel Band Purification Kit (Amersham) and ligated into $Pro_{CaMV35S}$:$MATE_{DTX2}$ or $Pro_{CaMV35S}$:$MATE_{DTX2}$GFP which were first digested with AscI and PacI. In order to obtain the destination vectors in their final form the DTX2 gene from Pro_{BAN5}:$MATE_{DTX2}$ and Pro_{BAN5}:$MATE_{DTX2}$GFP was replaced by the Gateway cassette. In this case BP recombination reaction was performed with equimolar amounts of the Pro_{BAN5}:$MATE_{DTX2}$ and Pro_{BAN5}:$MATE_{DTX2}$GFP vectors and pDONR207 (Invitrogen). The products were transformed by electroporation into competent *E. coli* strain DB 3.1. The growing colonies were selected on LB plates with 50µm/ml of kanamycin for resistant clones. Positive clones - Pro_{BAN5}:Gateway (pBAN5pr32) and Pro_{BAN5}:GatewayGFP (pBAN5pr83) were verified by PCR with the above mentioned primers, by restriction analysis and all constructs were subsequently sequenced as described in point 1.4.

1.3 Preparation of destination clones

All MATE full-length cDNAs were transferred into three independent destination vectors, (i) pMDC83 providing a $Pro_{CaMV\ 35S}$-$MATE_{XY}$GFP fusion (GFP C-terminal with respect to the MATE protein; Curtis and Grossniklaus, 2003), (ii) pBAN5pr32 and (iii) pBAN5pr83. The LR reaction were performed according to the manufacturer's instructions (Invitrogen) but setting up ½ of the recommended reaction volumes. 3µl of the product was used to transform by electroporation (Biorad) competent *E. coli* strain (XL1blue) and selected on LB plates containing 50µm/ml of kanamycin for resistant clones. All constructs were subsequently sequenced as stated in point 1.4.

1.4 Sequencing

DNA sequencing was conducted in house with the ABI 3730 sequencer. The sequencing mix contained: 1 µl Big Dye Terminator Mix v 3.1, 1.5µl 5x Sequencing Buffer (Applied Biosynthesis, USA), 1 µl DNA (~200ng), 0.5 µl primer (2.5 pmol/µl), 6 µl dH_2O and the reaction was performed using the following program:

1 cycle	94°C	2 min					
60 cycles	96°C	10 sec,	50°C	5 min,		60°C	3 min

2. Transient biolistic transformation of onion epidermal cells – described previously in chapter 2.

3. Stable transformation of *A. thaliana* using *Agrobacterium tumefaciens* by floral dipping and selection of transgenic plants.

Transformation was performed according to the protocol described by (Nesi *et al.*, 2000). The *Agrobacterium tumefaciens* strain GV3101 (Clough and Bent, 1998) was transformed by electroporation (Biorad) with constructs $Pro_{CaMV\ 35S}$-$MATE_{XY}$-GFP and selected on LB (Luria Bertani) agar plates containing 50 µg/ml kanamycin and rifampicillin respectively for 2 days at 28° C. Resistant colonies were subsequently grown in 10 ml liquid LB medium containing the same antibiotics for 2 days at 28°C on a shaker at 150 rpm. 5 ml of this pre-culture was used to inoculate 400 ml LB containing the same antibiotics and incubated over night at 28°C and 150 rpm until the OD_{600} reached a values of 0.6. Cells were harvested by centrifugation for 10 min at 1500g (4°C, Avanti, JL 10.500) and resuspended to a final OD_{600} 0.5-0.8 in infiltration medium containing ½ MS 1B medium, 50 g/l sucrose and 5 mmol/l $MgCl_2$. Silwet L-77 0.01% (v/v) was added to the suspension immediately before transformation. The flowers of Ws2 and *tt12* plants were dipped for 30 seconds into the *Agrobacterium* suspension. Subsequently the plants were placed for one hour horizontally on plastic wrap, and then they were completely covered with this film and left over night in the greenhouse. The following morning, the plastic wrap was removed and plants were brought back into a vertical position. After ripening, harvested seeds were surface-sterilized, stratified and selected on ½ MS+S plates containing 20 mg/l hygromycin B (Invitrogen). Antibiotic-resistant plants were transferred individually after about 2 weeks into soil and were grown in a greenhouse [16h light (150 µmol m^{-2} s^{-1}), 8h dark, 22°C, 60% relative humidity]. Dry seeds of several (usually 8-12 per construct) independent T1 plants were used for the analysis of *tt12* seed phenotype reversion.

4. PA mutant screen

Dry T2 seeds from individual stably transformed T1 plants carring $Pro_{CaMV\ 35S}$-$MATE_{XY}$-GFP constructs were stained according to published procedures (Debeaujon *et al.*, 2000; Abrahams *et al.*, 2002) using the *p*-dimethylaminocinnamaldehyde reagent (2% (w/v) DMACA in 3 M HCl/50% (w/v) methanol) for the presence of PAs. After 24h incubation at room temperature, seeds were washed three times with 70% (v/v) ethanol. DMACA-treated seed pools were then examined using a Nikon SMZ1500 binocular microscope coupled to a Nikon Coolpix camera for DMACA-specific black seed coloration.

For the vanillin assay intact seeds were incubated as described by Debeaujon *et al.* (2000) in a solution of 1% (w/v) vanillin and 6N HCl at room temperature for 5 or 20 min for immature and mature seeds, respectively. Vanillin turns red upon binding to flavan-3,4-diols

(leucoanthocyanidins), flavan-4-ols (catechin) or flavan-3-ols, which are present either as monomers or as terminal subunits of proanthocyanidins.

Results

1. Subcellular localization of MATE-GFP fusion proteins after transient biolistic transformation of onion epidermal cells.

Table 1. Summary of the data available after transient expression analysis

DTX code	MIPS code	Aramemnon predictions		Subcellular localization
		No. TMD	predicted place	
1	At2g04070	12	none	plasma membrane, Li *et al.*, 2002
2	At2g04080	12	none	tonoplast
3	At2g04050	12	none	
6	At2g04100	12	ch	tonoplast
9	At1g66760	11	none	
10	At1g15150	12	none	
12	At1g15170	12	none	plasma membrane, personal communication
13	At1g15180	12	none	
16	At5g52450	12	none	
18	At3g23550	12	none	tonoplast
19/ALF5	At3g23560	11	none	tonoplast
21	At1g33110	12	none	
23	At1g33080	11	mx	tonoplast
25	At5g17700	12	none	tonoplast
27	At5g65380	13	none	
29	At3g26590	11	none	
30	At5g38030	12	none	
31	At1g12950	12	none	
33	At1g47530	12	none	tonoplast
34	At4g00350	10	secretory pathways	
36	At1g11670	12	none	
37	At1g61890	12	none	
39	At4g21910	12	none	tonoplast
40	At3g21690	12	ch	tonoplast
41/TT12	At3g59030	12	mx	tonoplast
42/FDRL	At1g51340	12	secretory pathways	
43/FRD3	At3g08040	12	none	pericycle, Green & Rogers, 2004
44	At2g38330	12	ch	
46	At2g21340	12	ch	
47/EDS5	At4g39030	9	mx	
48	At1g58340	12	none	
50	At5g52050	10	mx	
56	At4g22790	12	none	

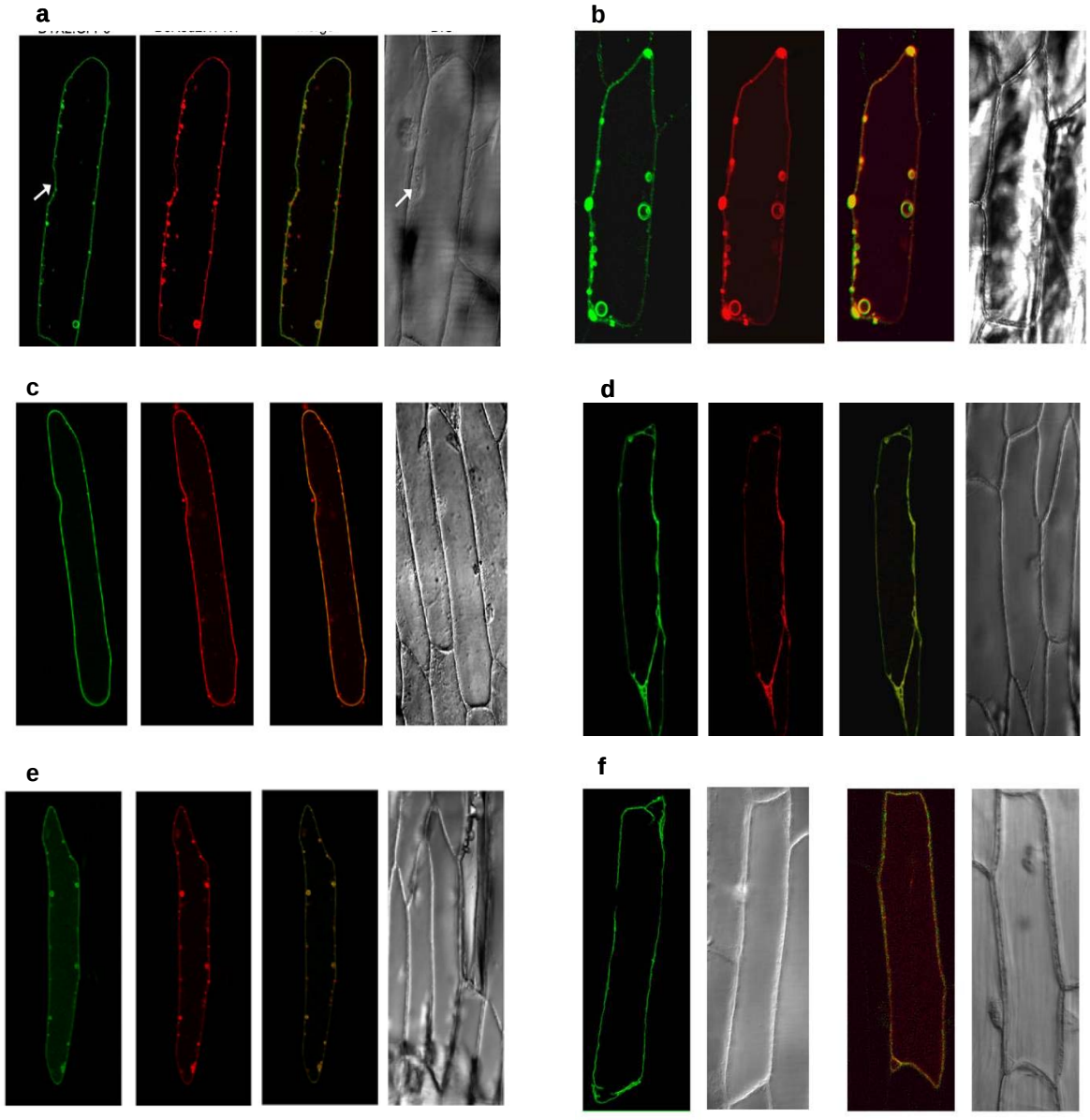

Figure 2. Subcellular localization of GFP fusions with (a) DTX2/At2g04080, (b) DTX6/At2g04100, (c) DTX19/At3g23560, (d) DTX23/At1g33080 (e) DTX25/At5g17700 and (f) DTX41 (GFP5:TT12) after transient expression on bulb onion epidermis cells.

The $Pro_{CaMV\ 35S}$-$MATE_{XY}$-GFP constructs containing *DTX2, 6, 18, 19, 23, 25, 33, 39, 40* and *41* (*GFP5:TT12*) constructs respectively were transiently expressed in onion bulb epidermis cells. Confocal images (A, B, C) are depicted together with corresponding differential interference contrast (DIC) images (D). (A) Transient expression of the GFP-fused constructs, false-colored in

green. (B) Transient expression of the tonoplast marker *DsRed2:TPK1*, false-colored in red. (C) The GPF-fused constructs and the tonoplast marker DsRed2:TPK1 shows colocalization on the vacuolar membrane and surround the nucleus (arrow) excluding plasma membrane localization.

Biolistic particle delivery on onion epidermal cells of each of the following $Pro_{CaMV\ 35S}$-$MATE_{XY}$-GFP constructs, where $MATE_{XY}$ stands for *DTX2, 6, 18, 19, 23, 25, 33, 39, 40* and *41* (GFP5:TT12), respectively resulted in GFP fluorescence on membranes surrounding the central vacuole and on membranes forming cytoplasmic strands, suggesting localization on the tonoplast (Figure 2A). In order to verify this localization we used separately (Figure 2B) or we cobombarded (Figure 2C) the onion epidermis with a DsRed2 tagged version of the two-pore ion channel TPK1 (formerly known as KCO1), whose tonoplast localization is well established (Czempinski *et al.*, 2002; Bihler *et al.*, 2005). Cobombardment of both constructs resulted in colabelling of the tonoplast (Figure 2C, merge), including the cytoplasmic strands that traverse the central vacuole and vesicles which represent the vacuolar invaginations which appeared in a given focal plane as a round structures. The pictures of the last panel (D) represent the DIC image of the same cells. Most probably due to the very high overexpression of the TPK1-DsRed absence of full localization was rare.

2. *TT12* cDNA driven by the *banyuls5* promoter complements the *tt12* mutant.

The ME MC gene identification strategy proposes to complement the seed-specific metabolic phenotype of the *tt12* mutant with MATE-transporter cDNAs using a promoter that is specifically active in cells actively synthesizing PAs in the seed coat. To this end, we have used the Pro_{ban5} promoter described by Debeaujon *et al.* (2003) which consists of the 5'UTR of the *BAN* gene and 413 bases of the promoter including the CAAT and TATA boxes, known to sufficient to determine *BAN*-specific expression in PA-synthesizing cells (Debeaujon *et al.*, 2003). This fragment was used to replace the constitutive CaMV 35S promoter in two binary, Gateway-compatible vectors suitable for stable plant transformation allowing either Pro_{ban}-driven expression of the cloned gene alone or of the gene fused in-frame with the cDNA encoding the GFP6 fluorescent reporter protein (work in progress).

In order to demonstrate functionality of the vectors and proof of concept, the *tt12* mutants was stably transformed with a binary vector containing the *Pro_{ban5}::cTT12-GFP* cassette. As shown in Figure 3, immature seeds of transgenic T1 plants exhibited red coloration with vanillin. Thus, unlike *tt12* seed, these T1 seeds produce PAs and are able to deposit them in the vacuole. Having demonstrated the functionality of the pBAN5prGFP vectors they were used to obtain further Pro_{ban5}::$cMATE_{XY}$ constructs followed by transformation of *tt12* plants.

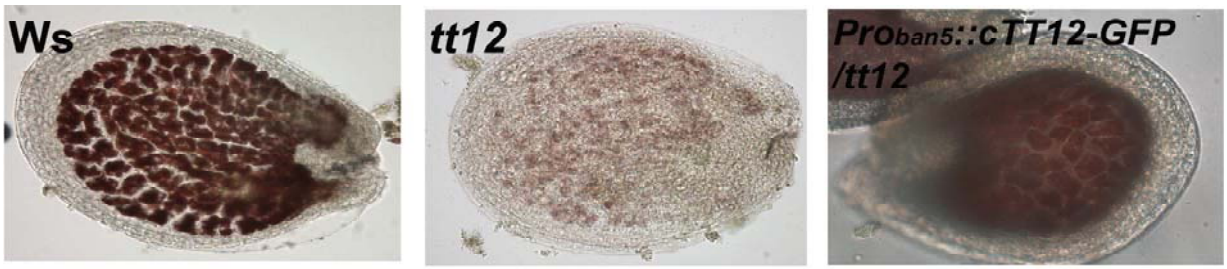

Figure 3. Whole-mount vanillin staining of immature seeds of wild type (Ws), *tt12* mutant and a *tt12* mutant complemented with the Gateway vector carrying TT12 cDNA C-terminally fused to GFP under control of the banyuls5 promoter (*Pro$_{ban5}$::cTT12-GFP/tt12*). Vanillin detects the otherwise colorless PAs in the endothelium. This experiment demonstrates proof of evidence that constructs used for the proposed misexpression strategy were functional.

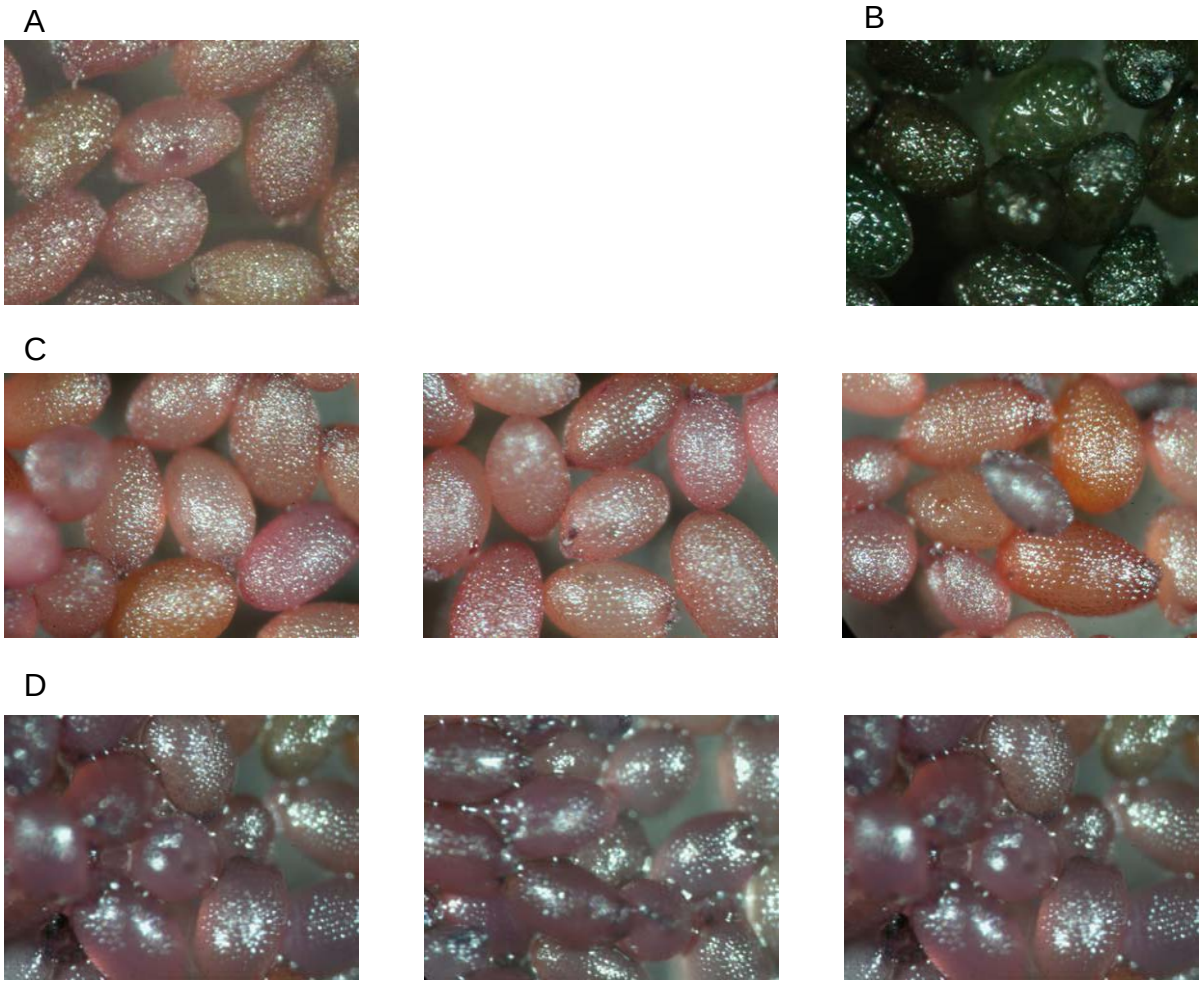

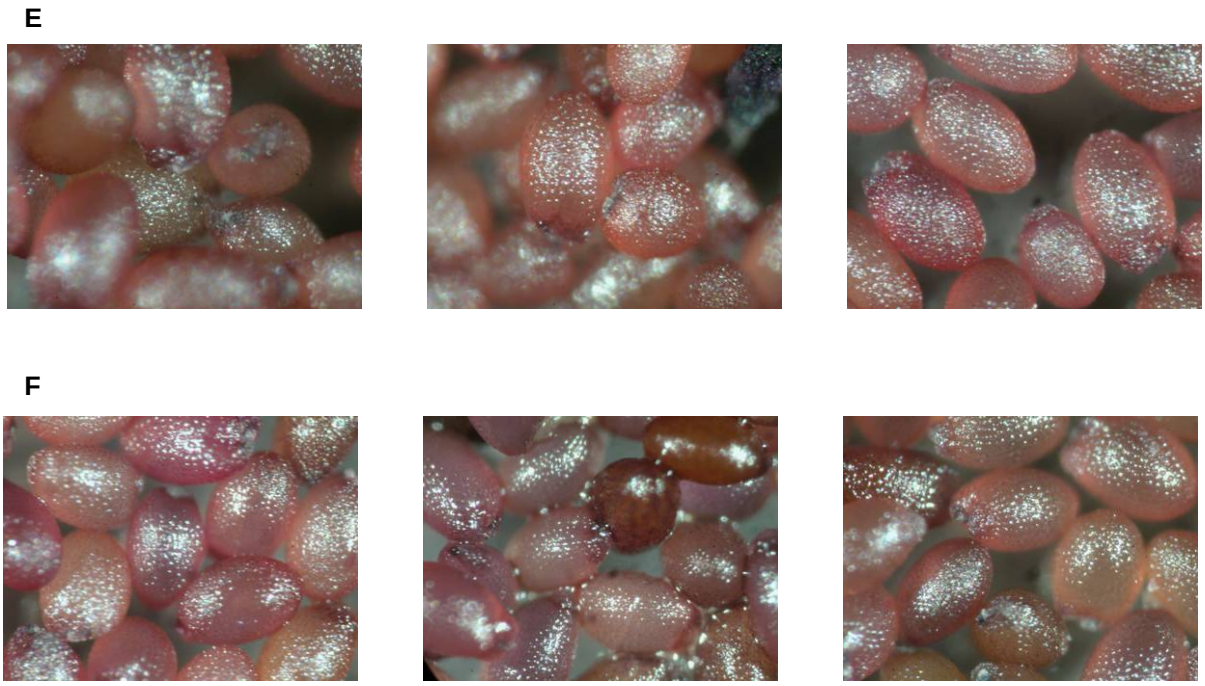

Figure 4. Proanthocyanidin pigment deposition in dry seeds of wild type (Ws, A), *tt12* (B) and seeds from stable transformed *tt12* plants with $Pro_{CaMV\ 35S}$-$MATE_{XY}$-GFP, where $MATE_{XY}$ stands for DTX2 (C), DTX6 (D), DTX12 (E) and DTX19 (F) respectively. Pictures of dry seeds were taken after histochemical staining with DMACA. Staining of dry seeds with DMACA resulted in black coloration of WT due to presence of PAs, or in light coloration of *tt12* seeds due to the absent of those compounds. T2 seeds of three independent hyg- resistant T1-lines (left, middle and right panel, respectively) were depicted.

Discussion

In Arabidopsis, the MATE family consists of 56 genes (Rogers and Guerinot, 2002; Li *et al.*, 2002), but only five of them have been characterized so far due to mutant phenotypes. Mutant analysis has revealed that four MATE genes are involved in lateral root formation (ALF5, Diener *et al.*, 2001), iron homeostasis (FRD3, Rogers and Guerinot, 2002), salicylic acid-dependent signaling for disease resistance (EDS5, Nawrath *et al.*, 2002) and PA accumulation, respectively (Debeaujon *et al.*, 2001 and chapter 2).

Functional complementation of an *E. coli acrAB* mutant deficient in multidrug resistance resulted in functional cloning of *AtDTX1* (At2g04070, Li *et al.*, 2002). AtDTX1 was shown to function in *E. coli* is as an efflux carrier of antibiotics, alkaloid berberine, and of other toxic compounds including ethidium bromide (Li *et al.*, 2002). The same authors predicted an AtDTX1-GFP fusion to the plasma membrane. *DTX2* (At2g04080) and *DTX1* can be found as direct neighbors in a cluster of the phylogenetic tree (Figure 1) which also includes *DTX6* (At2g04100) and *DTX3* (At2g04050). In our transient assay, $Pro_{CaMV35S}$*::DTX2-GFP* localizes *DTX2* to the tonoplast. GFP-fusions of DTX6 demonstrate localization on the tonoplast. In fact, the *DTX* genes *1* to *6* form a gene clade on chromosome 2 and are oriented in head-to-tail orientation and they share 72% of amino acid similarity (table 3).

Apart from *DTX2* and *6,* biolistic particle delivery on onion epidermal cells of *DTX18, 19, 23, 25, 33, 39, 40* and *41* (GFP5:TT12), respectively resulted in GFP fluorescence on membranes surrounding the central vacuole and on membranes forming cytoplasmic strands, suggesting localization on the tonoplast (Figure 2A). In contrast *DTX12* exhibit localization on the plasma membrane. Taken together, all tested MATE genes clustering to a clade of the phylogenetic tree together with *TT12* have been localized to the tonoplast. In contrast, the second clade defined by *DTX1-6, 9, 10* and *12*, *18* and *19* (*ALF5*) have diverse localizations on the plasma membrane and the tonoplast. If future work would show that all MATE transporters encoded by the *TT12* clade are found on the vacuolar membrane, one could therefore hypothesize that the tonoplast is a default location for integral membrane proteins while plasma membrane-localized membrane proteins such as *DTX 12* need a defined sorting signal.

In order to simplify the presentation of conserved or variable amino acids in individual DTX proteins, all amino acid position numbers refer to the numbering of the clustalW alignment in Figure 5, ignoring the gaps. The alignment represents two groups of proteins where the first group is localized on the plasma membrane while the second group (lower two proteins) localized on the tonoplast. We looked for differences between the two groups in order to define a peptide signal or residues which could be important for the final destination. We identified that the amino acids in positions 8, 14, 24, 63, 284, 410 and 432 in the first group (DTX1 and 3 – share 83% of amino acid similarity homology, but localization till the end not clear, red arrows) are conserved,

while the same amino acids are variable in the second group. More residues are conserved in the proteins localized on the plasma membrane in comparison to the tonoplast localized proteins. This led to the speculation that one or several of these conserved residues are required to target these proteins to the correct plasma membrane. In position 482 the situation is reversed, the conserved amino acids are in the 'tonoplast' group (DTX2 and 6) and could be the amino acids which define the tonoplast localization (brown arrow). Thus it would be interesting to perform some experiments, where we not only exchange the single amino acids between the groups, but also cutt out the residues after position 480 in order to obtain if this will change the final protein destination. Another way to find differential targeting signal is to create chimeras between members of both groups and look for their subcellular localizations. We recognized also that in positions 21, 247, 267 and 309 amino acids are not conserved in all 4 members (blue arrows). Taken all together we can assume that the sorting signal in this family could be based on a single amino acid or on 3D structural conformation, and further analysis is needed in order to describe better this transporter family.

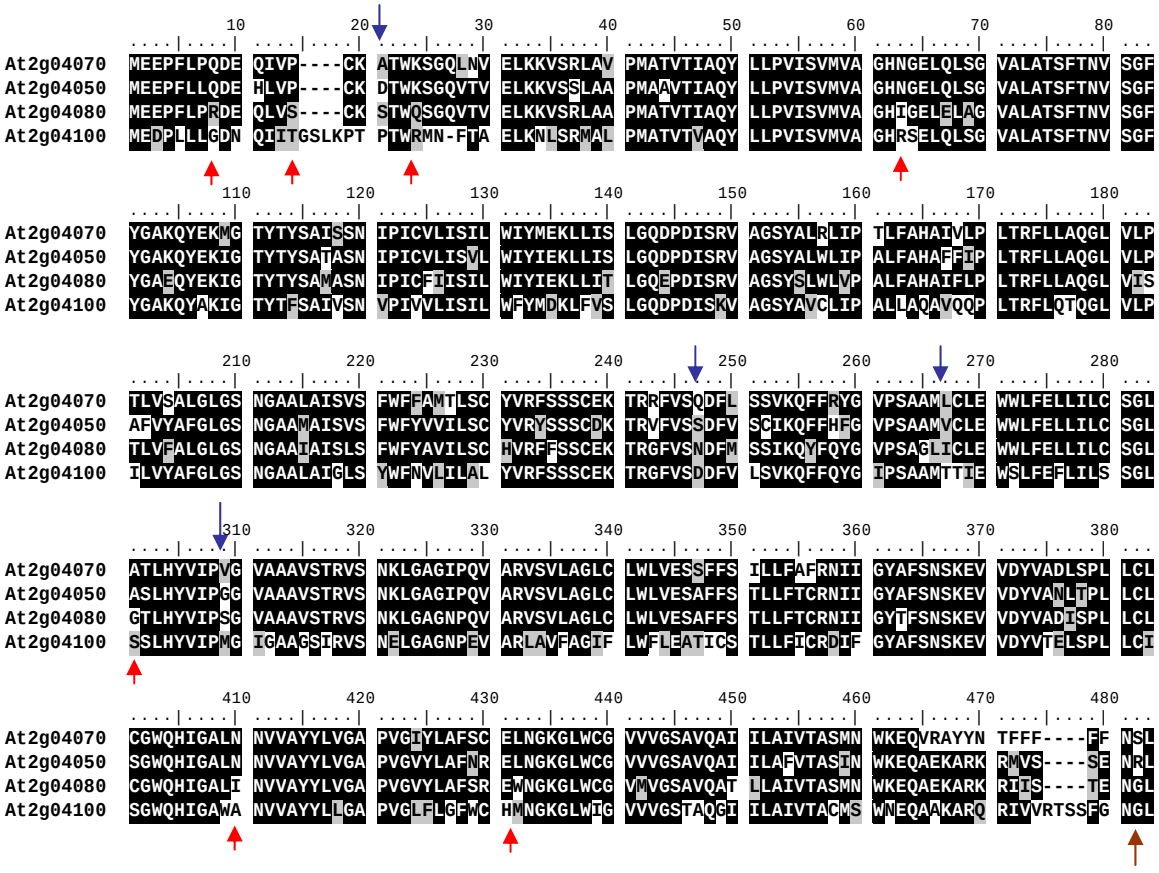

Figure 5. Multiple alignment of the amino acid sequences of DTX1/At2g04070/NP_178496.1, DTX3/At2g04050/NP_178492.1, DTX2/At2g04080/NP_178497.2 and DTX6/At2g04100/

NP_178499.2. Black and grey boxes indicate identical and similar amino acid residues, respectively. The protein sequences were aligned using ClustalW.

Table 3. % of amino acid identity between DTX1, 2, 3 and 6

% of amino acid identity	DTX1	DTX2	DTX3	DTX6
DTX1	100	85	87	72
DTX2	85	100	84	67
DTX3	87	84	100	71
DTX6	72	67	71	100

However, ectopic expression of the fusion protein between GFP and 23 amino acids of the transmembrane domain of the human lysosomal protein LAMP1 resulted in plasma membrane labeling suggesting that a non-plant transmembrane domain travels to this membrane by default (Brandizzi *et al.*, 2002). Alternatively, sorting signals defining either the tonoplast or plasma membrane are found in all MATE proteins and the tonoplast sorting signal is strictly conserved in the *TT12* clade. In contrast, the *DTX1-12* cluster is not defined by a unique subcellular localization suggesting that there is among the various members functional diversity. In view of the long-term goal – identification of sorting signals in related proteins traveling towards different target membranes, this cluster provides interesting genetic material to isolate these signals in the future.

The *ALF5* (at3g23560) gene was found to be expressed in the epidermis of Arabidopsis roots. A mutation in *ALF5* was shown to led to increased root sensitivity towards a variety of toxic compounds such as tetramethylammonium. The mutant was initially characterized by the reversibility of the lateral root elongation phenotype to wild-type when agar of higher purity was used for growth of sterile seedlings (Diener et al., 2001). These results suggested that ALF5 transports an inhibitory substance present in more contaminated agar preparations either out of the epidermal cells across the plasma membrane or into the vacuole as part of a detoxification mechanism. To this end we performed localization study using $Pro_{CaMV\ 35S}$-ALF5-GFP and the fusion localized ALF5 to the tonoplast which supports the proposed function as a vacuolar transporter for potentially toxic contaminants in soils. The identification of *ALF5* as a component of the detoxification system in roots suggests the possibility of engineering plants that overexpress particular MATE proteins to achieve increased resistance towards harmful compounds, *i. e.*, these transgenic plants might grow in soils containing chemicals that otherwise would inhibit the growth of wild-type plants.

It is suggested that TT12 homologs expressed in the vegetative tissues are responsible for vacuolar deposition of anthocyanins or flavonols in these plant parts. In the frame of this work

we tried to use the *tt12* mutant and specific misexpression of TT12-related MATE transporters in this mutant to assign functions as flavonoid transporters by *tt12* phenotype reversion.

Following histochemical assay described by Debeaujon *et al.* (2000) and Abrahams *et al.* (2002) the seed phenotype of *tt12* can be easily analyzed by histochemical staining of immature or dried seeds with DMACA. The DMACA staining of dry *tt12* seeds indicates the absence of the characteristic black color caused by PAs in the wild-type seeds (figure 4). We took advantage of the *tt12* phenotype and transformed plants with all $Pro_{CaMV\ 35S}$-$MATE_{XY}$-GFP we used for the localization study. Already in the T1 generation we hoped to score the phenotype(s) of transgenic plants by analyzing PA (*tt12* background) accumulation in immature or dried seeds. We expected that MATE transporters related to *TT12* complemented the mutant phenotype if the complementing gene encodes a protein involved in the transport compounds exhibiting structural similarity to anthocyanins or PA precursors. However, up to now we were not able to obtain any complementation of the *tt12* mutant with MATE transporter genes other than *TT12* itself.

In spite of this, the general feasibility of the misexpression approach is demonstrated by *ban5*-driven *TT12* expression in the *tt12* background where the PA-phenotype is restored to the wild-type as indicated by vanillin-staining of PAs in immature seeds (figure 3).

However, the cloning of 19 new genes with high homology to TT12 into the binary destination vectors followed by *tt12* transformation it is strongly hoped that MATE transporters complementing the *tt12* mutants will be found thereby defining novel flavonoid transporters.

Acknowledgements

The author thanks Mark Curtis for providing the vectors used in this study and RIKEN Bioresource Center for the MATE cDNAs. Christian Frey and Karl Huwiler (University of Zurich) for taking care of the plants. This work was supported by the Forschungskredit of the University of Zurich, Switzerland (MK) and the Roche Research Foundation, Basel, Switzerland (KM).

Reference list

Abrahams S., Tanner G.J., Larkin P.J., Ashton A.R. 2002 Identification and biochemical characterization of mutants in the proanthocyanidin pathway in Arabidopsis. Plant Physiol. 130:561-576.

Arabidopsis Genome Initiative 2000 Analysis of the genome sequence of the flowering plant Arabidopsis thaliana. Nature 408: 796–815.

Bihler H., Eing C., Hebeisen S., Roller A., Czempinski K., Bertl A. 2005 TPK1 is a vacuolar ion channel different from the slow-vacuolar cation channel. Plant Physiol. 139:417-424.

Brandizzi F., Frangne N., Marc-Martin S., Hawes C., Neuhaus J-M., Paris N. 2002 The destination for single-pass membrane proteins is influenced markedly by the length of the hydrophobic domain. Plant Cell 14:1077–1092.

Brown M.H., Paulsen I.T., Skurray R.A. 1999 The multidrug efflux protein NorM is a prototype of a new family of transporters. Mol. Microbiol. 31:394-395.

Clough S.J., and Bent A.F. 1998 Floral dip: a simplified method for Agrobacterium-mediated transformation of Arabidopsis thaliana. Plant J. 16: 735-743.

Czempinski K., Frachisse J.M., Maurel C., Barbier-Brygoo H., Mueller-Roeber B. 2002 Vacuolar membrane localization of the Arabidopsis 'two-pore' K^+ channel KCO1. Plant J. 29:809-820.

Debeaujon I., Leon-Kloosterziel K.M., Koornneef M. 2000 Influence of the testa on seed dormancy, germination, and longevity in Arabidopsis. Plant Physiol. 122:403-413.

Debeaujon I., Nesi N., Perez P., Devic M., Grandjean O., Caboche M., Lepiniec L. 2003 Proanthocyanidin-accumulating cells in Arabidopsis testa: Regulation of differentiation and role in seed development. Plant Cell 15:2514-2531.

Diener A.C., Gaxiola R.A., Fink G.R. 2001 Arabidopsis ALF5, a multidrug efflux transporter gene family member, confers resistance to toxins. Plant Cell 13:1625-1637.

Green L.S. and Rogers E.E. 2004 FRD3 Controls iron localization in Arabidopsis. Plant Physiol. 136:2523-2531.

Höfte H., and Chrispeels M.J. 1992 Protein sorting to the vacuolar membrane. Plant Cell 4:995–1004.

Jiang L.W., and Rogers J.C. 1998 Integral membrane protein sorting to vacuoles in plant cells: Evidence for two pathways. J. Cell Biol. 143:1183–1199.

Li L., He Z., Pandey G.K., Tsuchiya T., Luan S. 2002 Functional cloning and characterization of a plant efflux carrier for multidrug and heavy metal detoxification. J.Biol.Chem. 277:5360-5368.

Mathews H., Clendennen S.K., Caldwell C.G., Liu X.L., Connors K., Matheis N., Schuster D.K., Menasco D.J., Wagoner W., Lightner J., Wagner D.R. 2003 Activation tagging in tomato identifies a transcriptional regulator of anthocyanin biosynthesis, modification, and transport. Plant Cell 15:1689-1703.

Nesi N., Debeaujon I., Jond C., Pelletier G., Caboche M., Lepiniec L. 2000 The TT8 gene encodes a basic helix-loop-helix domain protein required for expression of DFR and BAN genes in Arabidopsis siliques. Plant Cell 12:1863-1878.

Rogers E.E. and Guerinot M.L. 2002 FRD3, a member of the multidrug and toxin efflux family, controls iron deficiency responses in Arabidopsis. Plant Cell 14:1787-1799.

Xie D.Y., Sharma S.B., Paiva N.L., Ferreira D., Dixon R.A. 2003 Role of anthocyanidin reductase, encoded by BANYULS in plant flavonoid biosynthesis. Science 299:396-399.

Chapter 4

Influence of mutation in the flavonoid biosynthesis on the vacuolar biogenesis

(work in progress in collaboration with Christina Ballmann)

Recent studies have used histological analyses and/or mutant characterization to focus on the development of the Arabidopsis seed coat (Léon-Kloosterziel *et al*., 1994). The Arabidopsis seed coat consists of five cell layers: two of them form the outer integument and three form the inner integument (Figure 1). Seed coat pigments in Arabidopsis are predominantly flavonoids—more precisely, proanthocyanidins (or condensed tannins) of the cyanidin type and flavonols of the quercetin type (Routaboul *et al*., 2006). Proanthocyanidins (PAs) are located specifically in the innermost cell layer of the seed coat, which also is called the endothelium (Devic *et al*., 1999; Debeaujon *et al*., 2003). They accumulate as colorless compounds during the early steps of embryogenesis and subsequently give the seed its brown pigmentation after oxidative reactions during seed maturation and desiccation processes (Debeaujon *et al*., 2000). The pigmentation of Arabidopsis seed bodies is not uniform and can be lost independently, suggesting that different genetic controls occur (Debeaujon *et al*., 2001). PAs have been shown to participate in the maintenance of seed coat–imposed dormancy as well as in seed longevity during storage (Winkel-Shirley, 1998; Debeaujon *et al*., 2000).

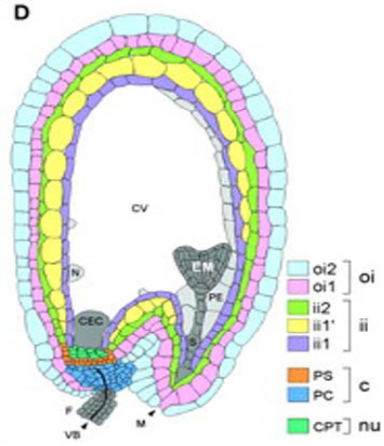

Figure 1. Schematic representation of an Arabidopsis seed. PAs are found mainly in the ii1 layer while flavonols are restricted to the oi1 layer of the outer integument. c, chalaza; e, embryo;

ii, inner integument (ii1 = endothelium); m, micropyle; oi, outer Integument; ps, pigment strand; t, testa. Adapted from Debeaujon *et al.*, 2003.

Numerous flavonoid mutants have been isolated in Arabidopsis on the basis of altered seed color. These mutants are named *transparent testa* (*tt*), because null mutations in *TT* genes result in reduced, abolished, or modified pigmentation of the seed coat, depending on the intermediate flavonoid pigments (Koornneef, 1990). Presence or absence of PAs in seeds can be detected histochemically either with vanillin or with DMACA (***p*-**Dimethylaminocinnamaldehye**)** which form red or black colored adducts with PAs (Figure 2). Remarkably, staining with DMACA and also vanillin is not completely absent in some of the *tt* mutants such as *tt6* or *tt7* which encode flavanone 3-hydroxylase (F3H) and flavonoid 3'H-hydroxylase (F3'H) suggesting that either less PAs are made or related compounds are synthesized. Yet, the appearance of black adducts with DMACA appears spotted suggesting that the PA-type compounds do no longer fill the entire cell of the seed coat. Thus, apart from differences in the amount of PAs synthesized, subcellular localization is affected.

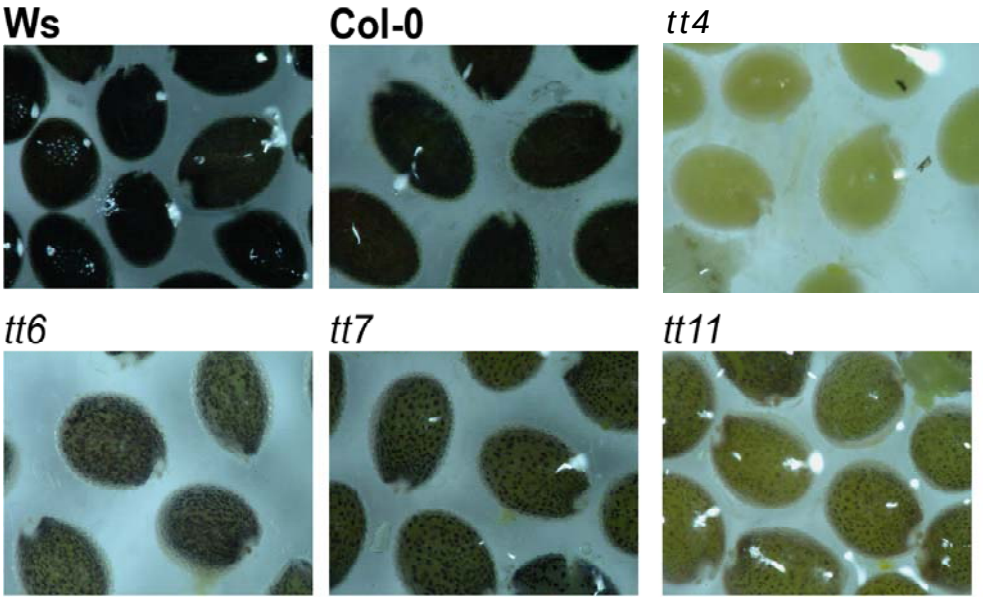

Figure 2. Dry seeds after histochemical staining with DMACA (*p*-dimethylaminocinnamaldehye**)** of WT (Ws and Ler) and *tt4*, *6*, *7* and *11*. In many *transparent testa*-mutants, black adducts formed between PAs and DMACA do not fill the entire cells as in wild-type seeds but appear in discrete spots. *tt4,* a mutant in CHS, exhibits no reaction due to complete absence of flavonoids.

Apart from the metabolic and histochemical PA-related differences between wild-type and *tt12* seeds (chapter 2) we discovered a third phenotype of *tt12* immature seeds. Accoding to two studies, mutants in the *TDS4* (tannin deficient seeds) gene encoding leucoanthocyanidin dioxygenase and mutants in the P-type H^+-ATPase gene *AHA10* are affected in PA biosynthesis and exhibited changes in vacuolar structures. These authors demonstrate mutant-related changes in vacuolar structures after loading seeds with the fluorescent dye carboxy-DCFDA (5-(and-6)-carboxy-2',7'-dichlorodihydrofluorescein diacetate): While carboxy-DCFDA labels the central vacuole of wild-type cells, *aha10* and *tds4* mutants display multiple fluorescent vesicular structures.

We repeated these experiments and demonstrate that *tt12* (Figure 3, see CD-ROM) as well as *tt4, 7, 11* (Figure 4) display 'vesicular' structures in seed coat cells when loaded either with carboxy-DCFDA or with the structurally unrelated fluorescent dye Cell Tracker Green (data not shown). Cell tracker green undergoes glutathione conjugation in the cytosol prior to loading into vacuoles.

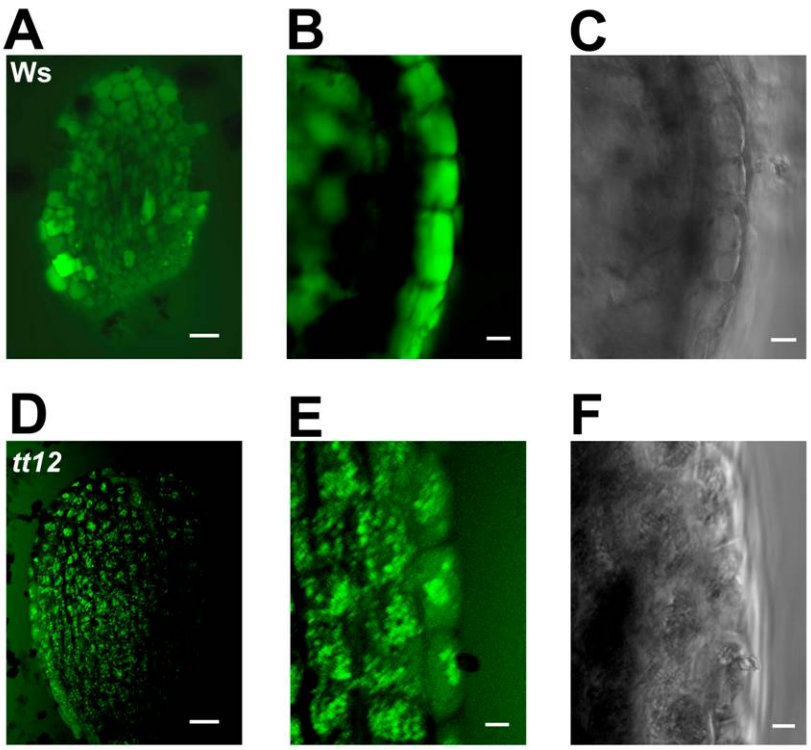

Figure 3. Confocal microscopy of immature wild type (Ws) and *tt12* seeds incubated with carboxy-DCFDA. Confocal images (left and middle panels) are depicted together with corresponding differential interference contrast (DIC) images (right panels). Bar = 50µm. Details of the outermost integument (oi2) (middle and right panels) demonstrate that presence of multiple vesicles in *tt12* was not restricted to the endothelial layer involved in PA biosynthesis.

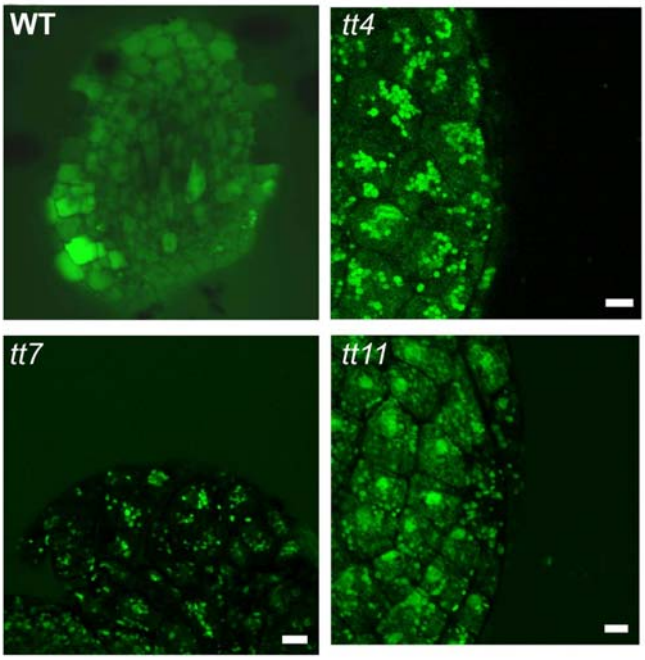

Figure 4. Confocal pictures of immature seeds of WT (upper left panel) *tt* seeds stained with carboxy-DCFDA. Bar = 50µm.

Together with the previous observations, it appears evident that absence of PAs leads to a defect in the cellular biogenesis of vacuoles at least as far as it can be followed by external loading of a fluorescent dye. Our results extend the published two genes to all steps in between the pacemaking chalcone synthase up to the PA precursor transporter. Thus, any step that leads to a perturbation of PA biosynthesis in immature seeds leads to vacuolar defects.

If we hypothesize that any disruption of the PA biosynthetic pathway leads to a defect in vacuolar biogenesis and to the appearance of vesicular, carboxy-DCFDA-stained structures, we must conclude that epicatechin or PAs acts as a metabolic signal for vacuolar fusion in the seed coat cells. Thus, the PAs may have very specific, cellular functions apart from general protection of seeds, and dormancy or longevity effects.

However, different points will have to be addressed to investigate this novel function in more detail:

1. Abrahams *et al*. have (2003) shown that vacuolar development is normal in vegetative cells even in the presence of the *tds4* mutation. We have confirmed this: root vacuoles of several *tt* mutants are not different from wild-type vacuoles in the presence of carboxy-DCFDA (data not shown). Thus, vacuoles in the seed coat must be functionally different from vegetative vacuoles. Alternatively, the control of vacuolar fusion absolutely depends on PAs in the seed coat while it is

independent of flavonoids in all other cell types investigated. In the latter case, the question arises, why this is so and what is the molecular mechanism defining this functional difference.

2. PAs are exclusively synthesized in the seed coat mainly in the endothelium but not in the outer integuments. *tt* mutants such as *tt12* or *ban* specifically affect PA production in the endothelium. Expression of *TT12* and *BAN* is also restricted to PA-producing cells. However, we loaded the dye to entire seeds without dissection which is in contrast to the treatment performed by Abrahams *et al*. 2004. As a result, with the laser intensities used and the chosen incubation time for carboxy-DCFDA, only the oi1 and oi2 layers appeared fluorescent but not the inner integuments including the endothelium. Thus, appearance of 'green vesicles' and synthesis of PAs does not appear necessarily in the same cell type or layer. If we assume that absence of PAs or precursors is ultimately responsible for absence of vacuolar fusion in *tt* seeds, we must conclude that PA biosynthesis and the effect of PA-related metabolites on vacuolar fusion can be spatially separated, at least for few cell layers. Consequently, a PA-related, metabolic signal must reach the outer integument controlling vacuolar biogenesis.

It will be interesting to conduct further experiments aiming at the identification of the type of vacuoles in the seed coat and the nature of the carboxy-DCFDA-stained vesicles in *tt* mutants with the help of endomembrane markers labeling different compartments or vacuolar subtypes.

Material and Methods

(Full protocols will be available in the diploma thesis of Christina Ballmann)

1. PA mutant screen

Dry *tt* seeds were stained according to published procedures (Debeaujon *et al.*, 2000; Abrahams *et al.*, 2002) using the *p*-dimethylaminocinnamaldehyde reagent (2% (w/v) DMACA in 3 M HCl/50% (w/v) methanol) for the presence of PAs. After 24h incubation at room temperature, seeds were washed three times with 70% (v/v) ethanol. DMACA-treated seed pools were then examined using a Nikon SMZ1500 binocular microscope coupled to a Nikon Coolpix camera for DMACA-specific black seed coloration.

2. Loading with fluorescent dyes

Developing siliques were dissected and liberated immature seeds were incubated with 10 µM carboxy-DCFDA in water (Invitrogen). After applying vacuum for 10 min the seeds were incubated for 12 h at room temperature after they were washed two times with water. Single optical sections were captured by confocal laser scanning microscopy (CLSM) using a TCS SP2-x1 full spectrum confocal microsope attached to a Leica DM IRE2 inverted fluorescence (Glattbrugg, Switzerland).

Reference list

Abrahams S., Lee E., Walker A.R., Tanner G.J., Larkin P.J., Ashton A.R. 2003 The *Arabidopsis* TDS4 gene encodes leucoanthocyanidin dioxygenase (LDOX) and is essential for proanthocyanidin synthesis and vacuole development. Plant J. 35:624-636.

Abrahams S., Tanner G.J., Larkin P.J., Ashton A.R. 2002 Identification and biochemical characterization of mutants in the proanthocyanidin pathway in *Arabidopsis.* Plant Physiol. 130:561-576.

Debeaujon I., Leon-Kloosterziel K.M., Koornneef M. 2000 Influence of the testa on seed dormancy, germination, and longevity in *Arabidopsis*. Plant Physiol. 122:403-413.

Debeaujon I., Peeters A.J.M., Leon-Kloosterziel K.M., Koornneef M. 2001 The TRANSPARENT TESTA12 gene of *Arabidopsis* encodes a multidrug secondary transporter-like protein required for flavonoid sequestration in vacuoles of the seed coat endothelium. Plant Cell 13:853-871.

Debeaujon I., Nesi N., Perez P., Devic M., Grandjean O., Caboche M., Lepiniec L. 2003 Proanthocyanidin-accumulating cells in *Arabidopsis* testa: Regulation of differentiation and role in seed development. Plant Cell 15:2514-2531.

Devic M., Guilleminot J., Debeaujon I., Bechtold N., Bensaude E., Koornneef M., Pelletier G., Delseny M. 1999 The BANYULS gene encodes a DFR-like protein and is a marker of early seed coat development. Plant J. 19:387-398.

Koornneef M. 1990 Mutations affecting the testa colour in *Arabidopsis*. *Arabidopsis* Inf. Serv. 27:1–4.

Leon-Kloosterziel K.M., Keijzer C.J., Koornneef M. 1994 A seed shape mutant of *Arabidopsis* that is affected in integument development. Plant Cell 6:385–392.

Routaboul J.M., Kerhoas L., Debeaujon I., Pourcel L., Caboche M., Einhorn J., and Lepiniec L. 2006 Flavonoid diversity and biosynthesis in seed of Arabidopsis thaliana. Planta 224:96-107.

Winkel-Shirley B. 1998 Flavonoids in seeds and grains: Physiological function, agronomic importance and the genetics of biosynthesis. Seed Sci. Res. 8:415–422.

Chapter 5

Flavonoid Biosynthesis in Barley Primary Leaves Requires the Presence of the Vacuole and Controls the Activity of Vacuolar Flavonoid Transport[1]

Krasimira Marinova, Katja Kleinschmidt, Gottfried Weissenböck, and Markus Klein*

Zurich Basel Plant Science Center, University of Zurich, Plant Biology, CH–8008 Zurich, Switzerland (K.M., M.K.); and University of Cologne, Botanical Institute, D–50931 Cologne, Germany (K.K., G.W.)

Barley (*Hordeum vulgare*) primary leaves synthesize saponarin, a 2-fold glucosylated flavone (apigenin 6-*C*-glucosyl-7-*O*-glucoside), which is efficiently accumulated in vacuoles via a transport mechanism driven by the proton gradient. Vacuoles isolated from mesophyll protoplasts of the plant line *anthocyanin-less310* (*ant310*), which contains a mutation in the chalcone isomerase (*CHI*) gene that largely inhibits flavonoid biosynthesis, exhibit strongly reduced transport activity for saponarin and its precursor isovitexin (apigenin 6-*C*-glucoside). Incubation of *ant310* primary leaf segments or isolated mesophyll protoplasts with naringenin, the product of the CHI reaction, restores saponarin biosynthesis almost completely, up to levels of the wild-type Ca33787. During reconstitution, saponarin accumulates to more than 90% in the vacuole. The capacity to synthesize saponarin from naringenin is strongly reduced in *ant310* miniprotoplasts containing no central vacuole. Leaf segments and protoplasts from *ant310* treated with naringenin showed strong reactivation of saponarin or isovitexin uptake by vacuoles, while the activity of the UDP-glucose:isovitexin 7-*O*-glucosyltransferase was not changed by this treatment. Our results demonstrate that efficient vacuolar flavonoid transport is linked to intact flavonoid biosynthesis in barley. Intact flavonoid biosynthesis exerts control over the activity of the vacuolar flavonoid/H^+-antiporter. Thus, the barley *ant310* mutant represents a novel model system to study the interplay between flavonoid biosynthesis and the vacuolar storage mechanism.

One of the major challenges of plant physiology in the postgenome era is to understand the overall regulation of metabolite flow in different pathways in response to developmental, tissue-, or cell-specific programs or environmental factors such as light or stress (Sweetlove and Fernie, 2005). Metabolic pathways often span more than one compartment at the cellular level. Compartmentation and controlled transmembrane metabolite transport hold the potential to establish the optimal concentrations of substances necessary for further enzymatic transformation in individual compartments. Subcellular compartmentation of metabolites results in individual pools of different sizes and is important for the local maintenance of high metabolite concentrations or for the separation of competing pathways such as anabolic and catabolic processes (Winkel, 2004). Thus, the analysis of biochemical pathways must also take account of transport processes and the spatial/subcellular organization of enzymes that catalyze consecutive synthetic reactions (Jorgensen et al., 2005). Despite the importance of transport steps for biosynthetic processes or the detoxification of xenobiotics, the mechanisms that allow a metabolic pathway to directly or indirectly control transport activities are largely unknown. This is reflected by the notion that under normal physiological conditions, transport steps are not considered rate limiting.

Flavonoid biosynthesis gives rise to structurally related, but functionally diverse, compounds such as flavonols, flavones, anthocyanins, proanthocyanidins, or isoflavonoids (Dixon and Paiva, 1995; Winkel-Shirley, 2001; Dixon et al., 2005) and represents an ideal model to study metabolic regulation in plant cells. Flavonoid synthesis branches from the general phenylpropanoid pathway and is subject to multiple levels of regulation, including transcriptional (Weisshaar and Jenkins, 1998; Lepiniec et al., 2006) and enzymatic regulation. Chalcone synthase (CHS), for example, catalyzes the first committed step in flavonoid synthesis and is regulated both at the level of enzyme activity (Knogge et al., 1986) and transcription (Block et al., 1990; Hartmann et al., 1998, 2005). CHS also responds strongly to environmental stimuli such as light or elicitors (Chappell and Hahlbrock, 1984; Schulze-Lefert et al., 1989; Christie and Jenkins, 1996; Faktor et al., 1997). In fact, the whole pathway is regulated developmentally (Schulz and Weissenböck, 1988) in specific tissues or cell types (Schulz and Weissenböck, 1986; Hutzler

[1] This work was supported by the Forschungskredit of the University of Zurich (M.K.) and the Deutsche Forschungsgemeinschaft (G.W.).

* Corresponding author; e-mail markus.klein@botinst.unizh.ch; fax 41–1–634–8204.

The author responsible for distribution of materials integral to the findings presented in this article in accordance with the policy described in the Instructions for Authors (www.plantphysiol.org) is: Markus Klein (markus.klein@botinst.unizh.ch).

www.plantphysiol.org/cgi/doi/10.1104/pp.106.094748

et al., 1998) and is affected by stress (e.g. by UV; Reuber et al., 1996).

Upon synthesis, many conjugated products of the flavonoid pathway such as flavonol and flavone glycosides or anthocyanins are found predominantly in the vacuole (Graham, 1998), while in other cases, conjugated and/or unconjugated flavonoids are secreted into the apoplastic space (Onyilagha and Grotewold, 2004). Isoflavonoids, for example, are secreted by the roots of legumes where they influence the interaction of the plant with microbes (Paiva, 2000). Isoflavonoid secretion affects the surrounding microflora in the rhizosphere (Weisskopf et al., 2006), attracts mutualistic microorganisms such as nitrogen-fixing bacteria, and enhances defense responses to pathogens (Paiva, 2000; Dakora and Phillips, 2002). Flavonol glycosides have been detected in the cell wall fraction of Scots pine (*Pinus sylvestris*) needles (kaempferol 3-glucoside; Schnitzler et al., 1996) and *Chrysosplenium americanum* (polymethylated flavonol glucosides; Ibrahim et al., 1987), while flavonoid aglycones, including flavones and flavonols, have been detected in exudates of numerous species (Valant-Vetschera and Wollenweber, 2001; Wollenweber et al., 2003).

It is generally accepted that flavonoid biosynthesis largely takes place in the cytosol. The prevailing spatial model suggests that the early proteins of the pathway are organized in a multienzyme complex centered around CytP450-dependent monoxygenases on the cytosolic side of the endoplasmic reticulum (ER) forming a functional metabolon (Saslowsky and Winkel-Shirley, 2001; for review, see Winkel, 2004; Jorgensen et al., 2005). Because histochemical analysis has repeatedly indicated that flavonoids are present in the nucleus (e.g. Peer et al., 2001; Saslowsky et al., 2005) and recent reports propose also the presence of CHS and chalcone isomerase (CHI), the function of flavonoids as regulators in the nucleus suggest additional layers of complexity and compartmentation in the process (Saslowsky et al., 2005). Interestingly, aureusidin synthase from *Antirrhinum majus* flowers, a polyphenol oxidase catalyzing the formation of aurones from chalcones, has recently been localized to vacuoles (Ono et al., 2006).

In contrast to our knowledge on flavonoid biosynthetic enzymes and the transcriptional regulation of the corresponding genes, the transport of phenolic compounds into subcellular compartments, facilitating the protection of cytosolic processes against the intrinsic toxicity of these compounds, is only marginally understood both at the mechanistic and regulation levels. While transport of flavonoids across the plasma membrane has not been investigated so far, biochemical analysis of vacuolar uptake mechanisms led to the proposition of different transport and accumulation mechanisms (for review, see Grotewold, 2004; Yazaki, 2005). Available data suggest that the conjugated moieties such as sugars or acyl residues are important determinants of transport specificity (Matern et al., 1986; Hopp and Seitz, 1987; Klein et al., 1996).

In barley (*Hordeum vulgare*), the 2-fold glucosylated saponarin (apigenin 6-*C*-glucosyl-7-*O*-glucoside) accumulates as the major compound during primary leaf development (Fig. 1; Reuber et al., 1996). Saponarin is synthesized from its precursor isovitexin (apigenin 6-*C*-glucoside) after the addition of Glc in the 7-*O* position catalyzed by a soluble UDP-Glc:flavone glucosyltransferase (Blume et al., 1979). Compared with saponarin, isovitexin is present only in trace amounts. Both saponarin and isovitexin are transported into and stored in barley vacuoles by a secondary energized proton antiport mechanism (Klein et al., 1996; Frangne et al., 2002). Arabidopsis (*Arabidopsis thaliana*) synthesizes conjugated flavonols instead of flavones (Graham, 1998). In contrast to the vacuolar saponarin/H^+-antiport found when barley vacuoles are used, uptake of saponarin into Arabidopsis cell culture vacuoles is ATP dependent and occurs via direct energization. The same has been found for the uptake of an abiotic glucoside, hydroxyprimisulfuron glucoside, which is synthesized during the detoxification of the sulfonylurea-type herbicide primisulfuron. Thus, an ATP-binding cassette protein-type transporter driving vacuolar uptake has to be hypothesized in addition to a proton antiport mechanism in certain cases (Klein et al., 1996; Frangne et al., 2002). On the molecular level, ATP-binding cassette-type transporters as well as secondary energized multidrug and toxic exchange transporters have been proposed to be involved in the transport of anthocyanins in maize (*Zea mays*) or proanthocyanidins in Arabidopsis, respectively (Debeaujon et al., 2001; Dean et al., 2005).

A model system that allows the analysis of a link between a metabolic pathway and the transport processes involved in metabolite translocation into compartments or organelles should fulfill several preconditions. First, it must be possible to control and manipulate the flow through the pathway experimentally. In other words, it must be possible to turn the pathway on and off. This can be done by selecting a mutant plant line with a lesion in a gene coding an enzyme involved in an early step in the pathway. This would allow the pathway to be switched on by applying the chemical product of the affected enzymatic reaction exogenously to effectively complement the mutation. Second, if the transport activity investigated is controlled by the flow through the metabolic pathway, transport is expected to decrease or increase in response to the absence (mutant) or presence of metabolites (chemically complemented mutant). Third, organelle or membrane isolation must be facile and quick to study transport activity changes and storage efficiency in response to alterations in the biosynthetic pathway.

Here, we present an experimental model to investigate the metabolic control mechanism of the flavonoid biosynthetic pathway through the vacuolar transport system. We use the barley *anthocyanin-less310* (*ant310*) mutant, which accumulates less than 5% of the flavonoids of the wild-type Ca33787 (Reuber et al., 1996). Instead,

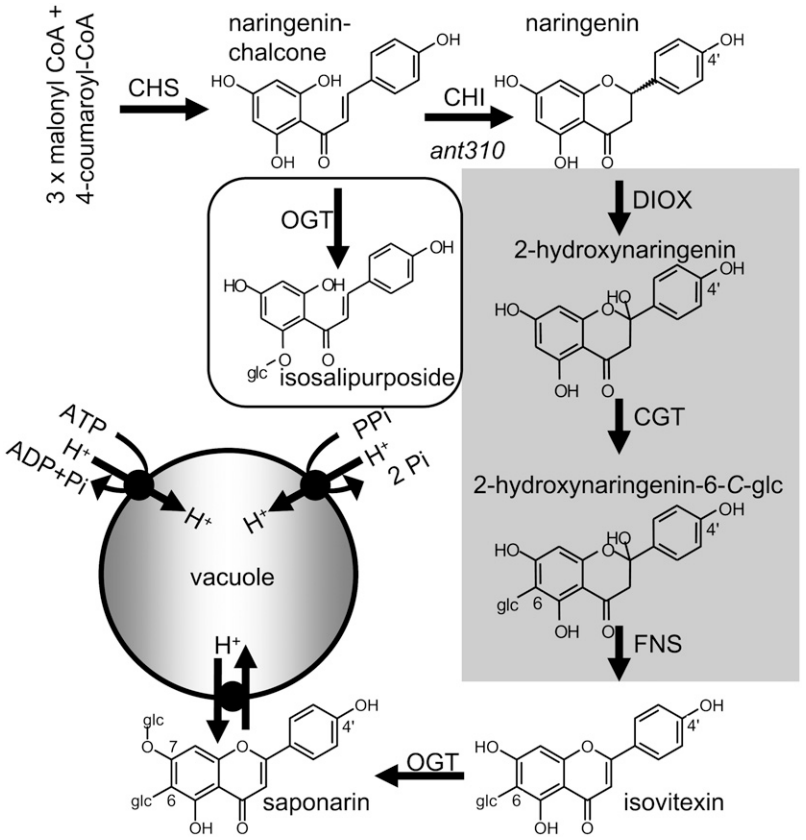

Figure 1. Scheme of the biosynthesis and compartmentation of saponarin in barley and the effect of the *ant310* mutation. Naringenin is formed by the condensation of three molecules of malonyl-CoA and one molecule of 4-coumaroyl-CoA via the CHS followed by ring closure catalyzed by CHI. The following steps of flavone formation toward isovitexin (apigenin 6-*C*-glucoside) have not been demonstrated in barley up to now, to our knowledge, and are adapted from buckwheat (Kerscher and Franz, 1987, 1988) and marked by a gray background. Isovitexin is detected in barley leaf extracts in low amounts and is processed to saponarin via an UDP-Glc:isovitexin OGT, which is soluble and cytosolic. OGT activity does not appear to be rate limiting (Blume et al., 1979). Finally, saponarin and isovitexin are transported into the vacuole via a flavone glucoside/H^+-antiporter that is energized by the pH gradient across the tonoplast generated by the activity of the two vacuolar proton pumps, the H^+-pumping ATPase and pyrophosphatase. The *ant310* mutation (italics) causes absence of CHI leading to the formation of a novel substance, isosalipurposide (boxed). CGT, UDP-Glc-dependent *C*-glucosyltransferase; DIOX, dioxygenase; FNS, flavone synthase (hypothetical).

mutant primary leaves contain isosalipurposide, which is a glucosylated form of 4, 2′,4′ 6′-tetrahydroxychalcone lacking the ring closure in the heterocyclus to flavanones, a step catalyzed by CHI (Fig. 1; Reuber et al., 1997). By diallelic crosses, four independent mutants including *ant310* were found to belong to the same complementation group (Reuber et al., 1997). Using the maize *CHI* gene as a probe, Druka et al. (2003) identified a barley ortholog and showed that the *ant310* mutant lacked a functional *CHI*. Surprisingly, transport of isovitexin and saponarin into vacuoles isolated from *ant310* primary leaves was strongly reduced when compared to vacuoles isolated from Ca33787 (Frangne et al., 2002). This result indicated that the intact flavonoid pathway was necessary for fully activated vacuolar flavonoid/H^+-antiport activity. Here, we show that micromolar concentrations of exogenously added naringenin, the product of the CHI reaction, restores saponarin biosynthesis in *ant310* leaves to levels of the wild type in only 5 to 6 h. Reconstitution of saponarin production is cell-type autonomous, because isolated *ant310* mesophyll protoplasts are able to synthesize saponarin after naringenin addition. Naringenin-induced saponarin biosynthesis in *ant310* protoplasts depends on the presence of the vacuole as a destination compartment and is strongly compromised if pH gradients necessary for vacuolar H^+-antiport transport activities are disrupted. Most importantly, naringenin reconstitution of saponarin biosynthesis in *ant310* reactivates the vacuolar transport activity for the barley flavone glucosides. We propose that the high-activity state of the vacuolar transporter is maintained by the biosynthesis of flavonoids in the pathway, while the presence of a mature lytic vacuole controls the metabolite flow.

RESULTS

Feeding of *ant310* Leaf Segments with Naringenin Fully Reconstitutes Saponarin Biosynthesis

When naringenin was fed externally to segments of 4-d-old *ant310* primary leaves, efficient saponarin biosynthesis was observed within 7 h of incubation (Fig. 2). In the presence of 50 μM naringenin in the medium, full reconstitution of saponarin biosynthesis was observed, because saponarin levels reached the amount present in the wild-type Ca33787 leaf segments incubated in the absence of naringenin. Saponarin production was absent in *ant310* leaves on control medium, indicating that presence of naringenin was necessary for saponarin production. Furthermore, feeding of *ant310* leaves with 100 μM naringenin resulted in less efficient saponarin production, which suggested that 50 μM naringenin was sufficient for efficient saponarin synthesis, while higher concentrations could be toxic. Saponarin production from naringenin in *ant310* leaves reached similar levels in 5- and 6-d-old primary leaf segments, while the biosynthesis was reduced in 7- or 8-d-old leaves. In the latter leaves, about 30% of

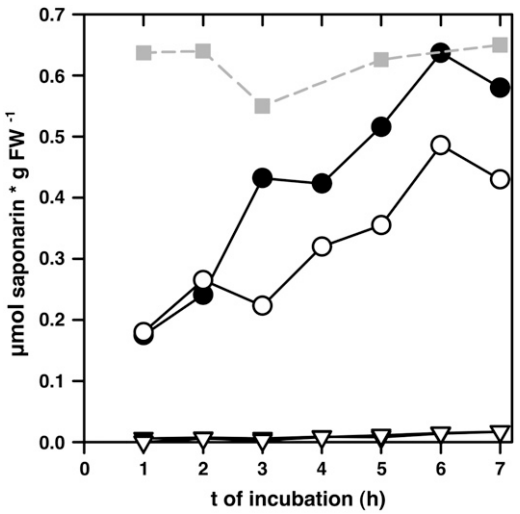

Figure 2. Naringenin incubation of *ant310* leaf segments fully reconstitutes saponarin biosynthesis. The 4-d-old primary leaf segments of *ant310* were incubated in the absence (triangles) or presence of 50 (black circles) or 100 μM (white circles) naringenin for the indicated times. Saponarin content in Ca33787 leaf segments without naringenin (gray squares) are depicted as a control. Saponarin content was measured by HPLC.

saponarin was formed from naringenin when compared to the corresponding Ca33787 flavonoid content (data not shown). In contrast, secretion of saponarin from leaf segments into the incubation medium never exceeded 5% of the amount formed within the tissue, suggesting that the flavonoids produced in *ant310* leaves in the presence of naringenin were efficiently stored within the cells. This result prompted us to investigate the cell autonomy of saponarin reconstitution and vacuolar compartmentation.

For all experiments with protoplast and fractions derived thereof, 7- to 8-d-old primary leaves were used. Older primary leaves were chosen because: (1) protoplast and vacuole experiments required the preparation of large amounts of primary leaf material; and (2) large-scale isolation of protoplasts and vacuoles from younger leaves is difficult. Starch production is marginal in young leaves, which results in the loss of mesophyll protoplasts during density centrifugation and fraction purification. In any case, saponarin production was still accurately measurable by HPLC in protoplasts derived from 7- to 8-d-old leaves.

Saponarin Biosynthesis from Naringenin in *ant310* Is Cell Autonomous

Mesophyll protoplasts isolated from 7-d-old *ant310* primary leaves were incubated in the absence or presence of 50 μM naringenin and the content of saponarin in protoplasts was analyzed by HPLC in a time-course study. As for the leaf segments, *ant310* protoplasts were able to synthesize saponarin in the presence of naringenin, reaching maximal levels after 2 to 3 h of incubation, while *ant310* protoplasts kept without naringenin did not synthesize saponarin (Fig. 3). As observed for leaf segments, protoplasts isolated from 7-d-old *ant310* leaves reached about 25% to 30% of the saponarin content of Ca33787 protoplasts (data not shown). We investigated whether the saponarin synthesized in *ant310* protoplasts during naringenin feeding was stored within the vacuole by performing a compartmentation analysis. The saponarin content was measured by HPLC in protoplast and vacuolar fractions isolated after 6 h of feeding *ant310* protoplasts with naringenin. To compare protoplasts and vacuoles, we determined acid phosphatase activity as a vacuolar marker enzyme in the same samples. Reconstituted saponarin synthesized during naringenin incubation of *ant310* protoplasts was efficiently transferred into the vacuole, because 95% $\pm$ 3% of the saponarin formed during naringenin feeding was found in the vacuolar fraction. Thus, in contrast to our former saponarin transport experiments into *ant310* vacuoles (Frangne et al., 2002), the tonoplast transport system for saponarin appeared to be fully active in *ant310* protoplasts in the presence of naringenin-driven saponarin biosynthesis.

We used diphenylboric acid-2-aminoethyl ester to microscopically visualize saponarin accumulation in *ant310* protoplasts during reconstitution from naringenin but found that the fluorescence signal obtained does not appropriately detect the vacuolar localization of the barley flavonoids in mesophyll protoplasts (data not shown).

Saponarin Biosynthesis from Naringenin Requires the Presence of the Central Vacuole and Is Independent from de Novo Protein Biosynthesis

Saponarin was formed during naringenin feeding of *ant310* protoplasts and was efficiently stored in the vacuole. We therefore examined whether presence of the vacuole was a prerequisite for saponarin biosynthesis from naringenin. We prepared evacuolated miniprotoplasts from *ant310* mesophyll protoplasts lacking the central, acidic vacuole as seen by the absence of a neutral red-stained compartment in miniprotoplasts (data not shown; Hörtensteiner et al., 1992). The efficiency with which central lytic vacuole was removed during evacuolization was further assessed by measuring the activities of different vacuolar hydrolytic enzymes in protoplast and miniprotoplast fractions. When compared to protoplasts (100%), evacuolated miniprotoplasts contained only 3.1% $\pm$ 0.6%, 0.3% $\pm$ 0.2%, and 1.2% $\pm$ 1.0% of the activities of acid phosphatase, β-*N*-acetylglucosaminidase, and α-mannosidase, respectively. In contrast to some dicotyledonous plants, barley was not able to regenerate a new vacuole. When evacuolated miniprotoplasts isolated from *ant310* leaves were incubated with naringenin, only very low amounts of saponarin were detected within 6 h, while the corresponding protoplasts reached maximal saponarin levels again after 2 h (Fig. 4). We concluded that

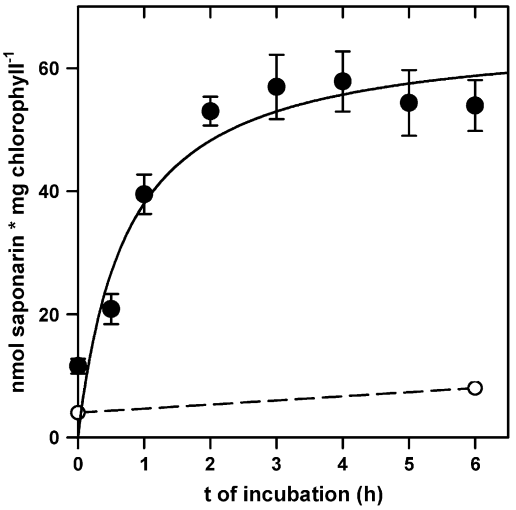

Figure 3. Naringenin incubation of *ant310* mesophyll protoplasts leads to cell-autonomous synthesis of saponarin. *ant310* mesophyll protoplasts isolated from 7-d-old primary leaves lacking flavonoids were incubated with or without 50 μM naringenin (black and white circles, respectively) in the light for the times indicated. Saponarin content in triplicate samples was determined by HPLC and is expressed based on the chlorophyll content measured in the same sample.

the presence of the vacuole as a destination compartment for saponarin accumulation was necessary for saponarin accumulation.

Because saponarin biosynthesis from naringenin in *ant310* was a rather quick process, already observed within up to 30 min (Figs. 3 and 4), we reasoned that the absence of CHI in the mutant did not affect the amount or in situ activity of the biosynthetic enzymes downstream of the isomerase. Indeed, addition of cycloheximid to *ant310* protoplasts did not affect saponarin production from externally fed naringenin, suggesting that de novo protein biosynthesis was not required for saponarin biosynthesis and vacuolar storage (Fig. 5). In contrast, when carbonyl cyanide 3-chlorophenylhydrazone (CCCP) or NH_4Cl, which dissipate pH gradients across membranes, were added to *ant310* protoplasts in the presence of naringenin, saponarin production was reduced by about 50% to values observed with protoplasts incubated on ice during naringenin treatment. Changes in the electrical membrane potential, caused by the addition of the K^+ ionophore, valinomycin, did not affect saponarin biosynthesis in naringenin-fed *ant310* protoplasts (Fig. 5). Thus, the overall inhibitor sensitivity of saponarin reconstitution in *ant310* protoplasts resembled the pharmacological profile of the vacuolar saponarin/H^+-antiporter (Frangne et al., 2002). Based on the absence of saponarin production in miniprotoplasts together with our previous observation of strongly decreased saponarin transport activity in isolated *ant310* vacuoles, we hypothesized that the absence of the vacuole or a decrease in the activity of vacuolar transport reduces the capacity to synthesize saponarin.

Naringenin Feeding of *ant310* Reactivates the Vacuolar Flavone Glucoside Transporter

Saponarin was efficiently stored in the vacuole during incubation of *ant310* protoplasts with naringenin. Thus, the vacuolar transport system should not have limited the overall biosynthetic capacity. In view of our previous data demonstrating strongly reduced saponarin transport in *ant310* vacuoles (Frangne et al., 2002), we tested whether resuming flavonoid biosynthesis in *ant310* affected the activity of the vacuolar flavone glucoside/H^+-antiporter.

We incubated *ant310* leaf segments and protoplasts without or with 50 μM naringenin for 3 h and isolated vacuoles in parallel followed by transport experiments. From our earlier experiments, it was known that the precursor isovitexin as well as saponarin itself were transported into vacuoles of the barley wild type by an H^+-antiport with K_m values of about 100 μM. Furthermore, saponarin and isovitexin competitively inhibited each other's transport, suggesting that both substances were taken up in barley vacuoles by the same transporter (Klein et al., 1996; Frangne et al., 2002). We therefore investigated uptake of both substances, isovitexin and saponarin, into *ant310* vacuoles after feeding the protoplasts with naringenin (Klein et al., 1996) with both substrate concentrations at the K_m value (100 μM).

In accordance with our former observation (Frangne et al., 2002), isovitexin was not taken up by vacuoles isolated from untreated *ant310* leaf segments. Figure 6A displays an HPLC trace of vacuoles after 18-min incubation with isovitexin in the presence of MgATP but without prior naringenin feeding of leaf segments. The only remarkable peak (denoted as peak no. 2)

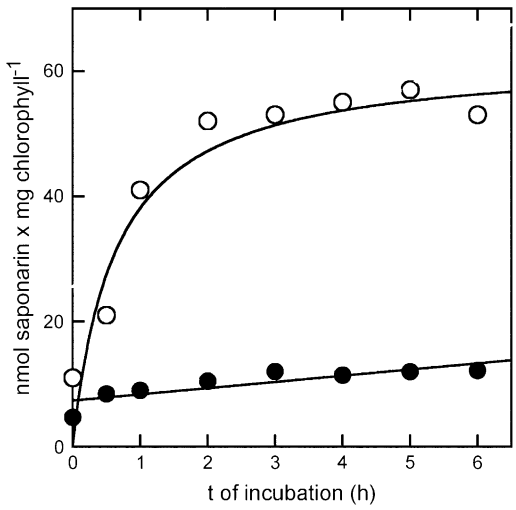

Figure 4. The presence of the vacuole as a destination compartment is necessary for saponarin reconstitution. *ant310* mesophyll protoplasts from 7-d-old primary leaves (white circles) and evacuolated miniprotoplasts (black circles) were incubated with 50 μM naringenin. Depicted is the reconstituted saponarin content based on chlorophyll after different times of naringenin incubation.

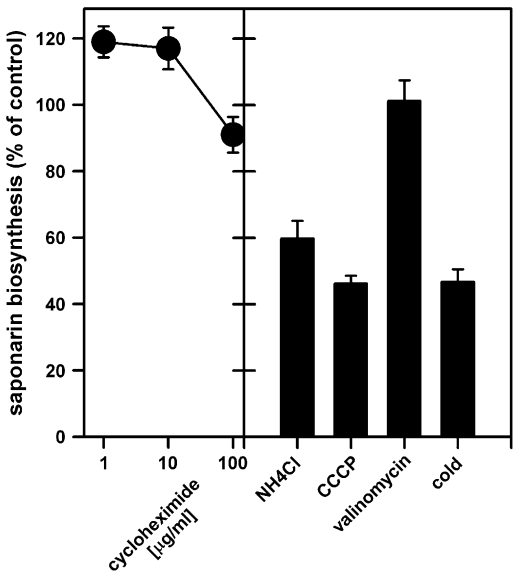

Figure 5. Inhibitor sensitivity of saponarin biosynthesis reconstitution by naringenin in *ant310* protoplasts. Isolated *ant310* protoplasts were incubated in the absence (control set to 100%) or presence of the inhibitors indicated together with 50 μM naringenin for 5 h at room temperature before protoplast-associated saponarin content was measured by HPLC. As a further control, naringenin incubation of protoplasts on ice was analyzed (cold). NH_4Cl was added at a final concentration of 5 mM, while CCCP and valinomycin concentrations were 10 μM.

corresponded to the *ant310*-specific compound isosalipurposide. In contrast, vacuoles isolated from naringenin-treated *ant310* material (3 h) exhibited after 18 min of uptake and presence of MgATP a peak (no. 1 in Fig. 6) that corresponded to authentic isovitexin. Figure 6C displays a comparable, time-dependent experiment with saponarin as substrate for the vacuolar uptake experiments. Only vacuoles isolated from *ant310* leaf segments, preincubated with naringenin, exhibited the vacuolar saponarin transport activity. The overall velocities of isovitexin and saponarin transport into vacuoles of naringenin-treated *ant310* leaves were comparable to expected transport rates for Ca33787 vacuoles calculated from our published kinetic constants for 100 μM substrate (Fig. 6, C and D; see Frangne et al., 2002). Furthermore, reactivation of vacuolar saponarin transport was independent of the time point of naringenin incubation during the isolation procedure. Results were identical when naringenin was added for 2 to 3 h during leaf segment preparation, cell wall digestion, and protoplast isolation or immediately to the purified protoplasts.

The latter notion prompted us to investigate whether naringenin feeding-induced vacuolar transport reactivation in *ant310* was a quick or slow process. For this experiment, *ant310* protoplasts were isolated and incubated in parallel for 10 min and 2 h with naringenin, before vacuoles were isolated and saponarin transport activities were determined. As a control, vacuoles were prepared from *ant310* protoplasts, omitting naringenin treatment (2 h). As can be seen from Figure 7, 10 min of naringenin treatment of protoplasts was not sufficient for an activation of the vacuolar saponarin transport activity when compared to vacuoles isolated after 2 h of protoplast feeding with naringenin. This result indicated that a metabolite derived from or induced by naringenin reactivated the vacuolar transport activity and not naringenin itself. We concluded that resumed flavone glucoside biosynthesis in *ant310* leaves by naringenin feeding restored the vacuolar transporter for these flavone glucosides to a high degree.

Naringenin Feeding Does Not Affect the Activity of the UDP-Glu:Isovitexin 7-*O*-Glucosyltransferase

Finally, we examined whether a metabolic regulation of a step in flavone glucoside biosynthesis was specific for the vacuolar transport system or also extended to other enzymes. As the only unequivocally defined step in late flavone glucoside biosynthesis in barley, we measured the activity of the UDP-Glc:isovitexin 7-*O*-glucosyltransferase (OGT) converting isovitexin to saponarin (Fig. 1; Blume et al., 1979). The activity of the OGT analyzed in crude extracts prepared from 5-d-old leaf segments was not affected either by the mutation in *ant310* nor by incubation of *ant310* leaf segments with naringenin (Table I). Thus, naringenin feeding of *ant310* leaves did not have an effect on the activity of a soluble biosynthetic enzyme when compared to the vacuolar flavone glucoside transport system.

DISCUSSION

We have previously shown that the vacuolar transport activity for the major barley flavone glucoside saponarin was strongly reduced when vacuoles isolated from *ant310* leaves were compared to the corresponding wild type (Frangne et al., 2002). The discovery that the mutation affected the *CHI* gene (Reuber et al., 1997; Druka et al., 2003) suggested that the absence of CHI activity in *ant310* in some way inhibited the vacuolar flavonoid transport activity. To examine whether intermediate(s) or products of flavonoid biosynthesis stimulate vacuolar flavonoid transport, we first analyzed whether it is possible to chemically complement the *chi* mutation in *ant310* by external application of naringenin.

We demonstrate that full chemical reconstitution of the flavonoid pathway by naringenin is possible in the *ant310* mutant, that naringenin conversion to saponarin needs the presence of an intact vacuole, and that reconstitution of the flavonoid pathway by naringenin in the *ant310* mutant reactivates the vacuolar flavonoid transporter to a high degree. Thus, we present an experimental model system that allows the detailed analysis of a metabolic linkage between a biosynthetic pathway whose activity can be externally manipulated

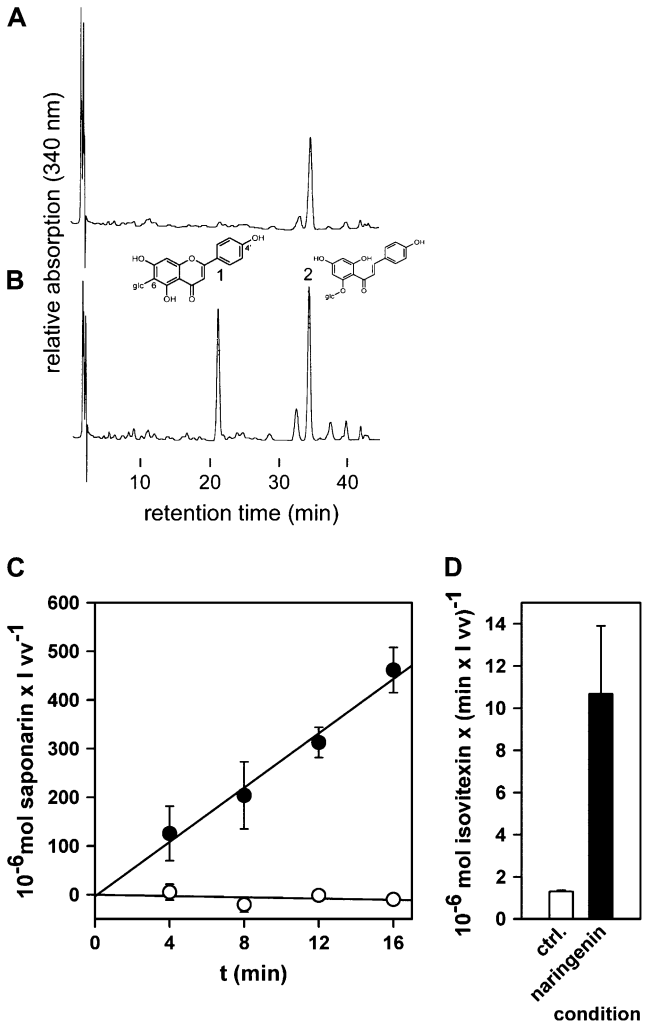

Figure 6. Naringenin incubation of *ant310* leaf segments or protoplasts reactivates the vacuolar flavone glucoside transport activity. Vacuoles isolated from 7-d-old *ant310* primary leaves incubated in the absence (A) or presence (B) of 50 μM naringenin for 3 h were subjected to transport experiments in the presence of 5 mM MgATP and 100 μM isovitexin for 16 min. Depicted are representative HPLC traces where comparable amounts of vacuole extracts were injected. Isovitexin (peak 1) was only taken up into vacuoles after naringenin preincubation of leaf segments (B). Peak 2 designates the *ant310*-specific compound isosalipurposide. C and D, Quantification of vacuolar transport experiments with 100 μM saponarin (C, time dependency) and isovitexin (D, uptake after 16 min) as substrates. White circles/bar, Vacuoles isolated from untreated *ant310* leaves. Black circles/bar, Vacuoles from *ant310* leaves incubated with naringenin. Efficient flavonoid transport reoccurs after treatment of leaf segments or protoplasts with naringenin. vv, Vacuolar volume.

and a transport step that appears to be necessary for the full activity of the pathway.

Efficient Chemical Reconstitution of a *chi* Mutant: Implications for the Flavonoid Biosynthesis Metabolon

The flavonoid biosynthetic pathway represents an important branch of the general phenylpropanoid pathway that also gives rise to other structurally and functionally diverse phenolic compounds, including soluble and cell wall-bound hydroxycinnamic acids, monolignols/lignin, sinapate esters, coumarins, and simple phenolics such as benzoic acid and salicylic acid (Dixon and Paiva, 1995). All these compounds are ultimately derived from trans-cinnamic acid, which is produced via Phe ammonia lyase (PAL). Because single cells are able to synthesize different products of the phenylpropanoid pathway at the same time, enzymes catalyzing the reactions at the branch points will compete for the precursors. Consequently, precursors should either be bound and converted with high affinity, exist in spatially separated cellular pools, or be directly handed over to downstream enzymes, most probably due to the close proximity of enzymes. In an attempt to explain competition for common intermediates, Stafford (1974) proposed that the different branches of phenylpropanoid metabolism are organized in enzyme complexes allowing channeled synthesis of different end products (Winkel, 2004). To date, it has become apparent, using metabolite feeding in combination with transgenic approaches, (co)localization, and interaction assays, that PAL and the proximate enzyme, cinnamate 4-hydroxylase converting trans-cinnamic acid to 4-hydroxycinnamate, are in close association on the ER, facilitating metabolic channeling at the entry point of the phenylpropanoid pathway (Rasmussen and Dixon, 1999; Liu and Dixon, 2001; Achnine et al., 2004). Furthermore, in the flavonoid pathway, Arabidopsis CHS, CHI, and flavonol 3-hydroxylase interact in association with the ER (Burbulis and Winkel-Shirley, 1999; Saslowsky and

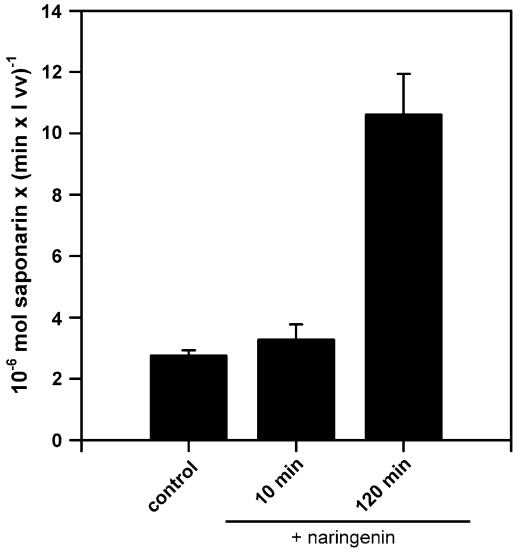

Figure 7. The reactivation of the vacuolar saponarin transport activity is not immediate. Protoplasts isolated from 7-d-old *ant310* leaves were in parallel incubated in the absence (control) or presence of 50 μM naringenin for 10 or 120 min, as indicated, followed by immediate vacuole isolation and saponarin uptake experiment.

Table I. *Activity of the UDP-Glc:isovitexin OGT in 5-d-old primary leaf segments incubated for 4 h in the absence (−) or presence (+) of 50 μM naringenin*

Condition		Activity
Line	Naringenin Incubation	
		pmol saponarin min^{-1} mg FW^{-1}
Ca33787	−	2.5 ± 0.3
ant310	−	2.7 ± 0.4
ant310	+	2.1 ± 0.4

Winkel-Shirley, 2001). Channeling, gel filtration, and cell fractionation studies performed by Hrazdina and Wagner (1985) suggested that a functionally intact multienzyme complex occurred loosely attached to the ER membrane, which contains all enzymes from PAL up to the late UDP-Glc:flavonoid glucosyltransferase. As a consequence, the question arises at which biosynthetic step is efficient feeding of precursors or intermediates possible, or, in other words, where and how many entry points for metabolites exist along the channel.

Here, we demonstrate that exogenous addition of naringenin resulted in efficient synthesis of saponarin, the major flavone glucoside in barley *ant310* primary leaves lacking functional *CHI* (Figs. 2 and 3). In the case of 4-d-old primary leaves, 50 μM naringenin in the medium led to the production of levels of saponarin within 7 h of incubation that are present in the wild type. This result suggests that naringenin is very efficiently taken up by barley leaf cells, is readily converted by all catalytic activities acting downstream of CHI, and is not, therefore, limiting the rate of metabolite flow in the *ant310* mutant. Furthermore, flavonoid production occurred in a cell-autonomous manner, because saponarin was synthesized from naringenin in isolated *ant310* mesophyll protoplasts (Figs. 3 and 4). Finally, the major end product is efficiently transferred into the vacuole, while in evacuolated miniprotoplasts, lacking the vacuole, saponarin production from naringenin it was completely blocked (Fig. 4).

Studies where exogenous feeding of naringenin is used to analyze the functionality of the flavonoid pathway in intact plants are rare. Using illuminated buckwheat (*Fagopyrum esculentum*) hypocotyls, Amrhein (1979) demonstrated that suppression of anthocyanin biosynthesis by the PAL inhibitor aminooxyacetate could be restored by exogenous addition of naringenin. Concentration-dependent experiments showed that 0.5 to 1 mM naringenin was needed to reverse the anthocyanin content to 70% of the control, while higher concentrations of naringenin were inhibitory. In our experiments, raising the exogenous naringenin concentration from 50 to 100 μM resulted in less efficient saponarin synthesis. Thus, higher naringenin concentrations have to be considered as toxic to the biosynthetic machinery. In Arabidopsis, different phenotypic features have been restored by chemical complementation of the *transparent testa4* (*tt4*) mutant, which affects CHS and therefore lacks all flavonoids (Shirley et al., 1995), with submicromolar concentrations of naringenin. These include anthocyanin accumulation in seedling cotyledons (Shirley et al., 1995), diphenylboric acid-2-aminoethyl ester-induced yellow/green fluorescence indicating presence of flavonols, and processes related to flavonoid regulation of auxin transport (Murphy et al., 2000; Brown et al., 2001; Buer and Muday, 2004; Peer et al., 2004). Thus, with regard to the metabolon organization of the phenylpropanoid pathway, the question arises whether naringenin represents a substrate that can efficiently enter the flavonoid biosynthesis channel downstream of Phe or whether lack of CHS (*tt4*) or CHI (*ant310*) leads to a structural rearrangement of the entire multienzyme complex, opening the complex to an exogenous pool of substrates that cannot enter the channel if the complex contains all functional subunits in the wild-type situation. However, submicromolar concentrations of naringenin significantly decreased auxin transport in both wild-type and *tt4* Arabidopsis seedlings when compared to controls not treated with naringenin (Peer et al., 2004). This suggests that also in the wild type, low, exogenously added concentrations of naringenin can still efficiently enter the metabolon and, if converted to flavonols, exert their regulatory role on auxin transport.

Metabolic Regulation of Vacuolar Flavonoid Transport: How and Why?

A clear advantage of the barley *ant310* primary leaf experimental system to study linkage between flavonoid biosynthesis and vacuolar transport of its products is the relative ease and speed of organelle isolation following the supply of the metabolic precursor. Although Arabidopsis or petunia (*Petunia hybrida*), as genetically well-defined systems with regard to flavonoid biosynthesis, offer more mutants in important biosynthetic genes, exogenous feeding of precursors followed by the isolation of lytic vacuoles in sufficient amounts for transport experiments is presently only well established in barley. Furthermore, the primary leaf is a well-defined system with respect to flavonoid biosynthesis (Klein et al., 1996; Reuber et al., 1996; Frangne et al., 2002), although important conversion steps still need unequivocal biochemical elucidation (see

Fig. 1). Finally, mesophyll protoplasts and lytic vacuoles represent a homogenous cell or organelle type, an advantage over the use of Arabidopsis rosette leaves to produce protoplasts; the differences in flavonoid composition of spongy and palisade parenchyma have not been experimentally determined in this model plant, nor are we aware of detailed investigations of flavonoid patterns in rosette leaves representing different developmental stages.

Here, we provide experimental evidence that the vacuolar flavonoid transport system in barley is linked to functional flavonoid biosynthesis. In vacuoles isolated from *ant310* leaves, uptake of saponarin and its precursor isovitexin was strongly reduced (Frangne et al., 2002). Uptake of these two flavone glucosides in barley vacuoles was previously characterized, occurring via a proton-antiport mechanism (Klein et al., 1996; Frangne et al., 2002). Furthermore, competitive inhibition of saponarin transport by isovitexin and vice versa, as well as comparable K_m values, suggested that both flavone glucosides were transported into barley mesophyll vacuoles by a membrane protein accepting both compounds as substrates. In contrast, when *ant310* leaf sections or protoplasts were supplied with naringenin prior to vacuole isolation, transport of saponarin and isovitexin was strongly reactivated from almost undetectable transport activity in the absence of naringenin. Taking all independent transport experiments into account, the vacuolar transport activities after naringenin incubation of *ant310* were 18 ± 6 and 21 ± 5 μmol substrate min^{-1} L vacuolar $volume^{-1}$ for isovitexin and saponarin, respectively. This suggests no preference of the transporter for saponarin or isovitexin at 100-μM substrate concentration (a value close to the K_m values). Using our kinetic values published for [^{3}H]saponarin transport into vacuoles isolated from barley var. Bakara (Frangne et al., 2002), we calculated that the expected vacuolar transport rate for the flavone glucoside concentration applied in the transport experiments here (100 μM) was 13 μmol saponarin min^{-1} L vacuolar $volume^{-1}$. Thus, the addition of naringenin fully reconstituted the flavone glucoside transport activity in *ant310* cells. We propose, therefore, that the vacuolar flavonoid transporter in barley is under the strict control of the functional flavonoid pathway. Because reconstitution of saponarin production, which was intimately linked to vacuolar compartmentation, was not affected by high concentrations of cycloheximide (Fig. 5), the regulation should occur at posttranslational level. It is tempting to speculate that transport regulation involves an unknown pathway intermediate binding to the flavonoid transporter. Alternatively, it could be hypothesized that the vacuolar transporter itself represents a part of the flavonoid metabolon. Based on the fact that the OGT activity representing the last biosynthetic step is neither influenced by the loss of CHI activity nor by naringenin feeding of *ant310* leaves (Table I), it can be argued that regulation of the pathway by its intermediates may be rather specific for the transport step.

If the flavonoid pathway generates a metabolite regulating the transport step, it cannot be naringenin itself, because reactivation required a naringenin incubation period of several hours while short (10 min) exposure of *ant310* protoplasts to naringenin was not sufficient for efficient transport reactivation (Fig. 7). Furthermore, this metabolite must be absent in *ant310* plants and should be specific for the flavonoid pathway. Transport reactivation occurred after naringenin feeding of *ant310* leaves and therefore in the presence of the mutant-specific compound isosalipurposide accumulating as a consequence of the absence of CHI. Consequently, isosalipurposide does not likely act as an inhibitor of vacuolar saponarin transport in *ant310* leaves (Figs. 1 and 6).

For an alternative proposition, a physical integration of the transport step into the hypothesized metabolon, an intriguing problem has to be addressed: How can an ER-associated biosynthetic complex interact with a vacuolar transporter? In this respect it is interesting to note that cellular inclusions containing flavonoids that may move between different compartments have been repeatedly described in different plant species, e.g. in pathogen-challenged *Sorghum bicolor* (Snyder and Nicholson, 1990; Nielsen et al., 2004). Maize 'Black Mexican Sweet' cells accumulate green and yellow autofluorescent bodies targeted to the cell wall and the vacuole, respectively, following expression of the Myb-type transcription factor P1 that continues along with production of *C*-glycosylflavones (Lin et al., 2003). In different species, anthocyanic vacuolar inclusions have been shown to be responsible for local high accumulation of anthocyanins, which is associated with color intensification (Pecket and Small, 1980; Markham et al., 2000; Irani and Grotewold, 2005). Furthermore, mutations in the genes *TDS4* and *AHA10* encoding leucoanthocyanidin dioxygenase and a P-type proton-translocating adenosine triphosphatase in Arabidopsis, respectively, resulting in defects in proanthocyanidin biosynthesis in the seed coat, are associated with alterations in vacuolar morphology visualized after addition of a fluorescent dye normally labeling the central vacuole (Abrahams et al., 2003; Baxter et al., 2005). Likewise, overexpression of the R and C1 regulators of anthocyanin accumulation in maize cells induces alterations in the subcellular distribution and vacuolar organization of anthocyanins in a light-dependent manner, which is also associated with changes in vacuolar morphology (Irani and Grotewold, 2005). The question of how glutathione *S*-transferases, such as BZ2 in maize (Marrs et al., 1995), TT19 in Arabidopsis (Kitamura et al., 2004), or AN9 in petunia (Alfenito et al., 1998), contribute to the accumulation of flavonoids in the vacuole remains unanswered. Despite overwhelming genetic evidence for the importance of these usually soluble enzymes in a late step of anthocyanin biosynthesis prior to vacuolar storage, their direct enzymatic action on flavonoids has not been established. Instead, a role as soluble flavonoid-binding proteins that could guide flavonoids in a protected

manner through the cytosol toward the vacuole has been proposed (Mueller et al., 2000).

We did not observe any changes in vacuolar morphology in *ant310* leaves or protoplasts, and also, isolation of vacuoles was possible from flavonoid-free protoplasts. It must be assumed, therefore, that the morphology of the central vacuole responsible for saponarin storage is not altered in *ant310.* Nevertheless, it is possible that the molecularly unidentified flavonoid transporter could travel between two compartments: the ER where it could be activated by a component of the metabolon and where it also could accept the flavonoid substrate as a cargo and the vacuole where transport would occur. Alternatively, flavonoids produced at the ER could be accepted by soluble glutathione *S*-transferases and handed over to the vacuolar transporter after traveling through the cytosol. Clearly, experiments testing these hypotheses will need to address the cellular localization of the transporter in response to naringenin treatment and the availability of substrates.

The absence and reduction of naringenin-induced saponarin biosynthesis in evacuolated *ant310* miniprotoplasts (Fig. 4) and NH_4Cl- or CCCP-treated *ant310* protoplasts (Fig. 5) suggest that an intact and acidic vacuole is required for saponarin biosynthesis. These experiments do not help determine which hypothesis, described above, is true; however, they do suggest that a destination compartment is necessary for efficient flavonoid production. The efficiency of the elimination of products of the flavonoid pathway from the cytosol to the vacuole appears to affect overall biosynthesis, which presumably involves feedback inhibition. Feedback inhibition of flavonoid biosynthesis resulting from the failure to store flavonoid end products in the vacuole agrees with observations made in antisense experiments of the anthocyanin transporter ZmMRP3 or using the Arabidopsis *tt12* mutation, which causes a lesion in the gene encoding a presumptive transporter for proanthocyanidin precursors (Debeaujon et al., 2001; Goodman et al., 2004). Together with the inducible vacuolar flavonoid transport system demonstrated here, this indicates that flavonoid biosynthesis is functionally linked to the transport step and to vacuolar compartmentation of flavonoids.

MATERIALS AND METHODS

Chemicals

Naringenin was obtained from Sigma (Buchs) and dissolved in 40% (v/v) ethanol/water (stock 1 mg mL^{-1}). The glucosylated apigenins, saponarin and isovitexin, were obtained from Extrasynthese, and flavonoid as well as inhibitor stocks were dissolved in dimethyl sulfoxide. Stock concentrations for saponarin and isovitexin were calculated after measuring the A_{340} using the molar extinction coefficient for apigenin ($\varepsilon_{apigenin,\ 340\ nm}$ = 20,800 M^{-1}; Weast, 1982). For the naringenin reconstitution experiments, controls without naringenin contained the corresponding amount of ethanol. All other flavonoid standards were taken from our laboratory collection. Cell wall-digesting enzymes were from Seishin Pharmaceuticals and UDP-Glc from Boehringer. For chemicals used during protoplast or vacuole isolation and HPLC analysis, see Klein et al. (1996) and Frangne et al. (2002).

Plant Material and Growth Condition

The barley (*Hordeum vulgare*) lines Ca33787 (wild type) and the *ant310* mutant (Jende-Strid, 1993; Reuber et al., 1997; Druka et al., 2003) were grown in standard soil (Einheitserde Typ ED 73) in growth cabinets. For the naringenin reconstitution experiments with entire leaf segments performed in Cologne, plants were grown with 13 h of fluorescent light (80 $\mu E\ m^{-2}\ s^{-1}$), while plants used for protoplast, miniprotoplast, and vacuole isolations performed in Zurich were grown with a photoperiod of 14 h. In both locations, phytotrons were set to 20°C and a relative humidity of 60% to 70%.

Naringenin Feeding of Leaf Segments and Flavonoid Extraction

To achieve maximal turgescence, plants were well watered approximately 30 min before primary leaf segments were cut once above the coleoptile and 1 cm from the tip. This resulted in leaf segments of 3 to 4 and 5 to 6 cm for 4- or 5-d-old primary leaves, respectively. The abaxial epidermis was removed mechanically and leaf segments (4–8 segments per experiment depending on leaf age) were transferred with their abaxial side on 5 or 10 mL 0.1 M KPi buffer, pH 7, in 5- or 9-cm petri dishes, respectively. Reconstitution started by the addition of naringenin solution or solvent to the medium followed by incubation at room temperature on a shaker (50 rpm) close to a window with daylight for the times indicated. Following incubation, the segments were quickly dried with filter paper and the sample fresh weight (FW) was determined. For flavonoid extraction, segment samples were pulverized in the presence of liquid N_2 and 5 mL/g FW of 50% (v/v) MeOH/water were added followed by 15-min extraction at room temperature with occasional vortexing. Prior to HPLC analysis, extracts were centrifuged in 1.5-mL reaction tubes at 18,000*g* for 10 min. Investigation of flavonoid exudates during leaf segment incubation was performed by directly subjecting incubation media aliquots to HPLC analysis.

Isolation and Naringenin Feeding of Mesophyll Protoplasts, Vacuoles, and Evacuolated Miniprotoplasts

In comparison to naringenin feeding of 4- or 5-d-old leaf segments, 7-d-old primary leaves were used for all protoplast experiments. Isolation of barley protoplasts and vacuoles followed published procedures (Rentsch and Martinoia, 1991) with the modifications reported by Frangne et al. (2002). The purity of barley mesophyll vacuoles was recently reassessed for vacuoles used in proteomic experiments (Endler et al., 2006). Marker enzyme activities detected less than 1% of chloroplast, mitochondrial, or cytosolic contamination in the vacuolar compared to the protoplast fraction, while western-blot analysis with compartment-specific antibodies suggests absence of contaminating membranes and compartments from vacuolar preparations. Evacuolated miniprotoplasts isolated from barley mesophyll protoplasts were obtained as described for tobacco (*Nicotiana tabacum*; Hörtensteiner et al., 1992).

When protoplasts were used for naringenin feeding without subsequent vacuole isolation, protoplasts were purified using the Percoll step gradient described by Rentsch and Martinoia (1991), but 0.5 M sorbitol, 1 mM $CaCl_2$, 10 mM MES KOH, pH 5.6 (medium A), was used instead of 0.4 M sorbitol, 30 mM KCl, 5 mM HEPES KOH, pH 7.2, which was prepared for the isolation of vacuoles from protoplasts.

Naringenin feeding experiments with Ca33787 and *ant310* protoplasts and miniprotoplasts were performed by adding naringenin to a final concentration of 50 μM to the illuminated cells kept in medium A. At times indicated, triplicate 0.25-mL aliquots were removed and added to 1.5 mL 0.5 M Gly betaine 1 mM $CaCl_2$, 10 mM MES KOH, pH 5.8 (medium B), followed by gentle centrifugation (50*g*, 5 min). The pellet was resuspended in 0.3 mL medium B, presence of protoplasts or miniprotoplasts was checked by microscopy, and flavonoids were extracted by the addition of 0.2 mL resuspended cells to 0.2 mL MeOH. After 2 h at −20°C, samples were centrifuged for 10 min at 18,000*g*, and the supernatant was subjected to HPLC analysis. To compare different isolations, 10-μL aliquots were taken from the remaining cell suspension in medium B, added to 1 mL of 80% (v/v) acetone, and total chlorophyll content was determined by spectrophotometric measurement of absorbances at 470, 647, and 663 nm using the equations of Lichtenthaler (1987).

Two different naringenin-feeding conditions were used for the demonstration of vacuolar flavonoid transport reactivation following naringenin

treatment of *ant310* without significant differences in their effectivity. For standard long-term naringenin incubation (2–3 h), 50 μM naringenin (control, solvent only) was present in all media during the preparation of leaf segments, cell wall digestion, and protoplast isolation up to the moment of vacuole lysis. Alternatively, only purified protoplasts were incubated in the presence or absence of naringenin. To avoid cell wall regeneration that would subsequently complicate vacuole isolation, medium A was supplied with 0.5% (w/v) cellulase Y-C and 0.05% (w/v) pectolyase Y-23. In all cases, flavonoid transport experiments were performed immediately after vacuole isolation.

For vacuole uptake studies, naringenin-feeding experiments and corresponding controls were in all cases performed in parallel, resulting in a minimum of two independent protoplast and vacuole isolations on the same day.

Flavonoid Compartmentation Studies, Marker-Based Assessment of Evacuolated Miniprotoplasts, and Uptake Experiments with Plant Vacuoles

Vacuolar compartmentation of saponarin reconstituted during naringenin incubation of *ant310* protoplasts (3 h) was analyzed by comparing the amount of saponarin in protoplasts and vacuoles isolated from the same naringenin-treated protoplast preparation. To compare both fractions, the activity of the acid phosphatase was determined as a vacuolar marker according to Hörtensteiner et al. (1992) using methylumbelliferyl phosphate as a substrate. Fluorescence emission of liberated methylumbelliferone was measured with a Fusion Universal Microplate Analyzer (Packard) and the following filters: $\lambda_{exc} = 380 \pm 20$ nm; $\lambda_{em} = 485$ nm. The calculation of the amount of product formed was performed using a methylumbelliferone standard curve. Likewise, absence of vacuolar marker enzymes in evacuolated miniprotoplasts was assessed by measuring the activities of the acid phosphatase, β-*N*-acetylglucosaminidase, and α-mannosidase in protoplast and miniprotoplast fractions using the corresponding methylumbelliferyl conjugates as substrates (final concentration 2.4 mM).

Flavonoid uptake experiments into vacuoles isolated from *ant310* leaves or protoplasts that were incubated either in the presence or absence of naringenin were performed in parallel using the silicone oil centrifugation technique as described previously (Klein et al., 1996; Frangne et al., 2002). In all cases, six 0.4-mL polyethylene tubes were prepared per condition and time point containing 5 mM MgATP, 0.1 μCi ^3H_2O per tube, and 0.1 mM unlabeled isovitexin and saponarin as substrates, which is close to the K_m value of saponarin transport (Frangne et al., 2002). The supernatants of two tubes containing the vacuolar content following centrifugation of the vacuoles through the silicone oil were pooled, resulting in 100 μL, of which 50 μL was injected for HPLC analysis of the amount of flavonoids transported into vacuoles, while 10 μL was subjected to scintillation counting for the calculation of vacuolar volumes. If not stated otherwise, the flavonoid uptake rates were calculated by subtracting values obtained after 18 min of transport from corresponding 3-min values.

HPLC Analysis of Flavonoids

The flavonoid composition of methanolic extracts of leaf segments, protoplasts, miniprotoplasts, and vacuoles was analyzed by HPLC performed identically either on a Shimadzu (experiments performed in Cologne) or on a Gynkothek HPLC system using the following reverse-phase conditions: Nucleosil 100 to 5 C18 column (125 × 4.6 mm; Macherey-Nagel); constant flow rate of 1 mL min^{-1}; solvent A, water/1% (v/v) H_3PO_4; solvent B, acetonitrile; gradient (B over A in % [v/v]; all changes linear) 0 to 1 min 10% to 10%, 1 to 16 min 10% to 14%, 16 to 26 min 14% to 14%, 26 to 41 min 14% to 22%, 41 to 42 min 22% to 100%, 42 to 43 min 100% to 10%, 43 to 48 min 10% to 10%; detection at 315 nm. The Gynkothek HPLC system was connected to a Dionex diode array detector. Peaks were therefore identified by coelution with authentic standards and due to identity of absorption spectra (220–370 nm).

Glucosyltransferase Assay

The activity of the uridine-diphosphate-Glc:isovitexin OGT was measured in crude extracts as follows: segments of 4- to 5-d-old Ca33787 and *ant310* primary leaves were incubated in the absence or presence of 50 μM naringenin for 4 h as described above. Liquid N_2-frozen samples were pulverized in a mortar and extracted with 6.25 mL/g FW of extraction buffer (0.1 M KPi, pH 7.5, 0.5 mM 1,4-dithioerythritol supplied with 0.2 g Polyclar AT, and 0.2 g Dowex Cl^-/g FW) for 15 min on ice. The homogenate was filtered through Miracloth and centrifuged (4°C, 20 min, 15,000*g*). The supernatant was purified on a PD-10 column that was previously equilibrated with extraction buffer and used immediately for the activity assay. A total of 10 to 50 μL of extract was incubated at 30°C in 0.1 M KPi, pH 7.5, 0.5 mM 1,4-dithioerythritol, 0.4 mg bovine serum albumin, 3 mM UDP-Glc, and 0.2 mM isovitexin in a total volume of 0.1 mL. Assays were stopped by the addition of 1 vol MeOH/1% (v/v) HCl, centrifuged, and the amount of saponarin formed from isovitexin was analyzed by HPLC. The glucosyltransferase activity was linear over time for at least 60 min, and for the protein concentrations, up to 45 μg per assay was used.

ACKNOWLEDGMENTS

The authors thank Christian Frey and Karl Huwiler for taking care of barley plants and Enrico Martinoia and Mark Curtis for discussion and help on the manuscript (all University of Zurich).

Received December 13, 2006; accepted March 9, 2007; published March 16, 2007.

LITERATURE CITED

Abrahams S, Lee E, Walker AR, Tanner GJ, Larkin PJ, Ashton AR (2003) The Arabidopsis *TDS4* gene encodes leucoanthocyanidin dioxygenase (LDOX) and is essential for proanthocyanidin synthesis and vacuole development. Plant J **35:** 624–636

Achnine L, Blancaflor EB, Rasmussen S, Dixon RA (2004) Colocalization of L-phenylalanine ammonia-lyase and cinnamate 4-hydroxylase for metabolic channeling in phenylpropanoid biosynthesis. Plant Cell **16:** 3098–3109

Alfenito MR, Souer E, Goodman CD, Buell R, Mol J, Koes R, Walbot V (1998) Functional complementation of anthocyanin sequestration in the vacuole by widely divergent glutathione S-transferases. Plant Cell **10:** 1135–1149

Amrhein N (1979) Biosynthesis of cyanidin in buckwheat hypocotyls. Phytochemistry **18:** 585–589

Baxter IR, Young JC, Armstrong G, Foster N, Bogenschutz N, Cordova T, Peer WA, Hazen SP, Murphy AS, Harper JF (2005) A plasma membrane H^+-ATPase is required for the formation of proanthocyanidins in the seed coat endothelium of *Arabidopsis thaliana*. Proc Natl Acad Sci USA **102:** 2649–2654

Block A, Dangl JL, Hahlbrock K, Schulze-Lefert P (1990) Functional borders, genetic fine structure, and distance requirements of cis elements mediating light responsiveness of the parsley chalcone synthase promoter. Proc Natl Acad Sci USA **87:** 5387–5391

Blume DE, Jaworski JG, McClure JW (1979) Uridinediphosphate-glucose: isovitexin 7-O-glucosyltransferase from barley protoplasts: subcellular localization. Planta **146:** 199–202

Brown DE, Rashotte AM, Murphy AS, Normanly J, Tague BW, Peer WA, Taiz L, Muday GK (2001) Flavonoids act as negative regulators of auxin transport in vivo in Arabidopsis. Plant Physiol **126:** 524–535

Buer CS, Muday GK (2004) The *transparent testa4* mutation prevents flavonoid synthesis and alters auxin transport and the response of Arabidopsis roots to gravity and light. Plant Cell **16:** 1191–1205

Burbulis IE, Winkel-Shirley B (1999) Interactions among enzymes of the Arabidopsis flavonoid biosynthetic pathway. Proc Natl Acad Sci USA **96:** 12929–12934

Chappell J, Hahlbrock K (1984) Transcription of plant defence genes in response to UV light or fungal elicitor. Nature **311:** 76–78

Christie JM, Jenkins GI (1996) Distinct UV-B and UV-A/blue light signal transduction pathways induce chalcone synthase gene expression in Arabidopsis cells. Plant Cell **8:** 1555–1567

Dakora FD, Phillips DA (2002) Root exudates as mediators of mineral acquisition in low-nutrient environments. Plant Soil **245:** 35–47

Dean JV, Mohammed LA, Fitzpatrick T (2005) The formation, vacuolar localization, and tonoplast transport of salicylic acid glucose conjugates in tobacco cell suspension cultures. Planta **221:** 287–296

Debeaujon I, Peeters AJ, Leon-Kloosterziel KM, Koornneef M (2001) The *TRANSPARENT TESTA12* gene of Arabidopsis encodes a multidrug

secondary transporter-like protein required for flavonoid sequestration in vacuoles of the seed coat endothelium. Plant Cell **13:** 853–871

Dixon RA, Paiva NL (1995) Stress-induced phenylpropanoid metabolism. Plant Cell **7:** 1085–1097

Dixon RA, Xie D-Y, Sharma SB (2005) Proanthocyanidins: a final frontier in flavonoid research? New Phytol **165:** 9–28

Druka A, Kudrna D, Rostoks N, Brueggeman R, von Wettstein D, Kleinhofs A (2003) Chalcone isomerase gene from rice (*Oryza sativa*) and barley (*Hordeum vulgare*): physical, genetic and mutation mapping. Gene **302:** 171–178

Endler A, Meyer S, Schelbert S, Schneider T, Weschke W, Peters SW, Keller F, Baginsky S, Martinoia E, Schmidt UG (2006) Identification of a vacuolar sucrose transporter in barley and Arabidopsis mesophyll cells by a tonoplast proteomic approach. Plant Physiol **141:** 196–207

Faktor O, Kooter JM, Loake GJ, Dixone RA, Lamb CJ (1997) Differential utilization of regulatory cis-elements for stress-induced and tissue-specific activity of a French bean chalcone synthase promoter. Plant Sci **124:** 175–182

Frangne N, Eggmann T, Koblischke C, Weissenböck G, Martinoia E, Klein M (2002) Flavone glucoside uptake into barley mesophyll and Arabidopsis cell culture vacuoles: energization occurs by H^+-antiport and ATP-binding cassette-type mechanisms. Plant Physiol **128:** 726–733

Goodman CD, Casati P, Walbot V (2004) A multidrug resistance-associated protein involved in anthocyanin transport in *Zea mays.* Plant Cell **16:** 1812–1826

Graham TL (1998) Flavonoid and flavonol glycoside metabolism in Arabidopsis. Plant Physiol Biochem **36:** 135–144

Grotewold E (2004) The challenges of moving chemicals within and out of cells: insights into the transport of plant natural products. Planta **219:** 906–909

Hartmann U, Sagasser M, Mehrtens F, Stracke R, Weisshaar B (2005) Differential combinatorial interactions of cis-acting elements recognized by R2R3-MYB, BZIP, and BHLH factors control light-responsive and tissue-specific activation of phenylpropanoid biosynthesis genes. Plant Mol Biol **57:** 155–171

Hartmann U, Valentine WJ, Christie JM, Hays J, Jenkins GI, Weisshaar B (1998) Identification of UV/blue light-response elements in the *Arabidopsis thaliana* chalcone synthase promoter using a homologous protoplast transient expression system. Plant Mol Biol **36:** 741–754

Hopp W, Seitz HU (1987) The uptake of acylated anthocyanin into isolated vacuoles from a cell suspension culture of *Daucus carota.* Planta **170:** 74–85

Hörtensteiner S, Martinoia E, Amrhein N (1992) Reappearance of hydrolytic activities and tonoplast proteins in the regenerated vacuole of evacuolated protoplasts. Planta **187:** 113–121

Hrazdina G, Wagner GJ (1985) Metabolic pathways as enzyme complexes: evidence for the synthesis of phenylpropanoids and flavonoids on membrane-associated enzyme complexes. Arch Biochem Biophys **237:** 88–100

Hutzler P, Fischbach R, Heller W, Jungblut T, Reuber S, Schmitz R, Veit M, Weissenböck G, Schnitzler J (1998) Tissue localization of phenolic compounds in plants by confocal laser scanning microscopy. J Exp Bot **49:** 953–965

Ibrahim RK, De Luca V, Khouri H, Latchinian L, Brisson L, Charest PM (1987) Enzymology and compartmentation of polymethylated flavonol glucosides in *Chrysosplenium americanum.* Phytochemistry **26:** 1237–1245

Irani NG, Grotewold E (2005) Light-induced morphological alteration in anthocyanin-accumulating vacuoles of maize cells. BMC Plant Biol **5:** 7

Jende-Strid B (1993) Genetic control of flavonoid biosynthesis in barley. Hereditas **119:** 187–204

Jorgensen K, Rasmussen AV, Morant M, Nielsen AH, Bjarnholt N, Zagrobelny M, Bak S, Møller BL (2005) Metabolon formation and metabolic channeling in the biosynthesis of plant natural products. Curr Opin Plant Biol **8:** 280–291

Kerscher F, Franz G (1987) Biosynthesis of vitexin and isovitexin. Z Naturforsch [C] **42:** 519–524

Kerscher F, Franz G (1988) Isolation and some properties of an UDP-glucose: 2-hydroxyflavanone-6(or8)-C-glucosyl-transferase from *Fagopyrum esculentum* M. cotyledons. J Plant Physiol **132:** 110–115

Kitamura S, Shikazono N, Tanaka A (2004) *TRANSPARENT TESTA 19* is involved in the accumulation of both anthocyanins and proanthocyanidins in Arabidopsis. Plant J **37:** 104–114

Klein M, Weissenböck G, Dufaud A, Gaillard C, Kreuz K, Martinoia E (1996) Different energization mechanisms drive the vacuolar uptake of a flavonoid glucoside and a herbicide glucoside. J Biol Chem **271:** 29666–29671

Knogge W, Schmelzer E, Weissenböck G (1986) The role of chalcone synthase in the regulation of flavonoid biosynthesis in developing oat primary leaves. Arch Biochem Biophys **250:** 364–372

Lepiniec L, Debeaujon I, Routaboul JM, Baudry A, Pourcel L, Nesi N, Caboche M (2006) Genetics and biochemistry of seed flavonoids. Annu Rev Plant Biol **57:** 405–430

Lichtenthaler HK (1987) Chlorophyll and carotenoids: pigments of photosynthetic biomembranes. Methods Enzymol **148:** 331–382

Lin Y, Irani NG, Grotewold E (2003) Sub-cellular trafficking of phytochemicals explored using auto-fluorescent compounds in maize cells. BMC Plant Biol **3:** 10

Liu CJ, Dixon RA (2001) Elicitor-induced association of isoflavone *O*-methyltransferase with endomembranes prevents the formation and 7-*O*-methylation of daidzein during isoflavonoid phytoalexin biosynthesis. Plant Cell **13:** 2643–2658

Markham KR, Gould KS, Winefield CS, Mitchell KA, Bloor SJ, Boase MR (2000) Anthocyanic vacuolar inclusions: their nature and significance in flower colouration. Phytochemistry **55:** 327–336

Marrs KA, Alfenito MR, Lloyd AM, Walbot V (1995) A glutathione S-transferase involved in vacuolar transfer encoded by the maize gene *Bronze-2.* Nature **375:** 397–400

Matern U, Reichenbach C, Heller W (1986) Efficient uptake of flavonoids into parsley (*Petroselinum hortense*) vacuoles requires acylated glycosides. Planta **167:** 183–189

Mueller LA, Goodman CD, Silady RA, Walbot V (2000) AN9, a petunia glutathione S-transferase required for anthocyanin sequestration, is a flavonoid-binding protein. Plant Physiol **123:** 1561–1570

Murphy A, Peer WA, Taiz L (2000) Regulation of auxin transport by aminopeptidases and endogenous flavonoids. Planta **211:** 315–324

Nielsen KA, Gotfredsen CH, Buch-Pedersen MJ, Ammitzboll H, Mattsson O, Duus JO, Nicholson RL (2004) Inclusions of flavonoid 3-deoxyanthocyanidins in Sorghum bicolor self-organize into spherical structures. Physiol Mol Plant Pathol **65:** 187–196

Ono E, Hatayama M, Isono Y, Sato T, Watanabe R, Yonekura-Sakakibara K, Fukuchi-Mizutani M, Tanaka Y, Kusumi T, Nishino T, et al (2006) Localization of a flavonoid biosynthetic polyphenol oxidase in vacuoles. Plant J **45:** 133–143

Onyilagha JC, Grotewold E (2004) The biology and structural distribution of surface flavonoids. Recent Res Devel Plant Sci **2:** 1–18

Paiva NL (2000) An introduction to the biosynthesis of chemicals used in plant-microbe communication. J Plant Growth Regul **19:** 131–143

Pecket RC, Small CJ (1980) Occurrence, location and development of anthocyanoplasts. Phytochemistry **19:** 2571–2576

Peer WA, Bandyopadhyay A, Blakeslee JJ, Makam SN, Chen RJ, Masson PH, Murphy AS (2004) Variation in expression and protein localization of the PIN family of auxin efflux facilitator proteins in flavonoid mutants with altered auxin transport in *Arabidopsis thaliana.* Plant Cell **16:** 1898–1911

Peer WA, Brown DE, Tague BW, Muday GK, Taiz L, Murphy AS (2001) Flavonoid accumulation patterns of *transparent testa* mutants of Arabidopsis. Plant Physiol **126:** 536–548

Rasmussen S, Dixon RA (1999) Transgene-mediated and elicitor-induced perturbation of metabolic channeling at the entry point into the phenylpropanoid pathway. Plant Cell **11:** 1537–1552

Rentsch D, Martinoia E (1991) Citrate transport into barley mesophyll vacuoles: comparison with malate-uptake activity. Planta **184:** 532–537

Reuber S, Bornman JF, Weissenböck G (1996) A flavonoid mutant of barley (*Hordeum vulgare* L.) exhibits increased sensitivity to UV-B radiation in the primary leaf. Plant Cell Environ **19:** 593–601

Reuber S, Jende-Strid B, Wray V, Weissenböck G (1997) Accumulation of the chalcone isosalipurposide in primary leaves of barley flavonoid mutants indicates a defective chalcone isomerase. Physiol Plant **101:** 827–832

Saslowsky D, Winkel-Shirley B (2001) Localization of flavonoid enzymes in Arabidopsis roots. Plant J **27:** 37–48

Saslowsky DE, Warek U, Winkel BS (2005) Nuclear localization of flavonoid enzymes in Arabidopsis. J Biol Chem **280:** 23735–23740

Schnitzler J-P, Jungblut TP, Heller W, Kofferlein M, Hutzler P, Heinzmann U, Schmelzer E, Ernst D, Langebartels C, Sandermann H (1996) Tissue localization of UV-B-screening pigments and of

chalcone synthase mRNA in needles of Scots pine seedlings. New Phytol **132:** 247–258

Schulz M, Weissenböck G (1986) Isolation and separation of epidermal and mesophyll protoplasts from rye primary leaves: tissue specific characteristics of secondary phenolic product accumulation. Z Naturforsch [C] **41:** 22–27

Schulz M, Weissenböck G (1988) Dynamics of the tissue-specific metabolism of luteolin glucuronides in the mesophyll of rye primary leaves (*Secale cereale*). Z Naturforsch [C] **43:** 187–193

Schulze-Lefert P, Becker-Andre M, Schulz W, Hahlbrock K, Dangl JL (1989) Functional architecture of the light-responsive chalcone synthase promoter from parsley. Plant Cell **1:** 707–714

Shirley BW, Kubasek WL, Storz G, Bruggemann E, Koornneef M, Ausubel FM, Goodman HM (1995) Analysis of Arabidopsis mutants deficient in flavonoid biosynthesis. Plant J **8:** 659–671

Snyder BA, Nicholson RL (1990) Synthesis of phytoalexins in sorghum as a site-specific response to fungal ingress. Science **248:** 1637–1639

Stafford HA (1974) Possible multienzyme complexes regulating the formation of C6-C3 phenolic compounds and lignins in higher plants. Recent Adv Phytochem **8:** 53–79

Sweetlove LJ, Fernie AR (2005) Regulation of metabolic networks: understanding metabolic complexity in the systems biology era. New Phytol **168:** 9–24

Valant-Vetschera KM, Wollenweber E (2001) Exudate flavonoid aglycones in the alpine species of *Achillea* sect. *Ptarmica*: chemosystematics of *A. moschata* and related species (Compositae-*Anthemideae*). Biochem Syst Ecol **29:** 149–159

Weast RC (1982) CRC Handbook of Chemistry and Physics. CRC Press, Boca Raton, FL

Weisshaar B, Jenkins GI (1998) Phenylpropanoid biosynthesis and its regulation. Curr Opin Plant Biol **1:** 251–257

Weisskopf L, Abou-Mansour E, Fromin N, Tomasi N, Santelia D, Edelkott I, Neumann G, Aragno M, Tabacchi R, Martinoia E (2006) White lupin has developed a complex strategy to limit microbial degradation of secreted citrate required for phosphate acquisition. Plant Cell Environ **29:** 919–927

Winkel BS (2004) Metabolic channeling in plants. Annu Rev Plant Biol **55:** 85–107

Winkel-Shirley B (2001) Flavonoid biosynthesis: a colorful model for genetics, biochemistry, cell biology, and biotechnology. Plant Physiol **126:** 485–493

Wollenweber E, Dorr M, Rivera D, Roitman JN (2003) Externally accumulated flavonoids in three Mediterranean *Ononis* species. Z Naturforsch [C] **58:** 771–775

Yazaki K (2005) Transporters of secondary metabolites. Curr Opin Plant Biol **8:** 301–307

Chapter 6

Sorghum bicolor as a model system to study induced synthesis and compartmentation of flavonoids in inclusions

Introduction

1. *Sorghum bicolor*

Sorghum [*Sorghum bicolor* (L.)] is ubiquitously used as a fodder and food crop, as well as in the beverage industry and is a member of the grasses (Poaceae). It is cultivated in tropical and temperate zones where they are naturally exposed to a broad range of pathogens. Sorghum plants are attacked by fungal, bacterial, and viral pathogens causing root, stalk, foliar, panicle, and caryopsis diseases. In Africa, where annual cereal production is around 89 million tones, sorghum is second only to maize in agronomic importance (Chantereau and Nicou, 1994). Sorghum is reported to contain simple phenols, hydroxybenzoic acids, hydroxycinnamic acids (with ferulic acid being the most abundant), anthocyanins, proanthocyanidins (PAs), and several other flavonoids (Awika *et al.*, 2004; Awika and Roony, 2004). The 3-deoxyanthocyanidins (3-DAs), namely, apigeninidins and luteolinidins, are particularly abundant in sorghum grain but rare or absent in other plants (Awika and Roony, 2004; Awika, 2004; Schutt and Netzly, 1991). Agronomic interest exists in sorghum grains containing flavan-4-ols, such as leucoapigeninidin (apiforol) and leucoluteolinidin (luteoforol), because they are known to confer resistance to fungal infections in grain crops (Schutt and Netzly, 1991; Melake-Berhan, 1996). Flavan-4-ols have also been shown to be anticarcinogenic (Ferreira and Slade, 2002). Sorghum phenols protect plants against insects and diseases (Taylor and Dewar, 2001), and they have also been demonstrated to act as antioxidants *in vitro* (Awika, 2004; Palé *et al.*, 1997; Dicko *et al.*, 2005).

Flavonoids are present at high levels in most plant seeds and grains. These compounds appear to play vital roles in defense against pathogens and foragers and contribute to physiological functions such as seed maturation and dormancy (Debeaujon *et al*., 2000). At the same time, particular subclasses of flavonoids, such as the proanthocyanidins (PAs, condensed tannins), negatively impact the use of seeds and grains in animal feed and can add undesirable qualities to food products for human consumption. Today, antioxidant phenolic compounds are generally regarded as desirable components of human food and they are considered to be of nutraceutical importance (Awika and Roony, 2004; Parr and Bolwell, 2000; Santos-Buelga and Scalbert, 2000). All phenolic compounds are able to scavenge free radicals due to their oxidizing properties (Parr and Bolwell, 2000). Some phenolic compounds have been linked to the

prevention of neurological disorders and cardio diseases based on their potent free-radical scavenging activities (Lu and Foo, 2001; Pellegrini *et al.*, 2003). Other roles of antioxidants include antifungal, antibacterial, and antiviral effects (Schutt and Netzly, 1991). Because sorghum is a source of phenols that have varying antioxidant potential, it is necessary to isolate and characterize these phenolic compounds. The antioxidant activity potential increases in sorghum due to the presence of tannins and depends on the number of conjugated unsaturated bonds (Rice-Evans, 1999; Bors *et al.*, 2001).

3. Sorghum flavonoids play roles in abiotic and biotic stress response

Plants synthesize a variety of secondary metabolites in response to a wide range of external stimuli. In some cultivars of sorghum, anthocyanin pigments (mainly cyanidin 3-dimalonyl glucoside) are produced naturally in response to light (Orczyk *et al.*, 1996; Weiergang *et al.*, 1996; Lo and Nicholson, 1998). Anthocyanins constitute a large class of flavonoid compounds and are one of the most important and widespread groups of plant pigments. They serve to attract animals for pollination and seed dispersal and are also believed to be important as protectants against UV irradiation and pathogen infections (Lo and Nicholson, 1998).

In response to infection by both pathogenic and nonpathogenic fungi (*Bipolaris maydis, Cochliobolus heterostrophus*, respectively*)*, sorghum synthesizes a complex mixture of 3-deoxyanthocyanidin phytoalexins (Aida *et al.*, 1996). The major components of this mixture of flavonoids are a group of structurally related compounds, the 3-deoxyanthocyanidins, apigeninidin, luteolinidin, luteolinidin 5-methylether, apigeninidin 7-methylether and the caffeic acid ester of arabinosyl 5-O-apigeninidin (Figure 1).

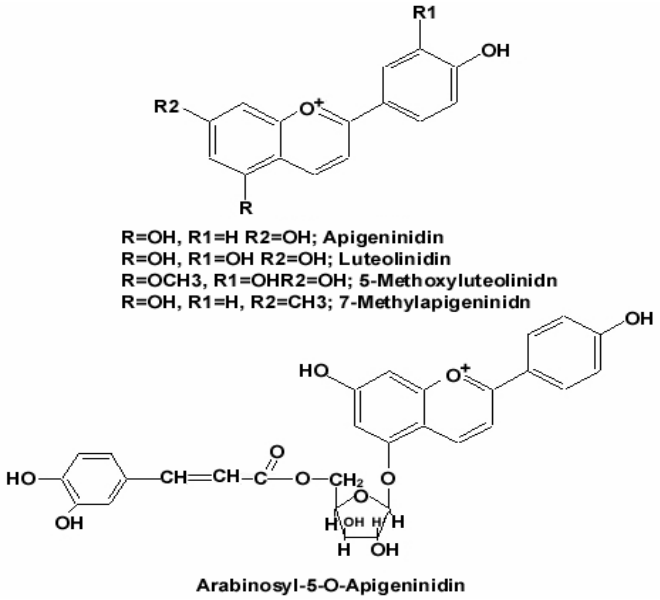

Figure 1. Chemical structures of the flavonoids present in sorghum leaves after fungal infection (modified from Lo and Nicholson, 1998)

Phytoalexins are low-molecular-weight antimicrobial compounds produced by plants in response to infection or stress (Van Etten *et al.*, 1994). In sorghum leaf tissue, these phytoalexins first appear in the cells which are being infected, accumulating in cytoplasmic inclusions (Snyder and Nicholson, 1990; Snyder, 1991; Wharton and Nicholson, 2000). These inclusions migrate to the site of infection, where they become pigmented, indicating the presence of the phytoalexins, lose their spherical shape and ultimately release their contents into the cytoplasm, killing the cell and restricting further development of the pathogen. Thus accumulation is a site-specific response localized to the cells representing the site of pathogen infection (Nicholson, 1987, 1988; Snyder and Nicholson, 1990).

The biosynthesis of anthocyanidins and 3-deoxyanthocyanidins represents two partially overlapping, competing pathways in sorghum. Both compounds are derived from the phenylpropanoid and flavonoid pathways. Activities of the key phenylpropanoid branch-point enzymes Phenylalanine ammonia-lyase (PAL) and chalcone synthase (CHS), and expression of their respective genes, are induced by light and by fungal infection (Lue *et al.*, 1989; Orczyk *et al.*, 1996). The compounds originate from the condensation of *p*-coumaroyl-CoA and malonyl-CoA to form naringenin chalcone, which is converted to the flavanone naringenin. In turn, naringenin is used for the synthesis of the anthocyanidins and the 3-deoxyanthocyanidins (Dixon and Paiva, 1995; Hipskind 1996b; Lo and Nicholson, 1998, and Figure 2). The repression of light-induced expression of anthocyanin genes by fungal inoculation supports the hypothesis that synthesis of 3-deoxyanthocyanidin phytoalexins does not occur via the same pathway as synthesis of 3-hydroxylated anthocyanidins and/or is differentially regulated (Hipskind *et al.*, 1996b). The accumulation is likely to proceed through *de novo* synthesis, and the 3-deoxyanthocyanidin precursor compounds are likely to be present at extremely low concentrations or to have a rapid turnover.

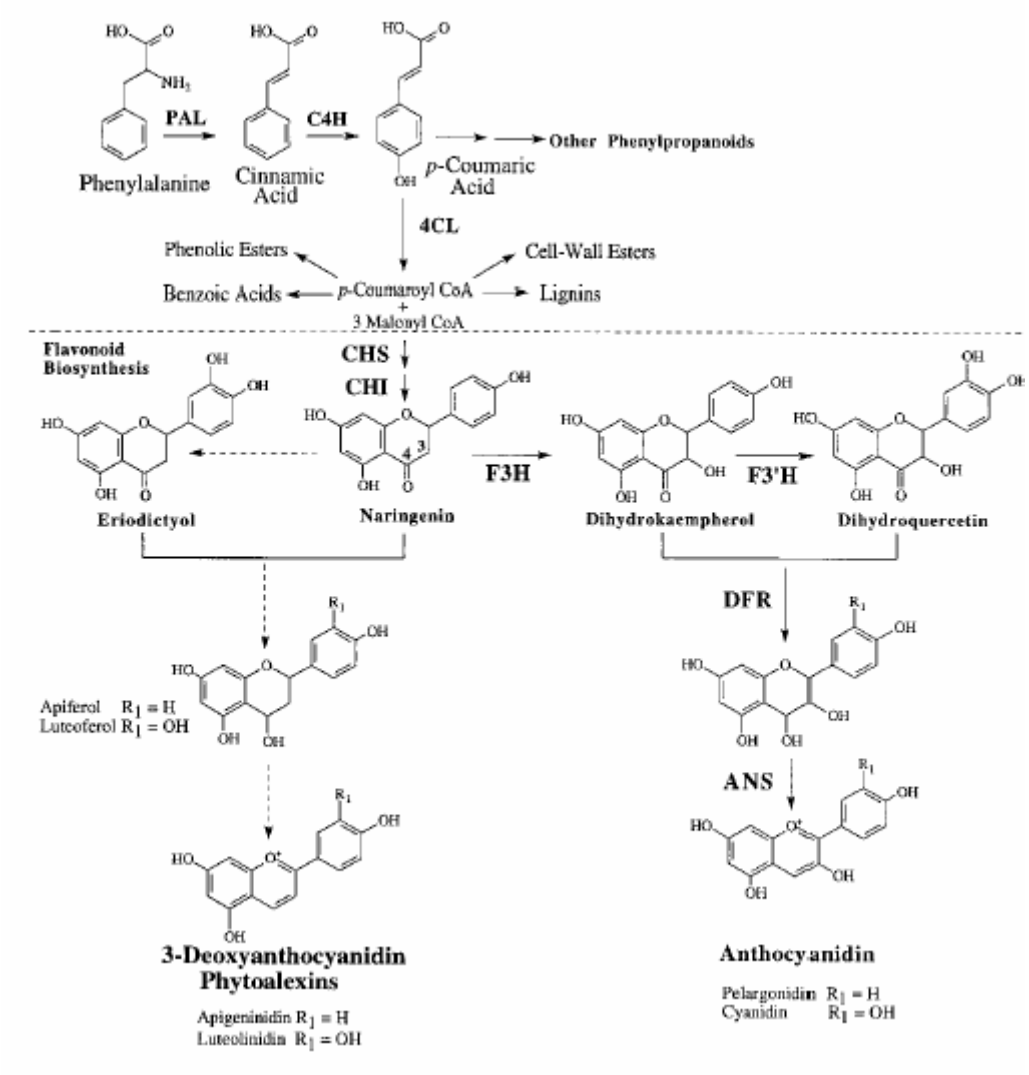

Figure 2. Biosynthetic pathways for 3-deoxyanthocyanidins and anthocyanidins. The proposed pathway of 3-deoxyanthocyanidin synthesis originates with the first committed step in phenylpropanoid biosynthesis. Phenylalanine is deaminated by PAL to form cinnamic acid, which is hydroxylated by C4H to form p-coumaric acid. Subsequently, p-coumaric acid is activated to a high-energy CoA thiol-ester by 4CL, which then serves as one of two substrates for flavonoid biosynthesis mediated by CHS. The routes for biosynthesis of normal anthocyanidins and 3-deoxyanthocyanidins are proposed to diverge after the synthesis of the flavanone naringenin. C4H, Cinnamic acid 4-hydroxylase; 4CL, 4-hydroxycinnamic acid:CoA ligase; CHI, chalcone isomerase; F3'H, flavonoid 3'-hydroxylase. Solid arrows indicate established pathways; dashed arrows indicate proposed metabolic steps in 3-deoxyanthocyanidin synthesis (Lo and Nicholson, 1998).

Plants have a wide array of physical and chemical strategies to defend themselves from infection by pathogens. Physical barriers such as the mechanical strength of the cuticle and epidermal wall and the resistance of their structural polymers to enzymatic degradation represent the first lines of defense. However, the active biochemical defense strategies are considered to be more important as these often determine the success of an infection. In sorghum, resistance is proposed to be correlated to the more complex phytoalexin compounds, in particular luteolinidin and luteolinidin 5-methylether, which appear to be synthesized only in incompatible interactions (Aida *et al.*, 1996; Wharton and Nicholson, 2000).

Phytoalexins represent one of the most classical of all defense responses, and one of the most intriguing examples of phytoalexin production comes from sorghum-fungal interactions. Snyder and Nicholson (1990) reported a localized accumulation of deoxyanthocyanidin phytoalexins in sorghum in response to *Colletotrichum graminicola*. Inoculation with the nonpathogenic fungus *Cochliobolus heterostrophus* drastically reduces the light-induced accumulation of anthocyanin by repressing the transcription of the anthocyanin biosynthesis genes encoding flavanone 3-hydroxylase, dihydroflavonol 4-reductase, and anthocyanidin synthase. In contrast to these repression effects, fungal inoculation results in the synthesis of the 4 known 3-deoxyanthocyanidin phytoalexins and a corresponding activation of genes encoding the key branch-point enzymes in the phenylpropanoid pathway, PAL and CHS. In this interaction, the phytoalexins (which are pigmented), were shown to migrate in inclusions toward the point of penetration by the fungus. Taking advantage of the pigmentation and via microspectrophotometry, Snyder *et al.* (1991) were later able to show that the concentration of the phytoalexins in the invaded cell was more than sufficient to inhibit the pathogen based on *in vitro* activity. However, these studies did not provide the nature of the inclusion, why the inclusion changed color as they migrated, and why the deoxyanthocynaidins were antifungal. Based on *in vitro* analysis Nielsen *et al.* (2000) showed that the inclusions form as a result of self-stacking of the phytoalexins and is conditioned by protons and acetate ions. Nielsen *et al.* also report that the color changes of the inclusions in the host cell appears to be due to changes in pH and not the conversion of colorless intermediates into the pigmented phytoalexins. The authors also present an interesting model of how cytoplasmic flow, cellular pH and nuclear migration help to coordinate the trafficking and delivery of the phytoalexins to the site of fungal infection. A possible mode of action of the deoxyanthocyanidin phytoalexins was presented by demonstrating that luteolindin, which was found in the form of an inclusion disrupts fungal and the plant plasma membranes. Taken together, these results clearly argue against the earlier hypothesis, that the pigmented inclusions are membrane bound structures.

Resistance (R) genes present in the host plant may be activated upon infection by pathogenic fungi, leading via signal transduction pathways to defense responses, such as the production of phytoalexins and antifungal proteins. A common feature of a host resistance

reaction expressed in response to infection is the rapid localized cell death and browning of host cells, known as a hypersensitive reaction (HR) (Bailey, 1982). In many resistant cultivars, single epidermal cells die as soon as they are in contact with the pathogen. This type of resistance, which depends on the localised accumulation of phytoalexins, has been referred as an example of HR based on host cell incompatibility (Bailey, 1983). The extent of symptom and pathogen development appears to depend on the time at which the infected cells die, turn brown and accumulate phytoalexins (O'Connell and Bailey, 1986). However, a critical investigation of the HR by Bailey *et al.* (1980) indicated that early death of infected cells occurred before phytoalexin formation.

The metabolic shift from the light-induced accumulation of anthocyanin pigments to the pathogen stimulated synthesis of 3-deoxyanthocyanidin phytoalexins in sorghum also represents a model to study the metabolic regulation in response to light and pathogen attack. The results obtained to date suggest that the plant represses less essential metabolic activities such as anthocyanin synthesis as a means of compensating for the immediate biochemical and physiological needs for the defense response (Lo and Nicholson, 1998). When exposed to an inducer, sorghum arrests the synthesis of anthocyanin pigments, in favor of 3-deoxyanthocyanidin phytoalexin synthesis (Lo and Nicholson, 1998). An understanding of the regulation in the diversion of metabolism leading to resistance would provide insights for the development of innovative strategies to enhance disease resistance in sorghum and related crop species. The content of 3-DAs is a good visible marker for sorghum resistance to both biotic and abiotic stresses because it correlates with resistance to all stresses except for photoperiod sensitivity. A second marker for stress resistance is the content of PAs.

The aims of this study were (i) to use the sorghum primary leaf as a model to study and analyze the second proposed model for trafficking of molecules into the cells – via vesicles, (ii) to establish a system replacing the fungus with an elicitor in order to provide a tool for studying the synthesis and accumulation of secondary compounds under stress, and (iii) to analyze and identify the mixture of compounds synthesized after this elicitor treatment.

Materials and Methods

1. Plant material and chemicals

Sorghum bicolor (ID 1272) plants were grown in soil in a controlled environment chamber [8h light (90 µmol m^{-2} s^{-1}), 22°C, 16h dark, 60% relative humidity] for 10 days, prior to being harvested for the experiments outlined below.

Table.1 Chemicals used in this work

Compound	Supplier	Solvent
Xylanase*	Fluka,CH	water
Cellulase YC	Kyowa Chemical product CO	water
Wortmannin	Agros organics, Belgium	DMSO
Cycloheximid	Fluka,CH	DMSO
Brefeldin A	Fluka,CH	methanol
Monensin	Fluka,CH	methanol
FM4-64•	Molecular probes, USA	DMSO
Lyso Tracker Red DND-99	Molecular probes, USA	DMSO
Monochlorobimane	Invitrogen, CH	DMSO
Apigeninidin	Extrasynthese, France	methanol
Luteolinidin	Extrasynthese, France	methanol

*Xylanase (EC 3.2.1.8) or endo-1,4-β-xylanase from *Trichoderma viride*

•FM4-64 ((N-[3-triethylammoniumpropyl]- 4-[p-diethylaminophenylhexatrienyl] pyridinium dibromide)

DMSO – dimethyl sulfoxide

2. Elicitation treatments, mechanical damage and microscopic observations

Primary leaves were collected on wet filter paper. Drops of 0.1µl of elicitation solution A (1% (w/v) xylanase, 0.1% (v/v) Triton) or B (1% (w/v) cellulase, 0.1% (v/v) Triton) were applied on the adaxial epidermis of the leaf with a glass syringe. Elicitation of a response to these treatments was gauged by the development of red spots at the point of application of the respective elicitor solution. Images of whole leaves were captured every 24h after applying the elicitors using a Nikon SMZ1500 binocular microscope coupled to a Nikon Coolpix camera. Microscopic observation of the treated areas was conducted using a Leica DMR microscope equipped with a Leica DC300F charge coupled device camera and controlled by Leica IM1000 software (Leica, Switzerland).

The light time-lapse microscopy was performed in EMZ (Laboratory of electron microscopy at the University of Zurich) using a Leica DMIRBE microscope coupled to a QImaging Glabler camera and controlled by Openlab software (Leica, Switzerland). Time-lapse DIC images were taken every ten seconds. The time-lapse series were converted into a movie at one frame per second. The movie can be visualized using either QuickTime player or Windows Media Player.

In order to investigate if mechanical damage of the leaves led to accumulation of the red compounds leaf segments were excised and placed on wet filter paper for 2 days or unexcised primary leaves were pricked with a needle.

3. High Performance Liquid Chromatography (HPLC) analysis

25 red areas which correspond to the spots after elicitor application were cut out of the leaves, ground and the compounds were extracted with 1ml extraction buffer (80% (v/v) MeOH/0.01% (v/v) HCl). For the analysis 3 replicates were performed. Compounds were separated on a CC 250/4 Nucleosil 100-5 C18HD column (Macherey–Nagel, Oensingen, Switzerland) with (A) water/acetic acid/ MeOH 71:10:9 and (B) MeOH/ acetic acid 9:1 at a total flow rate of 0.8 ml/min using a linear gradient 0% A / 100% B to 100% A / 0% B over 33 minutes. The chromatograms were analysed using a Gynkotek liquid chromatograph equipped with a UVD340S diode array detector (Dionex, Switzerland) whose detection was set to 405 and 420nm.

Two flavonoids were used as standards – luteolinidin and apigeninidin. Both were resuspended in 80% (v/v) MeOH/0.01% (v/v) HCl at a concentration of 5 mg/ml. Absorption spectra of dilutions of both standards were obtained with a Beckman Coulter DU 800 spectrophotometer (Beckman, Switzerland). In order to confirm the correct concentrations in the dilutions of the standards, the concentrations were recalculated based on their extinction at λ 405nm and using the extinction coefficient ($\varepsilon_{apigeninidin,\ 480nm}$ = 18 000 M^{-1} cm^{-1}, $\varepsilon_{luteolinidin,\ 495nm}$ = 13 800 M^{-1} cm^{-1} (Lo and Nicholson, 1998). Finally, to obtain a standard curve relating peak areas resulting from HPLC analysis to molar amount of standards, the dilutions were analysed by HPLC using the above mention analytical conditions.

4. Inhibitor assays

In a pharmacological approach, a number of inhibitors (cycloheximide, brefeldin A, monensin, wortmannin) were applied in droplets (as described in point 2) alone or together with the elicitor solution on the leaf surface for 48h, followed by the extraction procedure and HPLC analysis mentioned above. Images of the leaf segments were captured using a Nikon SMZ1500 binocular microscope coupled to a Nikon Coolpix camera.

Table.2 Inhibitors, and their concentration, used in combination with the elicitor.

Inhibitor + 1%xylanase (w/v)	Final amount in the droplets
cycloheximide	0.35nmol, 3,5nmol, 30nmol
brefeldin A	0.35nmol, 3.5nmol, 30nmol
monensin	0.1nmol, 1nmol, 10nmol
wortmannin	1nmol, 10nmol, 50nmol

5. Loading with fluorescent dyes

To obtain information about the nature of the red inclusions observed after the treatment with the elicitor, leaves were loaded, under vacuum for 10 min, 30 min, or without applying vacuum for 1h or 24h with fluorescent dyes as FM4-64 (8µM or 15µM), monochlorobimane (MClB; 10mM MES KOH, 1mM $CaCl_2$, pH 5.8) and Lyso Tracker Red (50nM, MES KOH, pH 6, or HEPES- Na, pH 7.5) respectively.

Results and discussion

It has been shown previously that young sorghum leaves accumulate a complex of phenolic compounds (Figure 1) in response to invasion by both pathogenic and non-pathogenic fungi and by light.

In leaf tissue, these phenolics first appear in the invaded cell, accumulating in inclusions in the cytoplasm (Snyder and Nicholson, 1990). These cytoplasmic inclusions migrate to the site of penetration, become pigmented, lose their spherical shape and ultimately release their contents into the cytosol, which then kill the cell and restrict further pathogen development. The fungi/sorghum pathosystem has been used as a model system to analyze phytoalexin mechanisms. Together with our new model system plant/elicitor it is an ideal system for this as most phytoalexins produced in sorghum are orange-red pigmented flavonoids which allow following easily their accumulation and distribution in plant tissue using light microscopy (Figure 3).

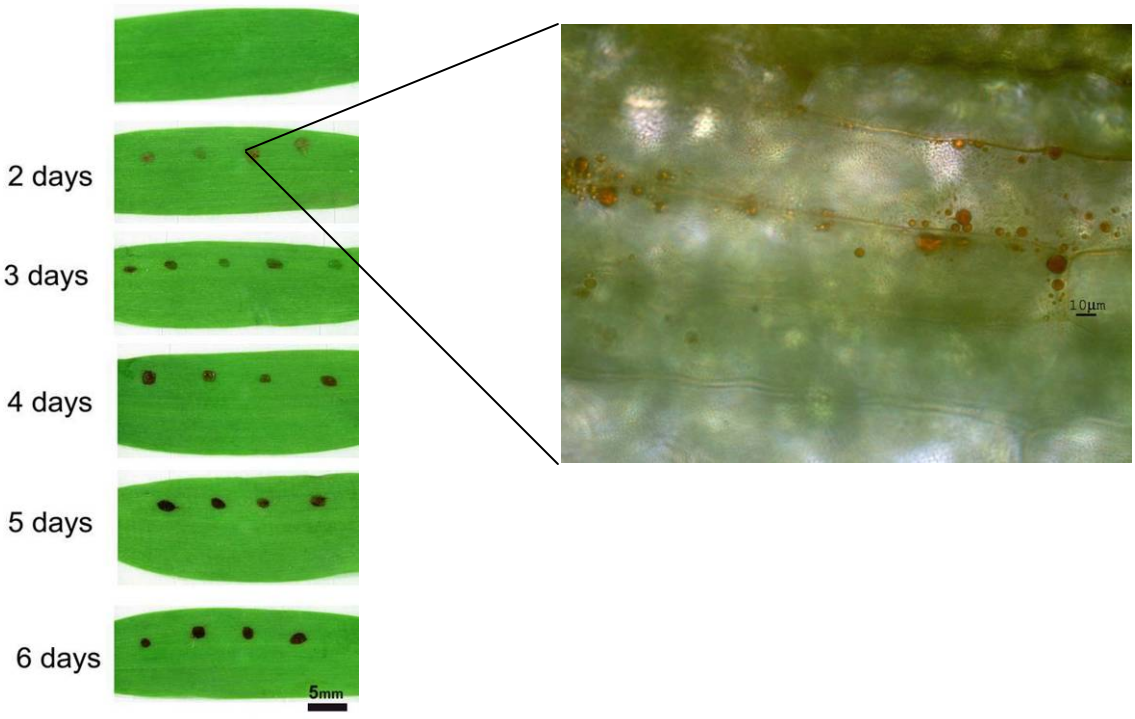

Figure 3. Surface view and microscopic observation of a sorghum leaf treated with xylanase. Time- dependent accumulation of red compounds in the places where the elicitor

drops were applied (left panel, bar=5nm) and microscopic close view into one of the red area (right panel, bar=10µm).

Here we demonstrate that treatment of sorghum primary leaves with an unspecific elicitor xylanase or cellulase led to a response which is comparable to the fungal invasion by *Colletotrichum graminicola* or *Cochliobolus heterostrophus*. Cells affected by the elicitor first accumulate colorless inclusions in the cytoplasm (Figure 4A, black arrows). After 36 hours post-inoculation, the inclusions increase in size and become orange pigmented (4B). Afterwards, the inclusions change color and appeared reddish whilst they start to accumulate in higher concentrations in the areas of xylanase application. After 48 hours the inclusions have started to coalesce and were intensely red pigmented (4C). In addition the inclusions start to release their contents into the cell and pigmented inclusions are starting to accumulate in surrounding cells (4D). After 54 hours post-inoculation, the inclusions in the surrounding cells have released their contents into the cells and the *apoplast* and the area is intensely red stained (4E). Rapid accumulation of the compounds is detected in stomatal cells (4F).

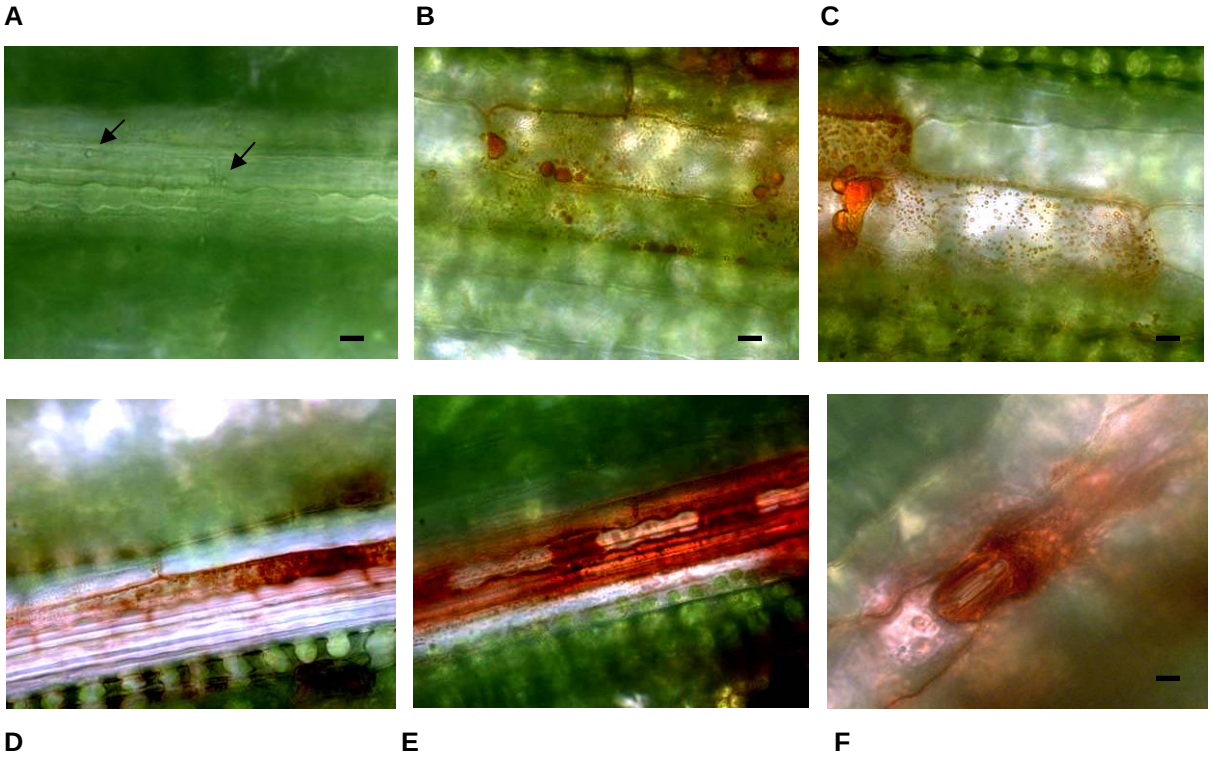

Figure 4. Bright-field microscopy of the red areas on the surface of the leaf after the treatment with xylanase. Depicted are representative pictures captured after 24 (A), 36 (B), 48

(C) and 54h (D) after addition of xylanase. Arrows in (A) highlight small, unstained vesicular structures, appearing before they turn red in the course of 3-DA biosynthesis. (F) Stomata are preferentially filled up with red inclusions after 36 h. Bar = 10µm.

Previous studies demonstrated that anthocyanins accumulated and were stored in inclusions that, when observed microscopically (see Figure 4), appeared round and regular in shape (Markham *et al.*, 2000). They started as vesicles in the cytoplasm and were defined in the past as membrane bound structures that occur in the leaves of various Brassicaceae (Pecket and Small, 1980, Nozzolillo and Ishikura, 1988). More recently, the intravacuolar structures observed in the flower petals of various plants, including carnation (*Dianthus caryophyllus*) and lisianthus (*Eustoma grandiflorum*) were termed anthocyanic vacuolar inclusions, or AVIs (Markham *et al.*, 2000). These inclusions were suggested to be membrane-less, proteinaceous matrixes that acted as anthocyanin traps, preferentially for anthocyanidin 3, 5-diglycosides (Markham *et al.*, 2000) or acylated anthocyanins (Conn *et al.*, 2003). Thus, in these examples the anthocyanins do not fill the entire cell, but they appear in high concentration in discrete spots.

The next step of our work was to analyze the composition of the mixture of phytoalexins which accumulate in the red inclusions emerging after application of the elicitor on the surface of the leaves (Figure 4). Samples were taken 2, 4, 6 and 8 days post inoculation and were extracted as described in material and methods. In the extract of untreated leaves no flavonoids were detected at wavelengths of 450 and 520nm, indicating absence of 3-DAF type substances. After 2 days of treatment we detected a major peak with retention time of 11.2 min. We were able to identify this peak as apigeninidin (peak 1) based on coelution with a commercially purchased apigeninidin standard and the identity of the absorption maxima (Figure 5F). We observed a positive correlation between apigeninidin accumulation and days after inoculation (Figure 6). Furthermore, after 4 days, a second peak with retention time 13.07 min appeared and also increased to concentrations similar to that of apigeninidin after 8 days. This substance possessed an absorption spectrum very similar to apigeninidin with an absorption maximum of 473.6 at 405 nm (Figure 5C). It did not correspond to luteolinidin which elutes after 10.8 min (see Figure 8, peak A). As a result we suggested that peak 2 corresponds to an apigeninidin-derivative. Finally, after 8 days a third peak with retention time 15.8 min appeared. Based on its absorption spectrum with maximum 372.0 at 405 nm we suspect that this substance could be a UV-absorbing flavonol or flavone.

A

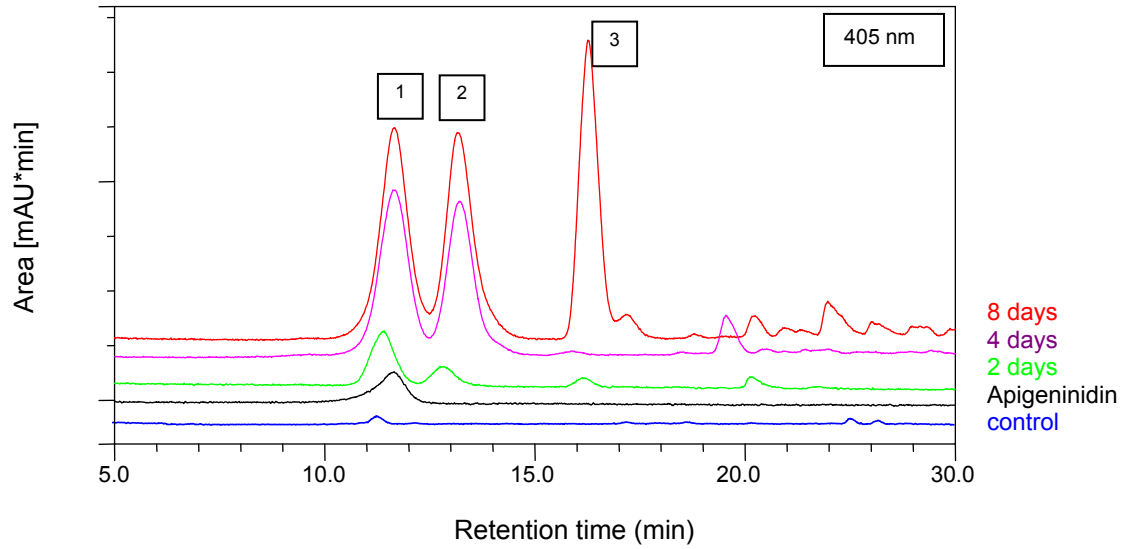

B – Absorption spectrum of peak 1 with retention time 11.2 min

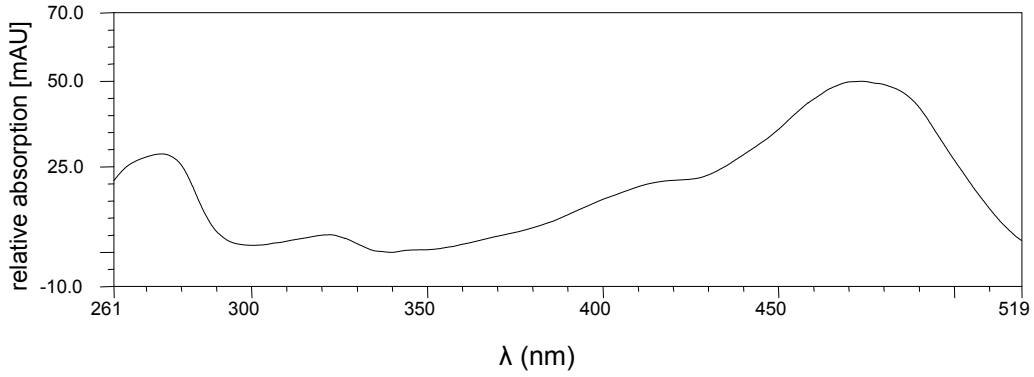

C – Absorption spectrums of peak 2 with retention time 13.07 min

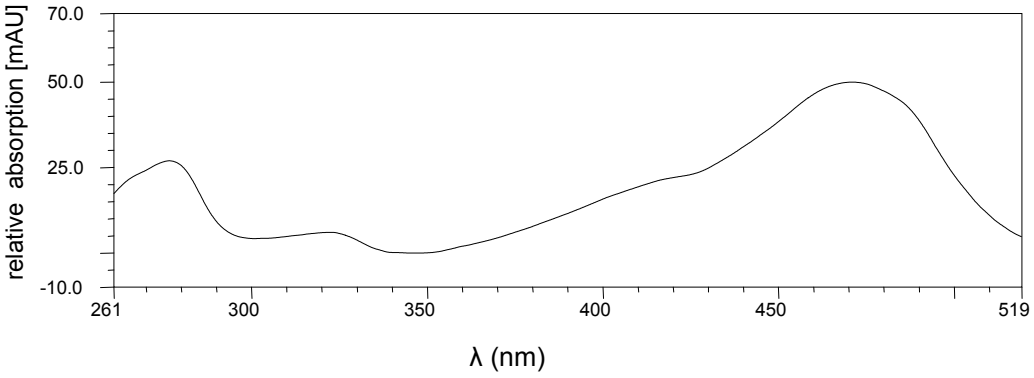

D – Absorption spectrums of peak 3 with retention time 15.79 min

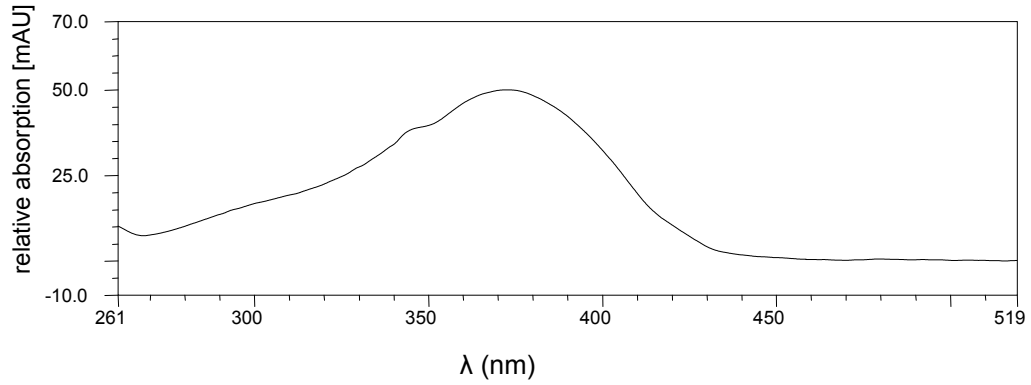

E – Absorption spectrums of the standard luteolinidin

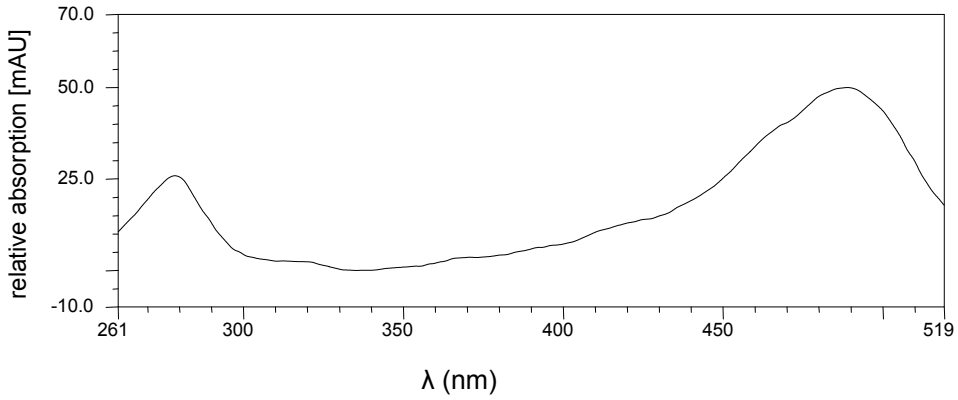

F – Absorption spectrums of the standard apiginindin

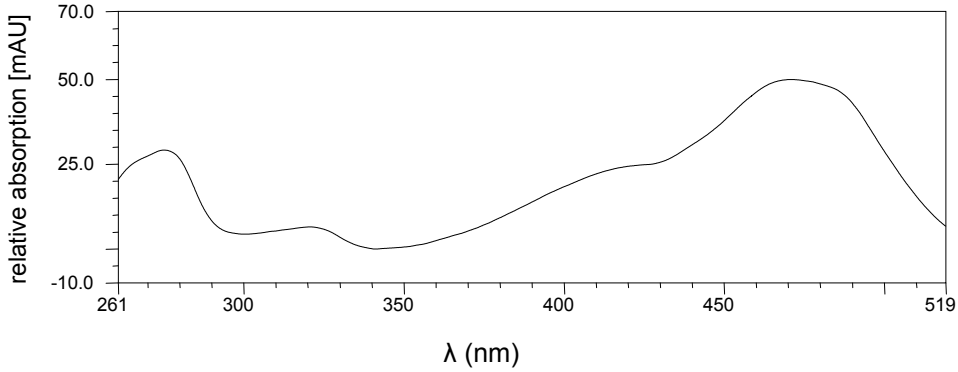

Figure 5. HPLC profiles (A) of the control extract (blue line) and treated leaves extracts after 2 (green line), 4 (rose line), 8 days (red line) after elicitation, standard – apigenindin (black line) and absorption spectra of the detected compounds (B – F).

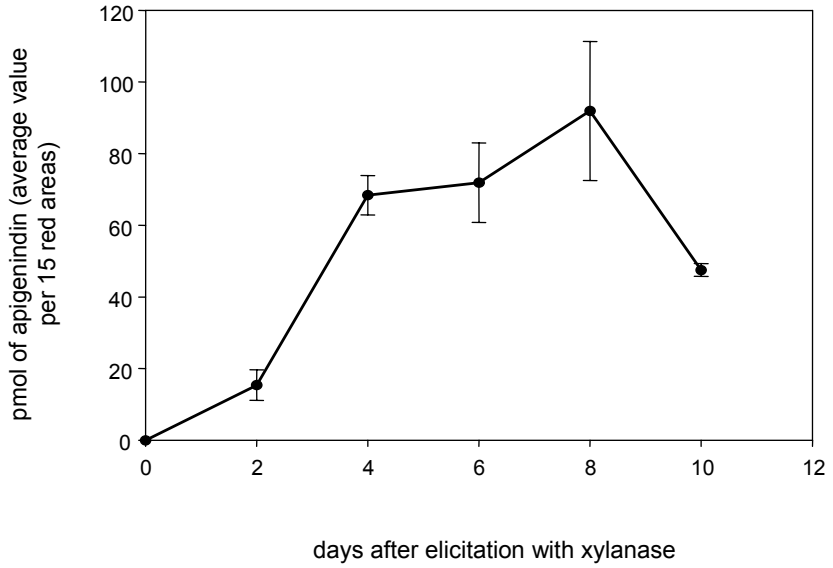

Figure 6. Time-dependent accumulation and quantification of apigeninidin (peak 1 in figure 5) in primary leaves of Sorghum treated with xylanase. The experiment was performed with 3 replicates each containing 15 red areas, which appeared after elicitation.

Our analysis shows that apigeninidin accumulates in a time dependent manner with the highest concentration observed after 8 days of elicitation (Figure 6). After this period the cells are collapsing which is obviously associated with a decrease in the amount of the compounds. Figure 6 also supports our microscopy observations that after 2 days there is an increase in the number of vesicles corresponding to the increased amount of apigeninidin in the first 2 days in contrast to 6-8 days when the pigmented compounds are released in the *apoplast*.

Using xylanase as an unspecific elicitor we observed similar structures as described by Snyder and Nicholson (1991) for the Sorghum – *Colletotrichum* interaction. However, in our case, luteolinidin is not produced in xylanase-treated Sorghum leaves suggesting metabolic differences between our elicitor and their fungal infection treatments. This suggests that the specificity of the flavonoid production in response to biotic stress in Sorghum might go beyond the published differences in anthocyanins and 3-DAF production. Probably, different signals produced either by elicitor treatment or fungus can results in remarkably different pattern of 3-DAF. This results is confirmed by analysis of flavonoid pattern present after mechanical stress (see bellow).

Evidence for structurally comparable flavonoid-filled cellular inclusions were also obtained by Markham *et al.* (2000) in *lisianthus* flower petals and by Irani and Grotewold (2005) who studied anthocyanin-filled ‘vacuoles’ in maize cells. In contrast to Markham *et al*., (2000) the anthocyanin-filled structures in maize were interpreted as membrane-surrounded compartments.

In order to gain further information on the nature of the red inclusions observed after xylanase-treatment of Sorghum leaves, we performed a time-lapse video analysis of elicited leaves focusing on cells producing the colored compounds. 24 hours post-inoculation we observed many small red 'vesicles' which were actively moving in the cytosol (Figure 7). The fraction of moving red structures (black arrows) was clearly distinguished from other droplets (blue arrows) that remained spatially static over time. After 48h and 56h of elicitation treatment we noticed that the pigments fill the entire cell and are also released on the cell surface (watch the attached CD-ROM covering 3 h of the observation under file names s1, s2). However because of technical reasons we were not able to follow the process within the cells at the moment of appearance of the red 'vesicle' after the treatment with the elicitor in order to describe the process fully.

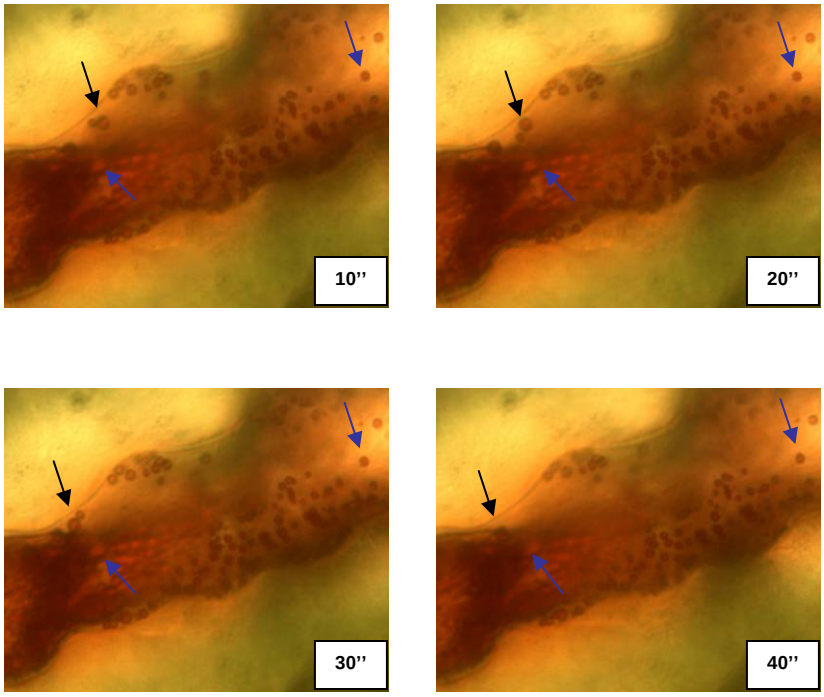

Figure 7. Time-lapse pictures taken every 10 sec at the site of xylanase application. Pictures were recorded 48h after xylanase treatment. Time is indicated in the right bottom of each picture. The black arrows indicate the movement of one 'vesicle' in contrast to the static vesicles marked with blue arrows.

Taken together, it can be speculated that the moving inclusions are still within the epidermal cell, while the subcellular localization of the static red structures could be either within or on the cell surface.

We decided to investigate if mechanical damage of leaves leads to accumulation of red compounds and whether their composition is different to that observed during elicitor treatment. Accumulation of red pigments was detected after cutting the leaves (Figure 8b), but red inclusions appeared later, after 3 days, when compared to xylanase treatment. It is not clear which type of mechanical damage caused this effect given that the response was not detected after pricking the leaves with a needle (data not shown). The composition of the *de novo* synthesized compounds showed differences as compared to the elicitation treatment. Due to the standards used during the analysis we identified two of the compounds in the mixture: 1) peak A with retention time 10.8 min and with maximum 487.6 at 405 nm which correspond to the absorption maxima of the standard luteolinidin (Figure 5E), and 2) peak 1 with retention time 11.3 min and maxima 469.2, which is identical to the absorption spectrum of the standard apigeninidin (Figure 5F).

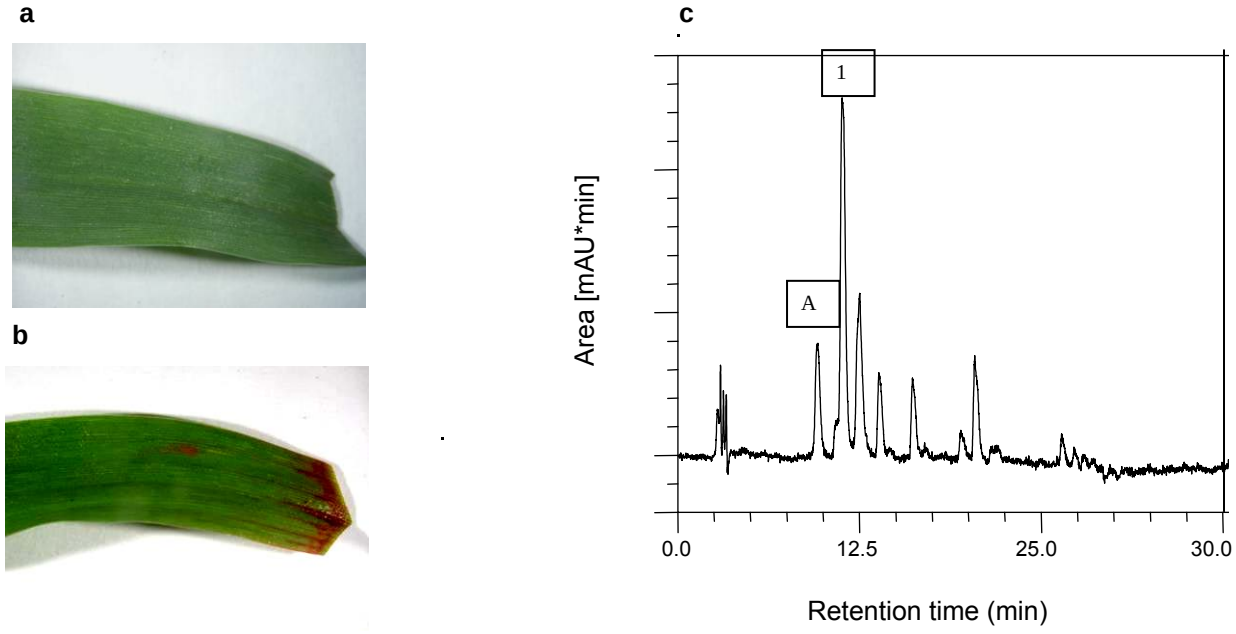

d – Absorption spectrums of peak A with retention time 10.8 min

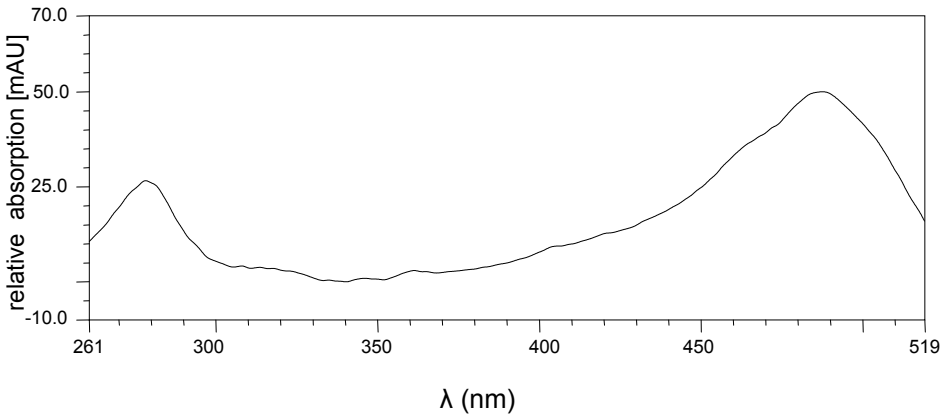

e – Absorption spectrums of peak 1 with retention time 11.3 min

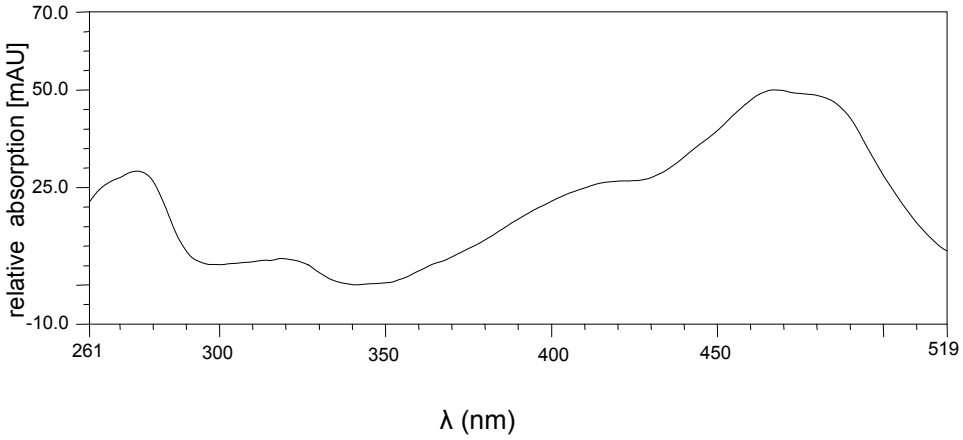

Figure 8. Effect of the mechanical damage of leaves on the accumulation of red pigments. Leaf after excision (a) and after 3 days incubation on wet filter paper (b), HPLC profile after extraction (c) and absorption spectra of the peaks (d and e)

In an attempt to define the nature of the red inclusions produced by xylanase treatment we used fluorescent dyes known to differentially label various cell compartments.

We used the styryl dye FM4-64 known from studies of vesicle trafficking (endocytic tracer, Samaj *et al.*, 2005) and membrane dynamics. When added to plant cells FM4-64 immediately stains the plasma membrane. After 5 to 10 min intracellular vesicles interpreted as endosomes are labelled, and finally FM4-64 accumulates in the tonoplast. Monochlorobimane (Invitrogen) is a nonfluorescent compound which is conjugated in the cytosol to reduced glutathione by cytosolic glutation-S-transferases and the resulting fluorescent bimane-glutathione is transported into the central vacuole via MRP-type ABC transporters (Li *et al.*, 1996). We obtained another fluorescent dye - Lyso Tracker Red DND-99 (Invitrogen) used for labeling and tracking of acidic organelles in living cells. This dye has been used to investigate the acidification of lysosomes and alterations of lysosomal trafficking in cells following diffusion across the plasmalemma.

Unfortunately we were unable to monitor any co-staining between these dyes and the inclusions. We had problems loading the dyes into the Sorghum leaf tissue before and after elicitation treatment. Even prolonged exposure to vacuum did not help to achieve access of these dyes into phytoalexin-producing cells.

Therefore, in order to evaluate the hypothesis that the appearance of the moving red inclusions is associated with vesicular movement in the phytoalexin-producing cells, we performed assays with inhibitors which are known to affect vesicle trafficking in plant cells.

Cycloheximide inhibits the cytoplasmic ribosomal protein synthesis and in our case inhibited completely the synthesis of 3-DAF-like compounds (Figure 9A and E). The inhibition of

the synthesis is complete after applying the highest amount of inhibitor (5nmol) suggesting that phytoalexin production is dependent on *de novo* protein synthesis. Cycloheximide also affects the whole leaf since serious sign of desiccation were visible.

Brefeldin A is a compound used to demonstrate constitutive cycling of plant proteins between the plasma membrane and endosomal compartment (Geldner *et al.*, 2001). It is a fungal toxin commonly used as a vesicle trafficking inhibitor (Robineau *et al.*, 2000; Nebenfuhr *et al.*, 2002). It also disturbs the endomembrane trafficking between Golgi and endoplasmic reticulum. After application of droplets of highly concentrated brefeldin A (35nM) and xylanase on the leaf we noticed that the synthesis of the flavonoids is reduced in the areas of treatment (Figure 9B). The synthesis of the red compounds was restricted to the surrounding zones of application, while the center did not contain them, appearing like a region of cell death. We can just assume that the synthesis of the red compounds in other regions occurred due to the fact that the brefeldin concentration was reduced when diffused out of the center where the defense response and accumulation was still active. The HPLC analysis (Figure 9A d) showed gradual decrease of apigeninidin and at the highest concentration of the inhibitor the apigeninidin was 60% less as compared to the control.

A similar effect of inhibition was observed after using monensin (Figure 9B). Monensin is a monovalent cation ionophore that excanges Na^+, K^+ and protons across membranes and thereby affects the acidification of acidic compartments (Pressman and Fahim, 1982). Furthermore, it drastically inhibits Golgi function. Red compounds appeared only in the surrounding zones of application. With respect to apigeninidin, monensin reduces its accumulation drastically, up to 20% of the value of the control.

Wortmannin causes a swelling of the prevacuolar compartments (PVC, Tse *et al.*, 2004) and blocks the vacuolar protein transport (Matsuoka *et al.*, 1995). Wortmannin treatment interferes with protein sorting to the lytic vacuole. In our case we did not obtained an inhibition of the synthesis of flavonoids in the treated areas (Figure 9D a). We assumed that the wortmannin did not block 3-DAF synthesis if applied in droplets together with the xylanase. Nevertheless, wortmannin caused a high accumulation of red pigmentation in leaf parts which were not directly treated (Figure 9D a), which could explain the high accumulation of the apigeninidin after the extraction and HPLC analysis in the presence of the inhibitor (Figure 9D b). Thus, wortmannin in combination with an elicitor can increase the production of 3-DAF-type compounds in an unknown manner.

A

a

b

c

d

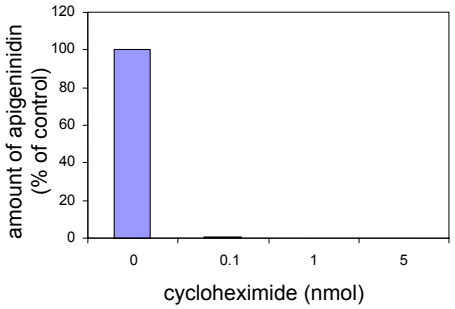

B

a

b

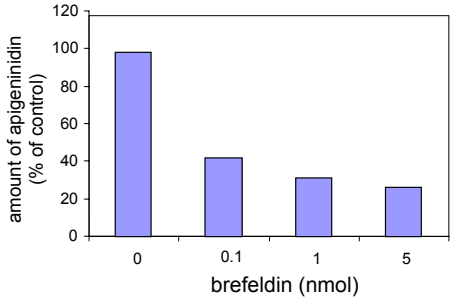

C

a

b

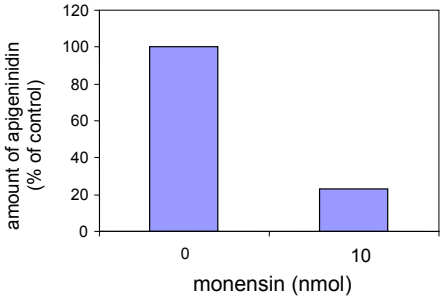

D

a

b

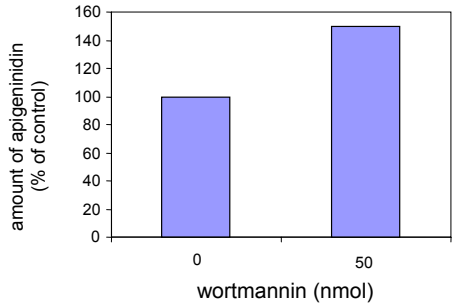

Figure 9. Effect of inhibitor application on the synthesis of apigeninidin.

To: A a, b, c, B a, C a and D a: surface view of leaves after application of droplets containing cycloheximide together with xylanase (A), brefeldin A together with xylanase (B), monensin together with xylanase (C) and wortmannin together with xylanase (D).

To: A d, B b , C b and D b: amount of apigeninidin expressed as % of that of the control detected after HPLC analysis. Values were registered 2 days after inhibitor application. Amounts of inhibitors applied onto leaves are indicated on the x axis of the graphs.

The interpretation of pure pharmacological data is hazardous in the absence of clear cell-biological effects. However, considering the targets of the brefeldin A, monensin, and wortmannin in plant cell vesicle trafficking it may be concluded that the ER to Golgi trafficking and the function of the Golgi apparatus are essential for xylanase induced 3-DAF biosynthesis. Since brefeldin A and monensin inhibited late vacuolar trafficking, wortmannin did not inhibit 3-DAF production.Thus, it can be speculated that the vacuolar trafficking in the case of 3-DAF synthesis during phytoalexin production is not crucial when compared to the proper function of ER and Golgi. Nevertheless, the *in vivo* experiments did not answer directly the question whether 3-DAF production and trafficking takes place in 'vesicles' or whether a general block of the vesicular machinery also disturb production of red membrane less inclusions.

In conclusion we have developed a new reproducible and effective 'plant – elicitor' system which can provide new information about the genesis and accumulation of secondary compounds under stress conditions without the restriction of working with pathogens.

There is increasing evidence for the role of flavonoids in defense response in many plant species, although the exact mechanism was not yet clearly defined. Engineering the flavonoid pathway for enhancement of specific flavonoids in selected tissues subjected to pathogen attack or environmental stress could be a novel strategy to improve disease resistance in cereals. In

addition 3-DAF in sorghum plants could be a source for production of pharmaceuticals and biopolymers with antioxidant potential.

Acknowledgements

The author thanks Prof. Bächi from EMZ (Laboratory of electron microscopy at the University of Zurich) for the kind collaboration, Réka Nagy and Shaun Peters for the suggestions on the manuscript.

Reference list

Aida Y., Tamogami S., Kodama O. and Tsukiboshi T. 1996 Synthesis of 7-methoxyapigeninidin and its fungicidal activity against *Gloeocercospora sorghi*. Biosci.Biotechnol.Biochem. 60:1495-1496.

Awika J.M. and Rooney L.W. 2004 Sorghum phytochemicals and their potential impact on human health. Phytochemistry 65:1199-1221.

Awika J.M., Rooney L.W. and Waniska R.D. 2004 Properties of 3-deoxyanthocyanins from sorghum. J. Agric.Food Chem. 52:4388-4394.

Bailey J.A. 1983 Biological perspectives of host-pathogen interactions. In: Bailey, J.A., Deverall, B.J., eds., The Dynamics of Host Defense. Academic Press, Sidney, pp 1-32.

Bailey J.A. 1982 Physiological and biochemical events associated with the expression of resistance to disease. In: Wood, R. K. S., ed, Active Defense Mechanisms in Plants. Plenum Press, New York, pp. 39-65.

Bailey J.A., Rowell P.M. and Arnold G.M. 1980 The temporal relationship between host cell death, phytoalexin accumulation and fungal inhibition during hypersensitive reactions of *Phaseolus vulgaris* to *Colletotrichum lindemuthianum*. Physiological Plant Pathology 17:329-339.

Bors W., Michel C., Stettmaier K. 2001 Structure-activity relationships governing antioxidant capacities of plant polyphenols. Methods Enzymol. 335:166-181.

Conn S., Zhang W., Franco C. 2003 Anthocyanic vacuolar inclusions (AVIs) selectively bind acylated anthocyanins in *Vita vinifera* L. (grapevine) suspension culture. Biotech Ltrs. 25:835-839.

Debeaujon I., Leon-Kloosterziel K.M., Koornneef M. 2000 Influence of the testa on seed dormancy, germination, and longevity in *Arabidopsis*. Plant Physiol. 122:403-413.

Dixon R.A., Paiva N.L. 1995 Stress-induced phenylpropanoid metabolism. Plant Cell 7:1085–1097

Irani N.G. and Grotewold E. 2005 Light-induced morphological alteration in anthocyanin-accumulating vacuoles of maize cells. BMC Plant Biology 5:7

Geldner N., Friml J., Stierhof Y.D., Jurgens G. and Palme K. 2001 Auxin transport inhibitors block PIN1 cycling and vesicle trafficking. Nature 413:425-428.

Ferreira D., Slade D. 2002 Oligomeric proanthocyanidins: Naturally occurring O-heterocycles. Nat. Prod. Rep. 19:517-541.

Hahn D.H., Rooney L.W., Earp C.F. 1984 Tannins and phenols of sorghum. Cereal Foods World 29:776-779.

Hipskind J., Hanau R., Leite B., Nicholson R.L. 1990 Phytoalexin synthesis in sorghum: identification of an apigeninidin acyl ester. Physiol Mol Plant Pathol. 36:381–396

Hipskind J., Wood K., Nicholson R.L. 1996a Localized stimulation of anthocyanin accumulation and delineation of pathogen ingress in maize genetically resistant to *Bipolaris maydis race O*. Physiol Mol Plant Pathol. 49:247–256

Hipskind J.D, Goldsbrough P.B, Urmeev F., Nicholson R.L. 1996b Synthesis of 3-deoxyanthocyanidin phytoalexins in sorghum does not occur via the same pathway as 3-hydroxylated anthocyanidins and phlobaphenes. Maydica 41:155–166.

Li Z.S., Szczypka M., Lu Y.P., Thiele D.J., Rea P.A. 1996 The yeast cadmium factor protein (YCF1) is a vacuolar glutathione S-conjugate pump. J Biol Chem 271: 6509-6517.

Lo S.C.C. and Nicholson R.L. 1998 Reduction of light-induced anthocyanin accumulation in inoculated sorghum mesocotyls . Implications for a compensatory role in the defense response. Plant Physiol. 116:979-989.

Lu Y., Foo L.Y. 2001 Antioxidant activities of polyphenols from sage (*Salvia officinalis*). Food Chem. 75:197-202.

Lue W.L, Kuhn D., Nicholson R.L. 1989 Chalcone synthase activity in sorghum mesocotyls inoculated with *Colletotrichum graminicola*. Physiol Mol Plant Pathol 35:413–422

Markham K.R., Ryan K.G., Gould K.S., Rickards G.K. 2002 Cell wal sited flavonoidsin lisianthus flower petals. Phytochemistry 54:681-687

Markham K.R., Gould K.S., Winefeld C.S., Kevin A. Mitchell K.A., Bloor S.J., Boase M.R. 2000 Anthocyanic vacuolar inclusiona and their nature and significance in flower colouration. Phytochemistry 55:327-336

Matsuoka K., Bassham D.C., Raikhel N.V., and Nakamura K. 1995 Different sensitivity to wortmannin of two vacuolar sorting signals indicates the presence of distinct sorting machineries in tobacco cells. J.Cell Biol. 130:1307-1318.

Melake-Berhan A., Butler L.G., Ejeta G., Menkir A. 1996 Grain mold resistance and polyphenol accumulation in sorghum. J.Agric. Food Chem. 44:2428-2434.

Nebenfuhr A., Ritzenthaler C., and Robinson D.G. 2002 Brefeldin A: Deciphering an Enigmatic Inhibitor of Secretion. Plant Physiol. 130:1102-1108.

Nielsen K.A., Nicholson R.L., Carver T.L.W., Kunoh H., Oliver R.P. 2000 First touch: an immediate response to surface recognition in conidia of Blumeria garminis. Physiol. Mol. Plant Pathol. 56:63-70.

Nicholson R.L., Hammerschmidt R. 1992 Phenolic compounds and their role in disease resistance. Annual Review of Phytopathology 30:369-389.

Nicholson R.L, Hipskind J.D. 1996. Resistance in the Poaceae: diferent roles for phenolic compounds. In: Mills D, Kunoh H, Keen NT, Mayama S, eds. Molecular aspects of pathogenicity and resistance : requirements for signal transduction. St Paul, MN, USA: APS Press, 209-217.

Nicholson R.L, Jamil F, Snyder B.A, Lue W.L, Hipskind J.D. 1988. Phytoalexin synthesis in the juvenile sorghum leaf. Physiological and Molecular Plant Pathology 33:271-278.

Nicholson R.L, Kollipara S.S, Vincent J.R, Lyons P.C, Cadena-Gomez G. 1987 Phytoalexin synthesis by the sorghum mesocotyl in response to infection by pathogenic and nonpathogenic fungi. PNAS USA 84:5520-5524.

Nozzolillo C., Ishikura N. 1988 An investigation of the intracellular site of anthocyanoplasts using isolated protoplasts and vacuoles. Plant Cell Rep 7:389-392

O'Connell R.J. and Bailey J.A. 1986 Immunogold labelling of fungal antigens in cells of *Phaseolus vulgaris* infected by *Colletotrichum lindemuthianum*. Physiological and Molecular Plant Pathology 28 (1):99-105.

Orczyk W., Hipskind J., deNeergaard E., Goldsbrough P., Nicholson R.L. 1996 Stimulation of phenylalanine ammonia-lyase in sorghum in response to inoculation with *Bipolaris maydis*. Physiol Mol Plant Pathol 48:55–64

Parr A.J., Bolwell G.P. 2000 Phenols in the plant and in man. The potential for possible nutritional enhancement of the diet by modifying the phenols content or profile. J. Sci. Food Agric. 80:985-1012.

Pellegrini, N., Serafini, M., Colombi, B., Del Rio, D., Salvatore, S., Bianchi, M., Brighenti, F. 2003 Total antioxidant capacity of plant foods, beverages, and oils consumed in Italy assessed by three in Vitro assays. J. Nutr. 133:2812-2819.

Pecket C.R., Small C.J. 1980 Occurrence, location and development of anthocyanoplasts. Phytochemistry 19:2571-2576.

Pressman B.C, Fahim M. 1982 Pharmacology and toxicology of the monovalent carboxylic ionophores. Annu Rev Pharmacol Toxicol. 22:465-90.

Rice-Evans, C. 1999 Screening of phenolics and flavonoids for antioxidant activity. In Antioxidant Food Supplements in Human Health; Packer, L.; Hiramatsu, M.; Yoshikawa, T. Eds.; Academic Press: New York, pp 239-253.

Riedl K.M., Hagerman A.E. 2001 Tannin-complexes as radical scavengers and radical sinks. J. Agric. Food Chem. 49:4917-4923.

Robineau S., Chabre M., and Antonny B. 2000 Binding site of brefeldin A at the interface between the small G protein ADP-ribosylation factor1 (ARF1) and the nucleotide-exchange factor Sec7 domain. PNAS 97:9913-9918.

Santos-Buelga C., Scalbert A. 2000 Proanthocyanidins and tanninlike compounds: Nature, occurrence, dietary intake, and effects on nutrition and health. J. Sci. Food Agric. 80:1094-1117.

Smith C.J. 1996 Accumulation of phytoalexins: defense mechanism and stimulus response system. New Phytol 132:1–45

Snyder B.A., and Nicholson R.L. 1991 Accumulation of sorghum phytoalexins induced by *Colletotrichum graminicola* at the infection site. Physiol. Mol. Plant Pathol. 39:463-470.

Snyder B.A., Leite B., Hipsind J., Butler L.G., Nicholson R.L. 1991 Accumulation of sorghum phytoalexins induced by *Colleotrichum graminicola* at the infection site. Physiol. Mol. Plant Pathol. 39:463-70.

Snyder B.A., and Nicholson R.L. 1990 Synthesis of phytoalexins in sorghum as a site specific response to fungal ingress. Science 248:1637-1639.

Taylor J.R.N., Dewar J. 2001 Developments in sorghum food technologies. AdV. Food Nutr. Res. 43:217-264.

Tse Y.C., Mo B., Hillmer S., Zhao M., Lo S.W., Robinson D.G., and Jiang L. 2004 Identification of multivesicular bodies as prevacuolar compartments in *Nicotiana tabacum* BY-2 cells. Plant Cell 16:672-693.

VanEtten H.D., Mansfield J.W., Bailey J.A., and Farmer E.E. 1994 Two Classes of Plant Antibiotics: Phytoalexins versus "Phytoanticipins". Plant Cell 6:1191-1192.

Waniska R.D.,Venkatesha R.T., Chandrashekar A., Krishnaveni S., Bejosano F.P., Jeoung J., Jayaraj J., Muthukrishnan S., and Liang G.H. 2001 Antifungal proteins and other mechanisms in the control of Sorghum stalk rot and grain mold. J. Agric. Food Chem. 49:4732-4742

Wharton P.S. and Nicholson R.L. 2000 Temporal synthesis and radiolabelling of the sorghum 3-deoxyanthocyanidin phytoalexins and the anthocyanin, cyanidin 3-dimalonyl glucoside. New Phytologist 145:457-469.

Weiergang I., Hipskind J.D, Nicholson R.L. 1996 Synthesis of 3-deoxyanthocyanidin phytoalexins in sorghum occurs independent of light. Physiol Mol Plant Pathol 49:377-388.

Chapter 7

Conclusions

Abiotic or biotic environmental stresses cause significant intracellular restructuring in plants and also lead to a production of phenolic secondary metabolites that are involved in many plant functions as protection against light, nutrient stresses, fungal parasites, herbivores, pathogens, and oxidative cell injury. Flavonoid biosynthesis, giving rise to structurally related but functionally varying compounds such as flavonols, flavones, anthocyanins, proanthocyanidins or isoflavonoids (Dixon and Paiva, 1995; Winkel-Shirley, 2001), represents an ideal model to study metabolic regulation in plant cells. Anthocyanins, a flavonoid subclass, are the main pigments in flowers and fruits, acting as insect and animal attractants (Harborne and Williams, 2000).

The presence and synthesis of secondary plant products require a strict compartmentation of the sites of production and storage. Recent studies demonstrate that proteins that are required for secretory vesicle targeting and fusion play an important role in plant defense against pathogens and stress adaptation (Schulze-Lefert and Robatzek, 2006). Since phenolic compounds are known phytoalexins, it will be interesting to see whether vesicles filled with such substances definitively help to control the invasion of the pathogen and how these vesicles are finally filled with their metabolic cargo.

New findings support the hypothesis that flavonoids possess regulatory roles in plant cells and that they act as negative regulators of auxin transport affecting trafficking of the auxin efflux facilitator PIN1 (Muday *et al*., 2003; Taylor and Grotewold, 2005). In Arabidopsis, at least two enzymes (CHS and CHI) have been found in the nucleus together with histochemical staining of flavonols in this organelle, pointing to the possible existence of a differential targeting of the biosynthetic machinery and potential roles of flavonoids in the regulation of gene transcription (Saslowsky *et al*., 2005). Here we demonstrate that absence of PAs in the seed coat of several Arabidopsis *tt* mutant seeds leads to changes in the appearance of the vacuole (Chapter 4). These results suggest that PAs are necessary for proper biogenesis of the cell vacuole. Taken together, it becomes evident that flavonoids have functions that go beyond stress protection or defense and are related to important cellular processes in plants.

The present work investigates cellular flavonoid transport on different levels. Figure 1 summarizes a model of flavonoid transport in Arabidopsis. One set of experiments aims at the biochemical identification of the function of the candidate flavonoid transporter TT12. TT12 is identified as a vacuolar membrane protein. Furthermore, it acts as a cyanidin-3-glucoside/H^+-antiporter after heterologous expression. The substrate specificities tested so far suggest strongly that glycosylation of the substrate is necessary for TT12-mediated transport which is in accordance with published data on vacuolar flavonoid transport in carrot, parsley and barley (Matern *et al*., 1986; Hopp and Seitz, 1987; Klein *et al*., 1996). Thus, it must be hypothesized that

the flavan-3-ol precursor of the PA polymers should be glucosylated to be an efficient TT12 substrate. In order to demonstrate the *in vivo* function of TT12, future experiments will be necessary which involve the identification of glycosylated epicatechin derivatives in Arabidopsis seeds, eventually identification of UDP-sugar-dependent glycosyltransferases and isolation or synthesis of this substance on a larger scale allowing direct transport experiments with TT12.

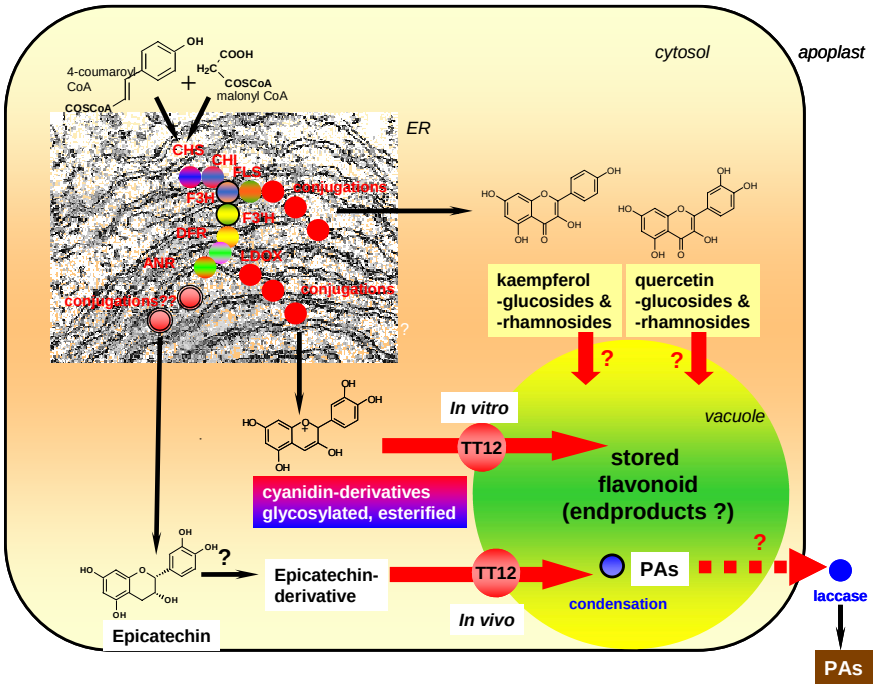

Figure 1. Scheme of the proposed biosynthesis and transport pathways of flavonoids in plant cell.

Based on the results in TT12 transport activity as a proton-antiporter and based on earlier results demonstrating flavonoid/H^+-antiport activity on barley mesophyll vacuoles, it is tempting to suggest that further MATE transporters are involved in the vacuolar accumulation of flavonoids related in structure to the PA precursors. Due to the well-defined, clear and rapidly-scorable seed-related phenotype of *tt12* mutants, we suggest a strategy to identify flavonoid transporters by misexpression of MATE transporter full-length cDNAs in cells involved in PA production. This strategy is based on the notion that MATE transporters possess rather broad substrate specificity (Routaboul *et al.*, 2006). As a consequence, MATE transporters functionally related to TT12 may be able to complement the *tt12* phenotype because they recognize similar substrates. To this end, we report the cloning of 19 MATE transporter full-length cDNAs into binary vectors suitable

for plant transformation that allow on the one hand localization of the corresponding proteins as GFP fusions in stable and transient assays. On the other hand, ongoing work aims at the construction of vectors which enable us to misexpress these cDNAs specifically in PA-producing cells in the *tt12* background. In order to do this, a fragment of the *BANYULS* promoter was chosen exhibiting high and specific expression in PA-producing cells of the Arabidopsis seed coat (Debeaujon, 2003). The fact that Pro_{BAN}-driven expression of the *TT12* cDNA complements *tt12* based on histochemical analysis allows the conclusion that the specific misexpression essentially works. Furthermore, overexpression of several cDNAs of MATE transporters exhibiting higher homology to *ALF5* and *DTX1* than to *TT12* are reported not to complement the *tt12* phenotype. In contrast, $Pro_{CaMV\ 35S}$*::-GFP-TT12* partially revert the *tt12* seed coloration and metabolite composition. As a consequence, it may be speculated that further flavonoid transporters are not related to *ALF5, DTX1* and further genes of this subclade but may share closer homology with *TT12*. Clearly, this strategy must be followed up in the future and needs to be completed for the Pro_{BAN5}*::MATE* constructs in order to find candidates complementing *tt12*. As a next step, expression analysis will help to find out, whether a candidate MATE transporter is involved in vacuolar flavonoid in vegetative plant parts.

At the same time, medium-scale localization by transient assays has been performed for 13 MATE transporters fused to GFP. Interestingly, most of them localize to the tonoplast and only 1 was found on the plasmalemma. As discussed in Chapter 3, alignments allow the clear identification of discrete, specific amino acids that are different in MATE proteins trafficking to different destinations. In the future, site-directed mutagenesis of these MATE transporters of individual amino acids that are specific for either the tonoplast or plasma-membrane MATE transporters will lead to the identification of the necessary signals required for proper sorting. Moreover, an approach to investigate sorting of different isoforms will also be helpful to identify components of the unknown machinery responsible for proper subcellular trafficking of membrane proteins.

A third approach was undertaken to understand in more detail the posttranslational regulation of the barley flavonoid/H^+-antiport system whose activity was reported to be reduced in the *ant310* biosynthetic barley line. The fact that naringenin is able to overcome and complement the mutation in *CHI* in ant310 on the level of saponarin production and on the level of the recovery of the vacuolar transport activity makes this system an ideal model to study the interplay between metabolism and transport. According to our data, it has to be suggested that flavonoid biosynthesis itself in an unknown way controls the activity of the transport system. Either an unknown intermediate of the flavonoid pathway (but not naringenin it self since short-term complementation were not sufficient for full transport activity reactivation) which acts as a signal or interaction between components of the metabolic pathways and the transporter could be involved in this regulatory mechanism.

The question how this regulation works on a molecular basis may be difficult to study in barley, most importantly because the biosynthetic steps between naringenin synthesis by CHI and isovitexin are not properly elucidated. Therefore, it must be suggested to transfer the experimental system to Arabidopsis in the future because of several advantages. (1) The core flavonoid pathway is known in Arabidopsis and tagged by mutants. Mutants in the chalcone synthase and isomerase (*tt4* and *tt5*) could be used to verify whether flavonoid absence leads to the deactivation of the vacuolar transporter and whether naringenin feeding reactivates as it did in barley. However, in order to establish the comparable experimental system, vacuolar flavonol transport into Arabidopsis mesophyll vacuoles needs a basic characterisation. (2) Most of the attempts to purify tonoplast proteins biochemically did not lead to the identification of secondary energized transporters. As a consequence it appears more probable to find the Arabidopsis flavonol transporter by genetic analysis (see above) than to isolate the barley flavone transporter. Nevertheless, regulation of the flavonoid transporter can only be studies further if the protein is known.

Another major topic under investigation during this work focused our attention on the question how the vesicle trafficking machinery works within the cell and to elucidate this process we used Sorghum bicolor as model. We established easy and reliable elicitor based system, which allowed the analysis of mechanisms involved in 'vesicular' flavonoid transport.

It has been shown previously that young sorghum leaves accumulate a complex of phenolic compounds (3-DA and anthocyanins) in response to invasion by both pathogenic and non-pathogenic fungi and by light. It was shown that also anthocyanins accumulated and were stored in inclusions that occur in the leaves of various Brassicaceae (Pecket and Small, 1980, Nozzolillo and Ishikura, 1988). More recently, the intravacuolar structures observed in the flower petals of various plants, including carnation (*Dianthus caryophyllus*) and *lisianthus* (*Eustoma grandiflorum*) were termed anthocyanic vacuolar inclusions, or AVIs (Markham *et al.*, 2000). These inclusions were suggested to be membrane-less, proteinaceous matrixes that acted as anthocyanin traps, preferentially for anthocyanidin 3, 5-diglycosides (Markham *et al.*, 2000) or acylated anthocyanins (Conn *et al.*, 2003).

Here we demonstrate that treatment of sorghum primary leaves with an unspecific elicitor xylanase or cellulase led to a response which is comparable to the fungal attack. Although, the response was visibly similar we monitor different composition of the compounds after the elicitation. We observed that mechanical damage also led to accumulation or red compounds but later, when compared with xylanase treatment. The different pattern could be in correlation with the different signals produced after treatment. Nevertheless, the *in vivo* experiments with different inhibitors did not answer directly the question whether 3-DA production and trafficking takes place in 'vesicles' or whether a general block of the vesicular machinery also disturb production of red membrane less inclusions. Future work is needed to evaluate if the moving 'vesicles' we monitor

in this study are membrane bound compartment using markers fused to fluorescent proteins (e.g. GFP).

Reference list

Conn S., Zhang W., Franco C. 2003 Anthocyanic vacuolar inclusions (AVIs) selectively bind acylated anthocyanins in *Vita vinifera* L. (grapevine) suspension culture. Biotech Ltrs. 25:835-839.

Dixon R.A., and Paiva N.L. 1995 Stress-induced phenylpropanoid metabolism. Plant Cell 7:1085–1097.

Debeaujon I., Nesi N., Perez P., Devic M., Grandjean O., Caboche M., Lepiniec L. 2003 Proanthocyanidin-accumulating cells in *Arabidopsis* testa: Regulation of differentiation and role in seed development. Plant Cell 15:2514-2531.

Harborne J.B. and Williams C.A. 2000 Advances in flavonoid research since 1992. Phytochemistry 55:481-504.

Hopp W., Seitz H.U. 1987 The uptake of acylated anthocyanin into isolated vacuoles from a cell suspension culture of *Daucus carota*. Planta 170:74-85

Klein M., Weissenböck G., Dufaud A., Gaillard C., Kreuz K., Martinoia E. 1996 Different energization mechanisms drive the vacuolar uptake of a flavonoid glucoside and a herbicide glucoside. J. Biol. Chem. 271:29666-29671.

Matern U., Reichenbach C., Heller W. 1986 Efficient uptake of flavonoids into parsley (*Petroselinum hortense*) vacuoles requires acylated glycosides. Planta 167:183-189

Markham K.R., Gould K.S., Winefeld C.S., Kevin A. Mitchell K.A., Bloor S.J., Boase M.R. 2000 Anthocyanic vacuolar inclusiona and their nature and significance in flower colouration. Phytochemistry 55:327-336.

Muday G.K., Peer W.A., Murphy A.S. 2003 Vesicular cycling mechanisms that control auxin transport polarity. Trends Plant Sci. 8(7):301-4.

Nozzolillo C., Ishikura N. 1988 An investigation of the intracellular site of anthocyanoplasts using isolated protoplasts and vacuoles. Plant Cell Rep 7:389-392.

Pecket C.R., Small C.J. 1980 Occurrence, location and development of anthocyanoplasts. Phytochemistry 19:2571-2576.

Routaboul J.M., Kerhoas L., Debeaujon I., Pourcel L., Caboche M., Einhorn J., and Lepiniec

L. 2006 Flavonoid diversity and biosynthesis in seed of Arabidopsis thaliana. Planta 224:96-107.

Saslowsky D.E., Warek U., Winkel B.S. 2005 Nuclear localization of flavonoid enzymes in Arabidopsis. J Biol Chem 280: 23735-23740.

Schulze-Lefert P., and Robatzek S. 2006 Plant pathogens trick guard cells into opening the gates. Cell 126(5):831-4.

Taylor L.P., and Grotewold E. 2005 Flavonoids as developmental regulators. Curr Opin Plant Biol. 8(3):317-23.

Winkel-Shirley B. 2001 Flavonoid biosynthesis. A colorful model for genetics, biochemistry, cell biology, and biotechnology. Plant Physiol. 126:485–493.

Chapter 8

Comparative mutant analysis of Arabidopsis Multidrug Resistance-Associated Proteins: Only AtMRP2 but not AtMRP1, 11 and 12 Contribute to Detoxification, Vacuolar Organic Anion Transport and Chlorophyll Degradation

Authors: Annie Frelet[1], Üner H. Kolukisaoglu[2], Louis Azevedo[1], Stefan Hörtensteiner[3], **Krasimira Marinova[1]**, Barbara Weder[1], Burkhard Schulz[4], and Markus Klein[1,5]

Affiliations:

[1] Zurich Basel Plant Science Center, University of Zurich, Plant Biology, Zollikerstrasse 107, CH-8008 Zürich, Switzerland

[2] University of Rostock, Biosciences, Plant Physiology, Albert-Einstein-Str. 3, D-18051 Rostock, Germany

[3] University of Bern, Institute of Plant Sciences Altenbergrain 21 CH-3013 Bern, Switzerland

[4] Purdue University, Horticulture and Landscape Architecture, 625 Agriculture Mall Dr.,West Lafayette, IN, 47907-2010, USA

[5] To whom correspondence should be addressed: E-mail: markus.klein@botinst.unizh.ch

Abstract

The enormous metabolic plasticity of plants allows them to detoxify many harmful compounds that are either generated during biosynthetic processes such as phenolics or are present as biotic or abiotic toxins in their environment. Ultimately, derivatives of toxic compounds such as glutathione conjugates are moved into the central vacuole via ATP binding cassette (ABC)-type transporters of the Multidrug Resistance-associated Protein (MRP) subfamily. The Arabidopsis genome contains 14 *AtMRP* isogenes, four of which (*AtMRP1*, *2*, *11* and *12*) cluster together in one of two major phylogenetic clades since they exhibit high amino acid identity between 68 and 90 %. We isolated T-DNA knockouts in all four *AtMRP* genes of this clade and subjected them to physiological experiments to elucidate the function of each *AtMRP* of this group. None of the single *atmrp* mutants displayed any visible phenotype under control conditions. In spite of the fact that AtMRP1 and AtMRP2 had been described as efficient ATP-dependent organic anion transporters in heterologous expression experiments, the contribution of most of the four single AtMRPs to detoxification is marginal. Only knockouts in *AtMRP2* exhibited a significant reduction in sensitivity towards 1-chloro-2,4-dinitrobenzene, however, not towards other herbicides. Vacuolar uptake studies demonstrated that the ATP-dependent transport of typical MRP substrates was reduced in *atmrp2*. *AtMRP2* but not *AtMRP1* is involved in chlorophyll degradation since ethylene-treated rosettes of *atmrp2* showed reduced senescence confirming a role for AtMRP2 in vacuolar transport of chlorophyll catabolites. GUS analysis of the *AtMRP1* and *2* promoter activities revealed that both genes are differentially expressed in Arabidopsis with strong and low GUS activity in rosette leaves of *ProAtMRP1-GUS* and *ProAtMRP2-GUS* lines, respectively, as one of the major differences. We conclude that only AtMRP2 contributes partially to overall glutathione conjugate pump activity and propose that the range of functions of the other AtMRPs in this cluster is beyond detoxification.

Keywords*:* T-DNA knockout, gene family, gene redundancy, herbicide resistance, senescence, glutathione conjugate

Addendum – CD-ROM